The Geology and Tectonic Evolution of the Western Approaches Trough

Richard R. Hillis

Doctor of Philosophy
University of Edinburgh
1988

DECLARATION

This thesis has been composed solely by myself. The work presented is my own unless otherwise acknowledged

Richard R. Hillis.

CONTENTS

ABSTRACT

The Western Approaches Trough is a composite sedimentary depocentre covering the extreme south-west of the British, and north-west of the French continental shelves. It is sub-divided into the Western Approaches Basin in the British sector and the Brittany and South-West Channel Basins in the French sector. This thesis investigates the geology and tectonic evolution of the area, concentrating on the driving mechanisms of vertical crustal movements. The database for the project comprises seismic reflection, gravity, magnetic and well data acquired largely in the recent search for commercial hydrocarbon deposits.

Terrestrial Permo-Triassic red-beds up to 6km thick and marine Jurassic shales and limestones were deposited during initial basin development. In the Western Approaches Basin subsequent late Jurassic-early Cretaceous erosion cut back as far as the Permian, whereas in the Brittany and South-West Channel Basins the Jurassic-Cretaceous sequence is nearly complete. In mid-late Cretaceous times transgression resulted in Chalk deposition over the entire area. However, much of the Chalk was removed from the Brittany and South-West Channel Basins by Tertiary uplift, but it is preserved beneath about 1.5km of Tertiary shelf clastics and carbonates in the Western Approaches Basin.

South-south-east-dipping basement events observed on seismic reflection data over the Western Approaches Basin were mapped and correlated with known onshore Variscan thrusts. The thrusts, together with a steep, perpendicular transfer fault set apparent on gravity data, impart a pronounced orthogonal structural grain to the area.

The magnitude of Permian-Jurassic tectonic subsidence in the Western Approaches Basin is inconsistent with "whole crustal" estimates of extension based on backstripped gravity and deep seismic data and with "cover" estimates based on summing fault heaves. A Permian subsidence phase driven by denudation of a Variscan high in the northern Western Approaches Basin/Cornubian Massif is consistent with the observed facies and distribution of the Permian red-beds and accounts for the discrepancy between crustal extension and subsidence. In the Western Approaches Basin extension-driven subsidence commenced in the Triassic

with local reactivation of the Variscan thrusts and transfer faults. Fault activity migrated southwards from the Western Approaches Basin into the Brittany and South-West Channel Basins where subsidence did not commence until the end of the Triassic/early Jurassic.

Late Jurassic-early Cretaceous Atlantic-related uplift of the Western Approaches Trough was synchronous with the second major phase of faulting and extension. Fault-controlled subsidence, within a sinistral strike-slip/extensional regime, counteracted regional uplift in the Brittany and South-West Channel Basins, accommodating the deposition of the continuous Jurassic-Cretaceous sequence. In contrast, a major angular unconformity associated with 1-2km of erosion was developed in the Western Approaches Basin. In the latter area, faulting and subsidence, involving further extensional reactivation of the Variscan thrust and transfer faults, was subsidiary to the uplift, preserving only fault-bounded outliers of Liassic rocks. Tectonic subsidence curves for the ensuing regional late Cretaceous-early Tertiary subsidence fit lithospheric cooling following a combination of extension and uplift/erosion.

Tertiary uplift driven by Alpine plate convergence interrupted regional subsidence. Porosity data have been used to quantify this uplift and it is shown to have occurred throughout the Western Approaches Trough. Compressional deformation is apparent only in the Brittany and South-West Channel Basins but it is proposed that sub-crustal compression occurred throughout the area.

ACKNOWLEDGMENTS

It would be impossible to acknowledge everyone who has helped me during the last three years, particularly those in the marine units of the BGS where I worked on a daily basis. However, I shall endeavour to thank those due special mention.

I would first of all like to acknowledge the help and encouragement of my supervisors, Roger Scrutton and Geoff Day, without whom the project could never have been carried out.

Secondly, I would like to thank the operating oil companies (and their partners) in the Western Approaches Trough who provided, in advance of its release into the public domain, the data on which the work has been based, namely; Amerada Hess (BCRIC Exploration UK Limited, Charterhall Oil Limited, Svenska Petroleum AB, THF Oil Limited, WL Explorations Limited), Arco British Limited (Elf UK plc), British Gas plc, Britoil plc (Amoco UK Exploration Company, British Gas plc, Mobil North Sea Limited and Svenska Petroleum AB), British Petroleum Exploration Company Limited (Elf UK plc, Total Oil Marine Limited), Chevron Exploration North Sea Limited (Britoil plc, Enterprise Oil plc, National Westminster Resources Limited), Murphy Petroleum Limited (Aran Energy Exploration Limited, Ocean Exploration Company Limited, Ultramar Exploration Limited, Viva Petroleum Limited), Phillips Petroleum Company UK Limited (Century Power and Light Limited, Fina Exploration Limited, Hispanoil (UK) Limited, Whitehall Petroleum Limited), Placid Oil Company (UK) (Britoil plc, Enserch International Exploration Incorporated).

Amerada Hess, Arco, Chevron and Murphy and their respective partners are due special thanks for allowing the inclusion of data in the thesis from as yet unreleased wells. I would like to also acknowledge Elf UK plc for providing the released well data from the French sector of the Western Approaches Trough. Particular appreciation is due to Steve Trueblood at Murphy for detailed data on their acreage in the Western Approaches Trough and Godfrey Spalton at Britoil for his comments on Chapter 2.

GECO Exploration Services allowed access to their speculative seismic data shot over the area in 1978 and 1979 and gave their

permission for the inclusion of Figures 2.9, 4.6, 4.8 and 4.11. Particular thanks are due to Tim Chapman (Merlin Exploration Services) for discussion on matters pertaining to the seismic data, and for his comments on Chapter 4. Thanks are also due for a pre-publication copy of his paper on the Melville Basin. Western Geophysical are acknowledged for speculative seismic data from the northern part of the French sector of the basin.

I would also like to thank P.A. Ziegler for comments on regional geology and palaeogeography, J.P. Lefort and C. Bois for information on the Brittany and South-West Channel Basins, and J.M. Hancock, B.K. Davis, P.A. Scholle and J. Jensenius for comments on the Chalk porosity data. Appreciation is due to R.A. Chadwick for discussion on Tertiary uplift mechanisms and his comments on Chapter 7, H.T. Genc and R.G. Hipkin for advice and considerable help in carrying out the gravity backstripping work, S. Egan for discussions on mixed shear extension and compression and J.M. Bull and A.G. Hulbert for help in digitizing and depth converting the seismic sections of Figure 1.2.

The authors of the forthcoming BGS offshore regional report on the area, Geoff Day, John Edwards and Bob Gatliff have been of great help during the project and I would particularly like to thank the report compiler Chris Evans for his comments both during the research and on the thesis manuscript. Thanks also to Martyn Stoker for his encouragement and comments on the manuscript.

In Murchison House special thanks go to Kate Forteath and Elaine McElvanney for their help in drafting, to Stuart Gillies for his computer drawn base maps, to Jane Taylor for copying seismic data, and to Fergus McTaggart for photography. Thanks also to Amarjit Chandhial for help in the preparation of the borehole correlation diagrams (Figures 2.1 and 2.2) and to Joe Bulat for the aeromagnetic map of Figure 2.8. Thanks also to Alan Dobinson for his support of the project.

The research students in the BGS marine units, Alastair Bent, Frankie Zervos and Fiona Stewart provided daily humour and encouragement not to mention valuable scientific comment, but special thanks are due to Pat Condon for his considerable help, if not his late tackles on Monday evenings. Allan Trench at Glasgow University encouraged me, as ever, to look at the broader perspectives.

Greatest thanks of all, however, go to my parents who have supported and encouraged my extended stay in higher education. Thanks a lot.

The project was carried out whilst in receit of NERC (CASE) research studentship GT4/85/GS/30.

CHAPTER 1

INTRODUCTION

1.1 PROJECT PHILOSOPHY, AIMS AND OUTLINE

In the 1960s and early 1970s geodynamical research focused on horizontal movements of the earth's crust. This work resulted in the development of the geological paradigm of plate tectonics. Subsequently attention has switched to analysing the mechanisms of vertical motions. Particularly, why does the crust of the earth subside to form deep sedimentary basins, and, why are previously formed basins uplifted? The aim of this project is to elucidate the causes of both post-Carboniferous subsidence, and subsidiary uplift in the Western Approaches Trough, south-west of the British Isles.

In order to successfully elucidate its tectonic evolution the geological setting of the Western Approaches Trough must be well constrained. Hence Chapter 2 describes the geology of the area. The subsequent chapters discuss the analytical techniques applied to the seismic, gravity and borehole data and the implications of the results for the crustal dynamics of the Western Approaches Trough.

1.2 PROJECT AREA AND GEOLOGICAL NOMENCLATURE

The project area covers the south-west British and north-west French continental shelves west of 5°W and between 48°N and 50°N (Figure 1.1). However, adjoining areas are also considered where relevant.

There has been some confusion over the geographical nomenclature of the sea area covered by the project. Western Approaches, South-Western Approaches, South Celtic Sea and western English Channel have all been used. The author prefers South-Western Approaches, although geographical nomenclature is avoided. The geological provinces referred to in this thesis are outlined below.

The Western Approaches Trough is a complex composite sedimentary depocentre divided into a number of sub-basins which must be distinguished if its geological and tectonic evolution are to be successfully described. The nomenclature used in this study is slightly modified from that of Ziegler (1987a; 1987c) and is consistent with that in the forthcoming British Geological Survey offshore regional report on the area (Evans et al, in press).

Figure 1.1 shows the geological elements of the Western Approaches Trough and surrounding areas. The ENE-WSW trending Melville Basin, containing up to 6km of post-Carboniferous sediments, forms the north-western part of the Western Approaches Trough (Figure 1.2). The Melville Basin has seen the greatest concentration of commercial activity, consequently borehole data, in particular, is biased towards this area (Appendix A). The Melville Basin passes eastwards into the similarly trending St. Mary's Basin (Figure 1.2) which in turn passes eastwards over a slight high, the Lizard-Morlaix axis, into the Plymouth Bay Basin. The Plymouth Bay Basin is circular in plan and contains over 9km of largely Permo-Triassic rocks. To the east another structural high, the Start-Cotentin line (a prolongation of the Sticklepath-Lustleigh fault zone onshore south-west England) separates the Plymouth Bay Basin from the Channel Basins. Together the Melville, St. Mary's and Plymouth Bay Basins comprise the Western Approaches Basin which covers the entire British sector of the Western Approaches Trough and the northern part of the French sector. The terms Western Approaches Basin and Western Approaches Trough should not be confused (Table 1.1).

The ENE-WSW trending Brittany Basin lies to the south of the Melville and St. Mary's Basins being clearly distinguishable by the absence of a major middle Mesozoic, Cimmerian unconformity and also by Tertiary inversion (Figure 1.2). The South-West Channel Basin lies along strike to the ENE of the Brittany Basin and is geologically similar.

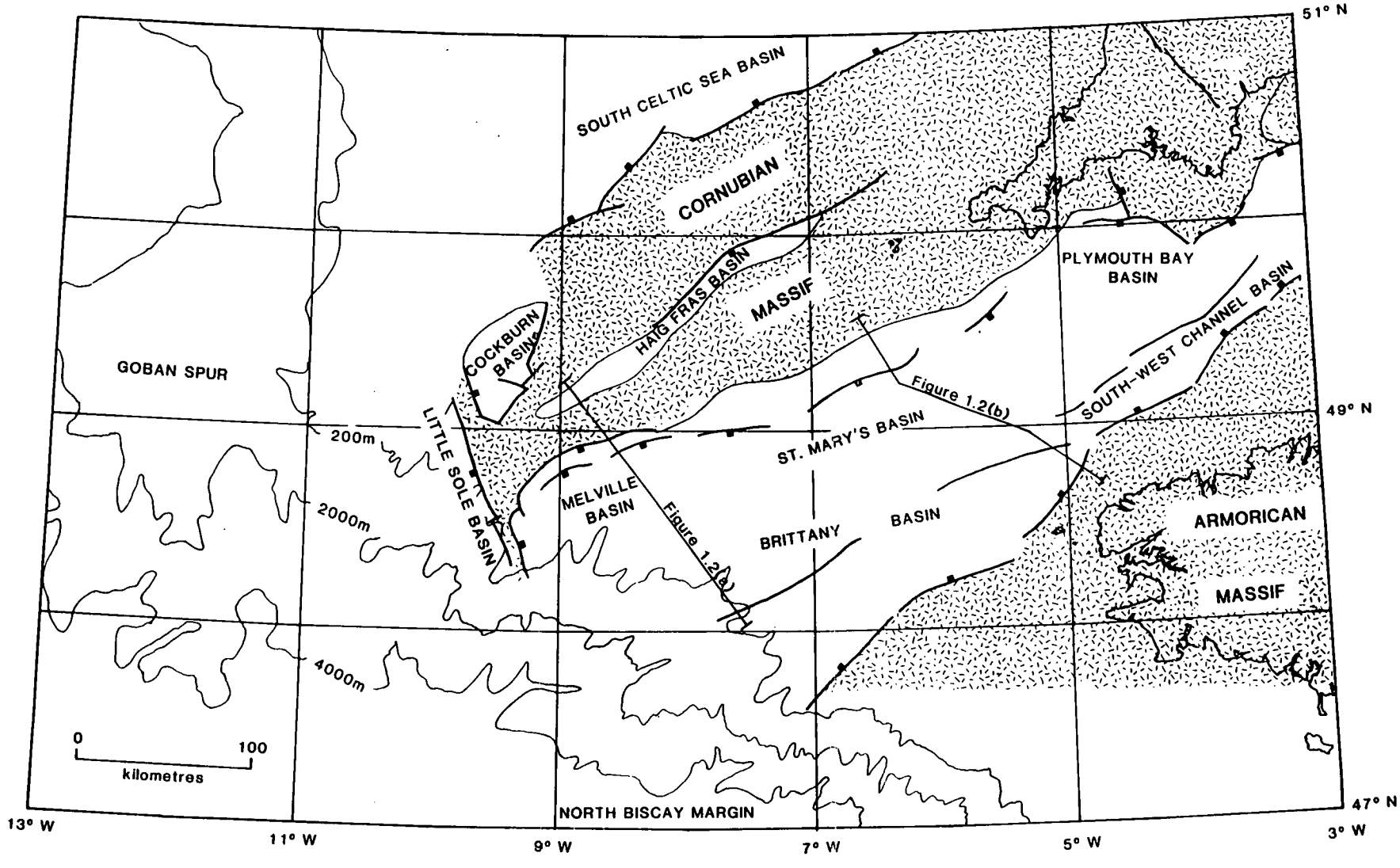

Figure 1.1 Major tectonic elements of the Western Approaches Trough and Cornubian Massif. Patterned areas show Palaeozoic basement at or near surface. Continental slope bathymetry is also shown.

Table 1.1 Hierarchy of basin nomenclature within the Western Approaches Trough.

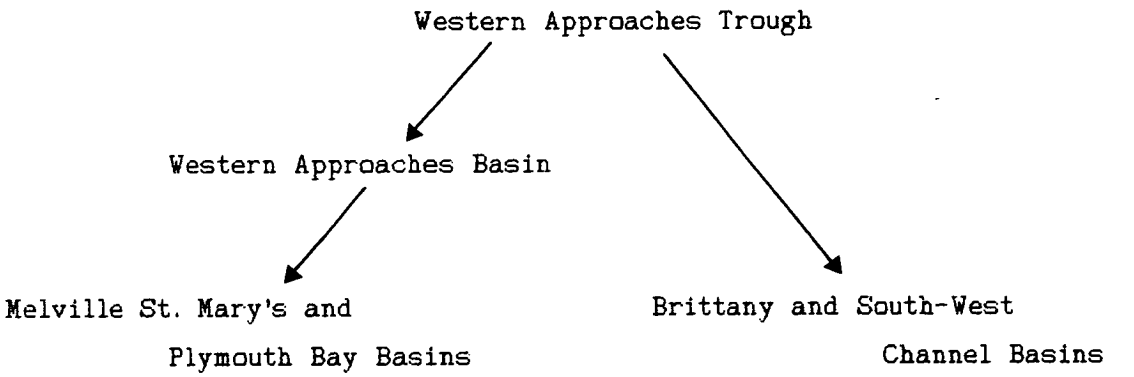

The Cornubian Massif forms the northern flank of the Western Approaches Trough and extends north to the southern flank of the South Celtic Sea Basin. It comprises the Cornubian and Haig Fras Batholiths, surrounding Devono-Carboniferous metasediments, and the shallow Haig Fras Basin and Cockburn Basin . The southern margin of the Western Approaches Trough is formed by the Armorican Massif of Brittany and its offshore extension.

The Cornubian Massif is truncated to the south-west by the Little Sole Basin, the most inbound (easterly) of the half-grabens stepping down to the North-East Atlantic Basin. The continental slope west of the Little Sole Basin is formed by the north-south trending promontory of Goban Spur, whereas the NW-SE trending north Biscay margin forms the continental slope in front of the Western Approaches Trough.

1.3 HISTORY OF RESEARCH IN THE WESTERN APPROACHES TROUGH

The Western Approaches Trough has a long history of marine geoscientific exploration. Dredging in the early part of this century suggested the possible presence of a sedimentary basin (Crawshay, 1908; Worth, 1908). This was confirmed by an early seismic refraction

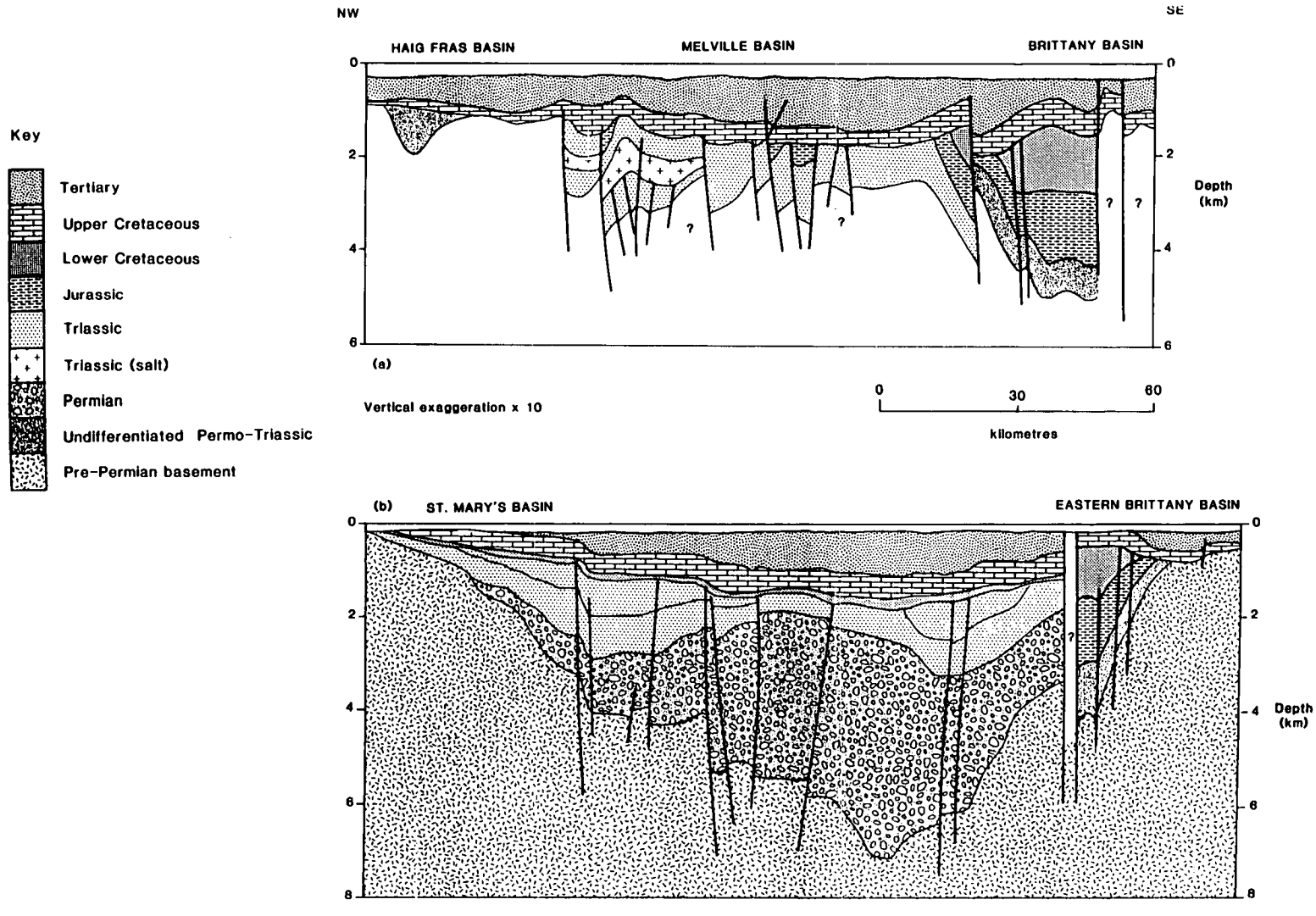

Figure 1.2 Depth converted regional seismic interpretations (assuming v = 2.297 + 0.431 TWT), locations as marked on Figure 1.1. Section (a) is based on an early regional commercial line on which pre-Triassic horizons could not be picked, section (b) is based on BIRPS SWAT 6 and 7.

experiment which ran from Plymouth Bay to the edge of the shelf (Bullard and Gaskell, 1941).

Seismic refraction and gravity work in the late 1940s and early 1950s resulted in Day et al's (1956) maps showing depth to the metamorphic basement and the Palaeozoic floor and also the thickness of post-Carboniferous strata. Subsequent commercial data has, however, shown these to underestimate the thickness of the sedimentary sequence in the Western Approaches Trough.

Shallow seismic reflection, sparker and boomer profiles, and gravity coring by research groups at Bristol University (e.g. Curry et al, 1962; Curry et al, 1965; Smith et al, 1965; Curry et al, 1971) and the Bureau de Recherches Géologiques et Minières (BRGM) (e.g Pomerol, 1972; Andreieff et al, 1972; Andreieff et al, 1975) led to a better understanding of the geometry and stratigraphic relationships of horizons exposed at or near the seabed.

Further reviews on the area were published in the 1970s (e.g. Owen, 1974; Blundell, 1975; Naylor and Mounteney, 1975; Blundell 1979; Hamilton, 1979). However, the available data still constrained detailed study to the shallower part of the sedimentary sequence.

Between 1973 and 1981 the British Geological Survey (BGS) carried out an extensive reconnaissance programme of shallow sampling and geophysical exploration in the British sector of the Western Approaches Trough culminating in the production of the 1:250000 map series (e.g. Evans, 1986; Fletcher and Evans, 1987). Desriptions of the Quaternary (Pantin and Evans, 1984) and Neogene (Evans and Hughes, 1984) successions were also published. Shallow boreholes drilled by the drillship "Wimpey Sealab" in 1976 as part of the mapping programme tested the Lower and base Upper Cretaceous stratigraphy south and west of Cornwall (Lott et al, 1980).

The advent of commercial hydrocarbon exploration brought in a new era of exploration in the Western Approaches Trough. Although French companies had begun multi-channel seismic work in the 1960s the first commercial well, Lizenn-1, was drilled in 1975. The first commercial well in the British sector, 72/10-1, was drilled in the Melville Basin in 1979. Although no commercially viable hydrocarbon deposits have been recorded in the area a total of 32 deep exploration wells have been

drilled in association with the shooting of numerous multi-channel seismic reflection surveys. The majority of the work in this project has been based on these commercially acquired data.

Until recently much of the commercial data has remained confidential and relatively few publications have been forthcoming. However, the largely stratigraphical accounts of Evans et al (1981) on four BGS wells which tested sub-Chalk stratigraphy, Bennet et al (1985) on well 72/10-1 and Naylor and Shannon's (1982) general review of the area are notable exceptions. Ziegler's (1981; 1982) reviews of the geology of north-west Europe include the Western Approaches Trough and other publications (Ziegler, 1987a; 1987c) cover the area specifically. Along with Chapman's (in press) discussion of the Permian-Cretaceous structural evolution of the Melville Basin based on seismic reflection data these provide the most detailed previously published tectonic studies of the area.

Much published material does, however, cover the continental slope adjacent to the Western Approaches Trough. Leg 48 of the Deep Sea Drilling Project (DSDP) covered sites 399/400, 401 and 402 on the north Biscay margin in 1978, and in 1980 leg 80 drilled sites 548, 549, 550 and 551 on Goban Spur (Appendix A). These legs were accompanied by seismic reflection profiling. The north Biscay margin and Goban Spur have both been relatively starved of sediments since Atlantic separation in mid Cretaceous times and the results of leg 48, in particular, have played an important role in the development of the theory of continental separation and passive margin formation by extension (e.g. Montadert et al, 1979; LePichon and Sibuet, 1981; Chenet et al, 1982).

The British Institutions Reflection Profiling Syndicate (BIRPS) together with the Etude de la Croûte Continentale et Océanique par Réflexion et Réfraction Sismiques (ECORS) shot the South West Approaches Traverse (SWAT) deep reflection seismic profiles to 15s two-way-time (TWT) in the Celtic Sea area in 1984 (BIRPS and ECORS, 1986). SWAT 6,7, 8 and 9 lie at least partially within the Western Approaches Trough (Appendix A) and reveal much information on deep crustal and upper mantle structure in the area (e.g. Beach, 1987; Pinet et al, 1987). SWAT 6 and 7, in particular, have been an important part

of the dataset in this project. In 1985 another deep seismic reflection profile, the Western Approaches Margin (WAM) line, was shot westwards from the Haig Fras Batholith across the continental shelf and slope and onto oceanic crust in order to test the hypothesis that lower crustal reflectivity increased across the progressively extended continental slope (Hobbs et al, 1987).

1.4 BASIN SUBSIDENCE AND UPLIFT MECHANISMS

Chapters 4,5,6,7 and 8, which discuss the tectonic evolution of the Western Approaches Trough, assume a basic knowledge of the principal driving mechanisms of vertical crustal motions. In the final part of this introduction an attempt has been made to briefly review this subject, concentrating on gravity loading and unloading, thermal processes and crustal thickness changes.

1.4.1 Gravitational Loading and Unloading

1.4.1.1 Local Isostatic Response

The gravitational load caused by a sediment pile will itself cause subsidence of the crust, displacing mantle material at depth (Dietz, 1963). If local, Airy isostasy is assumed then the relation between the magnitude of an initial air- (d_a) or water- (d_w) filled depression and its depth (d_s) after being infilled with sediment is simply obtained by balancing the mass of lithospheric columns prior to, and following, infill,

$$d_s = d_w[(\rho_m-\rho_w)/(\rho_m-\rho_s)] = d_a[\rho_m/(\rho_m-\rho_s)] \qquad (1)$$

where ρ_m, ρ_w and ρ_s are mantle, water and sediment densities respectively

Similarly, if uplifted crust is eroded isostatic rebound resulting from gravitational unloading will amplify the initial air-loaded uplift (u_a),

$$u_e = u_a[\rho_m/(\rho_m-\rho_e)] \qquad (2)$$

where u_e is the magnitude of uplift allowing for unloading and ρ_e is the density of the eroded material

Taking mantle, sediment and water densities of $3.33gcm^{-3}$, $2.3gcm^{-3}$ and $1.03gcm^{-3}$ respectively, equation (1) becomes,

$$d_s \simeq 2.2d_w \simeq 3.2d_a \qquad (3)$$

Hence thick sedimentary sequences may be produced by the infilling of subaerial intermontane depressions and submarine continental slopes and rises. However, in shelf seas, which are generally less than 200m deep, only a few hundred metres of marine sediments can accumulate in this way (Bott, 1980). An additional "tectonic" (Steckler and Watts, 1978) element of subsidence is required to explain the deposition of thick shallow water sequences, such as the post-Triassic sequence of the Western Approaches Trough.

1.4.1.2 Flexural Response

Local isostatic compensation will only occur if the lithosphere has no lateral strength (flexural rigidity). If the lithosphere has a finite flexural rigidity then, like an elastic plate, the effects of sediment loading and unloading will be accommodated over a larger area than that of the loading/unloading itself. The higher the elastic thickness of the lithosphere (the parameter that controls flexural rigidity) the larger the total area of response.

Perhaps the classic example of flexural subsidence is the formation of foreland basins. The load caused by the orogenic emplacement of thrust nappes causes subsidence in front of the nappes, forming a

depression into which the erosional products of the nappes are shed (Beaumont, 1981).

Flexural subsidence associated with a sedimentary load may account for the onlap often observed over tectonically undisturbed basin flanks (e.g. Watts et al, 1982). A more subtle flexural load on passive margins and their adjacent shelf areas, such as the Western Approaches Trough, is imposed by cooling, and associated density increase, of the adjacent oceanic crust as the passive margin moves away from the oceanic spreading centre.

Theoretical and experimental estimates of the elastic thickness of the continental lithosphere (Kusznir and Karner, 1985) suggest that flexure may play an important role in basin subsidence, particularly when the lithosphere is cool. However, gravity (Barton and Wood, 1984), seismic (Warner, 1987) and subsidence (Hellinger et al, in press) modelling suggest that the crustal structure of the British continental shelf is almost in local isostatic equilibrium. Gravity admittance studies of passive continental margins (Karner and Watts, 1982; Beaumont et al, 1982) have produced similar results. Following Warner (1987) it is proposed that the weak zones presented by major faults (e.g. BIRPS and ECORS, 1986), rather than average crustal rheology, control the flexural rigidity of the continental lithosphere.

1.4.2 Thermal Uplift and Subsidence

Noting the difficulty of explaining deep sedimentary basins purely by gravitational loading, Hsü (1965) invoked mantle density changes combined with supra-crustal erosion. A decrease in the density of the mantle above the level of isostatic compensation will cause crustal uplift. With a return of the mantle density to its initial value the elevated crust will subside to its initial level. If supracrustal erosion accompanies uplift, then following mantle re-equilibration the new erosional surface will subside beneath its initial level forming a sedimentary basin.

Sleep (1971) observed that the exponentially decaying subsidence rate of passive margins resembled that of cooling oceanic crust and

suggested that heating associated with continental separation and subsequent cooling could drive the mantle density changes and hence passive margin subsidence.

The relationship between the magnitude of erosion (u_e) and later sediment-loaded subsidence (d_s) can again be determined by simple isostatic mass balancing (Figure 6.8),

$$d_s = u_e[(\rho_m-\rho_e)/(\rho_m-\rho_s)] \qquad (4)$$

where the symbols are as equations (1) and (2)

Taking mantle and sediment densities of $3.33gcm^{-3}$ and $2.3gcm^{-3}$ respectively, a sedimentary sequence lying directly on basement (density $2.8gcm^{-3}$) will only attain a thickness of approximately half the magnitude of erosion. Hence the deposition of thick sedimentary sequences overlying basement, such as the post-Carboniferous sequence of the Western Approaches Trough, by the thermal uplift process requires an unreasonably large amount of pre-depositional erosion (c.f. Bott, 1980; Royden et al, 1980). However, intra-basinal uplift driven by re-equilibrating mantle density changes will result in approximately the same magnitude of post-uplift subsidence as initial uplift ($\rho_e \simeq \rho_s$). In this way basin uplift and subsidence may be intimately linked.

1.4.3 Lithospheric Extension

1.4.3.1 Introduction

The problem of excessive uplift required by the thermal hypothesis can be avoided if there is crustal extension and thinning in association with basin subsidence (Artemjev and Artyushkov, 1969). McKenzie's (1978) quantitative development of the lithospheric stretching model (Figure 1.3) requires no external heat sources and is justifiable in terms of widely accepted horizontal lithospheric movements.

Instantaneous horizontal extension of the crust and upper mantle by a factor β causes a rapid isostatically driven subsidence due to the

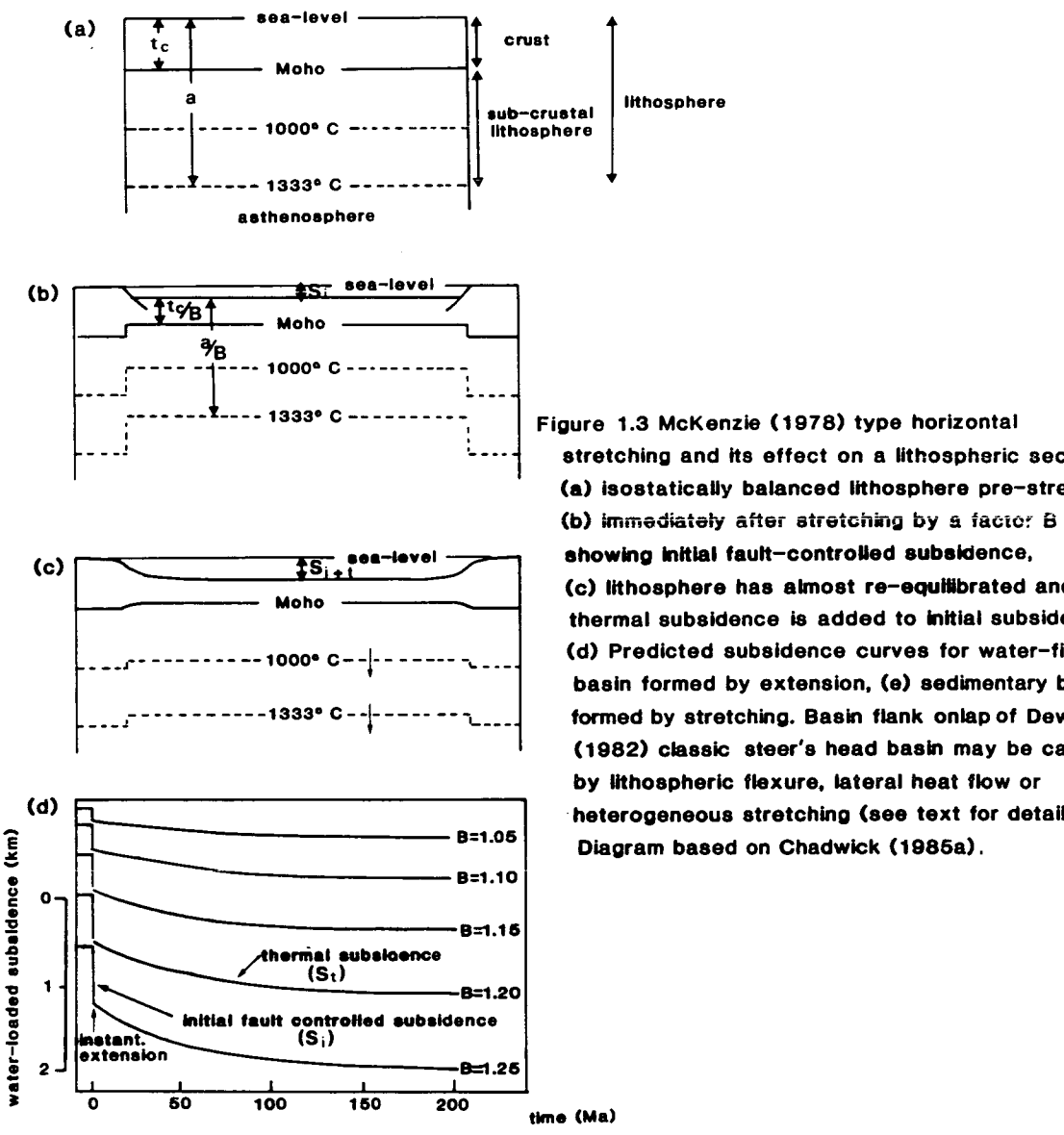

Figure 1.3 McKenzie (1978) type horizontal stretching and its effect on a lithospheric section: (a) isostatically balanced lithosphere pre-stretching, (b) immediately after stretching by a factor β showing initial fault-controlled subsidence, (c) lithosphere has almost re-equilibrated and thermal subsidence is added to initial subsidence. (d) Predicted subsidence curves for water-filled basin formed by extension, (e) sedimentary basin formed by stretching. Basin flank onlap of Dewey's (1982) classic steer's head basin may be caused by lithospheric flexure, lateral heat flow or heterogeneous stretching (see text for details). Diagram based on Chadwick (1985a).

replacement of light crustal material at depth by denser mantle material. This phase of subsidence is accompanied by crustal faulting and is generally termed the initial or fault phase (Figure 1.3). Thinning also elevates the lithospheric isotherms resulting in a second, thermal subsidence phase due to the density increase associated with the relaxation of the perturbed isotherms during subsequent cooling (Figure 1.3). The thermal subsidence phase is characterized by an exponentially decaying subsidence rate of the type previously described by Sleep (1971). Progressive basin flank onlap, the horns of Dewey's (1982) classic "steer's head" basin (Figure 1.3(e)), may be caused by thermal relaxation of the elevated isotherms resulting in increasing lithospheric flexural rigidity and hence increasing wavelength of flexural response.

McKenzie's (1978) model remains the foundation of modern extensional basin analysis although several modifications have been proposed. The most important of these are discussed below.

1.4.3.2 Finite Extension and Lateral Heat Flow

Jarvis and McKenzie (1980) and Cochran (1983) examined the effects of finite rift duration. If the lithosphere is able to thermally relax during extension then some of the thermal subsidence will be "transferred" to the initial subsidence phase which will increase in magnitude at the expense of the thermal phase (Figure 5.4). However, Jarvis and McKenzie (1980) showed that for a rift duration less than $60/\beta^2$ (27Ma for a β-factor of 1.5, 15Ma for a β-factor of 2) the difference between the subsidence paths predicted by instantaneous and finite rifting is negligible. Cochran (1983) showed that lateral heat flow out of the zone of elevated isotherms also decreases the magnitude of post-rift subsidence in the rift axis by transferring heat to the basin flanks. The unfaulted basin flanks will be elevated, in a manner similar to that invoked by Sleep (1971), due to heating without accompanying crustal thinning. Erosion of the elevated basin flanks followed by cooling and sediment loaded subsidence may also produce the horns of the classic "steer's head" basin (Figure 1.3(e)).

1.4.3.3 The "Extension Problem" and Heterogeneous Extension

Following thermal re-equilibration of the lithosphere after stretching isostatic considerations show that the only factor which controls the total amount of subsidence is the magnitude of crustal thinning or extension. Many sedimentary basins and passive margins show less crustal extension than would be predicted from their observed subsidence as tested by boreholes (e.g. Royden and Keen, 1980; Sclater et al, 1980; Chenet et al, 1982; Bessis, 1986; Hegarty et al, 1988). Two-layer, or heterogeneous stretching has been invoked to account for this phenomenon. Excess stretching of the sub-crustal lithosphere may cause greater subsidence than that predicted by homogeneous extension if, like Sleep's (1971) thermal hypothesis, it generates initial uplift and erosion (Figure 1.4(c)). In this case the total magnitude of subsidence will be determined by the crustal thinning caused by both extension and supracrustal erosion. Without erosion excess thermal perturbation of the upper mantle simply reduces the magnitude of initial subsidence and increases the magnitude of thermal subsidence (Figure 1.4(b)).

Unless there is a dynamic heat input into the upper mantle a space problem is associated with excess thinning of the sub-crustal lithosphere over that of the crust. Rowley and Sahagian (1986) and White and McKenzie (1988) argued that although the stretching in the two layers may be differently distributed it should be of the same total magnitude. It is generally considered that extension in the ductile sub-crustal lithosphere will be distributed over a larger area than that in the brittle crust (Rowley and Sahagian, 1986; Kusznir et al, 1987; White and McKenzie, 1988). Hence balanced detached two-layer stretching may account for flank onlap as the basin margins, which were originally uplifted due to excessive sub-crustal extension, subside, but it can not account for subsidence exceeding that predicted by crustal thinning (Figure 1.4(d)).

Discrepancies between apparent extension of the crust and the amount of subsequent subsidence may be due to the limited resolution of seismic reflection data and/or the geometrical simplicity of summing-

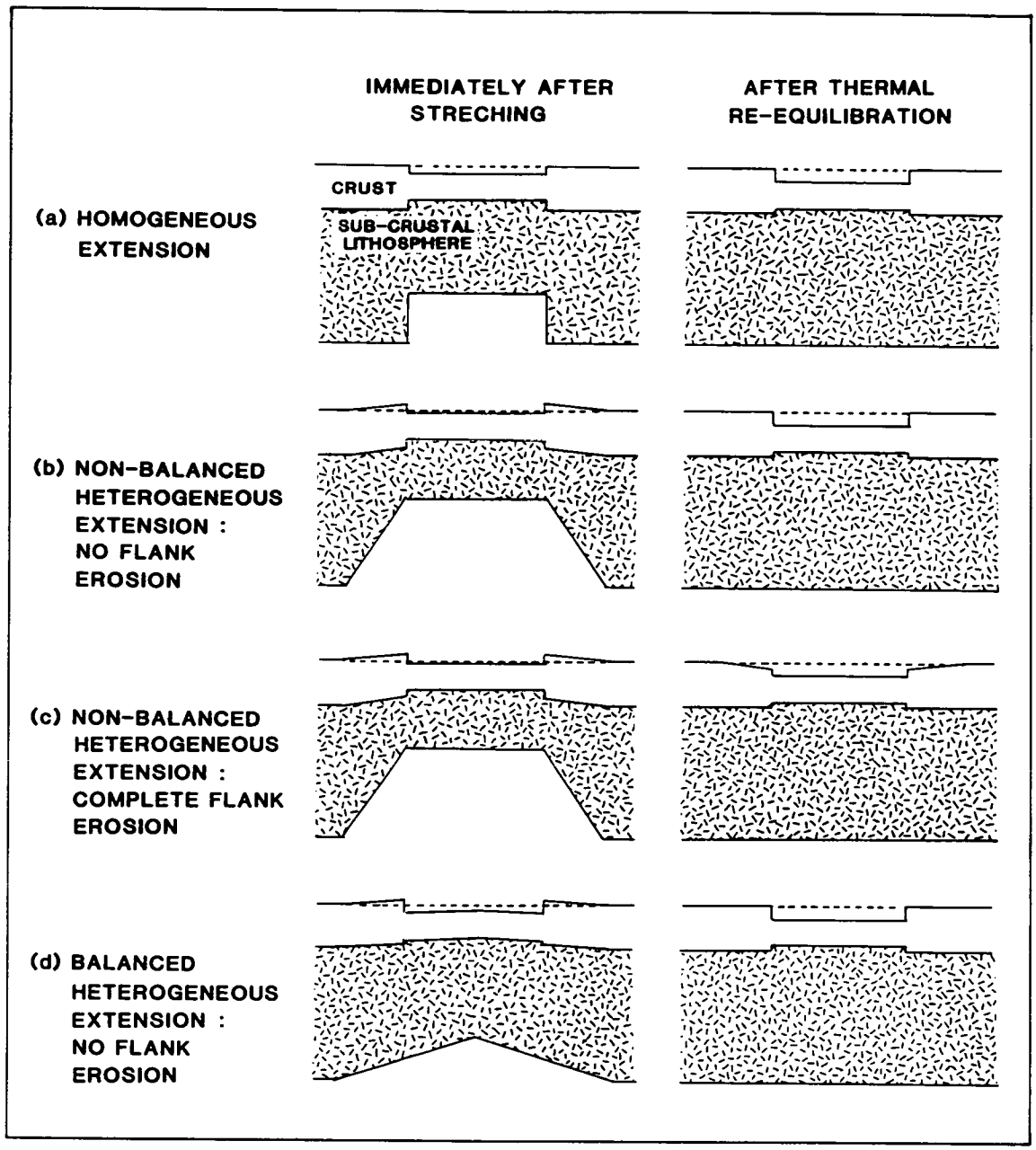

Figure 1.4 A comparison of the effect of different extensional mechanisms on a lithospheric section immediately after stretching and after thermal re-equilibration. In all cases Airy isostasy assumed and crustal stretching is as in homogeneous extension. N.B. Crustal thinning whether by extension or supracrustal erosion is the only factor which determines the total magnitude of subsidence.

the-heave type estimates of extension. Deformation at a scale not resolved by the seismic data, the blanketting effect of salt (Shorey and Scalter, in press), extension out of the plane of section, pure shear of the sediments (bed thinning), non-vertical collapse of the hanging wall (White et al, 1986) and low angle faulting (Shorey and Sclater, in press) may all result in extension being greater than that apparent on seismic reflection data. Until all these, and possibly other factors can be quantified, debate will continue as to whether basins such as the Viking Graben can (e.g. White, 1988) or can not (e.g. Ziegler and Van Hoorn, in press) be explained purely in terms of extension.

1.4.3.4 Simple and Mixed Shear Extension

Wernicke (1981) and Wernicke and Burchfiel (1982), looking principally at the Basin and Range province of the western United States, suggested that extension was accommodated along major, low angle faults which penetrate the entire crust (Figure 1.5). In the model, further developed by Wernicke (1985), extension in the crust is laterally displaced, along the detachment, from that in the upper mantle. Detailed quantification of the simple shear process was carried out by Mudford (1987), but the essential difference from the pure shear model is that thermal uplift and subsequent subsidence is laterally displaced from the fault-controlled basin (Figure 1.5).

Coward (1986) proposed that the pure and simple shear models were end members of a spectrum of lithospheric responses to extension and that sedimentary basins could exhibit a corresponding spectrum of superposed, partially displaced and totally displaced fault and thermally controlled subsidence.

Considering deep seismic reflection data, such as that acquired by BIRPS, Beach (1987) applied the simple shear model to north-west Europe. The resulting linked tectonic model elegantly explains, by compressional reactivation of former extensional faults, the preferential uplift of previous sedimentary basins over surrounding lows (Figure 7.6). However, detachments are not often seen to displace the Moho as required by the crustal simple shear model. Consequently

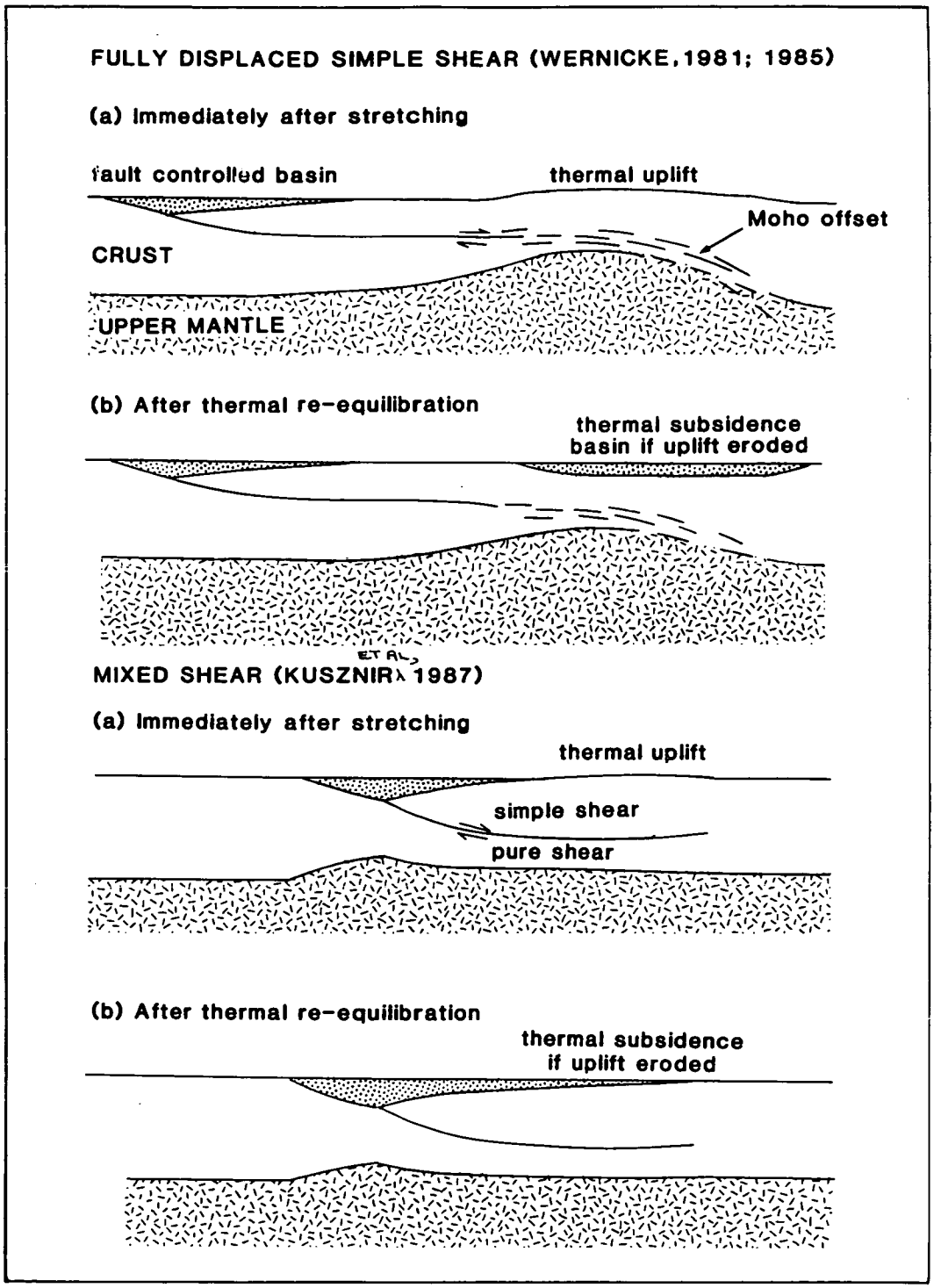

Figure 1.5 A comparison of simple shear and mixed shear extensional mechanisms. In the mixed shear model pure shear is more widely distributed than simple shear and the response is similar to that of partially displaced lithospheric simple shear.

Kusznir et al (1987) and Klemperer (1988) suggested a mixed shear extensional mechanism (Figure 1.5). In their models the upper or whole crust deforms by simple shear along faults which sole out in rheologically induced horizontal detachments either within or at the base of the crust. Beneath the detachment level pure shear processes dominate. In subsequent chapters pure heterogeneous and mixed shear deformations are generally assumed to detach at the Moho and deformations are considered either to affect the crust or the sub-crustal lithosphere. It is, however, noted that intra-crustal rheological detachments may occur (Kusznir et al, 1987).

1.4.4 Lithospheric Compression

Lithospheric compression will cause crustal uplift analogous to extension-driven subsidence (e.g Chadwick, 1985a; Murrell, 1986). Compression-driven uplift, and modifications to the basic hypothesis comparable to those applied to McKenzie's (1978) simple stretching model are discussed in Chapter 7. As with extension-driven subsidence, compression-driven uplift allows vertical motions to be placed in the context of widely accepted horizontal lithospheric movements.

1.4.5 Density Increases in the Lower Crust: Metamorphism and Igneous Intrusion

Density increases in the lower crust caused by metamorphism or igneous intrusion may cause crustal subsidence and sedimentary basin formation without crustal thinning. Falvey (1974) and Falvey and Middleton (1981) suggested that the high temperatures associated with continental separation could cause greenschist facies rocks in the lower crust beneath a passive margin to be metamorphosed to amphibolite facies with an associated density increase. Royden et al (1980), citing the dyke swarms of the east Greenland margin, suggested that cracking of the continental lithosphere and the intrusion of dykes of dense ultrabasic or basic mantle material could cause crustal subsidence.

A number of related mechanisms of lower crustal density increase have been proposed (e.g. Beloussov, 1960; Haxby et al, 1976). However, such a high density layer in the lower crust will have a correspondingly high seismic velocity and should be apparent on seismic refraction data. Falvey and Middleton (1981) related such a high velocity layer under the Queensland Plateau to their metamorphism hypothesis and White et al (1987) observed a similar layer under the north-west British continental margin associated with deep igneous processes. The velocity structure of the Western Approaches Trough and its adjacent continental margin does not support the presence of underlying anomalously dense, high velocity lower crustal material (Avedik et al, 1982; Ginzburg et al, 1985).

1.4.6 Lower Crustal and Asthenospheric Flow

Bott (1971) suggested that creep of lower crustal material driven by the unequal topographic loading across a passive margin may cause subsidence of that margin. This mechanism can not, however, readily account for the subsidence of a shelf basin aligned approximately perpendicular to the margin such as the Western Approaches Trough.

Sloss and Speed (1974) argued that widespread variations in the rate of flow of melt from continental to oceanic asthenosphere could cause vertical crustal movements. Periodic trapping of melt beneath continents causes uplift, while draining causes deflation of entire cratonic areas and an increase in the rate of sea-floor spreading. This model has received little attention, perhaps because it can not be readily tested by geological or geophysical observation. Furthermore, it implies similar behaviour over whole cratonic areas and can not account for the observed intra-basinal variations in the timing and magnitude of vertical crustal movements in the Western Approaches Trough.

1.4.7 Conclusions

Following the above discussion Chapters 4,5,6,7 and 8, which discuss the processes responsible for driving vertical crustal movements in the Western Approaches Trough, concentrate on the effects of thermal

changes, changes in the thickness of the crust (extension and supra-crustal erosion) and gravitational loading and unloading. These are generally discussed within the framework of local, Airy isostasy.

CHAPTER 2

GEOLOGY OF THE WESTERN APPROACHES TROUGH

2.1 INTRODUCTION

The geology of the Western Approaches Trough is described in the light of both published and previously unreleased data. Figure 2.1 (foldout) is a borehole correlation of nineteen exploration wells in the British sector of the basin and three wells in the French sector. Figure 2.2 (foldout) is a correlation of the Deep Sea Drilling Project (DSDP) wells on the northern Bay of Biscay margin (Leg 48) and Goban Spur (Leg 80). Interpretations from commercial and British Institutions Reflection Profiling Syndicate (BIRPS) reflection seismic lines are also included. Gravity and magnetic data have been utilized where they elucidate the subsurface geology of the basin. Appendix A summarizes the database for the project. Published information from the surrounding areas has also been incorporated where appropriate.

This chapter provides the necessary geological framework for the following chapters on the tectonic evolution of the area, and concentrates on pertinent geological problems. Additional lithological, biostratigraphical and geochemical data, may be found in the British Geological Survey offshore regional geology report on the area (Evans et al, in press).

2.2 DEEP AND MIDDLE CRUST

This section describes the crust beneath proven Armorican and Variscan basement, as inferred from deep seismic data.

The BIRPS South West Approaches Traverse (SWAT) profiles 6,7, 8 and 9 and Western Approaches Margin (WAM) profile were shot over or near the Western Approaches Trough (Appendix A). In general a relatively seismically transparent upper crust is underlain by a well developed zone of sub-horizontal reflectors within the lower crust, from 6 to 10s two-way-time (TWT) (Figure 2.3). There is an extensive literature on the possible origin

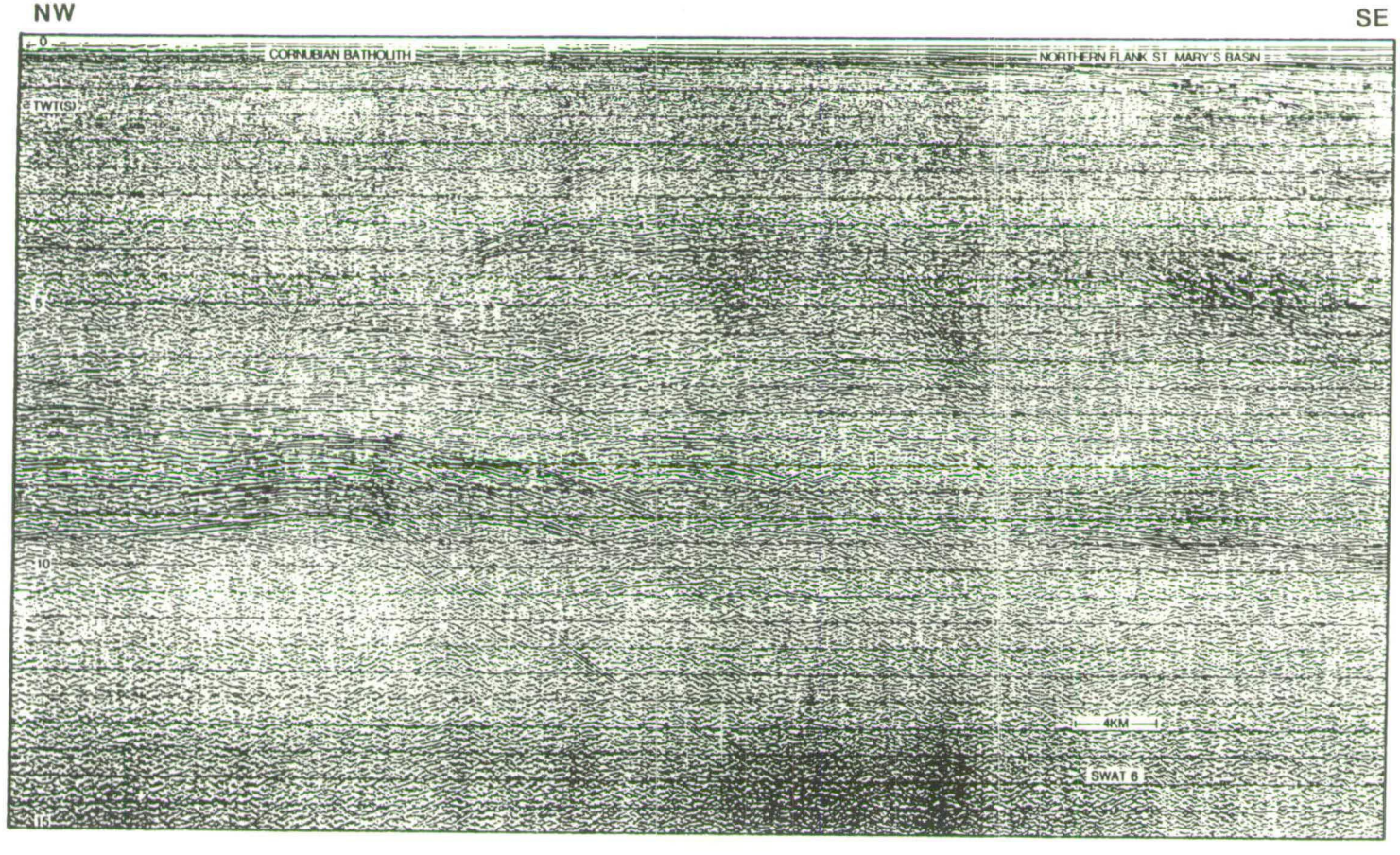

Figure 2.3 BIRPS SWAT line 6 over the Cornubian batholith and the northern flank of the St. Mary's Basin. Under the batholith lower crustal reflectivity is well developed between 7 and 9s TWT, and unusually shallow lower crust-type reflections occur at 3.5 to 4.5s TWT. Under the St. Mary's Basin lower crustal reflectivity occurs between 8 and 10s TWT, the events around 4 to 6s TWT are associated with the offshore extension of the Carrick Thrust (Chapter 4).

of these lower crustal reflectors, and an attempt has been made to summarize this in Table 2.1.

The WAM line was shot across the continental shelf to the north of the Western Approaches Trough, and onto oceanic crust (Appendix A) in order to test the hypothesis that the origin of the lower crustal reflections is in some way related to extension. If related to extension through lithological differentiation (Table 2.1, 1) or strain fabrics (Table 2.1, 2) they should increase in density across the progressively thinned continental slope from the shelf edge to the ocean basin. In spite of processing problems, no such relationship is apparent (Hobbs et al, 1987).

Although the WAM line failed to show an unequivocal link with extension, lower crustal reflectivity is related to geological age and heat flow (Klemperer and the BIRPS group, 1987; Trappe et al, 1988). Under continental shields reflectivity is generally poor, whilst Caledonian and Variscan provinces (such as the Western Approaches Trough) show strong reflecting lamellae in the lower crust. Kusznir and Park (1987) and Trappe et al (1988) proposed that low viscosity, weak zones were developed in the lower crust, particularly of younger, warmer terranes. Sub-horizontal reflecting layers may be generated or enhanced by the smoothing out of inhomogeneities such as those cited in Table 2.1 in the warmer, ductile lower crust of younger terranes. Hence, the top of the reflective lower crust may represent a transition between the brittle, unreflective upper crust and the ductile, reflective lower crust (Chadwick, 1986). Such a rheological boundary will have important consequences on the behaviour of crust under extension or compression (Section 1.4.3.4).

The lower crustal events terminate at approximately 10s TWT under the Western Approaches Trough. Under the Cornubian Batholith on SWAT 6 this level rises to approximately 9s TWT (Figure 2.3) and is coincident, at an average crustal velocity of $6kms^{-1}$, with Bott et al's (1970) 27km estimate of Moho depth from seismic refraction data. Refraction data in the North Sea and wide angle reflection data in northern France have similarly shown the base of the reflective lower crust to represent the Moho (Barton et al, 1984; Bois et al, 1986). The apparent rise, in two-way-time, of the Moho under the Cornubian Batholith may be due to the absence of the low velocity sediments present in the Western Approaches Basin. Indeed, Warner (1987) demonstrated that the crustal thinning associated with extensionally-formed

Table 2.1 Origin of seismic reflections from the lower crust with selected references.

1. Primary Lithological Variation	
(i) Sedimentary/Metamorphic	
Sedimentary layering now deeply buried and metamorphosed, possibly due to overthrusting or subduction	Brown et al (1986)
(ii) Metamorphic	
Layered metamorphic terrane	Hurich and Smithson (1987)
(iii) Igneous	
(a) Volcanic layering now deeply buried and metamorphosed, possibly due to overthrusting or subduction	Brown et al (1986)
(b) Layered basic/ultrabasic intrusions	Meissner (1973)
(c) Basic sills	McKenzie (1984)
(d) Lenses of (partial) melt	Hale and Thompson (1982)
2. Strain Fabrics	
(i) Rotation of primary lithologic variation into horizontality and parallelism generating or improving reflections	Phinney and Jurdy (1979)
(ii) Primary strain fabrics such as cracks, cataclasites and mylonite zones	Jones and Nur (1984)
3. Fluid-rich horizons possibly combined with 1 and/or 2	Hall (1986)
4. Geometrical effects modifying the seismic response of 1 and/or 2 and/or 3	
(i) Reflections from out of the plane of section	
(ii) Undulating single horizon producing several events	both Blundell and Raynaud (1986)
(iii) Interference patterns	
(a) Constructive interference between horizontal lamellae	Fuchs (1969)
(b) Focussing by lens-shaped bodies	Reston and Blundell (1987)
5. Artefacts of the Seismic Method	
(i) multiples	
(ii) side swipe	
(iii) diffractions	
(iv) reflected refractions	
(v) processing induced	

basins was almost exactly compensated for, in time, by the low velocity sedimentary basin-fill. Hence, crustal thinning will only be apparent on depth converted seismic data. The depth to the Moho in the area as derived from deep seismic and gravity data is discussed in Chapter 8.

The TWT to the top of the zone of lower crustal reflectivity rises by about 3s under the offshore extension of the Cornubian Batholith on SWAT 6 (Figure 2.3). Similar observations have been made under the Haig Fras Batholith on SWAT 5, and the granites off the coast of France at the southern end of SWAT 10 and 11. This effect may be caused by a higher seismic velocity in the granite, or lower attenuation allowing weaker events to be imaged. Alternatively, it may be a real phenomenon such as an increased density of fluid filled veins and microcracks associated with granite emplacement, as seen in the exposed granite aureole of south-west England.

Several sub-Moho events can be seen on the unmigrated SWAT profiles, although most of these are diffactions. After 2-D migration of the line drawings only one event remains in the vicinity of the Western Approaches Trough, under the Plymouth Bay Basin on profile 8 (BIRPS and ECORS, 1986). This may be a continuation of the reactivated Variscan thrust underlying the Plymouth Bay Basin and, like the Flannan structure seen on the BIRPS DRUM (Deep Reflections from the Upper Mantle) profile off north-west Scotland, may be a tectonic discontinuity or shear zone in the upper mantle (McGeary and Warner, 1985).

2.3 BASEMENT

A heterogeneous suite of Palaeozoic, largely Deveno-Carboniferous rocks deformed during the Variscan orogeny, form the Cornubian Massif to the north of the Western Approaches Trough. In contrast the Armorican Massif, south of the Western Approaches Trough, is composed of Proterozoic rocks, deformed and metamorphosed prior to and again during the Variscan orogeny. Under the Western Approaches Trough itself, however, the distinction between these two basement types becomes less clear.

Well and seismic data allow the basement under the Western Approaches Basin to be studied in some detail, and it is described in Section 2.3.2. In

contrast, only one available well penetrated basement under the South-West Channel and Brittany Basins. Section 2.3.1 briefly describes the Armorican basement as seen in north-west France and the Channel Islands and believed to underlie the Brittany and South-West Channel Basins.

2.3.1 Armorican Basement

The oldest rocks of the Armorican Massif are pre-900Ma Pentevrian granodioritic and quartz-dioritic ortho-gneisses, schists and amphibolites. The monzonitic gneisses recovered at the base of well Lennket-1 (Table 2.2) are speculatively compared with the Pentevrian of onshore north-west France. The Pentevrian orogeny produced an angular unconformity which separates these rocks from the overlying Brioverian series. The Brioverian comprises somewhat less metamorphosed shales and siltstones with subordinate sandstones and conglomerates deposited between 700 and 900Ma. The Brioverian rocks were deformed during the late Precambrian-Cambrian Cadomian orogeny with associated granite intrusion and volcanism. In northern and central Armorica the Brioverian is overlain with angular unconformity by Cambrian to Devonian Palaeozoic shelf sediments. There is no evidence of any Caledonian deformation, although igneous activity continued through the early Palaeozoic with further granite intrusion (concentrated around 450-460Ma) and volcanism (Matthews et al, 1980). From Devonian times the entire sequence was involved in the Variscan orogeny.

The interaction of orogenic phases produced the rather intermediate structural grain of the Armorican Massif (Figure 2.4). In the northern part, from Brest to Cherbourg, the structural trend is north-east to south-west. This is the Variscan trend and is similar to the structural trend in the Ardennes, the Rheinisches Schiefergebirge and south-west England. The north-west to south-east structural trend of the southern part of the Armorican Massif (Figure 2.4) can be followed into the Massif Central and is termed the Armorican direction. Both directions are mainly a product of the Variscan orogeny, though earlier foldbelts may have followed the same general lines (Rutten, 1969).

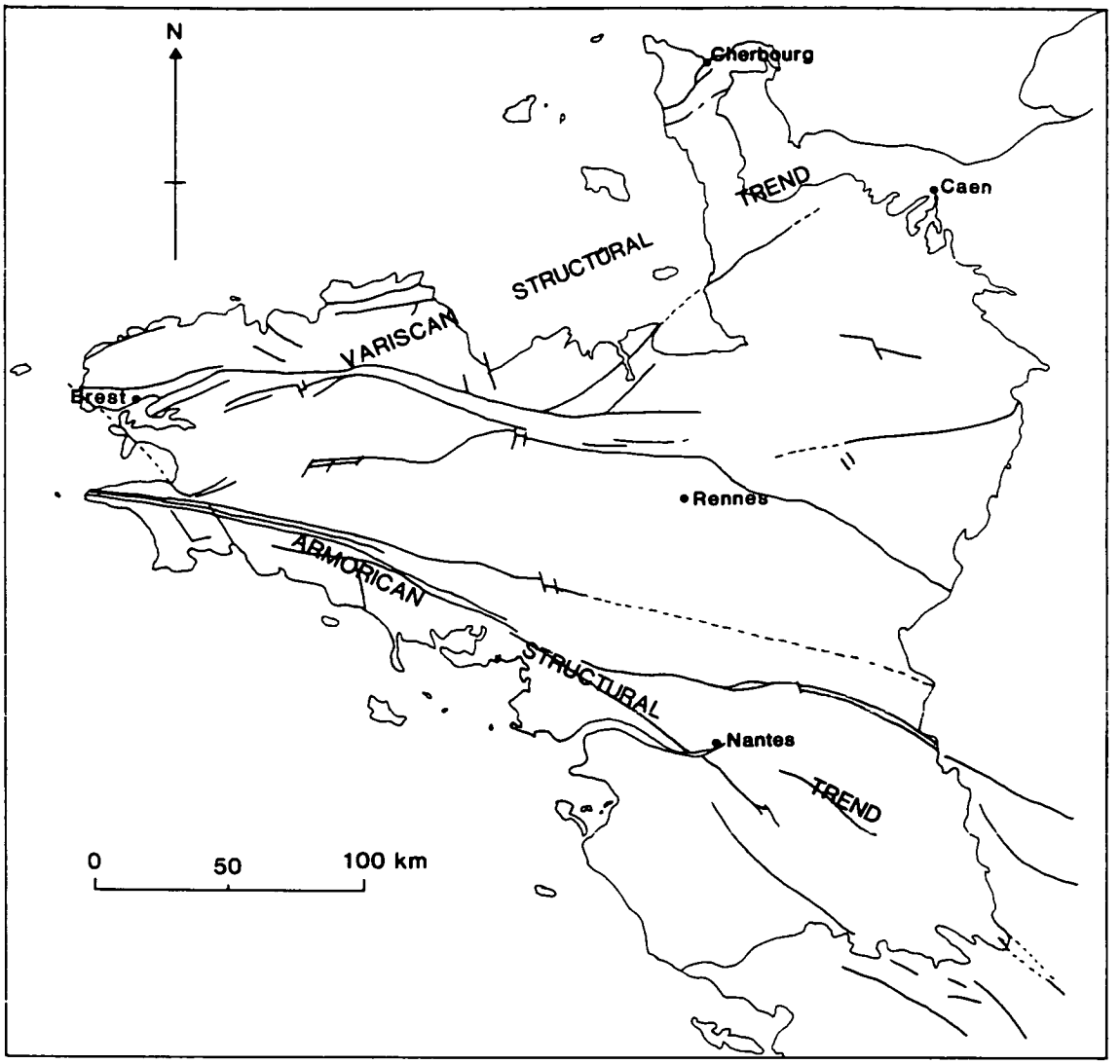

Figure 2.4 Structural trends of the Armorican Massif (modified from Matthews et al, 1980).

2.3.2 Cornubian Basement

Cornubian basement is defined as the pre-Permian rocks deformed only in the Variscan orogeny which form the Cornubian Massif and extend southwards under the Western Approaches Basin. There are insufficient data from the offshore record (Table 2.2) to fully interpret the basement geology of the basin, but combined with seismic data it may be reconciled with our more detailed knowledge of the Variscan foldbelt as a whole, and more specifically the onshore geology of south-west England.

Table 2.2 Pre-Permian basement rocks recovered from the Western Approaches Trough and the adjacent continental slope. Appendix A shows well and dredge locations.

Location		Lithology	Age
73/2-1	64m	brecciated conglomerate and (?) amphibolite	Cambrian
83/24-1	140m	sandstone, mudstone and slate	(? Devonian-) Carboniferous
86/18-1	110m	indurated shale	late Devonian-Carboniferous
87/12-1	324m	limestone (above)	middle Devonian
	140m	sandstone and mudstone	middle Devonian
Lennket-1	72m	monzonitic gneiss	(?)Pentevrian
SLS 66A	65m	phyllite with arenaceous bands	Devonian-Carboniferous
DSDP 548	21m	shale and quartzite	middle Devonian
DSDP 549	37m	sandstone	Devonian-(? Carboniferous)
SU 01 11	dredge	chlorite- and mica-schist	(?) Palaeozoic
CH 67 08	dredge	limestone	Carboniferous (? Visean)
CH 67 10	dredge	limestone	Carboniferous (? Visean)
CH 67 18	dredge	limestone	Carboniferous (? Visean)
	dredge	sandstone	(?) Palaeozoic
	dredge	schists	(?) Palaeozoic

2.3.2.1 Tectonic Setting

Although a variety of detailed models of the tectonics of the Variscan foldbelt have been proposed, the broad picture is of northward movement of Gondwanaland relative to northern Europe and North America closing a Rheic, or palaeo-Tethyan ocean of debated size and continuity and deforming the northern plate(s).

There are many published models of the Variscan evolution of south Cornwall, but there is a consensus that the rocks of the Lizard Peninsula represent a thrust ophiolite mass (Strong et al, 1975; Kirby, 1979; Floyd, 1984). The Lizard Complex comprises an upper sheet containing all the elements of classic ophiolite stratigraphy except pillow lavas, tectonically overlying a lower sheet of ultramafics welded to a sole complex of amphibolites and metasediments (Badham, 1982). This ophiolite may have come from a major ocean basin, possibly the Rheic or palaeo-Tethyan ocean itself (e.g. McKerrow and Ziegler, 1972; Scotese et al, 1979; Cocks and Fortey, 1982), or from a back arc basin with major ocean subduction occuring to the south (e.g. Leeder, 1982; Floyd, 1982; 1984), or from an extensional basin in an intracontinental transform system (e.g. Badham, 1982; Sanderson, 1984; Barnes and Andrews, 1986).

Whatever the specific affinity of the Lizard ophiolite, it has long been suggested that it was emplaced by thrusting (e.g. Hendriks, 1939). Coward and McClay (1983) described the evolution of south Cornwall in terms of two major northward verging thrust nappes. Day and Edwards (1983) suggested that dipping events observed on seismic data offshore south of Cornwall represented similar, ENE-WSW striking, south dipping Variscan thrusts, and these were subsequently correlated with thrusts on land by Leveridge et al (1984), who again described the evolution of south Cornwall in terms of a series of such stacked nappes (Figure 2.5). The thrusts were subsequently shown to be extensive throughout the basement of the Western Approaches Basin (Hillis and Day, 1987; Chapter 4).

As the thrusts moved northwards a series of foreland basins were sequentially developed and deformed ahead of them (Figure 2.5(b)). It was in deep water basins such as these that the turbidite and fan deposits of the early to middle Devonian Gramscatho Group and the quieter water slates of the middle to late Devonian Mylor Group of south Cornwall were deposited

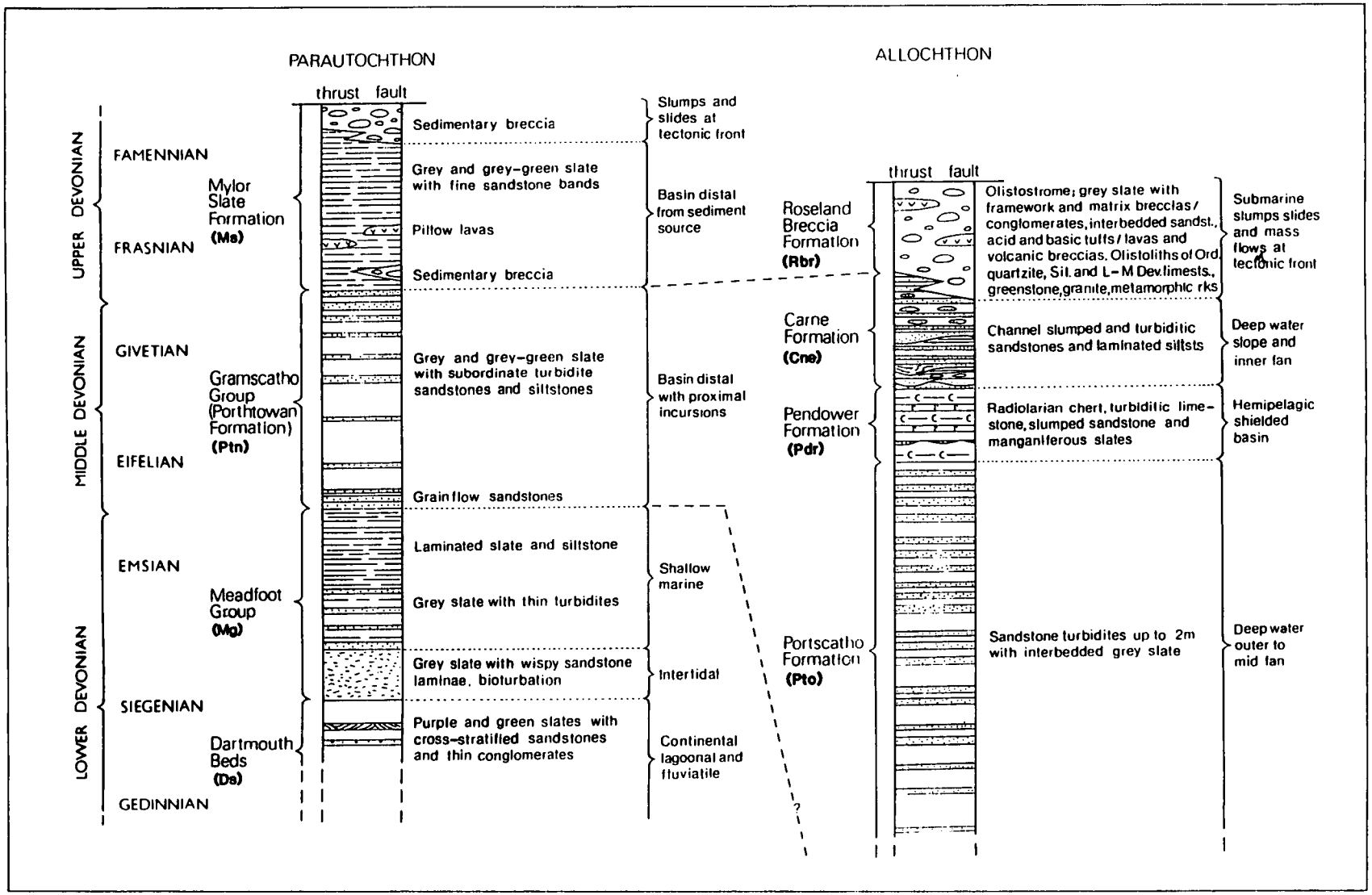

Figure 2.5(a) Lithostratigraphic sequences of south Cornwall (Holder and Leveridge, 1986)

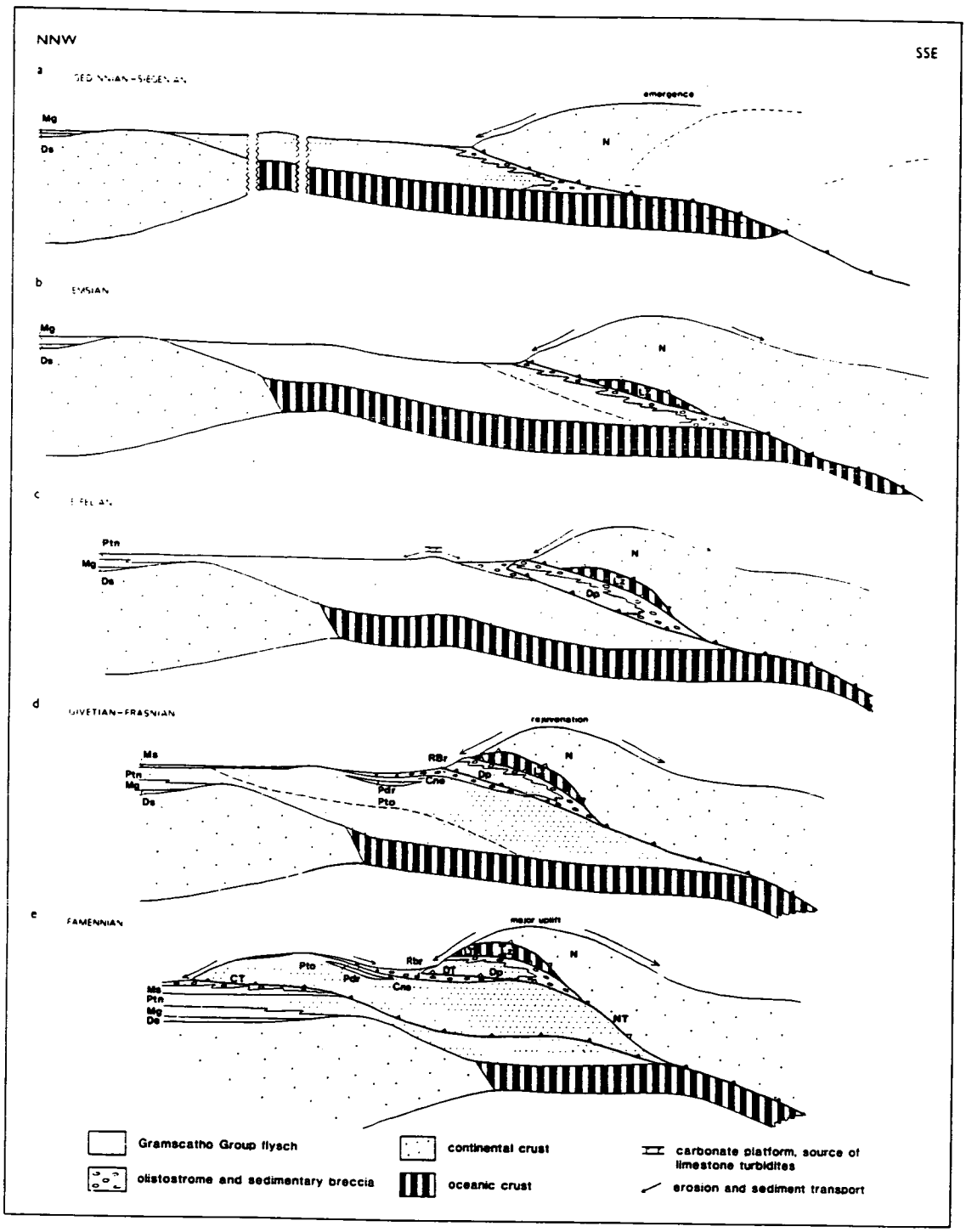

Figure 2.5(b) A model for the tectonic evolution of south Cornwall (Holder and Leveridge, 1986). Lithostratigraphic units as Figure 2.5(a). Tectonic units: Ck, Carrick Nappe, CT, Carrick Thrust, Dp, Dodman Nappe, DT, Dodman Thrust, LT, Lizard Thrust, Lz, Lizard Nappe, N, Normannian Nappe, NT, Normannian Thrust

(Figures 2.5 and 2.6). Sedimentary structures in these Groups suggest that the source was from the south (Wilson and Taylor, 1976), possibly the advancing thrust nappes. These Groups were overthrust by the Lizard Complex, and then themselves thrust northwards as the deformation front progressed (Figure 2.5(b)). The thrusts were driven by the movement of Gondwanaland relative to northern Europe during the Devonian and Carboniferous, but the depositional setting of the sediments in the thrust nappes may either have been an orthogonally closing basin of reasonable lateral continuity (e.g. Holder and Leveridge, 1986), or transpressional, following transtensional formation of a localized basin (e.g. Badham,1982; Barnes and Andrews, 1986).

While Armorican and Cornubian basement may be readily distinguished in the respective massifs the distinction becomes somewhat blurred under the intervening Western Approaches Trough. Beneath the sedimentary cover well 73/2-1 in the Melville Basin, which lies above a Variscan thrust, penetrated Armorican-type breccciated conglomerates underlain by altered amphibolite radiometrically dated at 570±10Ma. Like the Lizard Complex, and other allochthonous material this unit was transported northwards into the "Cornubian province" as part of the northward moving nappes. Indeed, Armorican-type (?)Precambrian lithologies occur at Eddystone Reef (Edmonds et al, 1975) and as xenoliths in late Devonian basalts near the the Land's End Granite (Goode and Merriman, 1987), while phyllite, schist and granite clasts in the Roseland Breccia Formation of south Cornwall are comparable to the Brioverian and Palaeozoic sequences of Armorica (Holder and Leveridge, 1986).

2.3.2.2 The Offshore Basement Record

The clastic Devonian sediments and metasediments of wells 83/24-1, 86/18-1, 87/12-1A and SLS 66A (Table 2.2 and Figure 2.1) are equivalents of the Gramscatho and Mylor Groups of south Cornwall (Figure 2.5(a)), and may represent similar (?)deep water deposits from the advancing nappes. Investigation of a cored interval of the limestone above these metasediments in well 87/12-1 (Table 2.2 and Figure 2.1), however, reveals a fine-grained carbonate mud containing crinoid debris interbedded with fossiliferous units rich in brachiopod, bivalve, crinoid, coral and

stromatoporoid fragments. This is suggestive of a fore or back reef facies. If in place, the occurrence of these shallow water limestones puts the deep water origin of the underlying clastics into doubt (no cored clastic material is available for sedimentological analysis). However, it supports Edmonds et al's (1975) Devonian palaeogeographic reconstruction of south-west England which shows shallower water facies developed beyond the Gramscatho Group deep water sequence on the south side of the basin (Figure 2.6). The limestones of well 87/12-1 may represent such a shallower water facies developed due to the proximity of the northwardly migrating nappes from which the deeper water facies observed onshore in south Cornwall were being contemporaneously shed. Alternatively, it may be that we are simply seeing a series of discrete terranes emplaced by strike-slip motion (e.g. Badham, 1982; Dewey, 1982; Barnes and Andrews, 1986), and that the present distribution of sedimentary facies cannot be sensibly interpreted in terms of a palaeogeographic reconstruction of south-west England. The undisputed thrust faulting will further confuse palaeogeographic reconstructions.

The Devonian clastics of the DSDP wells on the continental slope (Figure 2.2) are of shallower water affinities (Lefort et al, 1985) than those of the Gramscatho Group and its possible equivalents offshore. They are very speculatively compared (in view of the large distance of correlation, and the possible complications introduced by strike-slip and thrust faulting) with the shallower water facies of the middle Devonian to the north of the Gramscatho Group, such as the Hangman Grits of north Devon and Somerset (Figure 2.6). These fringed the still emergent Old Red Sandstone continent further to the north. Indeed, Lefort et al (1985), considering the samples of Palaeozoic basement from the continental slope, proposed a sandstone ridge to the north-west of a shale and slate basin, with the transition passing close to DSDP 548 in a north-easterly direction. This may be equivalent to the transition from the shallow water Hangman Grits to the deeper water Gramscatho Group (Figure 2.6).

The early Carboniferous shallow water limestones dredged from the continental slope (Auffret et al, 1979 and Table 2.2) are equivalent to early Carboniferous limestones in south-west England (e.g. Edmonds et al, 1975), and were deposited either towards the end of Variscan thrusting (Sanderson, 1984; Barnes and Andrews, 1986), or after the system had locked up (Styles and Rundle, 1984; Holder and Leveridge, 1986).

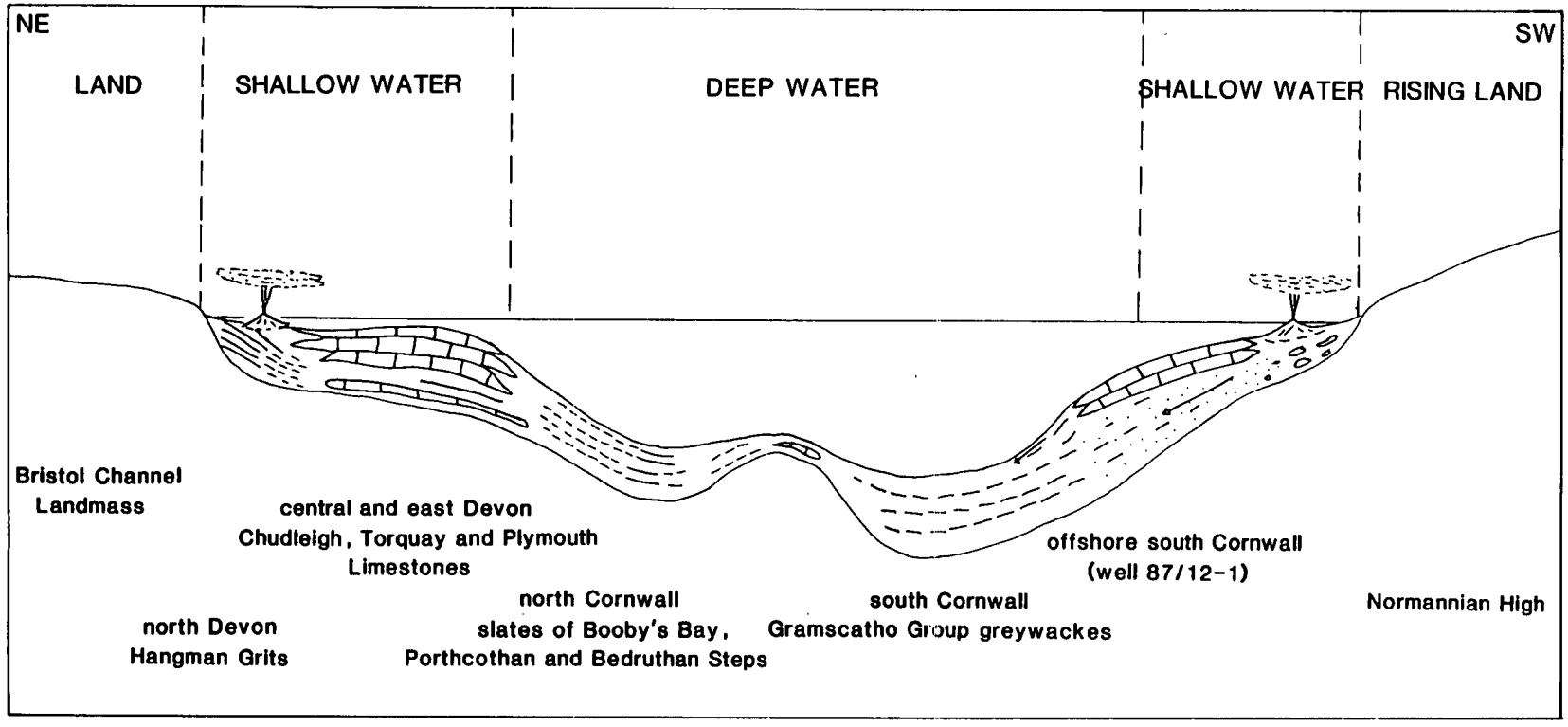

Figure 2.6 Middle Devonian facies model for south-west England and the adjacent offshore area with examples of onshore lithological formations (modified from Edmonds et al, 1975)

The Palaeozoic schists dredged from the continental slope (Table 2.2) occur in close proximity to samples of Permo-Carboniferous granites (Auffret et al, 1979), and are probably contact metamorphosed sandstones and mudstones, rather than Armorican or Lizard Complex type rocks.

2.3.2.3 Structural Trends

The dominant structural trend of the basement is the ENE-WSW direction imparted by the Variscan thrusts (Chapter 4). This trend appears to have controlled the development of the major tectonic elements of the continental shelf from northern Armorica to southern Ireland. The South-West Channel, Brittany, Western Approaches, Haig Fras and Celtic Sea Basins and the Cornubian Massif all follow this trend. In contrast, the limit of Variscan deformation (Variscan Front) has a WNW-ESE trend through southern Britain and Ireland. The present day trend of the Variscan Front is, however, a function of both Variscan structure and later erosion, and may not everywhere represent the same structure level. Hence it does not follow the more precise ENE-WSW trend of individual Variscan structures (thrusts).

In addition to the ENE-WSW striking thrusts, a series of NNW-SSE trending strike-slip faults were developed. Coward and Smallwood (1984), noting the similarity in trend of the NNW-SSE strike-slip faults to the Variscan transport direction in south Cornwall, suggested that they developed synchronously with the thrust faults as lateral ramps linking blocks moving northwards at different rates. Ziegler (1982), however, proposed that the northward moving Variscan system locked up in the late Carboniferous, and as Gondwanaland continued northward a change of relative motion from north to north-west or west occured causing dextral shearing along a system of NNW-SSE trending strike-slip faults. Arthaud and Matte (1977) also argued that these faults were created late in the Variscan orogeny. Whatever their precise origin, together with the ENE-WSW striking thrusts, they impart a strong orthogonal structural grain on the basement. The influence of this structural grain during later basin evolution is discussed in Chapter 4.

2.4 PERMO-CARBONIFEROUS

This section deals with igneous activity in the Western Approaches Trough and surrounding areas during the late Carboniferous and early Permian. This activity was manifested by the intrusion of granite batholiths in the Armorican and Cornubian Massifs and the extrusion of volcanics onshore south-west England and in the Western Approaches Trough itself.

2.4.1 Granite Batholiths

Together with the flanking Variscan metasediments the Cornubian and Haig Fras Batholiths form the Cornubian Massif. The Cornubian Batholith can be traced offshore from exposures in south-west England by an ENE-WSW trending negative Bouguer anomaly associated with the low density granite (Figure 2.7, anomaly A). Granites of similar age have also been dredged from the foot of the continental slope around 48°W 12°N (Auffret et al, 1979). However, gravity evidence for continuous granites between 8°W and those recovered from the foot of the continental slope is less convincing. The gravity low on the shelf west of 8°W (Figure 2.7, anomaly C) is displaced slightly to the south of the trend of the Cornubian Batholith and is at least partially caused by thick salt in the northern Melville Basin (Section 2.5.1).

According to radiometric dating the Cornubian Batholith was emplaced during the latest Carboniferous to earliest Permian, 280-290Ma (Darbyshire and Shepherd, 1985). Onshore it is dominantly composed of quartz, coarse orthoclase, plagioclase and biotite with secondary muscovite. Tourmaline, zircon and apatite are the most common accessory minerals (Edmonds et al, 1975).

The shape of the batholith, as determined by gravity modelling, has varied somehat (Bott et al, 1970; Edwards, 1984a), possibly due to along strike variation. However, it is generally shown to widen from approximately 10km at or near surface to 30-50km at its base which has been fairly consistently placed at 10-12km depth.

Out to about 8°W there is a striking relationship between the spatial extent of the mapped Variscan thrusts (Figure 4.1) and the gravity field,

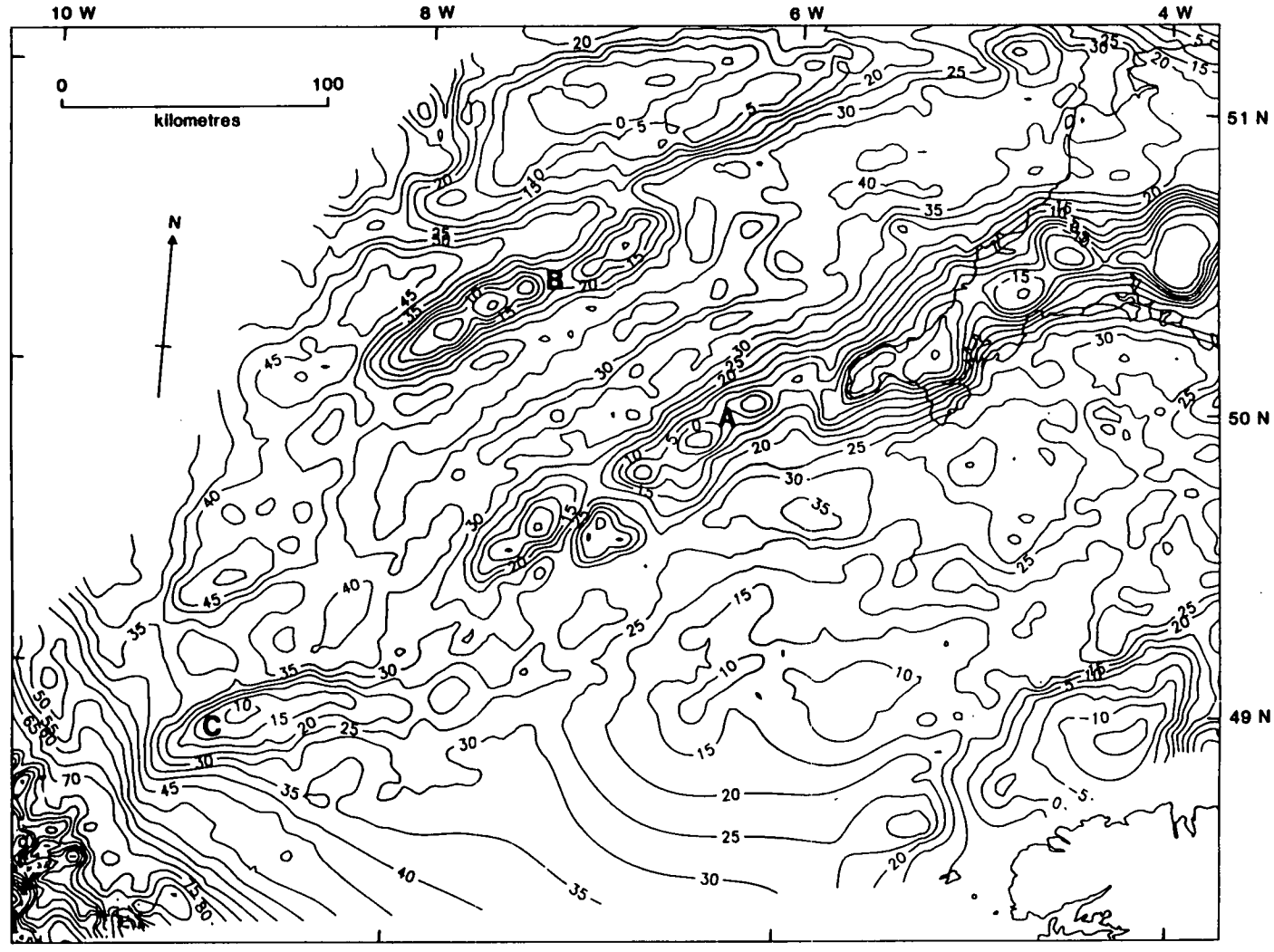

Figure 2.7 Bouguer gravity map, Western Approaches Trough (UTM projection). Lows A and B are caused by the Cornubian and Haig Fras batholiths respectively. Low C is largely due to salt in the northern Melville Basin. The anomalies to the extreme south-west are due to the continental slope effect. Contours are in mgals.

gravity lows defining granites occupying a large area where no thrusts have been mapped. This might be expected since thrusting predates granite emplacement in Cornwall (Shackleton et al, 1982), and presumably also along tectonic strike, offshore in the Cornubian Massif.

The origin of late orogenic granites such as the Cornubian Batholith is often linked to the subduction and partial melting of oceanic crust and sediments lying thereon. The lighter, granitic fraction of the melt rises and is intruded as an acidic batholith in the upper crust. Such an origin would support the existence of an ENE-WSW striking Variscan subduction zone either dipping north from the Western Approaches Basin or south from the Celtic Sea Basin. Alternatively, the granites may have been generated by mantle activity, or by *in situ* partial melting of crust thickened by Variscan compression. However, Shackleton et al (1982) argued that there was insufficient Variscan crustal thickening to account for *in situ* generation by crustal melting.

Whatever its specific origin, the trend of the batholith, which can be traced from 4°W in south-west England offshore to 8°W, and even possibly to the base of the continental slope at 12°W, is consistent with the known NNW closure direction in the area (Coward and McClay, 1983). Its extent suggests greater lateral continuity in the Variscan foldbelt than implied by strike-slip models such as those of Badham (1982) and Dewey (1982).

A separate but parallel batholith, the Haig Fras Batholith, lies to the north of the Cornubian Batholith between 6°W and 8°W. Its seabed outcrop measures some 45 by 15km and it is also associated with a significant gravity low (Figure 2.7, anomaly B). Intruded 277±10Ma (Exley, 1966), the Haig Fras Batholith is of similar age to the Cornubian Batholith and their origins are likely to be closely related.

Variscan granites are also found in the Armorican Massif. They occur as a number of batholiths scattered throughout the Massif, which range in age from 340-290Ma (Matthews et al, 1980).

2.4.2 Volcanics

Extrusive igneous activity in a belt between west Somerset and south Devon, the Exeter Volcanic Series, was broadly contemporaneous with emplacement of the Cornubian Batholith (Miller and Mohr, 1964). Lava types

range from basalts through trachybasalts to rhyolites. They are mostly vesicular and scoriaceous units from 1 to 20m thickness. In some places they are brecciated and contain red sandstone clasts (Durrance and Laming, 1982). Although presently rather insignificant in outcrop the original extent of the volcanics is shown to be much greater by the enormous quantities of volcanic detritus in the overlying Permian red-bed breccias of south-west England. Volcanics have also been proven at the base of the Permo-Triassic succession in the Western Approaches Basin in wells 73/12-1 and 74/1-1 (Figure 2.1). Unfortunately the volcanics recovered from these wells are too heavily altered to be radiometrically dated, and a similar Permo-Carboniferous age is tentatively proposed in view of the recorded igneous activity in south-west England, and indeed the Variscan externides of northern Germany and Poland, at this time (Ziegler, 1982).

The basal 294m of well 73/12-1 passes through extrusive volcanics interbedded with locally derived sediments. Morton (1987) described a cored sample from the base of this sequence as highly altered trachyandesites, and showed that while their geochemistry was grossly similar to the volcanics of south-west England it differed in detail. This was taken to confirm the suggestion of Thorpe et al (1986), deduced from the geochemistry of the volcanics onshore, that there was considerable mantle heterogeneity under south-west England at the time. Morton (1987) also showed that the material from well 73/12-1 possessed geochemical characteristics of subduction zone volcanics, as Thorpe et al (1986) had suggested for the Exeter Volcanic Series. This supports the hypothesis that Variscan subduction occurred in the area.

Well 74/1-1 terminated in 570m of weathered crystalline to microcrystalline tuff interbedded with locally derived sediments and crystalline trachyte which may represent lava flows (Evans et al, in press). No detailed analysis of core material from this well has been undertaken.

Like the Cornubian Batholith, the Permo-Carboniferous volcanics have distinctive geophysical signatures. However, in this instance seismic and magnetic data are more instructive than gravity data. The volcanics appear as short, sub-parallel, high amplitude events on the seismic reflection data (Figure 2.9). As such they are extensive throughout the southern Melville Basin (Figure 2.10) and correlate with a broadly circular magnetic high

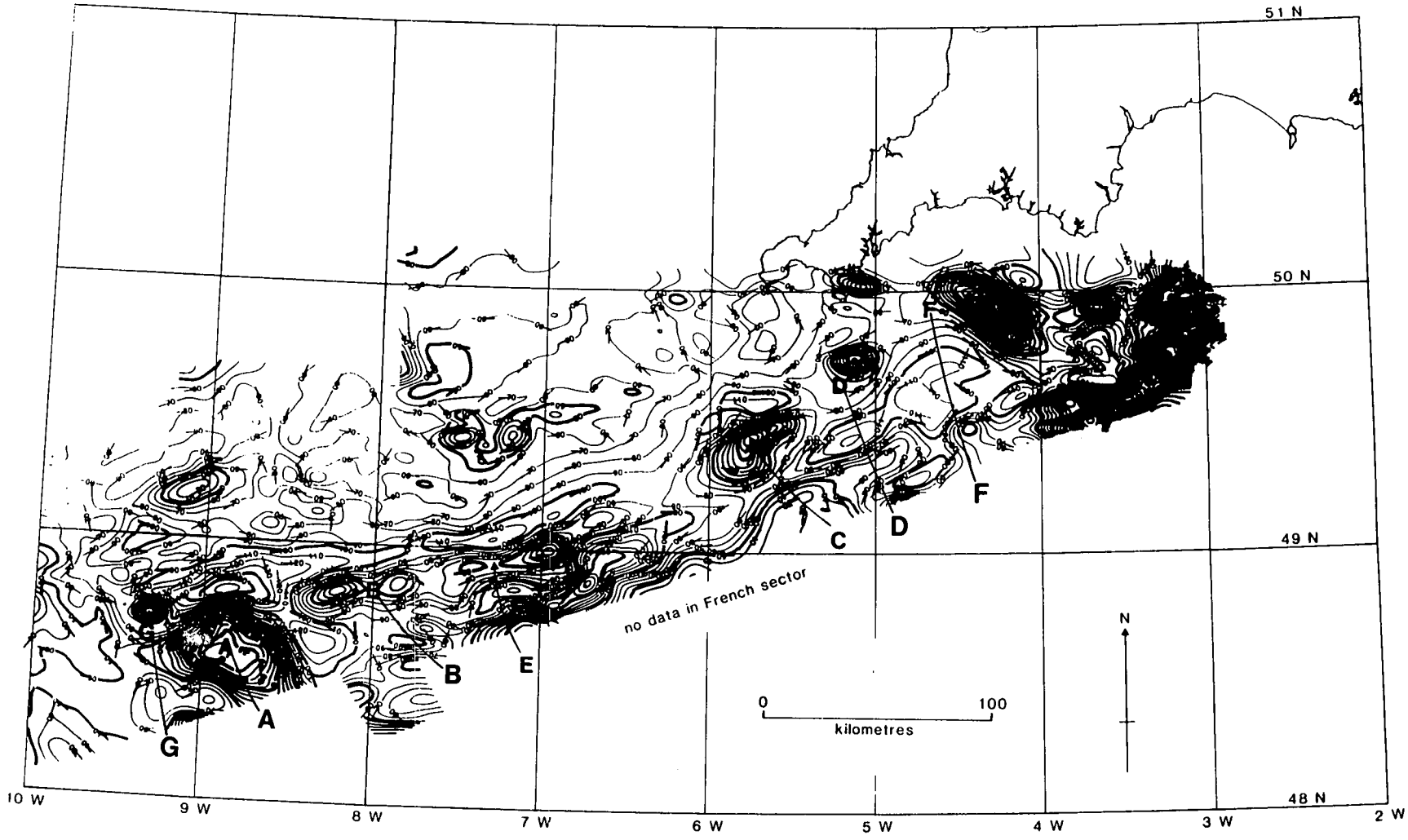

Figure 2.8 Aeromagnetic map, Western Approaches Basin (Evans et al, in press). Contours are in nTeslas. Highs A-F are caused by Permo-Carboniferous volcanics, high G may be caused by a Cretaceous volcanic centre.

(Figure 2.8, anomaly A). The volcanics recovered from well 74/1-1 similarly coincide with a magnetic anomaly (Figure 2.8, anomaly B), in this case trending more axial to the basin. Volcanic-type events can again be seen on the seismic data. Similar magnetic highs and evidence of volcanics on the seismic data can be seen in the southern St. Mary's Basin near wells 86/18-1 and 86/17-1 (Figure 2.8, anomalies C and D). The magnetic anomalies E, in the eastern Melville Basin, and F, in the Plymouth Bay Basin, probably also originate from Permo-Carboniferous volcanics. The ENE-WSW trending magnetic anomaly running along the axis of the Brittany Trough which Lefort (1977) suggested might be due to ophiolites in the basement marking the line of an old suture is more likely to be caused by similar volcanics.

There is a degree of parallelism between the magnetic anomalies generated by the volcanics (Figure 2.8) and the structural grain of the basement as imparted by the Variscan thrusts. The volcanics may, like the granites, have utilized the former thrusts as zones of weakness from which fissure eruptions were fed forming extensive floods.

2.5 PERMO-TRIASSIC

Following its late Carboniferous to early Permian consolidation, of which the Variscan orogeny was a major part, the Pangean supercontinent showed signs of instability during the Permian, and even more so during the Triassic (Ziegler, 1982). This transition from plate convergence to divergence was marked by the development of fault controlled troughs in which a major terrestrial red-bed succession, the New Red Sandstone, was deposited.

Due to differential movement on the faults separating the Western Approaches Basin and the Brittany and South-West Channel Basins the New Red Sandstone is very much more thickly developed in the former area (Figure 1.2). This section thus concentrates on the northern part of the Western Approaches Trough. In keeping with Smith et al (1974) and Warrington et al (1980), the Geological Society correlations of rocks of the Permian and Triassic respectively, a lithostratigraphic correlation of the area is introduced (Figure 2.1). The New Red Sandstone sequence is

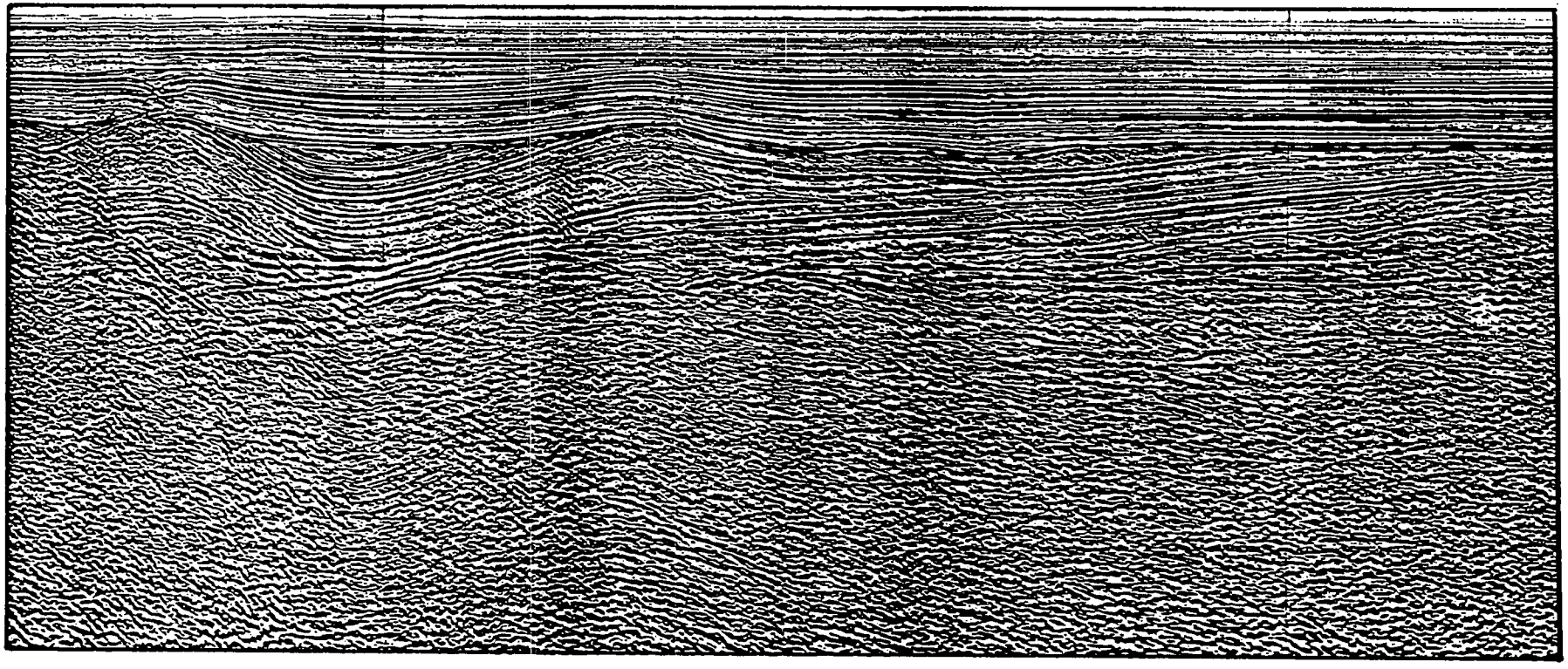

Figure 2.9(a) GECO line through Melville Basin (interpretation on following page).

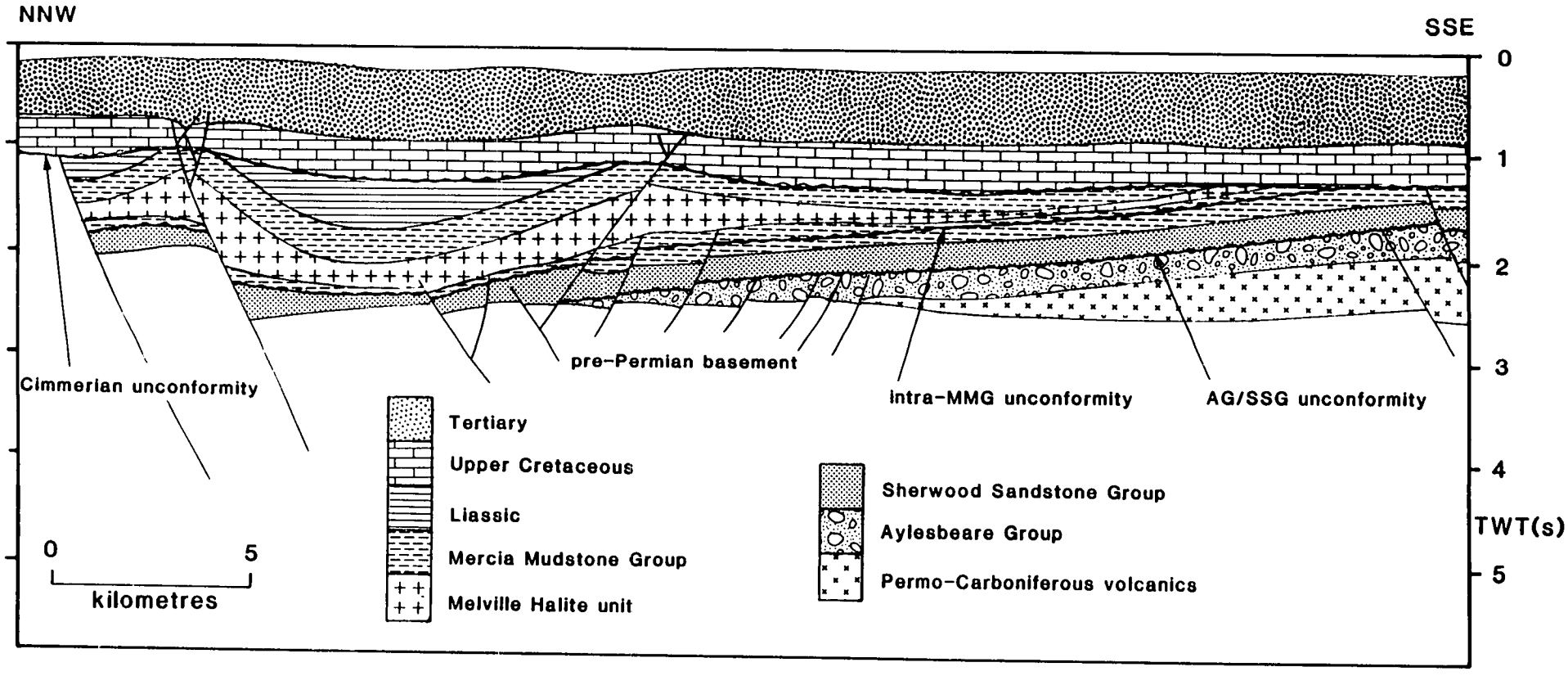

Figure 2.9(b) Interpretation of GECO line through Melville Basin (modified from Chapman (in press)).

discussed from the youngest to the oldest formations, as limited palaeontological data is available in the late Triassic.

2.5.1 Triassic

The marine sediments at the top of the Triassic sequence belong to the Penarth Group, formerly the Rhaetic (Warrington et al, 1980). They are only present in wells 72/10-1, 73/1-1, 73/13-1, 73/14-1 and 88/2-1 (Figure 2.1). In the remaining wells late Triassic sediments were removed by Cimmerian erosion (Section 2.7). In the absence of ammonites of the genus *Psiloceras*, the top of the Penarth Group, hence the Triassic/Jurassic boundary, is lithostratigraphically taken as the top of a distinctive limestone unit formerly known onshore southern England as the White Lias (Warrington et al, 1980; Warrington, 1983). This is in contrast with Bennet et al (1985) who took the base of the White Lias in well 72/10-1 as the Triassic/Jurassic boundary. The Group thus defined comprises the upper limestone unit (Langport Member of the Lilstock Formation) and a lower unit of calcareous mudstones locally grading to siltsones and interbedded with argillaceous limestones (Cotham Member of the Lilstock Formation and Westbury Formation). These sediments were deposited in low energy, generally shallow marine, but occasionally brackish nearshore conditions, and are equivalent to similar sediments deposited throughout England and Wales following the Rhaetian transgression (Warrington et al, 1980). In well 73/14-1 Cimmerian erosion has removed the upper limestone, leaving only the underlying unit.

The Mercia Mudstone Group, formerly that part of the Keuper above the Keuper sandstones (Warrington et al, 1980) underlies the Penarth Group and was widely deposited throughout the basin (Figure 2.1). Like the Penarth Group, however, the unit has been thinned by Cimmerian erosion, particularly in the southern parts of the Western Approaches Basin (Figures 2.1 and 2.9). Carnian to Rhaetian ages have been obtained from the Group (Bennet et al, 1985; Evans et al, in press).

The Mercia Mudstone Group comprises calcareous mudstone with common anhydrite and occasional interbedded dolomitic limestone, siltstone and sandstone. The mudstones lack marine fauna and they were deposited under shallow subaqueous conditions in playa lakes formed by impersistent rivers

charged by flash floods. The thin siltstones and sandstones represent distal alluvial facies. The lakes were subject to intense evaporation and periodic emergence producing anhydrite and evaporites. Thin, well sorted, well rounded sandstone interbeds suggest occasional aeolian deposition.

Thick Carnian-early Norian salt deposits, the Melville Halite unit, became interbedded with these mudstones (Figure 2.1) due to intense evaporation. The thickness of the Melville Halite unit suggests saline waters may have penetrated the basin at this time. Its subcrop can be mapped from seismic data (Figures 2.9 and 2.10(b)), and is also delineated by a gravity low (Figure 2.7, anomaly C). The Melville Halite unit is presently restricted to the northern Melville Basin. However, analysis of the dipmeter log of well 73/7-1, to the south of its present limit, shows a confused zone 200m thick under the Cimmerian unconformity from which salt appears to have withdrawn. Evaporites of similar age have been recorded onshore in south-west England (the Somerset Halite Formation), the Cheshire Basin and the Worcester Graben, and in the offshore Celtic Sea, Fastnet and Bristol Channel Basins and also on the Iberian and Canadian Atlantic margins.

There were two main periods of halokinetic activity in the area. The onlap of Tertiary sediments against the salt swells of Figure 2.9 shows that there was active movement during the Tertiary, and the preservation of Jurassic in the syncline between the salt domes (Figure 2.9) indicates that there was also a Cimmerian phase of movement. The dominant direction of salt movement was northwards, down the slope of the Triassic half graben forming the Melville Basin (Figure 2.9) and out of the southern Melville Basin (e.g. well 73/7-1). The effect of halokinesis should be considered, and if possible removed, when analyzing the vertical movements of wells over salt in terms of more regional mechanisms (Section 5.2.4).

Chapman (in press) described a pre-salt intra-Mercia Mudstone Group unconformity. It is apparent on seismic data (Figure 2.9) and is best developed in the northern Melville Basin underlying the Melville Halite unit. This unconformity may be the product of a period of erosion (Chapman, in press). However, it can not be traced into the St. Mary's Basin (T.J.C. Chapman, personal communication, 1988) and its association with the Melville Halite unit suggests that the halokinetic movements, responsible

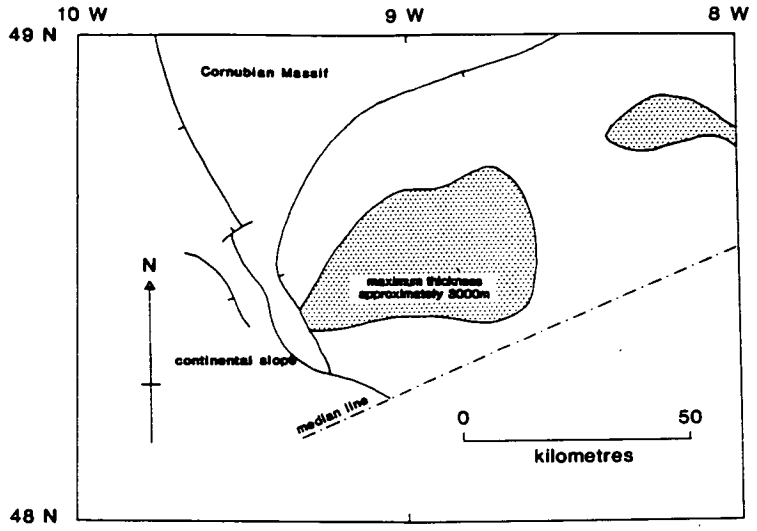

(a) Permo–Carboniferous volcanics subcrop

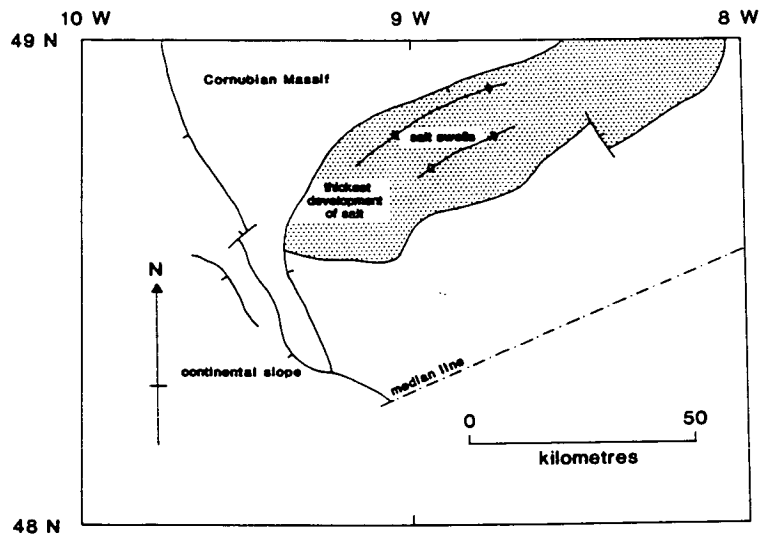

(b) Triassic salt subcrop

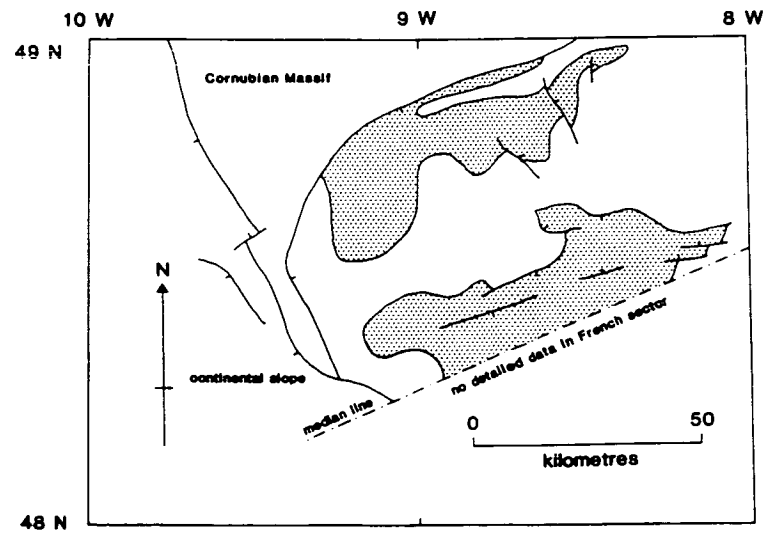

(c) Jurassic subcrop (all Liassic)

Figure 2.10 Subcrops in the western Melville Basin (modified from Evans, 1988)

for the creation of the disturbed zone in well 73/7-1, have enhanced this feature.

The Sherwood Sandstone Group, formerly the Keuper Sandstone and Bunter (Warrington et al, 1980) underlies the Mercia Mudstone Group. The top of the Sherwood Sandstone Group is lithostratigraphically defined as the top of the arenaceous units under the Mercia Mudstone Group, and as such it is present throughout the Western Approaches Basin (Figure 2.1). Limited palynological data suggests that the sandstones may be as young as Ladinian to Carnian (Evans et al, in press). Hence, they may be younger than their onshore lithostratigraphic equivalents such as the Otter Sandstone Formation of south-west England which has been dated as latest Permian to Ladinian (Warrington et al, 1980).

The Sherwood Sandstone Group generally comprises fine to medium grained quartz and arkosic sandstones set in an argillaceous matrix, with many fining upward units. It is locally conglomeratic, particularly towards its base, with the inclusion of poorly sorted angular grains of lithics, quartz, chert and volcanics. The sandstone and conglomerate units show planar and trough cross-stratification. Anhydrite is less common than in the Mercia Mudstone Group and thick salt is absent. The Sherwood Sandstone Group is clearly the product of a higher energy environment than the Mercia Mudstone Group. The conglomerates are interpreted as proximal alluvial fan and channel lag deposits, while the sandstones represent more distal fan facies and channel bars. These facies graded upwards and outwards into the playa lakes of the Mercia Mudstone Group. Onshore in south-west England, in addition to alluvial and fluviatile deposits, this Group contains subordinate well sorted well rounded aeolian sands (Laming, 1969). No unequivocal aeolian sandstones of this age have been recovered from the offshore wells, but the water-borne material is likely to be associated with aeolian deposits.

2.5.2 Permo-Triassic Boundary

The base of the Triassic in south-west England is commonly taken as the base of the conglomeratic sequence underlying the Sherwood Sandstone Group, the Budleigh Salterton Pebble Beds and equivalents (Warrington et al, 1980). Hence the base of the Triassic in Figure 2.1 has been taken as the base of

the arenaceous units of the Sherwood Sandstone Group, a horizon which is locally conglomeratic, and rests with slight unconformity on the underlying Aylesbeare Group. Since limited palynological evidence suggests that the Sherwood Sandstone Group may be slightly younger in the Western Approaches Basin than onshore south-west England its base may also be somewhat younger. It should be emphasized that the Permo-Triassic boundary as taken in this study is purely lithostratigraphic.

The proposed correlation of Figure 2.1 becomes somewhat speculative beneath the Sherwood Sandstone Group. For example, in well 72/10-1 the entire New Red Sandstone sequence may belong to the Sherwood Sandstone Group, with its chosen base simply a coarser facies within the Sherwood Sandstone Group, an interpretation favoured by Evans et al (in press). Alternatively, as proposed by Bennet et al (1985), the Sherwood Sandstone Group of Figure 2.1 may belong to the Aylesbeare Group, with the top Aylesbeare Group unconformity developed at the top of this arenaceous unit. The former hypothesis is not favoured because the clay mineralogy studies of Fisher and Jeans (1982) support a Permian age for the basal sequence (clay mineral zones G and H), and because these conglomerates are possible lateral equivalents of those at the base of wells 73/12-1 and 74/1-1 which are interbedded with volcanics of probable Permo-Carboniferous age. The latter interpretation is not favoured because it requires the absence of the widely developed Sherwood Sandstone Group which Fisher and Jeans (1982) suggested was present in the well (clay mineral zone F). The preferred interpretation of well 72/10-1 lies somewhere between the above hypotheses and is similar to that of Chapman (in press). In contrast with Chapman (in press), however, the entire New Red Sandstone sequence of well 86/18-1 in the St. Mary's Basin has been assigned to the Permian. Seismic data show the New Red Sandstone of well 86/18-1 to be entirely below the Sherwood Sandstone Group as seen in to the north in well 86/17-1.

Unequivocal palynologically dated Permian sediments have been recovered from wells 86/18-1 and 87/12-1 in the St. Mary's Basin and well Brezell-1 in the Brittany Basin. This supports the general interpretation that the Aylesbeare Group, as defined above, belongs to the Permian and is not a fine-grained facies developed within the Sherwood Sandstone Group. The presence of a demonstrable Permian sequence in the Western Approaches Trough contrasts with the surrounding basins where only Triassic sediments

have been proven (Kamerling, 1979; Jansa et al, 1980; Van Hoorn, 1987), and a Triassic age tentatively proposed for the entire New Red Sandstone sequence (Masson and Miles, 1986).

2.5.3 Permian

The Aylesbeare Group, as defined above, is thickest in the southern Western Approaches Basin and progressively thins to the north, downlapping Variscan basement. It is absent from the northern Melville Basin where the Triassic lies directly on Variscan basement (Figure 2.9). The Aylesbeare Group comprises dominantly calcareous mudstones grading to siltstones and thin argillaceous arkosic and lithic sandstones, and is generally siltier than the Mercia Mudstone Group. Gypsum and anhydrite occur in small quantities, and occasional cavities may be associated with the dissolution of evaporites, but, unlike the Mercia Mudstone Group, there is no thick salt. An essentially arid lowland, sabkha-type environment is proposed.

The lowermost unit of the New Red Sandstone comprises the breccio-conglomerates and sandstones found in wells 72/10-1, 73/12-1, 86/18-1 and 87/12-1 (Figure 2.1). In well 72/10-1 the unit consists of conglomeratic horizons and individual pebbles set in a very fine sandstone matrix containing significant argillaceous material. The clasts are altered igneous and pyroclastic rock of a predominantly acidic nature and are derived from the nearby Cornubian Batholith (Bennet et al, 1985). The material in well 73/12-1 is texturally similar, but clasts from the underlying, more basic lavas predominate. This reflects the proximal nature of the sediments accumulating in alluvial fans, and is typical of the Permian of the British Isles (Smith et al, 1974). No detailed correlation is implied between the wells exhibiting this facies, although there may be a broad equivalence through their association with early degradation of the Variscan highlands. This may extend to the conglomeratic horizons in the St. Mary's Basin in wells 86/18-1 and 87/12-1 which are thinner and contain a variety of sedimentary clasts, probably reflecting the lack of a proximal high relief volcanic source, and even to the early Permian breccias of south-west England such as the Teignmouth and Crediton Breccias.

Deposition of the New Red Sandstone in the Western Approaches Trough may have commenced in the Stephanian. New Red rocks underlie the Exeter

Volcanic Series in south-west England, and their deposition is thus believed to have commenced in the late Carboniferous. No red-beds have been proven underlying the volcanics in the Western Approaches Trough, but they may exist in undrilled locations.

2.5.4 Summary and Tectonic Implications of the Permo-Triassic Geology

The geological interpretation of the Permo-Triassic has been discussed in some detail because it plays an important role in elucidating early basinal development. This is particularly so in the Permo-Triassic where the absence of reliable age dating inhibits quantitative well subsidence analysis (Chapter 5).

The Permo-Triassic broadly comprises two fining upwards sequences. The first commenced with the basal Permo-Triassic breccio-conglomerates and sandstones and passed up into the shaly sandstones and shales of the Aylesbeare Group (the "Permian" sequence). The second commenced with the locally conglomeratic base of the Sherwood Sandstone Group and passed up into the Mercia Mudstone Group (the Triassic sequence). An unconformity separates these sequences. Coarser facies below the unconformity are dominated by lithic arenites, while quartz arenites dominate coarser facies below the unconformity. The two sequences correspond to two distinct periods of subsidence separated by a period of non-deposition.

Similar "two-stage" interpretations of the New Red Sandstone have been made onshore south-west England (Durrance and Laming, 1982) and in other exposed sequences of the British Isles (Smith et al, 1974; Warrington et al, 1980), and also in borehole analysis of the Worcester and Wessex Basins (Chadwick, 1985c; 1986). Durrance and Laming (1982) interpreted the first stage as due to the progressive denudation of the Variscan highlands, and the second as initiated by increased rainfall. In contrast, Chadwick (1985c, 1986) proposed that rifting preceded the deposition of each of the coarse units. Progressive denudation of rift-induced topography would produce the fining up sequences. In view of the topographic lows intrinsically associated with Variscan uplift, and the onlap of the Permian sequence towards the Cornubian Massif, from which it was in part shed (well 72/10-1), it does not seem necessary to invoke an early Permian rift phase. Sedimentation at this time was essentially molasse facies in a major

intermontane low. The driving forces of basin subsidence which accommodated the deposition of the Permian and Triassic sequences are discussed in more detail in Chapter 5.

2.6 JURASSIC

Eustatic transgression at the end of the Triassic (Haq et al, 1987) combined with regional subsidence of the Western Approaches Trough (Chapter 5) led to a change in lithology from the continental red-beds of the Permo-Triassic to the marine shales and limestones of the Jurassic.

Jurassic sediments in the Western Approaches Basin are spatially restricted to two outliers (Figures 2.1 and 2.10) and are temporally restricted to the early Liassic. However, due to differential movement on the faults separating the Western Approaches Basin from the Brittany and South-West Channel Basins, there is a much more widespread and complete Jurassic sequence in the latter basins. Liassic sediments have also been recovered from the south of the Plymouth Bay Basin in well 88/2-1 (Figure 2.1).

2.6.1 Liassic

Liassic (early Jurassic) sediments in the Western Approaches Basin comprise slightly carbonaceous calcareous mudstones with interbeds of muddy, micritic limestone and contain a fairly abundant fauna of Hettangian to Sinemurian age (Bennet et al, 1985; Evans et al, in press). They rest conformably on the late Triassic Penarth Group and were deposited in similar nearshore marine to sublittoral environments of low energy. These facies are typical of the early Jurassic of the surrounding basins on the British continental shelf (e.g. Kamerling, 1979; Robinson et al, 1981) and were also developed in the Brittany and South West Channel Basins. The similarity of facies in now isolated Liassic subcrop suggests it was originally more widespread than its present distribution. The Liassic was probably deposited over a very wide area following the Rhaetian transgression across a peneplained late Triassic surface.

In the South West Channel Basin well Lennket-1 passed through approximately 1km of Jurassic sediments (Figure 2.1). The base of this sequence, which rests on Armorican monzonitic basement, comprises 19m of undifferentiated (?)Lias or (?)Dogger microconglomerate underlain by 14m of Liassic shaly sandstone and shaly dolomite. Liassic sandstones are not found further west in the Brittany Basin (Figure 2.1). However, Sinemurian sandstones have been recovered from the Fastnet Basin (Robinson et al, 1981) and Pliensbachian sandstones occur in the Bristol Channel Basin (Kamerling, 1979). The latter are equivalent to the mid Liassic sandstones of south-west England. The distribution of these sands suggests they were sourced from nearby Variscan massifs such as Cornubia and Armorica rather than a dome to the west margining early Atlantic rifting as was proposed by Hallam and Sellwood (1976). The massifs were reactivated by a combination of local tectonism and eustatic sea-level change. A similar local source is postulated for the 15m of Hettangian sands in well 73/1-1 (Figure 2.1), equivalents of which have not been recognised in any other wells in the Western Approaches Basin.

2.6.2 Dogger

In the South West Channel Basin (well Lennket-1) the Dogger (mid Jurassic) is represented by 187m of undifferentiated dolomite (Figure 2.1). In the Brittany Basin the early Dogger calcareous mudstone facies is similar to the Liassic sequence and a tranquil shelf environment is suggested. A regressive phase occurs in the late Dogger with increased sandy input into the mudstones in well Lizenn-1, and an end Dogger (Callovian/Oxfordian) unconformity in well Brezell-1 and possibly also in wells Lennket-1 and Lizenn-1. Increasingly shallower conditions are also seen in the late Dogger of the South Celtic Sea Basin (Van Hoorn, 1987) and the unconformity in the Brittany Basin may be broadly equivalent to the disconformity separating the Kimmeridgian-Berriasian from the Callovian in the western Bristol Channel Basin (Kamerling, 1979). More regionally, mid/late Jurassic unconformities are also recorded in the Wessex Basin (Lake and Karner, 1987) and the North Celtic Sea Basin (Tucker and Arter, 1987). Unlike the late Jurassic-early Cretaceous movements (Section 2.7) the Callovian/Oxfordian unconformity of the south-west British continental

shelf was not associated with significant deformation. In the Jeanne d'Arc Basin on the Canadian Grand Banks, which juxtaposed Goban Spur prior to Atlantic opening (Masson and Miles, 1986), a similar late Callovian unconformity marks the initiation of a phase of late Jurassic-early Cretaceous rifting (Tankard and Welsink, 1987).

2.6.3 Malm

The Malm (late Jurassic) of the South West Channel Basin (well Lennket-1) is represented by Tithonian (possibly Kimmeridgian-Oxfordian at their base) calcareous sandstones and shales with interbedded anhydrite (Figure 2.1). In the Brittany Basin an Oxfordian to Tithonian aged dominantly fine grained facies with interbedded limestones overlies the Dogger/Malm unconformity, and anhydrite is again present in well Lizenn-1. These sediments are broadly equivalent to the late Jurassic calcareous shales and sandstones of the Bristol Channel Basin (Lloyd et al, 1973) and the Kimmeridgian-Tithonian limestones of the Fastnet Basin (Robinson et al, 1981) and were deposited in a similar shallow marine to brackish and freshwater environment with anhydrite suggesting periods of emergence.

The Malm of the present continental slope west of the Western Approaches Trough shows an open marine facies with reefal or peri-reefal limestones of Kimmeridgian-Tithonian age at DSDP site 401 (Montadert et al, 1979; Figure 2.2) and late Jurassic open marine limestones recovered from several dredges (Auffret et al, 1979). A westward decrease in continentality is supported by the disappearance of anhydrite in the west of the Brittany Trough (Brezell-1), but the abundance of lignite suggests that only on the proto-slope did true open marine conditions prevail.

It is not clear to what extent the eroded post-Sinemurian Jurassic sequence of the Western Approaches Basin is analogous to that of the Brittany Basin and other surrounding basins. However, from regional considerations the main period of tectonic activity appears to have been late Jurassic/early Cretaceous (Section 2.7) so that broadly similar conditions probably prevailed throughout the region until the end of the Jurassic (P.A. Ziegler, personal communication, 1988).

2.7 LATE JURASSIC/EARLY CRETACEOUS AND THE CIMMERIAN UNCONFORMITY

A major middle Mesozoic angular unconformity is developed throughout the Western Approaches Basin. It was associated with the removal of most of the Jurassic and locally cuts down to the Permian (Figure 2.1). The term "Cimmerian" has been widely, if imprecisely, used to describe several regional or local unconformities observed in the Mesozoic of north-west Europe (Fyfe et al, 1981; Rawson and Riley, 1982). In this thesis the term Cimmerian refers specifically to movements around the Jurassic/Cretaceous boundary which produced this angular unconformity and is hence equivalent to the late Cimmerian movements of Ziegler (1982). However, late Jurassic-early Cretaceous erosion in the Western Approaches Basin was so great that the Cimmerian unconformity now also incorporates the Dogger/Malm (mid/late Jurassic) disconformity seen across the south-west British continental shelf, assuming it did previously exist as a discrete event in the Western Approaches Basin. Locally it even incorporates the Sherwood Sandstone Group/Aylesbeare Group unconformity.

The Cimmerian unconformity, as described above, is seen in the Western Approaches Basin, the Plymouth Bay Basin, the Fastnet Basin (Robinson et al, 1981) and South Celtic Sea/Bristol Channel Basin (Kamerling, 1979). It is not so well developed in the North Celtic Sea Basin (Tucker and Arter, 1987) and is not seen in the Brittany and South West Channel Basins. Particular attention is paid to the distribution and timing of Cimmerian movements as they have a crucial bearing on the mechanisms of post-Cimmerian subsidence (Chapter 6).

(?)Tithonian-Berriasian brackish water mudstones and sands tones in well 87/12-1 in the St. Mary's Basin overlie the Cimmerian unconformity, hence Cimmerian uplift and deformation in the area occurred prior to the (?)latest Jurassic-earliest Cretaceous. Well 87/12-1 is, however, atypical and elsewhere in the Western Approaches Basin the oldest sediments overlying the Cimmerian unconformity are Barremian-Albian in age with structurally high areas not transgressed until the Albian (Figure 2.11). Since the youngest sediments recovered from beneath the unconformity in the Western Approaches Basin are Sinemurian there is very little direct control on the timing of the onset of deformation.

In the Fastnet Basin Valanginian sediments are the oldest recorded units overlying the Cimmerian unconformity and Tithonian the youngest underlying it (Robinson et al, 1981). Hence, Cimmerian deformation in the area was concentrated in the Berriasian. Similarly, Kamerling (1979) dated the major Cimmerian movements of the western Bristol Channel as late Berriasian to pre-Aptian.

The Cimmerian unconformity, as defined above, has been widely linked to rifting in the Bay of Biscay and North Atlantic (e.g. Hallam and Sellwood, 1976; Kamerling, 1979; Ziegler, 1982; Lake and Karner, 1987). The most complete sequence of syn-rift sediments on the continental slope was penetrated in a half-graben at site 549 on Goban Spur where the oldest syn-rift deposits are (?)Hauterivian-Barremian (Masson et al, 1985; Figure 2.2). Only in the Albian, with the onset of sea-floor spreading and regional subsidence, were structurally high areas of the slope transgressed. On the north Biscay margin continental separation and regional subsidence occurred in the Aptian (Montadert et al, 1979). Similarly, in the Jeanne d'Arc Basin on the Canadian Grand Banks the end of the late Jurassic-early Cretaceous rifting period is marked by an Aptian unconformity (Tankard and Welsink, 1987). These dates are consistent with the Western Approaches Basin where only in the Albian were the highs transgressed. Unlike the continental slope and the Brittany and Jeanne d'Arc Basins, however, the pre-Albian Cretaceous, where present, is not fault-controlled and sits only as a highly condensed veneer above the Cimmerian unconformity.

2.8 CRETACEOUS

This section describes in more detail the post-Cimmerian Cretaceous sequence of the Western Approaches Trough. In addition to the borehole correlation of Figures 2.1 and 2.2 the Cretaceous of the Western Approaches Trough and its adjacent margin are described by a series of palaeogeographic maps (Figure 2.11). These maps reconcile the variable quality of biostratigraphic dating in different wells in the region and their time intervals represent the best widely applicable constraints. Following these maps the discusssion is chronostratigraphically arranged

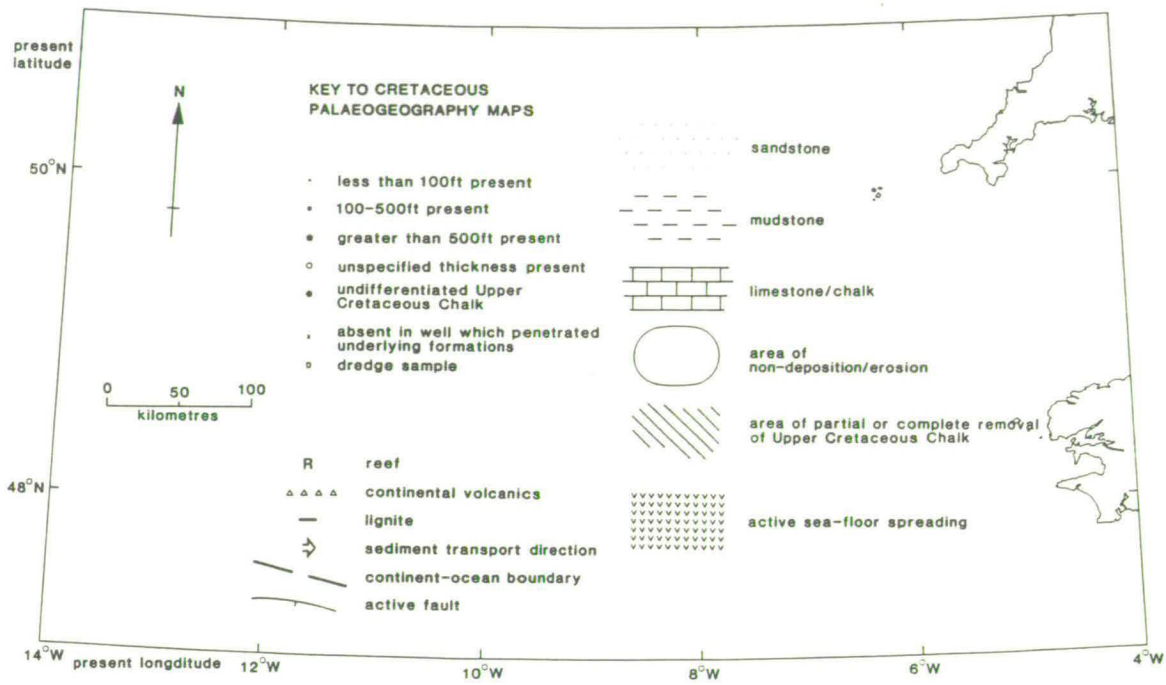

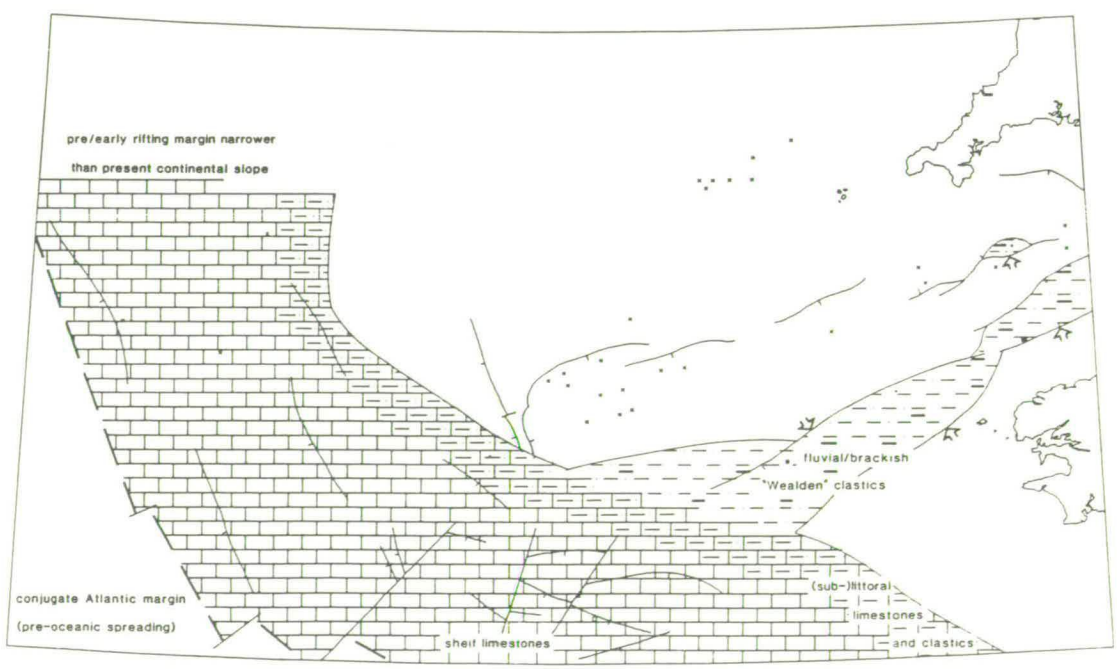

Figure 2.11(a) Berriasian–Valanginian

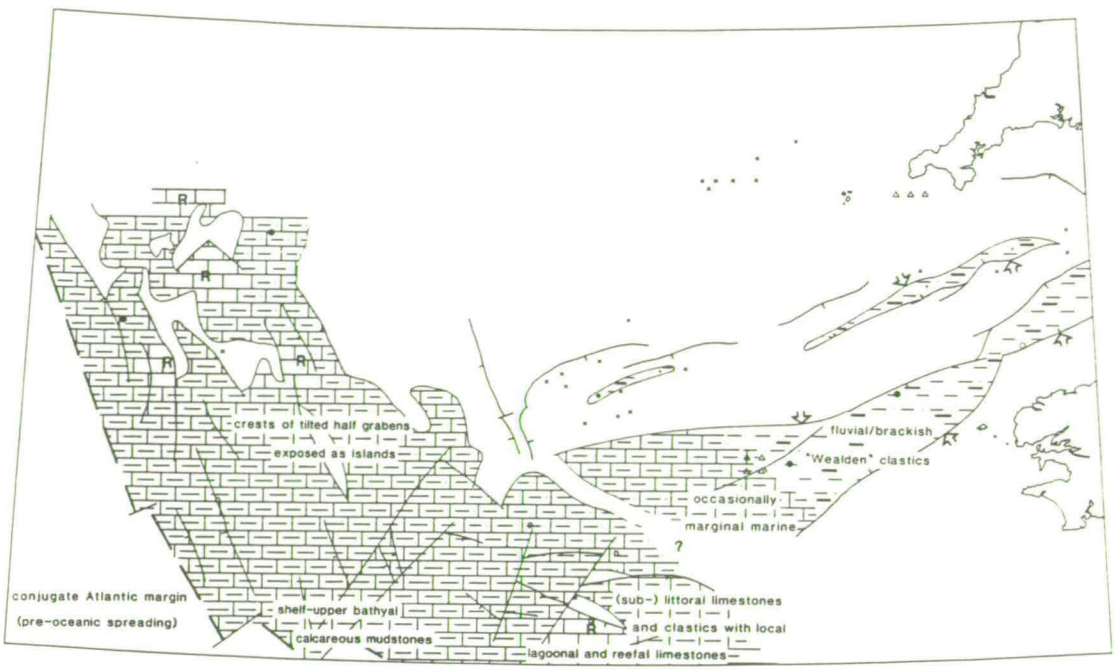

Figure 2.11(b) Hauterivian–Barremian

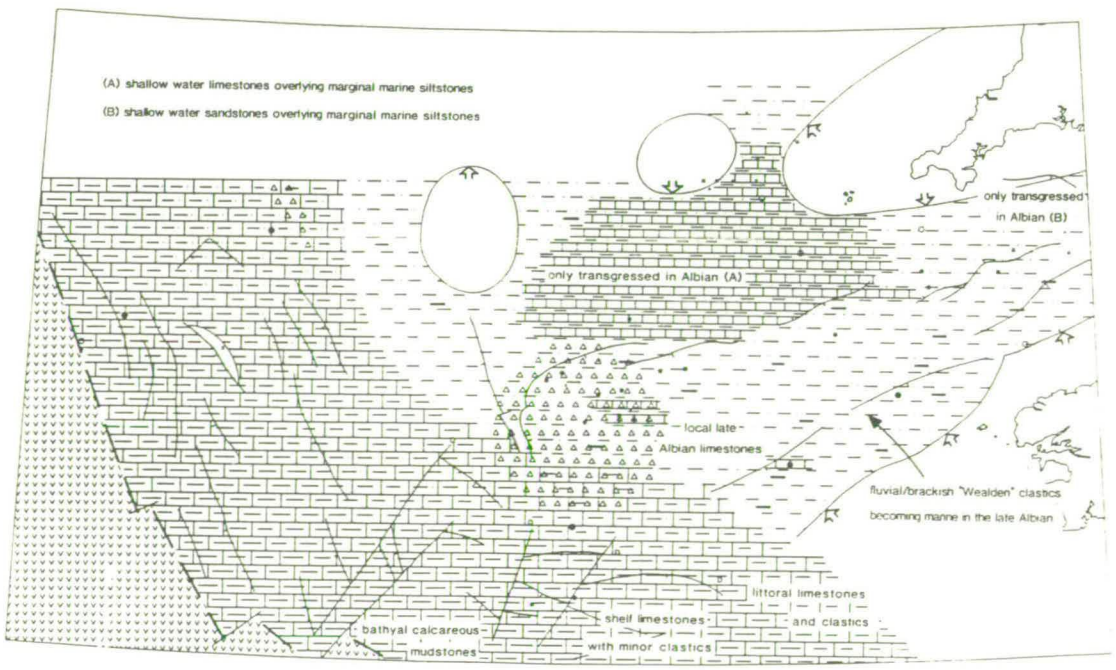

Figure 2.11(c) Aptian–Albian

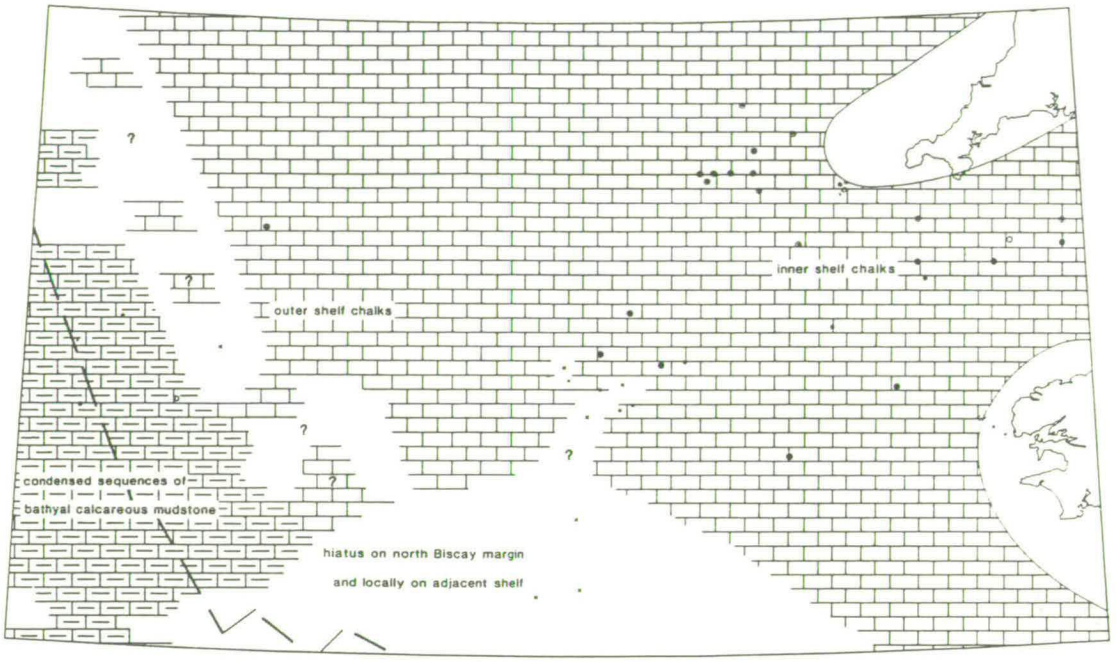

Figure 2.11(d) Cenomanian–Santonian

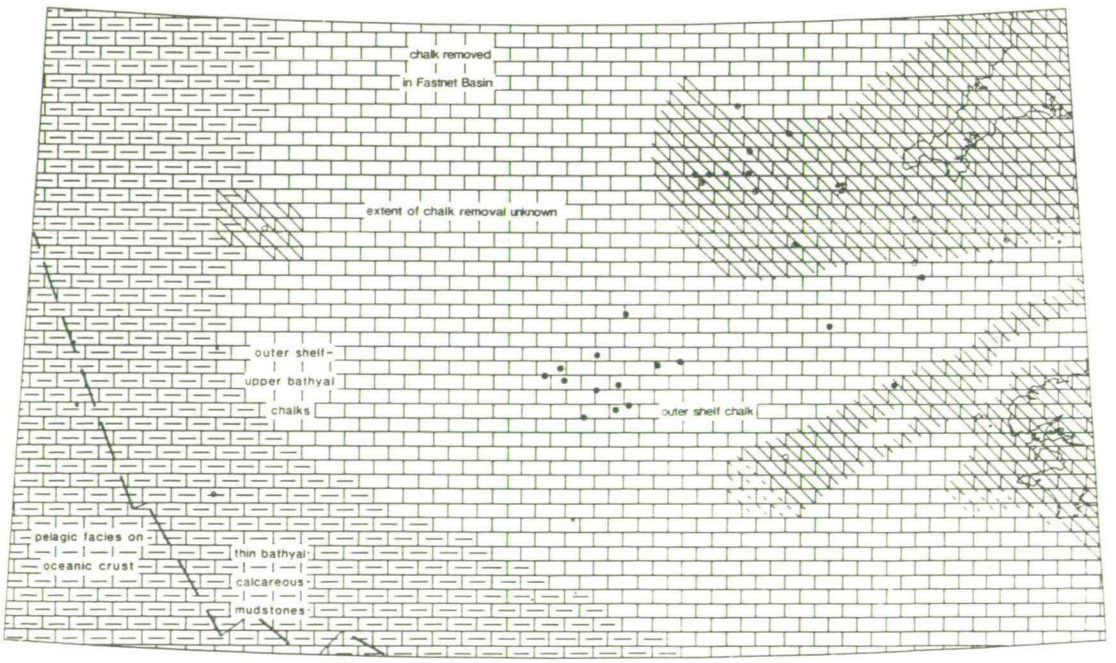

Figure 2.11(e) Campanian–Maastrichtian

although some formations have lithostratigraphic equivalents in the classic Weald-Wessex area.

2.8.1 Berriasian-Valanginian

Berriasian-Valanginian sediments are almost entirely restricted to the Brittany and South-West Channel Basins and the present continental slope (Figure 2.11(a)). Lignitic mudstones and sandstones deposited in Wealden-type fluvio-lacustrine conditions were recovered in wells Lennket-1, Brezell-1 and Lizenn-1, while well 87/12-1 in the St. Mary's Basin recovered Berriasian-(?)Valanginian sediments of similar facies. Sediments were only deposited during this period where tectonic subsidence and eustatic sea-level rise was more rapid than regional Cimmerian uplift. These processes were nearly in balance in wells Lizenn-1 and 87/12-1 where only a few tens of metres of sediment represent this interval.

On the continental slope dredged samples suggest there was an extensive marine carbonate platform at this time (Auffret et al, 1979). Possible undifferentiated Neocomian sediments from DSDP site 401 on the northern Biscay margin (Figure 2.2) and well 62/7-1 on the upper part of Goban Spur (Cook, 1987) support this interpretation.

2.8.2 Hauterivian-Barremian

Hauterivian-Barremian sediments are slightly more widespread than those of the Berriasian-Valanginian (Figure 2.11(b)). In the Western Approaches Basin post-Cimmerian sedimentation commenced in wells 73/5-1, 73/7-1, 85/28-1 and 86/18-1 during this period. Lignitic mudstones and sandstones similar to the Berriasian-(?)Valanginian of well 87/12-1 were deposited. Hauterivian-Barremian deposits across the Brittany and South-West Channel Basins and are of similar facies.

The syn-rift half-graben fill at DSDP site 549 on Goban Spur was deposited during this period (Masson et al, 1985; Figure 2.2). A transgressive sequence of shallow water (?)Hauterivian-Barremian carbonates overlain by outer shelf calcareous, sandy mudstones was recovered (Rat et al, 1985). Reefs or carbonate banks interpreted on reflection seismic data

have also been preserved within the half-grabens (Masson and Roberts, 1981; Cook, 1987).

Although rifting across the entire continental slope need not have occurred at this time DSDP site 549 provides the only cored interval through a half-graben in the area and has been taken to be representative. The erosion of the crests of the tilted blocks must also have occurred at this time and the pattern of exposed islands on Figure 2.11(b) has been compiled from Montadert et al (1979), Masson and Roberts (1981) and Masson et al (1985). The north Biscay margin was subject to less sub-aerial erosion during rifting. This difference presumably reflects the difference in pre-rift geology of the two areas: on Goban Spur rifting affected a pre-existing basement high continuous with the Cornubian Massif, whereas on the north Biscay margin a Mesozoic basinal sequence continuous with the Western Approaches Trough had been deposited.

Isolated volcanism on the continental shelf accompanied active rifting. The peralkaline volcano of Wolf Rock 15km south-west of Land's End has been dated as 131±5Ma, earliest Barremian (Harrison et al, 1977). The petrologically similar Epson Shoal was probably emplaced at the same time. Further volcanism is witnessed by late Neocomian-Barremian sills in the Brittany Basin (Ziegler, 1987a).

2.8.3 Aptian-Albian

During the Aptian conditions on the shelf were broadly similar to those of the Barremian with slight expansion of the area of deposition of lignitic mudstones and sandstones. Wells 73/2-1 and 73/8-1, in the Melville Basin, and 86/17-1 in the St. Mary's Basin are the only wells in which post-Cimmerian sedimentation demonstrably commenced in the Aptian.

In the Albian, however, most of the area was transgressed (Figure 2.11(c)). On the southern flanks of the Cornubian Massif Lott et al (1980) recognised two distinct periods of Albian sedimentation. A sandy carbonaceous clay unit deposited in quiet water with both marine and terrestrial influences during the mid Albian overlies the Wealden-type lignitic mudstones and sandstones and transgressed all but the most positive areas. Following a short-lived marine regression, renewed late Albian transgression resulted in the development of true marine conditions

in the Western Approaches Trough for the first time since the Jurassic. Late Albian-early Cenomanian open marine bioclastic limestones were deposited with a minor unconformity over the sandy carbonaceous clays between the Haig Fras and Cornubian Batholiths (wells SLS 28 and 74). To the east (wells SLS 64 and 76) the limestone unit is interbedded with shallow marine high energy bioclastic sandstones of the same age into which it passes laterally (well SLS 31A).

The mid Albian sandy carbonaceous clay unit appears to be widespread throughout the Western Approaches Basin, although it is difficult to distinguish from the underlying lignitic mudstones and sandstones in poorly dated wells. Late Albian sandstones which occasionally extend into the early Cenomanian are also widely developed, but the limestone unit only shows a patchy distribution (wells 73/13-1, 73/14-1, 83/24-1, 86/18-1).

A volcanic unit not described by Lott et al (1980) is present in the western Melville Basin where the Aptian-Albian is represented by lavas and tuffs with thin claystones (wells 72/10-1, 73/1-1 and 73/12-1). The volcanics are up to 46m thick in the westernmost wells, thin eastwards, and are absent from the eastern Melville Basin. A near circular magnetic high (Figure 2.8, anomaly G) which sits directly over, but is not displaced by and appears to post-date movement on, the northern bounding fault of the Melville Basin may be caused by similar Apto-Albian volcanics. The lavas are porphyritic olivine-rich basalts (Bennet et al, 1985) and appear to have been erupted in submarine conditions. Albian-Aptian volcanics have also been described from reflection seismic data over Goban Spur (Cook, 1987). In spite of these occurrences, and the isolated Hauterivian-Barremian volcanism, Biscay/Atlantic rifting and sea-floor spreading in the area was not associated with extensive volcanic activity on the adjacent proto-slope and shelf, unlike the Tertiary opening of the North-East Atlantic between the north-west British margin and Greenland.

Thick Aptian-Albian sequences are observed in the Brittany and South-West Channel Basins. Wells Lennket-1 and Lizenn-1 contain lignitic mudstones and sandstones of Wealden-type. Well Brezell-1 contains possible equivalents of the late Albian units to the north with limestones interbedded near the top of some 200m of Aptian-Albian lignitic mudstones and sandstones. It is not clear if these limestones are continuous with

those of the eastern Melville Basin, or possibly even those of the Cornubian Massif.

The transition from rifting to active sea-floor spreading took place in the Aptian on the north Biscay margin (Montadert et al, 1979), and in the Albian on Goban Spur (Masson et al, 1985). Albian tholeiitic basalt has been recovered at DSDP sites 550 and 551 which penetrated oceanic basement (Graciansky and Poag, 1985; Figure 2.2). Regional subsidence of the continental slope associated with the onset of sea-floor spreading caused an increase in water depths. Most of the crests of the tilted half-grabens became submerged and the Hauterivian-Barremian reefs and lagoons are overlain by Aptian-Albian shelf and upper bathyal limestones, marls and mudstones (Montadert et al, 1979). Only DSDP site 548 on Goban Spur is without Aptian-Albian sediments. It may have remained emergent during this period due to its location on a prominent structural high.

2.8.4 Cenomanian-Santonian

Regional subsidence (Chapter 6) combined with continued sea-level rise from the late Albian (Haq et al, 1987) led to the development of Cenomanian-Santonian marine conditions over an even greater area than that covered by the late Albian.

Cenomanian-Santonian chalks were deposited over the Brittany, South-West Channel, St. Mary's and Plymouth Bay Basins in addition to much of the Cornubian and Armorican Massifs and the eastern Melville Basin (Figure 2.11(d)). Continued emergence of significant land areas during the Cenomanian is witnessed by the early Cenomanian sandstones of the Cornubian Massif (Lott et al, 1980), and of well 86/18-1 in the St. Mary's Basin. Even where the Cenomanian comprises only chalk significant detrital shale is present (e.g. well 87/16-1, Figure 7.2). Glauconite is also abundant in the Cenomanian chalks. Flints are relatively rare in the Cenomanian but become more abundant in the purer Turonian-Santonian chalks.

On the continental slope at Goban Spur, DSDP sites 549, 550 and 551, condensed sequences of bathyal calcareous mudstones were deposited at this time (Figure 2.2). No sediments from this interval were recovered from site 548 which probably remained above sea-level (Graciansky and Bourbon, 1985).

A widespread Cenomanian-Santonian hiatus is recorded on the north Biscay margin (Montadert et al, 1979; Figure 2.2) and in the western Melville Basin (Figure 2.1). The north Biscay margin was clearly submarine during this interval and the hiatus may be linked to a major palaeoceanographic event observed throughout the Atlantic synchronous with the Cenomanian-Turonian eustatic sea-level rise (Montadert et al, 1979). Strong ocean currents may have swept the area clean of sediment. This may also be the cause of the hiatus in the western Melville Basin, but it is striking that once sedimentation commenced in the western Melville Basin Campanian-Maastrichtian subsidence was very rapid. The tectonic implications of this sudden change in behaviour are discussed in Chapter 6.

2.8.5 Campanian-Maastrichtian

Continued regional subsidence (Chapter 6) and the late Cretaceous sea-level highstand (Haq et al, 1987) led to the deposition of Campanian-Maastrichtian chalks over the entire shelf and the adjacent present land area, largely in outer shelf conditions. Bathyal pelagic facies, dominantly calcareous mudstones, were deposited on the slope and ocean basin. In the Tertiary, however, uplift caused widespread erosion of these chalks (Figures 2.1 and 2.11(e)).

Tertiary uplift caused partial or complete removal of the late Cretaceous Chalk over the entire Armorican Massif and South-West Channel Basin and also over the Cornubian Massif and Brittany Basin east of 8°W. The Chalk of the Melville Basin was not, however, subject to significant erosion (Figure 2.1). West of 8°W in the Brittany Basin and Cornubian Massif the extent of late Cretaceous Chalk removal is unclear (Figure 2.11(e)). In the latter areas late Tertiary sediments crop out at the sea-bed and few wells are available. The uppermost Maastrichtian is absent from well 62/7-1 on Goban Spur (Cook, 1987) suggesting removal may have occurred on the crest of the Cornubian Massif along its entire length, however, a complete late Cretaceous Chalk sequence in well 83/24-1 shows that removal did not occur on the flanks of the Massif west of 8°W. Seismic data suggest that Tertiary uplift and erosion in the western Brittany Basin did not cut down to the top of the late Cretaceous Chalk. The quantification and causes of Tertiary uplift are discussed in Chapter 7.

The Campanian-Maastrichtian interval recovered from wells in the Melville Basin comprises up to 510m of white-grey biomicritic chalk with flints and occasional glauconite and pyrite. Campanian-Maastrichtian chalks contain less detrital material than Cenomanian-Santonian chalks reflecting the absence of nearby land. Seismic data indicate that where preserved in the western Brittany Basin the late Cretaceous Chalk sequence is up to 750m thick, somewhat thicker than in the Melville Basin.

2.9 TERTIARY

The Tertiary history of the Western Approaches Trough reflects the interaction between continued post-Cimmerian regional subsidence (Chapter 6), eustatic sea-level changes and uplift associated with compressions in the Alpine foldbelt (Chapter 7). The resulting Tertiary sequence comprises up to 1.5km of Tertiary mudstones, sandstones and limestones cut by hiatuses of varying magnitude and lateral extent.

The Tertiary of the Western Approaches Basin forms a broad syncline, outcropping over much of the sea-bed (Figure 1.2). Tertiary uplift and erosion is responsible for the absence of Tertiary strata over the Cornubian Massif and its flanks east of 8°W and the South-West Channel and eastern Brittany Basins.

2.9.1 Palaeocene

Danian sediments are preserved in several wells in the Western Approches Basin where they comprise white-grey biomicritic shelf chalks with flints (Figure 2.1). Over much of the area, however, they have been removed by erosion concentrated at a mid-late Palaeocene hiatus (Figure 2.1). The magnitude of this erosion is variable. In the eastern Melville Basin (well 74/1-1) where the Maastrichtian and early Palaeocene are absent and the St Mary's Basin (well 85/28-1) where the Maastrichtian and entire Palaeocene are absent, up to 200-250m of sediments may have been removed (the thickness of the Maastrichtian-Palaeocene interval in wells 73/13-1 and 73/14-1). However, in the southern Melville Basin (wells 73/13-1 and 73/14-1), where 50-60m of Danian chalk is preserved, the mid-late

Palaeocene unconformity is expressed only by regressive shallow marine mid-late Palaeocene mudstones, sandstones and limestones. Similar shallow/marginal marine late Palaeocene sediments demonstrably post-date the unconformity (wells 74/1-1 and 83/24-1), but generally sedimentation did not recommence until the Eocene (Figure 2.1).

On the adjacent continental slope early Palaeocene deposition was characterised by the deposition of bathyal nannofossil chalks. This was terminated by a mid-late Palaeocene hiatus seen throughout the slope (Masson et al, 1985; Figure 2.2). As in the Western Approaches Trough erosive downcutting accompanied this unconformity (Poag et al, 1985). Late Palaeocene sediments overlying the unconformity contain increased clastic material.

2.9.2 Eocene

The Eocene sequence of the Melville Basin, up to 600m thick in wells, commences with a basal mudstone deposited in open marine shelf conditions assigned to the early Eocene and probably equivalent to the London Clay Formation of southern England (Bennet et al, 1985). The mudstone is overlain (disconformably in wells 72/10-1 and 73/1-1) by a variety of mid Eocene shelf calcareous sandstones and limestones which locally extend into the late Eocene and even the Oligocene (Figure 2.1). Late Eocene sediments have, however, been widely removed by later uplift and erosion (Section 2.9.3).

In the St. Mary's Basin there is only limited data on the Eocene as it has either been removed by uplift and erosion or is within the zone of no well returns. However, in well 85/28-1 the "basal" mudstone unit is underlain by 68m of early Eocene calcareous sandstones and limestones and is overlain by early-mid Eocene sandstones. In well 87/16-1 the Eocene is represented by similar sandstones and limestones, but the mudstone is absent.

Bathyal calcareous mudstones and marly chalks similar to the late Palaeocene continued to be deposited on the continental slope during the Eocene but are cut by several intra-Eocene hiatuses (Hailwood et al, 1979; Snyder et al, 1985). On Goban Spur the most important of these is an early-middle Eocene unconformity (Figure 2.2) which correlates with the

unconformity observed in wells 72/10-1 and 73/1-1 in the western Melville Basin. This marks the end of the period of increased clastic input on the continental slope which started following the mid-late Palaeocene hiatus. The upper boundary of the phase of relatively high clastic input on the north Biscay margin is marked by a mid Eocene-early Oligocene unconformity (Masson et al, 1985; Figure 2.2). The relationship of these unconformities to a major period of Eocene-Miocene deformation on the slope and adjacent shelf is discussed in the next section.

2.9.3 Eocene-Miocene Deformation

Masson and Parson (1983) described a faulted monocline at the foot of the north Biscay slope generated by compression during the mid Eocene-early Oligocene hiatus. This hiatus can be traced northward onto Goban Spur where it correlates with the early-mid Eocene hiatus (Masson and Parson, 1983). However, on Goban Spur this hiatus lies within the deformed sequence and at DSDP site 548 the deformation is associated with an early-late Oligocene hiatus of 4Ma duration (Poag et al, 1985; Sibuet et al, 1985).

In the western Melville Basin a significant unconformity separates the Oligocene from the Eocene. Unlike the continental slope, however, compressional deformation was absent during this interval. In well 72/10-1 late Oligocene calcareous mudstones overlie mid Eocene limestones (Bennet et al, 1985), and in well 73/1-1 mid Oligocene calcareous mudstones overlie mid Eocene sandstones. Early Oligocene sediments, apparently continuous with the Eocene sequence, were proven in wells 73/5-1, 73/7-1 and 73/14-1. Taken with the data from wells 72/10-1 and 73/1-1 this suggests that the erosional event in the Melville Basin was concentrated in mid Oligocene times, as at DSDP site 548 on Goban Spur.

In some areas the unconformity extends into the Miocene. In well 73/2-1 in the Melville Basin Miocene limestones overlie Eocene limestones. A similar hiatus has been described by Evans and Hughes (1984) in the western St. Mary's Basin where Miocene sediments overlie an Eocene palaeokarst surface (Figure 2.12(b)). The unconformity reaches its maximum magnitude over the western Cornubian Massif where the Miocene overlies Variscan basement from which Palaeogene and Cretaceous Chalk had been eroded during the preceding uplift (Figure 2.12(a)). Moving north-east from

the Melville Basin onto the Cornubian Massif the age of this transgression (the base of the Jones Formation) changes from late Oligocene to Miocene and progressively onlaps Palaeogene then Cretaceous and finally Variscan basement (Figure 2.12(a)).

In the central and eastern St Mary's Basin and the Brittany and South-West Channel Basins uplift was of greater magnitude than in the Melville Basin and pre-unconformity sediments outcrop on the seabed. The lack of post-unconformity sediments suggests that uplift in these areas may have continued into Miocene (Ziegler, 1987a) and possibly Pliocene times. In the Brittany and South-West Channel Basins, like the continental slope, this hiatus is associated with compressional deformation, and a major anticline was created (Figure 1.2).

In summary, a period of tectonic instability in the region is associated with a sedimentary hiatus of laterally variable extent. On the continental slope and in the Melville Basin, where the unconformity is of least magnitude, uplift appears to be concentrated in the early-mid Oligocene. However, in the surrounding areas, where the unconformity is larger, the mid Oligocene event is either of longer duration or incorporates discrete Eocene and Miocene erosional events. The variation in timing of the hiatus reflects complicated interaction between inherited post-Cimmerian subsidence, eustatic sea-level change, and compressional uplift. The Tertiary uplift of the Western Approaches Trough is discussed in Chapter 7.

2.9.4 Oligocene

Eocene-Miocene erosional event(s) have restricted the Oligocene and later sequence to the continental slope, the Melville Basin and isolated outliers.

The preserved pre-unconformity Oligocene sequence of the Melville Basin (wells 73/5-1, 73/7-1 and 73/14-1) comprises a thin sequence of early Oligocene shelf sandstones and limestones similar to that of the mid and late Eocene (Figure 2.1). On the continental slope pre-unconformity Oligocene sediments are restricted to Goban Spur where they comprise bathyal marly chalks (Figure 2.2).

After the Oligocene unconformity the region became tectonically quiescent and eustatic sea-level rise from the mid Oligocene to the mid

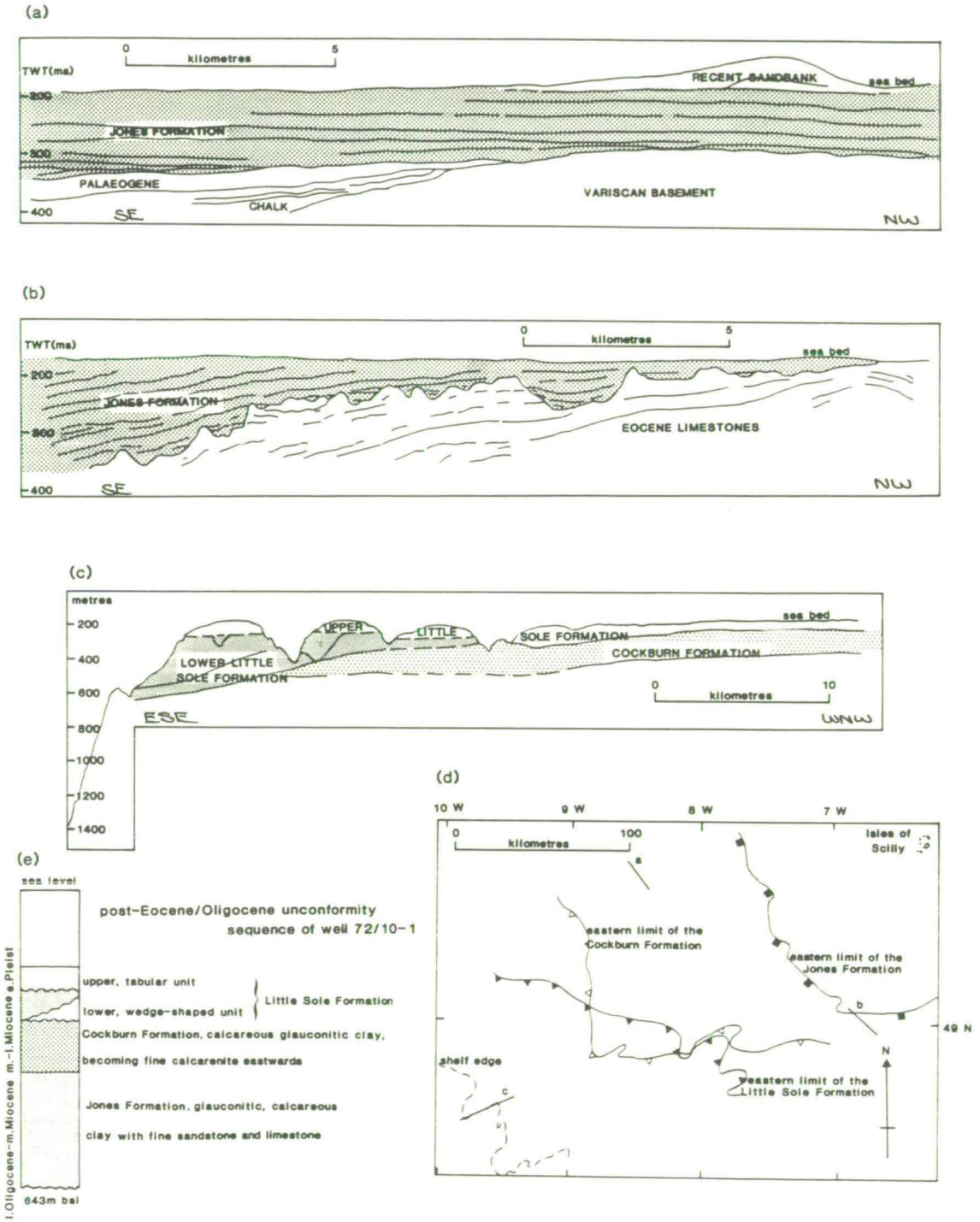

Figure 2.12 The post-Eocene/Oligocene sequence of the Western Approaches Trough.
(a)-(d) Evans and Hughes (1984) (e) modified from Evans (1986)

Miocene (Haq et al, 1987) led to the deposition of the transgressive Jones Formation in the Melville Basin (Figure 2.12). Jones Formation sediments have been recovered from wells 72/10-1 and 73/1-1 in the western Melville Basin (Figure 2.1) where they comprise calcareous mudstones and marly chalks grading upwards in the latter well into fine sandstones. In well 74/1-1 in the eastern Melville Basin they comprise limestones with fine sandstones. During the Oligocene Jones Formation sediments were largely restricted to the Melville and western Brittany Basins and the continental slope, in water depths progressively deepening as the transgression continued.

Post-unconformity sediments on Goban Spur comprise late Oligocene-Recent marly chalks and turbiditic silts cut by several submarine unconformities (Figure 2.2). The only unconformity correlatable between the wells is a mid-late Miocene hiatus probably associated with oceanic current circulation (Graciansky and Poag, 1985).

2.9.5 Miocene-Pliocene

In the Western Approaches Trough during the early Miocene the Jones Formation progressively onlapped more structurally positive areas including the western Cornubian Massif (Figure 2.12) and much of north-west France where isolated outliers are preserved. Its limits over south-west England are, however, problematical (Evans et al, in press). During the Miocene the Jones Formation was deposited in a shelf sea slightly deeper than the present (Jenkins and Shackleton, 1979).

The initiation of a regressive phase following the early Miocene transgression is indicated by the deposition of tidal sand ridges, assigned to the Cockburn Formation, in the Melville Basin (Evans and Hughes, 1984). The Cockburn Formation comprises a silty calcarenite, coarser than the Jones Formation, with carbonate content generally in excess of 80%. It was deposited in water depths less than 100m during the mid Miocene (Evans and Hughes, 1984). This shallowing was a precursor to the more significant mid-late Miocene regressive phase.

The Cockburn Formation is unconformably overlain by the dominantly clastic late Miocene-Pleistocene Little Sole Formation (Figure 2.12). Deposition of the late Miocene-Pliocene Lower Little Sole Formation was

restricted to within 15km of the shelf break (Figure 2.12(c)). Hence, the Lower Little Sole Formation and its basal unconformity represent a major mid-late Miocene regressive phase possibly correlatable with the mid-late Miocene hiatus on Goban Spur (Figure 2.2). The earliest Pleistocene Upper Little Sole Formation is conformable on the Lower Little Sole Formation on the continental slope. On the continental shelf, however, where it is more widespread than the Lower Little Sole Formation, they are separated by a Pliocene unconformity (Evans et al, in press).

Early Miocene transgression followed by mid Miocene regression culminating in the mid-late Miocene correlates well with the eustatic sea-level curve of Haq et al (1987). Hence these changes may be controlled by sea-level changes. However, tectonic uplift associated with Alpine compressions may also be a factor. The Pliocene unconformity on the outer continental shelf may similarly be associated with low late Pliocene sea-level (Haq et al, 1987), although Evans and Hughes (1984) suggested that the magnitude of Pliocene sea-level changes were not sufficient to account for the observed unconformity and that the outer shelf was uplifted during the Pliocene.

The Quaternary geology of the Western Approaches Trough is not discussed in this thesis and the reader is referred to Pantin and Evans (1984) and Evans et al (in press).

CHAPTER 3

POROSITY EVALUATION, SEDIMENT DECOMPACTION AND TECTONIC SUBSIDENCE

3.1 INTRODUCTION

Formation porosities are an essential "building block" in any quantitative basin history evaluation. Direct physical measurement from sidewall cores is the most reliable method of porosity evaluation. However, such rigorous analysis is generally only undertaken in potential reservoir horizons, and even in such horizons will not usually be available to the academic. In the absence of sidewall core data, porosities must be estimated remotely using readily available wireline log data.

In order to reconstitute the original depositional thickness of a buried sedimentary unit pore space lost during compaction must be replaced. This process, termed sediment decompaction, is described. Particular attention is given to the decompaction of uplifted, or overcompacted sediments. Decompacted sedimentary sequences can in turn be used to calculate the basement subsidence of a sedimentary basin in the absence of surface loads. This quantity, known as tectonic subsidence, can be compared with geophysical models of basin subsidence (Chapters 5 and 6).

3.2 POROSITY DEFINITIONS

Porosity is the ratio of void space, generally filled by liquids or gases, to the total bulk volume of the rock. It may be expressed either as a fraction of one or as a percentage, the latter being preferred in this study. Porosity type may be categorized in a number of ways, three of which are important in the following discussion.

3.2.1 Absolute and Effective Porosity

Absolute (or total) porosity encompasses both interconnected and isolated pores. Effective (or productive) porosity encompasses only the interconnected part of absolute porosity.

3.2.2 Primary and Secondary Porosity

Primary porosity originates during sedimentation due to void spaces between the matrix grains. Secondary porosity is generated during diagenesis by such processes as fracturing and chemical dissolution.

3.2.3 Intergranular and Intragranular Porosity

Intergranular porosity consists of void spaces between grains. Intragranular porosity occurs inside grains, and in the case of clay minerals is also referred to as interlayer porosity due to its position between sheets or layers of silicate minerals.

3.3 POROSITY ESTIMATION FROM WIRELINE LOGS

Single or paired sonic and nuclear (formation density and compensated neutron) logs are used for the estimation of formation porosities. The techniques have been widely reviewed (e.g. Dresser Atlas, 1974; Merkel, 1981; Schlumberger, 1987). The following draws on these reviews but highlights techniques of porosity evaluation appropriate for the decompaction and maximum depth of burial studies addressed here rather than for hydrocarbon exploration and production. Since details may be found in the above references only a very simplified outline of the operating principles of the tools is included.

3.3.1 Sonic Porosities

Sonic logs measure the shortest time for an acoustic pulse to travel through the formation. The acoustic pulse travels through a mixture of fast

matrix grains and slow formation fluids in the pore spaces. Hence the higher the porosity the slower the pulse travels through the formation as a whole. If matrix grain and formation fluid velocities are known, then the porosity of the formation may be calculated from its bulk velocity using Wyllie et al's (1956) equation.

$$\phi_s=(\Delta t_{log}-\Delta t_{ma})/(\Delta t_f-\Delta t_{ma}) \qquad (1)$$

where ϕ_s is the sonic porosity and Δt_{log}, Δt_{ma} and Δt_f are sonic log, grain matrix and formation fluid interval transit times (inverses of velocity) respectively

Since the sonic log measures the shortest time for an acoustic pulse to travel through the formation it circumvents any fracture or vugular porosity. Porosity of this type is generally secondary porosity, and may constitute a significant part of the total porosity, particularly in carbonate rocks (Merkel, 1981). The unsuitability of the sonic log for estimating total porosity is a serious drawback in the hydrocarbon field, but if porosities are being used to decompact a unit, or estimate its maximum depth of burial, it can be an advantage. Unless the "normal compaction curve" takes account of secondary porosity generation, its inclusion in the formation porosity will lead to an underestimate of the decompacted thickness of a sedimentary unit, or alternatively, an underestimate of maximum depth of burial.

Sonic logs do, however, have two serious drawbacks when used for porosity estimation. Firstly, in poorly consolidated, high porosity formations the sonic velocity is strongly influenced by the composition of the formation fluids through which it will be travelling for the majority of the time. Although most pronounced when the pore fluids change from brine to oil to gas, variations in brine concentration alone can influence sonic-derived porosity estimates in poorly consolidated formations. If, for example, a chalk of 50% porosity was wrongly assumed to have formation fluids of 20% NaCl brine, with the $\Delta t=189\mu sft^{-1}$ value typically used, when the formation fluid was actually a 10% NaCl brine ($\Delta t=208\mu sft^{-1}$), then with a calcite matrix velocity of $47.6\mu sft^{-1}$ the sonic porosity would be erroneously given as 56.7%. Merkel (1981) suggested that sonic porosities

are not reliable above 20%. Sonic porosities derived using 189μsft^{-1} as the interval transit time for formation fluids are significantly higher than density and neutron porosities in unconsolidated Chalk and Tertiary formations, and this is the probable cause.

Secondly, sonic porosities can be unreliable in shaly formations. Although the volumetric fraction of shale present in a unit can be readily estimated from gamma ray logs or paired log crossplots (e.g. Schlumberger, 1987), its precise effect on matrix velocities is difficult to assess. This is due both to the strong velocity anisotropy of shales and the actual variation in velocity of different clay minerals. The latter is largely associated with variation in the amount of interlayer porosity, and hence digenetic state, of the shale (Section 3.3.4).

3.3.2 Density Porosities

Density logs measure the electron density of the formation. Gamma rays fired into the formation are deflected by collisions with electrons (Compton scattering). The higher the electron density of the formation the greater the number of gamma rays which are deflected, through multiple collisions, back to the detector on the tool. For most common lithologies the ratio of the number of electrons per atom to the atomic mass number is very close to 0.5, hence electron density can easily be related to bulk density. If the density of the matrix grains and the formation fluids are known then porosity may be derived from the bulk density of the formation using an equation of the same form as equation (1).

$$\phi_D = (\rho_b - \rho_{ma}) / (\rho_f - \rho_{ma}) \qquad (2)$$

where ϕ_D is the density porosity and ρ_b, ρ_{ma} and ρ_f are density log, grain matrix and formation fluid densities respectively

On its own the density log is probably the most powerful tool for porosity evaluation (Merkel, 1981). However, in common with the sonic log it is difficult to determine matrix parameters in a shaly formation (Section 3.3.4).

3.3.3 Neutron Porosities

Neutron logs measure the hydrogen ion concentration of the formation. High energy neutrons fired into the formation lose energy on collision with larger atoms but the greatest energy loss occurs in "billiard ball"-type collisions with hydrogen nuclei of equal mass. When sufficiently slowed down the neutrons may be captured by nuclei such as chlorine, hydrogen or silicon which in turn emit a gamma ray of capture. Either gamma rays of capture, or slowed neutrons, are counted by the tool detector. These give a measure of the "hydrogen index" of the formation. No equation is required to determine neutron porosity, simply calibration of the tool against a standard.

"Hydrogen index" is equivalent to porosity if all the formation's hydrogen is contained in the form of liquids, and if these liquids completely occupy the total pore volume. Where hydrogen exists in a chemically bonded, intragranular state, such as in shales and gypsum, the neutron log will give an anomalously high porosity.

3.3.4 Neutron/Density Crossplot in Compaction Studies

It can be seen from the above that a single density or neutron log or, in compacted sequences, sonic log will suffice to derive porosities suitable for compaction studies in clean (shale-free) water-filled formations. Clean sandstones and limestones occur at certain limited stratigraphic horizons, but are far less common than shaly lithologies in the Western Approaches Trough. Even the Chalk contains a significant shale component. Assuming a two component system (e.g. shaly sandstone or shaly limestone) the data from any two of the above three logs may be combined to correct porosities for shaliness. The neutron/density combination (or crossplot) is the most popular technique because even when compositional volumes are in error (e.g. the formation is not a simple two component system) the porosity value will be essentially correct (Schlumberger, 1987). Due to this, and the unreliability of sonic porosities in uncompacted formations, the neutron/density combination has been used in this study.

Figure 3.1 shows typical neutron/density crossplots for determining porosity and shale volume in a shaly sand and their construction is

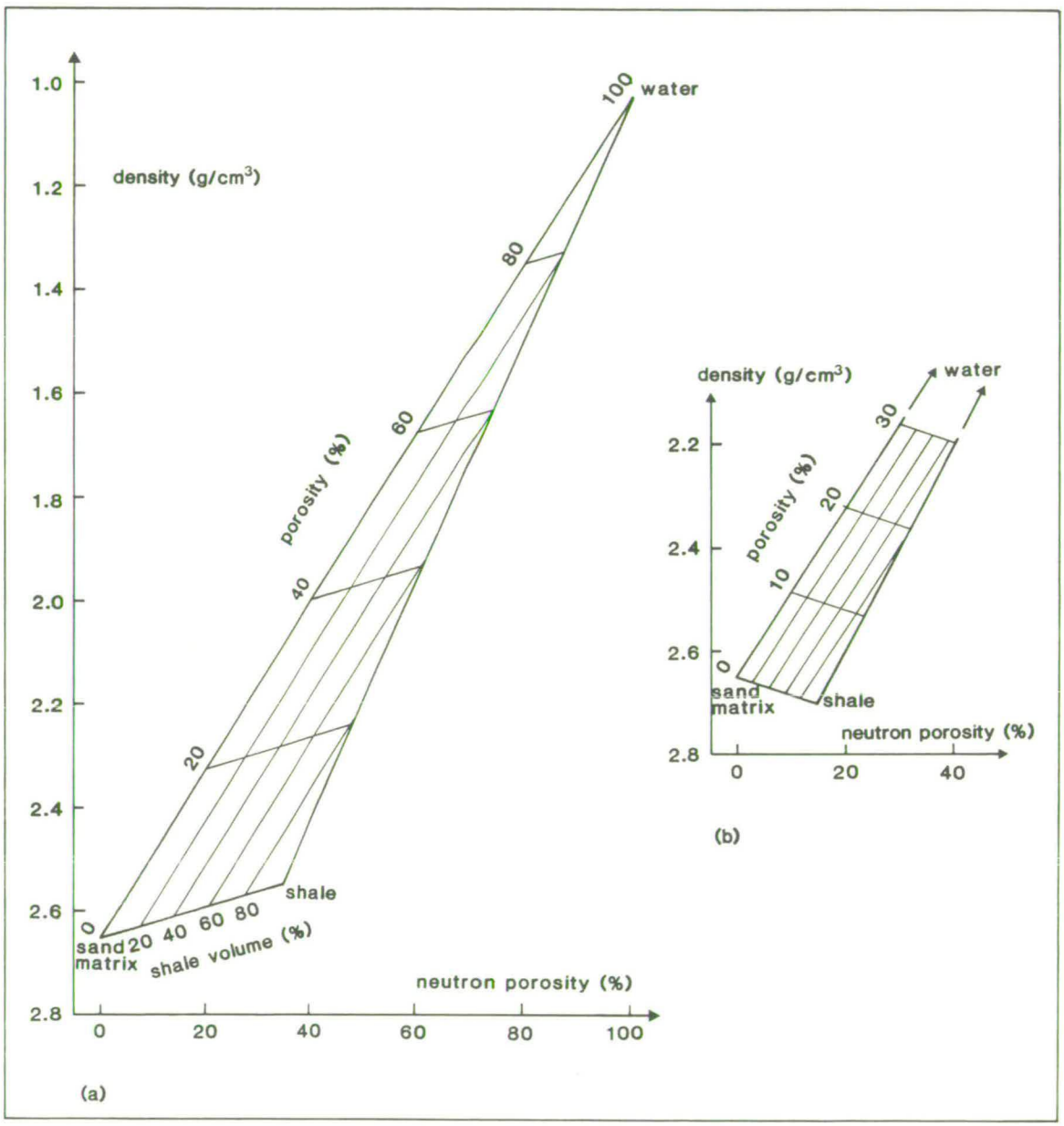

Figure 3.1 Typical neutron–density crossplots used for porosity and lithology evaluation in shaly sands
(a) shale point for clay mineral assemblage dominated by swelling clays
(b) shale point for clay mineral assemblage dominated by non-swelling clays

explained below. The procedure for shaly carbonates is identical except that the sand point is replaced by a calcite or dolomite point as appropriate.

The triangle of Figure 3.1(a) is similar to that used by sedimentary petrographers in classifying the lithology of a three component rock type. Here the triangle is defined by a water point (density=1.03gcm^{-3}, neutron porosity=100%), a sand matrix point (density=2.65gcm^{-3}, neutron porosity=0%) and a more problematical shale point. Points will plot in the triangle according to their percentage volume of water, sand and shale components. Clay minerals are the dominant matrix components of shales, and to position the shale point their properties must be understood.

Clay minerals may be divided into swelling (e.g. smectite and vermiculite) and non-swelling (e.g. illite and chlorite) types. The swelling types contain interlayer (intragranular) water and may be converted during diagenesis by expulsion of water from the interlayer sites to mixed phases and, with further dehydration and cation exchange, to non-swelling types (right hand side Figure 3.2). The water escape curve (left hand side Figure 3.2) for this diagenetic sequence shows an early peak of water escape due to intergranular water expulsion, and a second peak due to interlayer water expulsion as the swelling clays alter to non-swelling clays. The problem is how to define the shale matrix point when clay minerals, unlike quartz or calcite, change their physical properties during diagenesis.

Shales have no effective (productive) porosity due to their low permeability, hence for hydrocarbon applications the shale point is simply taken from the nearest pure shale in the sequence (Schlumberger, 1987). This will have zero effective porosity. Such a shale point will not necessarily have zero absolute porosity. In compaction studies the absolute intergranular porosity is the quantity with which we are concerned. Consider, for example, a shale unit of any given thickness. It would always decompact to the same thickness, regardless of its present burial depth, if its effective porosity (zero) was considered. Decompaction of the shale component of a dirty sandstone would similarly be independent of burial depth. Ideally in compaction studies the shale point would be defined by the neutron and density responses to the appropriate clay mineral assemblage with zero absolute intergranular porosity. Swelling clay assemblages with zero absolute intergranular porosities are, however, rare because the overburden pressure and/or temperature required to expel all

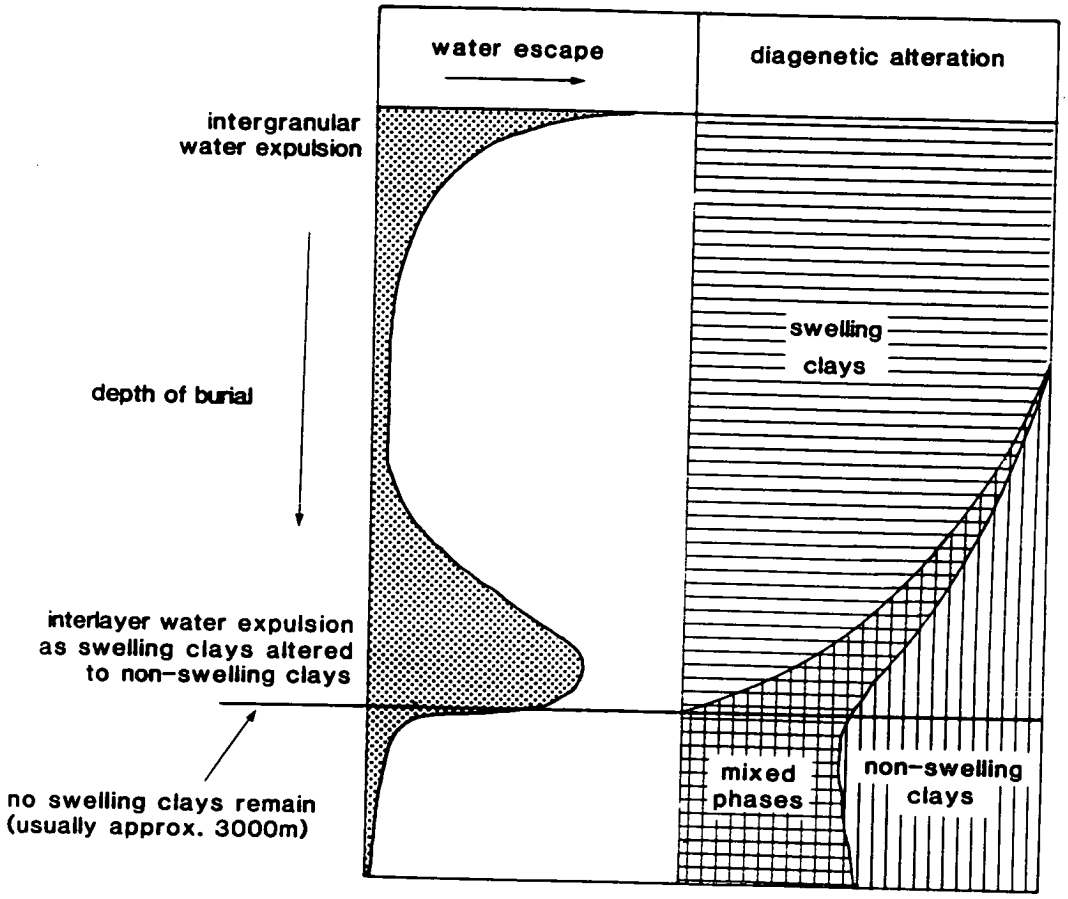

Figure 3.2 Compaction history of a swelling clay (modified from Powers, 1967).

the intergranular water will also tend to expel the intragranular water, converting them to non-swelling clays (Figure 3.2).

An empirical solution to this problem has been derived from Powers' (1967) model for the diagenesis of clay minerals (Figure 3.2). Pure shales in the depth range 1.5-2.0 km were used to position the shale point for all overlying shaly lithologies (Figure 3.1(a)). Clay minerals in this depth range should not have undergone significant alteration from swelling to non-swelling types but should have lost the majority of their intergranular water. Reasonably pure shales can usually be found in this depth zone in the late Triassic of the Western Approaches Trough. Since this shale point will still have some absolute intergranular porosity the technique will still underestimate the absolute intergranular porosity, but less so than if

shallow shales had been used to position the shale point. Considering Figure 3.1, if the absolute intragranular porosity of the shale point is 5% then actual porosity is approximately 1% greater than apparent porosity for a sandstone with 20% clay mineral content increasing to approximately 3% greater at 60% clay mineral content (shales with a clay mineral content greater than 60% are rare in the Western Approaches Trough).

The shale point for pre-late Triassic units was taken from the most deeply buried shale in the well (Figure 3.1(b)). This should give the density and neutron log responses of a zero absolute porosity shale dominantly composed of mixed and non-swelling clay mineral phases. If pure shales in the appropriate depth zone were not present in the well under consideration shale points were taken from the nearest suitable well. This is an approximate technique, but without independent data on the amount of intragranular water in every shaly unit being decompacted greater accuracy is not possible.

Although neutron/density crossplots are only required for porosity estimation in shaly units, all units were crossplotted in order to obtain consistent lithology identification. Clean sandstones were defined as containing $\leq$15% clay mineral volume, shaly sands between 15 and 40%, and shales $\geq$40%. In order to reduce the influence of localized porosity variation, whether due to processes such as secondary porosity creation, or due to data spikes, the values for each recorded depth represent an average value. Each data point is the midpoint of a 10m or 40ft interval, in wells recorded in metric and imperial units respectively. The logs were sampled every 20m in metric wells and every 100ft in imperial wells. In the French wells neutron logs were not always run in combination with density logs; over such intervals shaliness was estimated from the gamma ray log and combined with density to crossplot the formation.

Unreleased core analysis data show that for certain cored sandstones in wells 73/4-1, 73/14-1, 87/14-1, Brezell-1, Lennket-1 and Lizenn-1 log-derived porosity estimates are accurate within 1-2%.

Porosity-depth plots derived using the above neutron-density technique for individual wells are shown in Figure 3.3 while Figure 3.4 shows summarized plots for the major lithologies.

Figure 3.3 Well porosity–depth plots from neutron–density crossplots

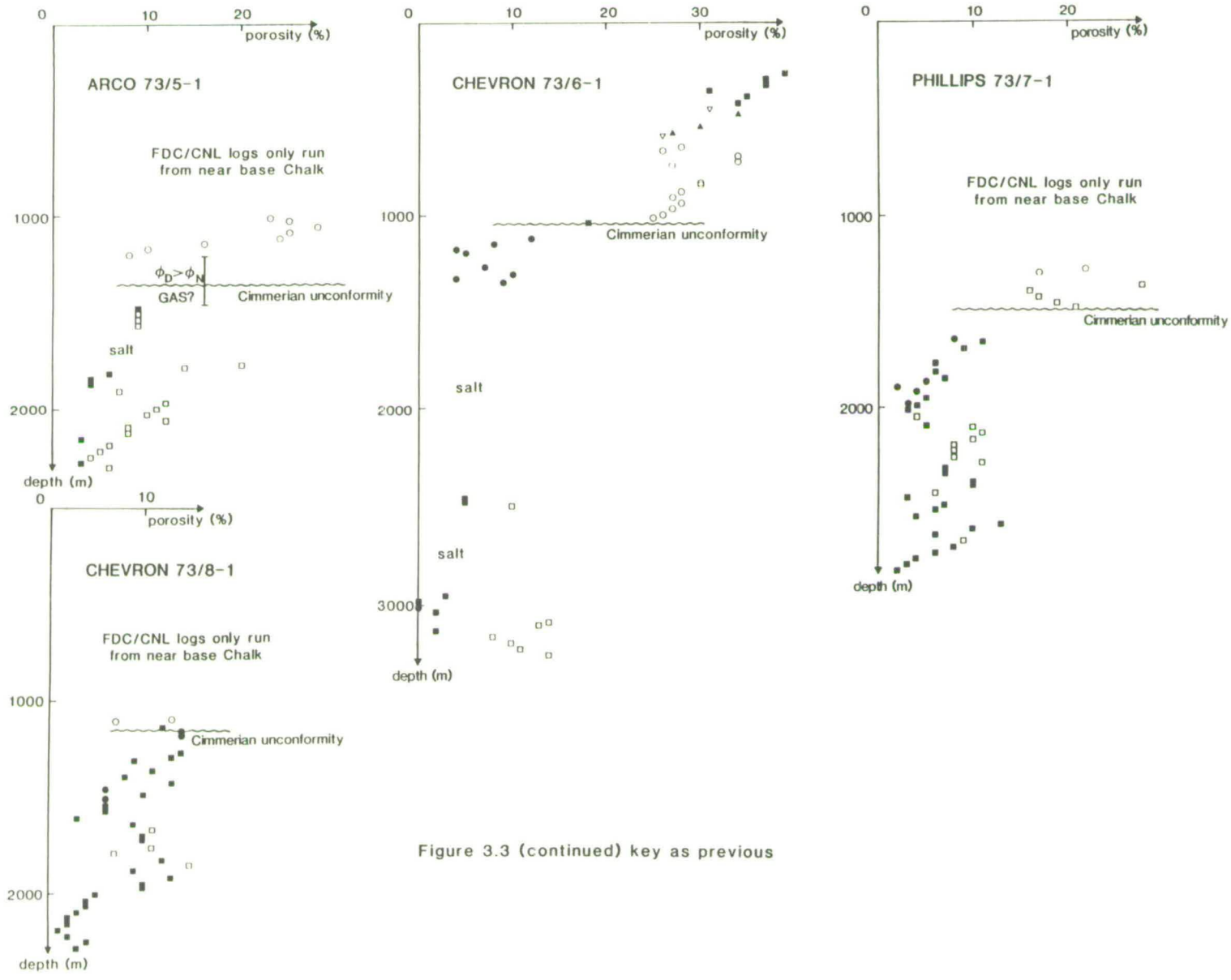

Figure 3.3 (continued) key as previous

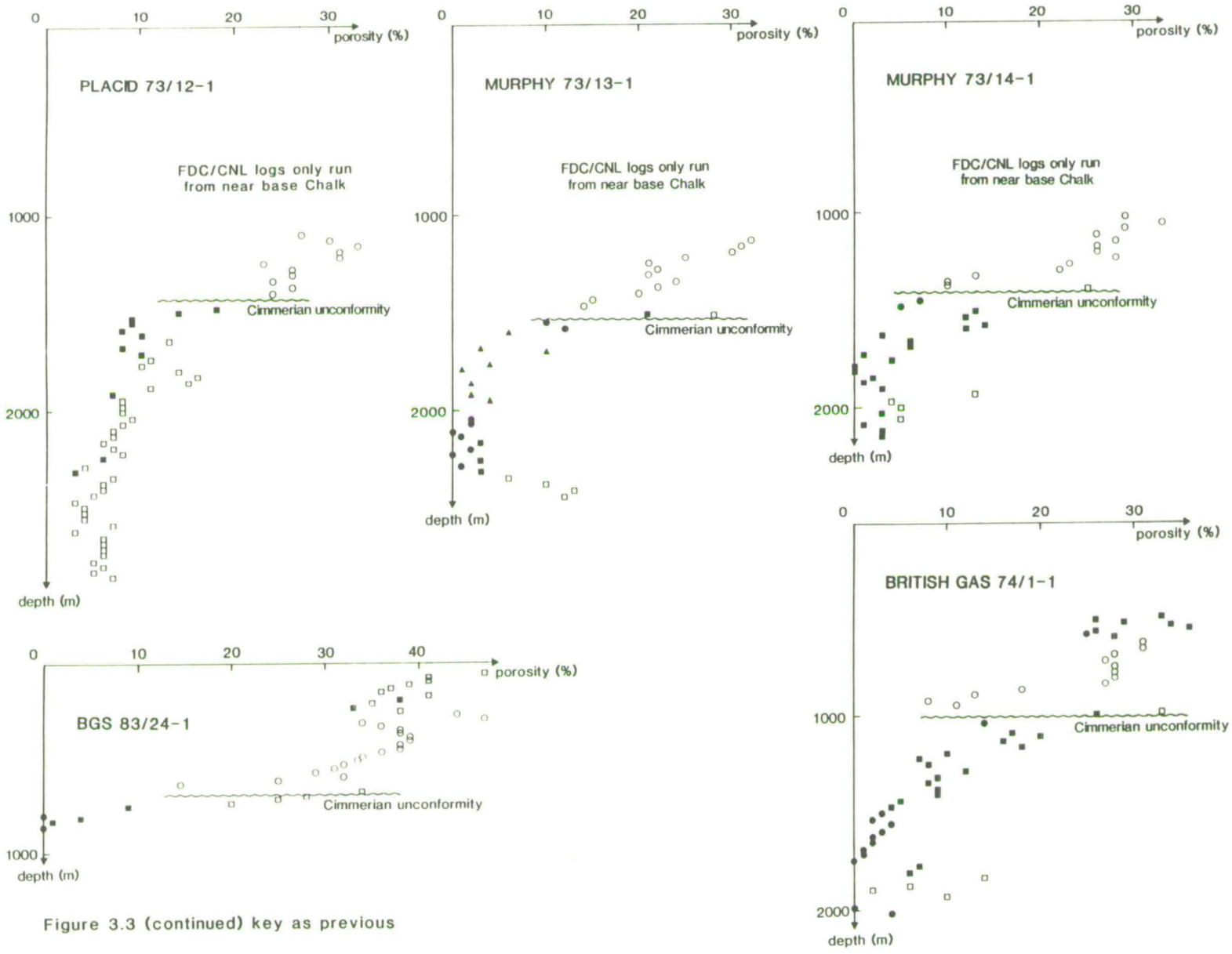

Figure 3.3 (continued) key as previous

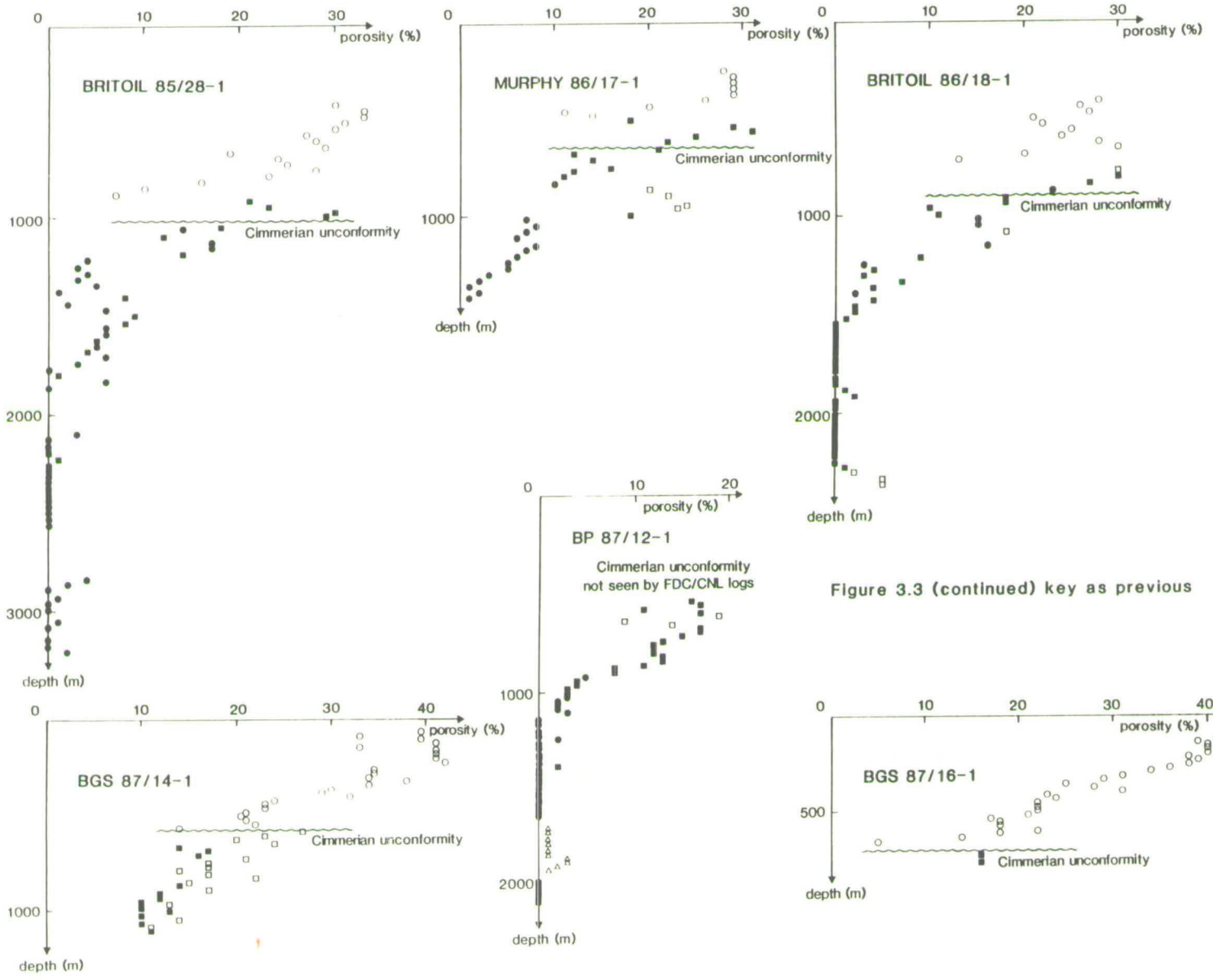

Figure 3.3 (continued) key as previous

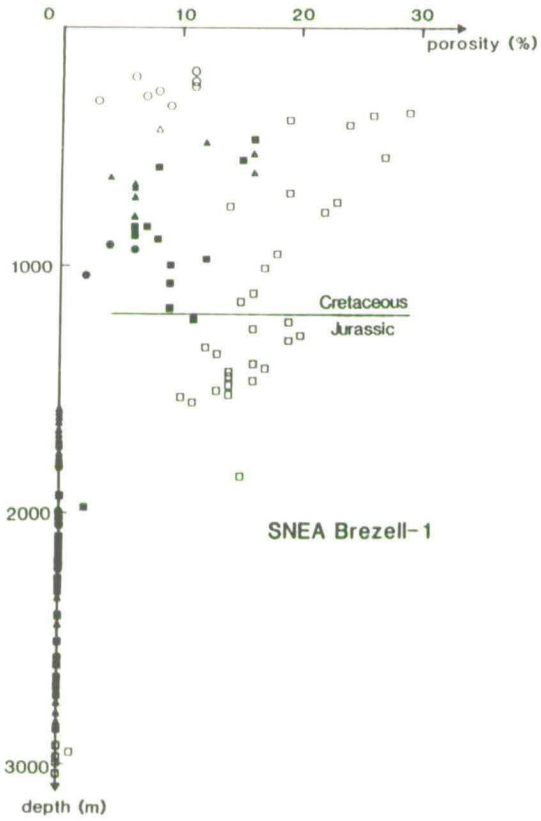

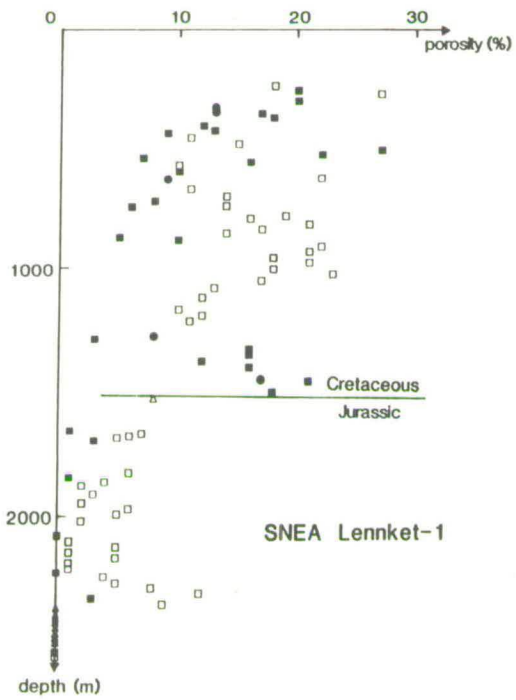

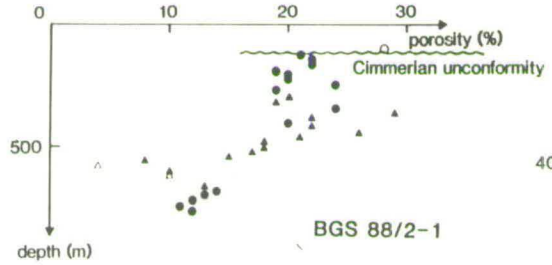

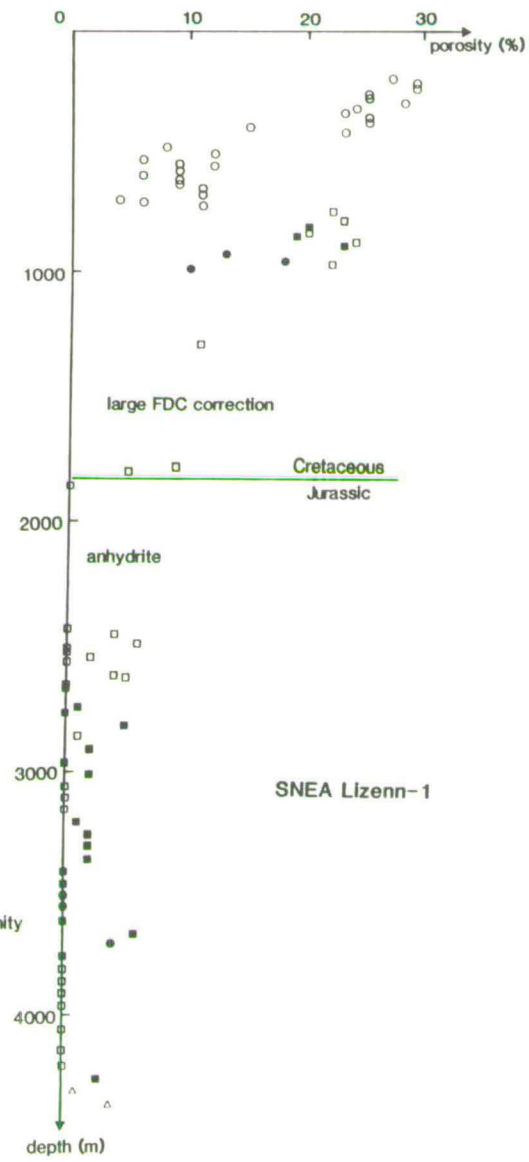

Figure 3.3 (continued) key as previous

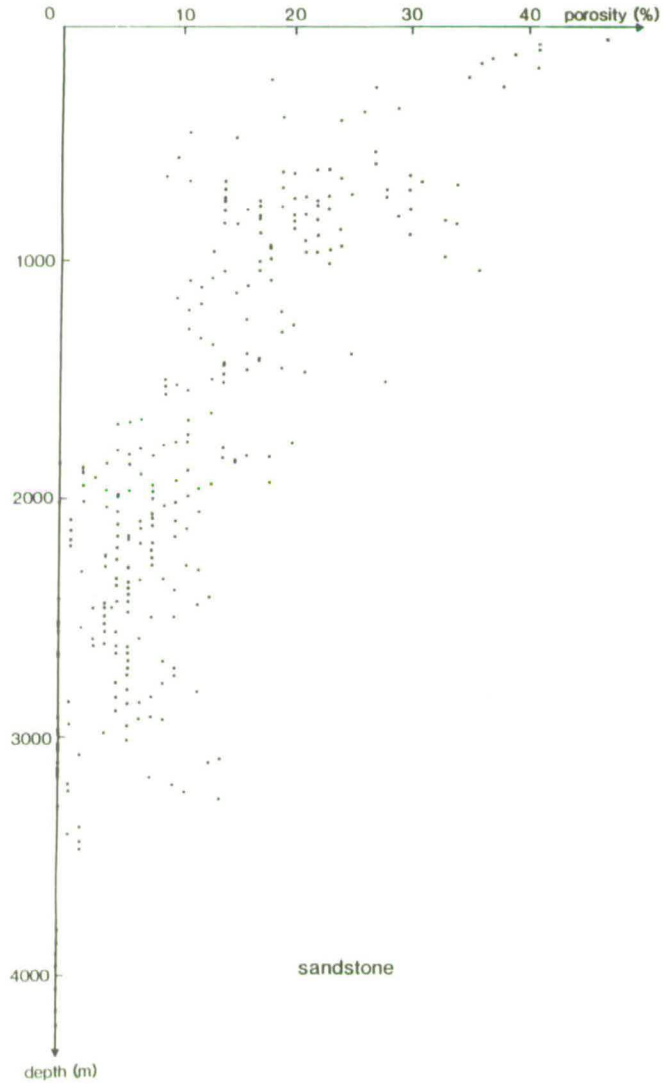

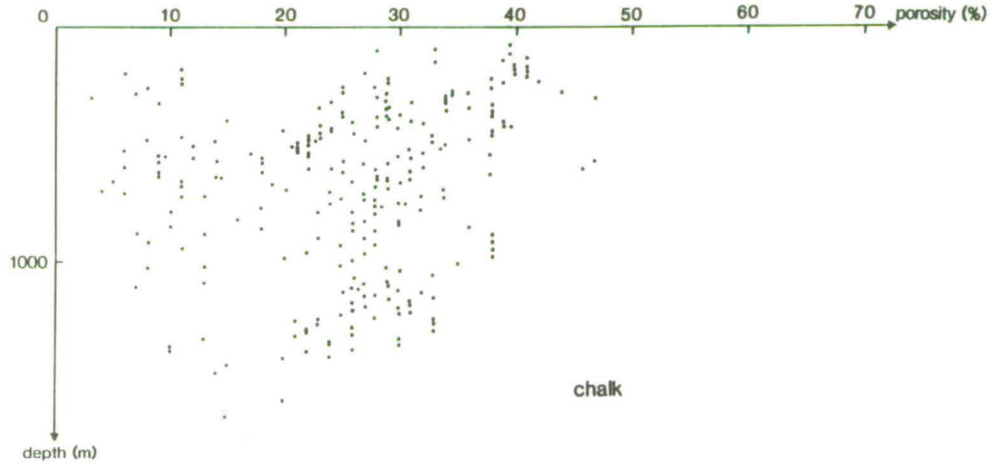

Figure 3.4 Lithology porosity–depth plots from neutron–density crossplots

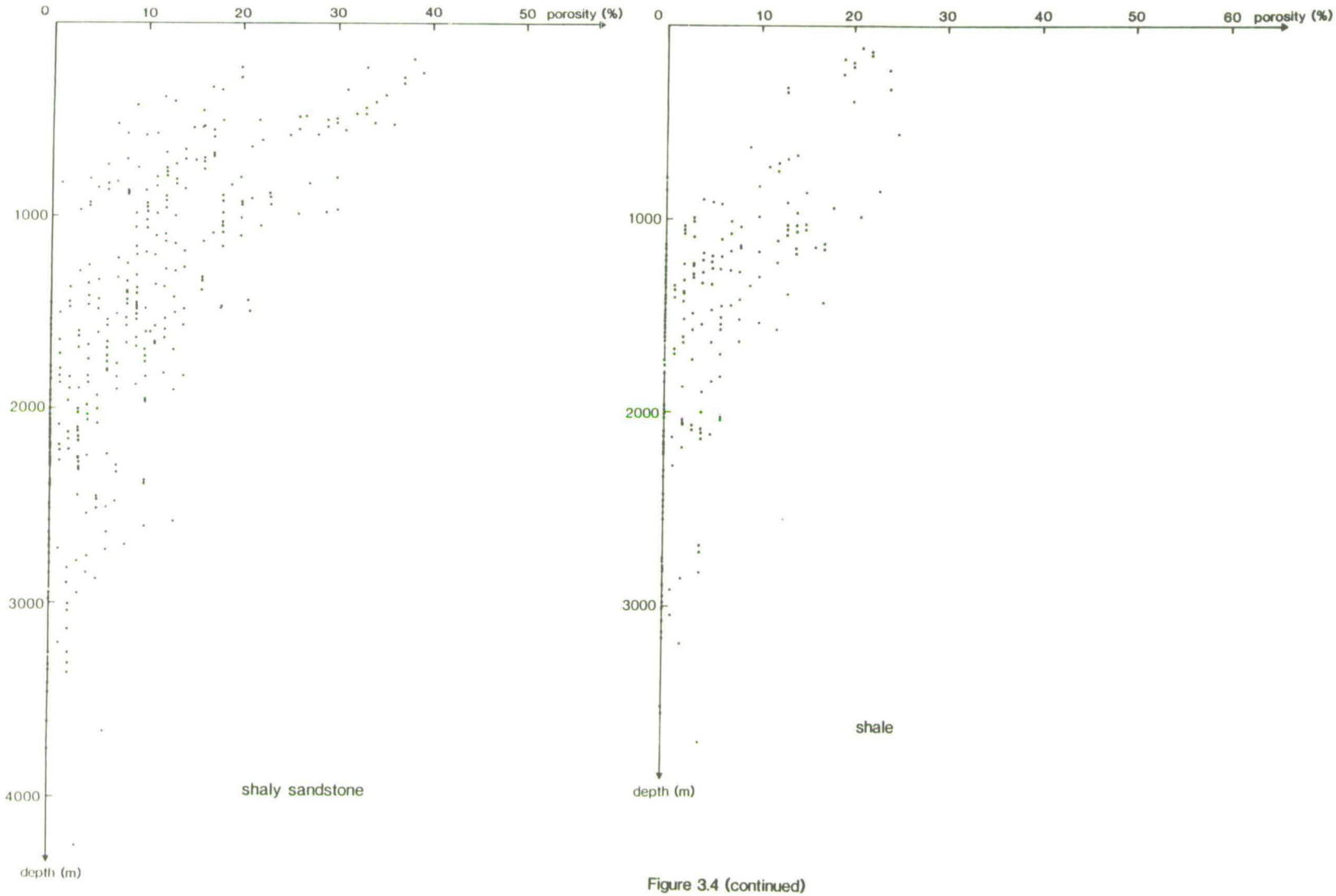

Figure 3.4 (continued)

3.4 PRINCIPLES OF SEDIMENT DECOMPATION

In order to reconstruct a curve of basement subsidence beneath a sedimentary sequence the loading effect of successive layers of sediments must be backstripped. In doing this, account must be taken of the decompaction of the sediments. As a unit is buried pore fluids are expelled and its volume, or thickness, decreases, as illustrated by the porosity-depth plots of Figures 3.3 and 3.4. To reconstitute the initial thickness of a sedimentary unit as it decompacts the pore space is "replaced", by sliding it back up its porosity-depth curve.

The mean density of a sediment pile will generally decrease as units are backstripped and the total thickness of the sediment pile drops. This must be taken into account when calculating the gravitational loading effect of the sediment column on the subsidence of the underlying basement (Sections 3.6.4 and 3.7).

To illustrate the technique of backstripping in Figure 3.5 the decompacted depth to the Cimmerian unconformity "basement" in well 73/13-1 is calculated by removing and decompacting the overlying sediment sequence unit-by-unit. The top unit (1), from which there are no well returns, is removed first and the underlying units are decompacted, increasing in thickness. This thickness increase counteracts the removal of the top 400m of sediments, hence the decrease in decompacted depth to "basement" from the present to the end of the Eocene with removal of the topmost 400m is only 240m. The late Eocene limestone is removed next, its thickness has increased from 150m (2) to 200m (2a) due to the removal of the top unit, however, the decompaction of the underlying sediments as the 200m of limestone is removed counteracts this. Hence the decrease in depth to the "basement" from the end to the beginning of the late Eocene with removal of the 200m of limestone is only 130m. This continues until approximately the middle of the sequence when the decompaction of the unit being removed becomes greater than the decompaction of the underlying units due to its removal, and decompacted depths to "basement" change by more than the present-day thickness of the unit being backstripped. Decompacting a sediment sequence hence predicts more rapid early and slower later subsidence than present well thicknesses. An important assumption is that

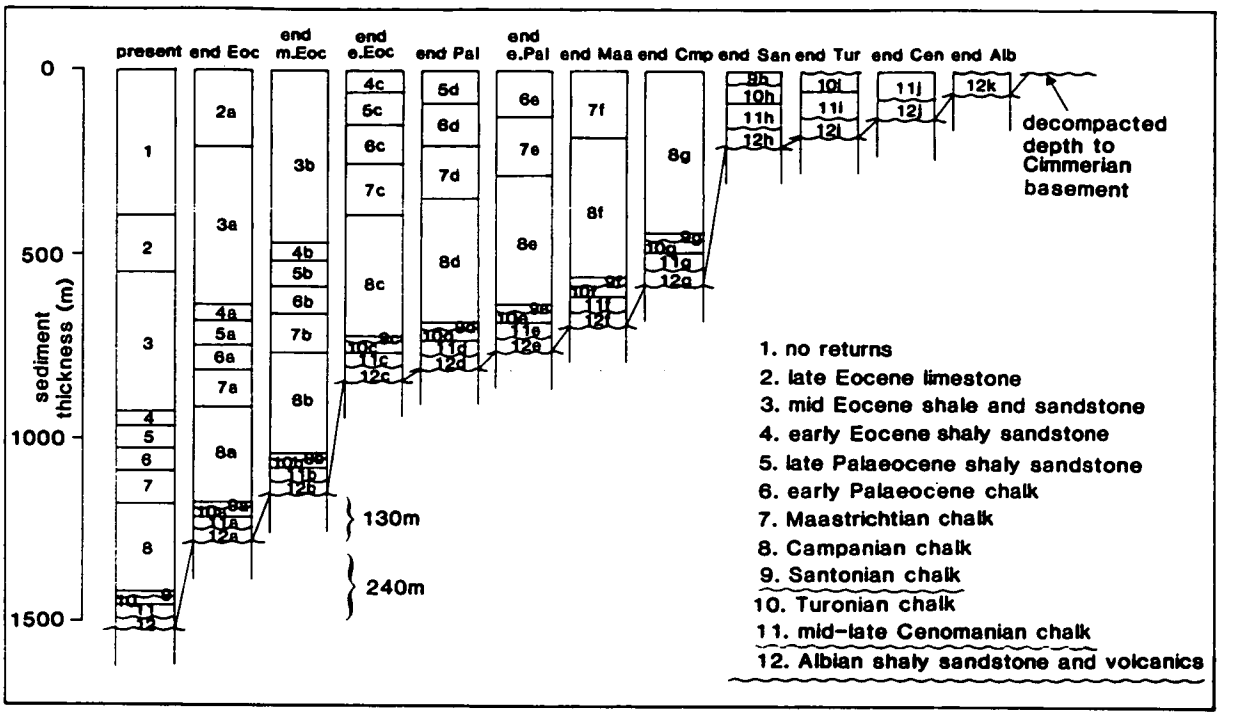

Figure 3.5 Progressive decompaction of the post-Cimmerian sequence, well 73/13-1.

levels beneath compaction basement are fully compacted prior to the onset of sedimentation and do not compact further during subsequent deposition.

This sediment decompaction technique is adopted from that of Sclater and Christie (1980). It has been used in this study with porosity-depth parameters derived from the Western Approaches Trough (Section 3.5) and modifications for the effect of uplift (Section 3.6).

3.5 POROSITY-DEPTH RELATIONS AND SEDIMENT DECOMPACTION IN THE WESTERN APPROACHES TROUGH

A variety of well- and lithology-specific porosity-depth curves have been used in sediment decompaction. Steckler and Watts (1978) decompacted all lithologies by sliding them up a well-average porosity-depth profile. Sclater and Christie (1980) and Falvey and Deighton (1982) decompacted units up lithology-specific porosity-depth curves; the former of the form,

$$\phi_z = \phi_o e^{-cz} \qquad \text{(after Rubey and Hubbert, 1959)} \qquad (3)$$

and the latter of the form,

$$1/\phi_z = 1/\phi_o + kz \qquad (4)$$

where ϕ_z and ϕ_o are porosity at depth and surface porosity respectively, z is the depth of the sediment, and c and k are constants.

The irregularity of porosity-depth relations in individual wells (Figure 3.3) suggests that decompaction should be lithology- rather than well-specific. However, even the lithology-specific data are so scattered that the best fit curves (ii) and (iii) shown in Figure 3.6 poorly constrain them. Hence decompaction up these curves will be inaccurate. It is not apparent, due to the scatter of the data in Figure 3.6, whether the Rubey and Hubbert (1959) relation, curve (ii), or that of Falvey and Deighton (1982), curve (iii), gives a better fit.

The wide scatter of porosity data is largely due to Tertiary uplift (Chapter 7). Formations with low porosities have been buried to greater depth than those at which they are now seen and the low porosities acquired at these depths have been retained following uplift. In order to decompact sediments in uplifted wells their undisturbed porosity-depth trend and the amount of uplift must be known. Undisturbed porosity-depth relations have been defined by combining likely surface porosity values with the "maximum envelope" to the present porosity data (Figure 3.6 curve (i) and Table 3.1). In an uplifted basin any normally compacting sediments, either post-uplift, or in wells not subject to significant uplift, will define the "maximum envelope" to the observed porosity-depth data.

Likely surface porosities have been taken from the literature. Scholle (1977, Figure 5) suggested 70% for normally compacting chalk. Limestone surface porosity was also taken to be 70%. Schlumberger (1974) suggested 63% for North Sea shales, while Pryor (1973) showed that sandstone surface porosity is facies-dependent; river point bars averaged 41%, beach sands 49%, and dune sands 49%. A simple average of these facies, 46%, was taken to represent the varied sandstone facies of the Western Approaches Trough. Shaly sandstone surface porosity was taken as the average of the shale and sandstone values.

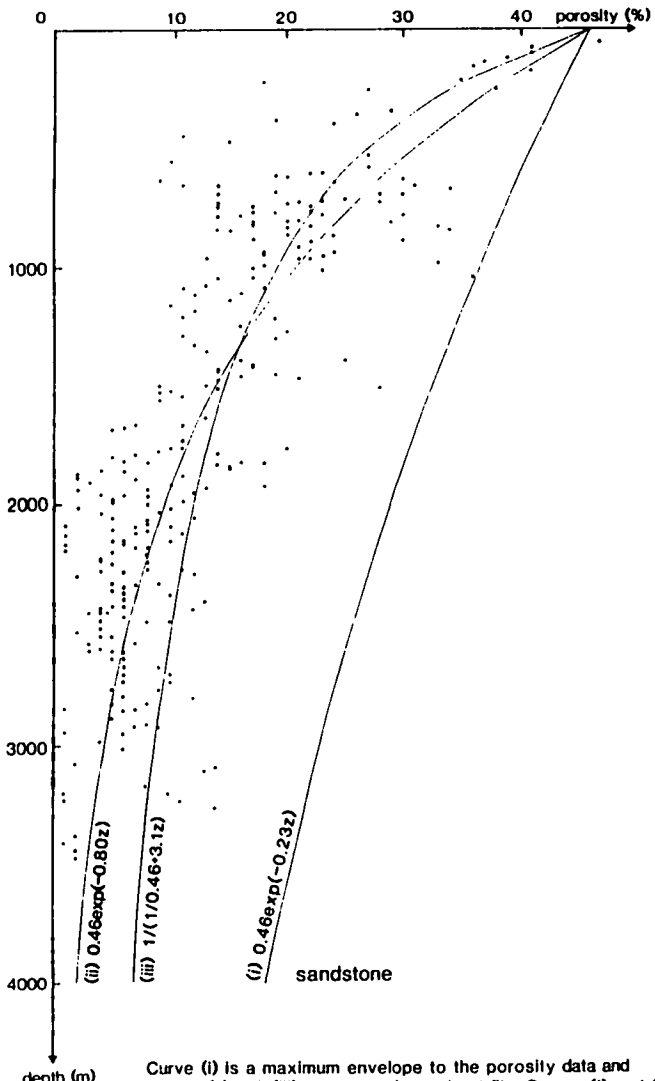

Curve (i) is a maximum envelope to the porosity data and curves (ii) and (iii) are approximate best fits. Curves (i) and (ii) are of the form of Rubey and Hubbert (1959) and curve (iii) is after Falvey and Deighton (1982).

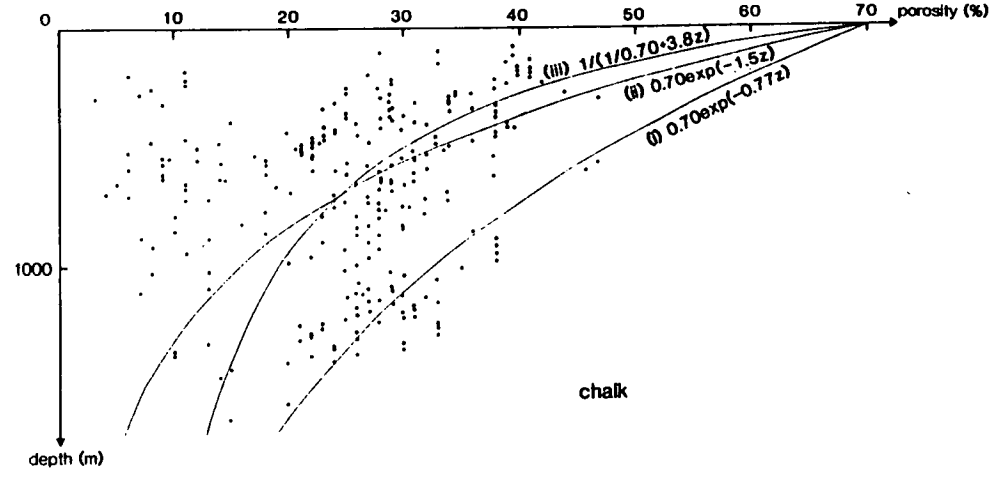

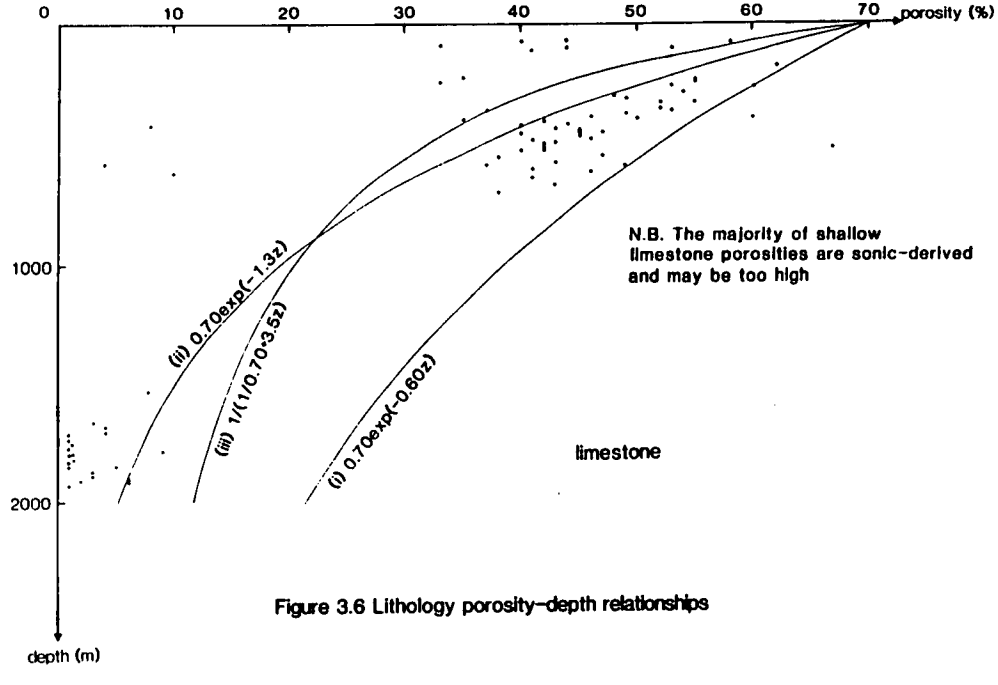

Figure 3.6 Lithology porosity–depth relationships

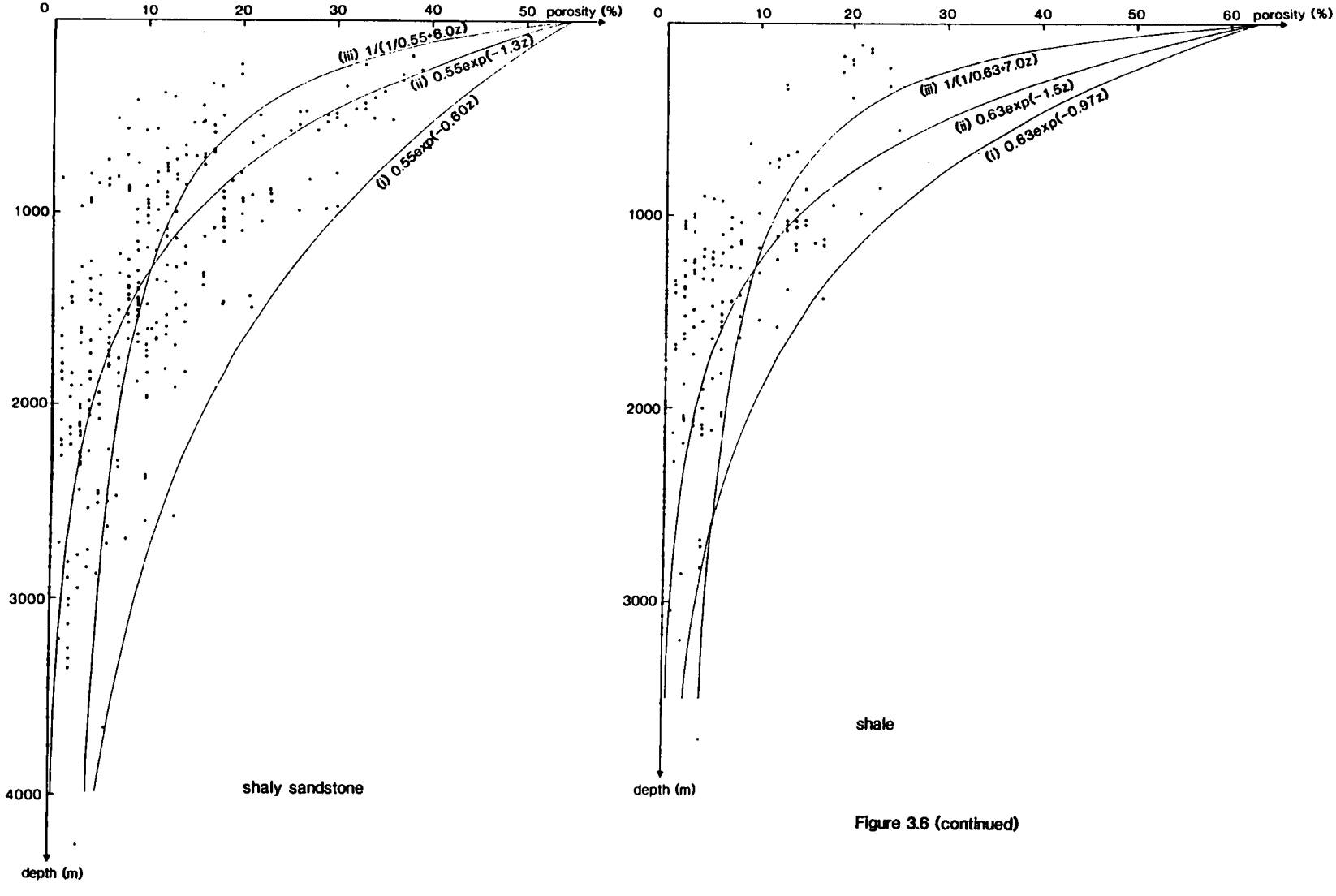

Figure 3.6 (continued)

There is, in fact, a large body of sedimentological data on surface porosity values, and those used here may be in error for individual units. However, detailed sedimentological analysis of each unit being decompacted, such as is only undertaken over cored horizons, would be required to systematically remove this error.

Table 3.1 Porosity-depth parameters and sediment grain (matrix) densities used in decompaction and sediment unloading. Derivation of porosity-depth parameters discussed in text; sediment grain densities after Schlumberger (1987), except the density of volcanics which was taken from density log data.

lithology	ϕ_0 (%)	c ($\times 10^{-5} cm^{-1}$)	ρ_{ma} (gcm^{-3})
sandstone	46	0.23	2.65
shaly sandstone	55	0.60	2.68
shale	63	0.97	2.72
chalk	70	0.77	2.71
limestone	70	0.60	2.71
salt	1	0.01	2.15
volcanics	1	0.01	2.50

The empirical curves for sandstone, shaly sandstone, shale, chalk and limestone (Figure 3.6 and Table 3.1) were combined, with appropriate weighting, to predict the decompaction behaviour of any mixed litholgy units, such as early Jurassic interbedded shales and limestones. Salt and igneous intervals both lack primary porosity and do not change in thickness during well decompaction.

3.6 DECOMPACTION OF UPLIFTED SEDIMENTARY SEQUENCES

If a sedimentary sequence, such as that of the Western Approaches Trough, has been uplifted, overcompaction of the pre-uplift units, and their non-compaction during later burial must be considered. Three types of uplift and later subsidence patterns can be distinguished in terms of their treatment in sediment decompaction.

3.6.1 Uplift With No Later Subsidence

This is the most straightforward case. The amount of uplift is simply added to the present burial depths and the sequence is then decompacted up the undisturbed porosity-depth curve. Figure 3.7 shows decompacted depths to the Cimmerian unconformity in well 86/17-1 with (dashed) and without (dotted) allowance for Tertiary uplift. The solid line shows backstripped depths to the Cimmerian unconformity uncorrected for decompaction. The inclusion of sediments removed during Tertiary uplift produces a subsidence pulse in the Eocene-Oligocene due to the deposition of these sediments, as shown by the dot-dash line. It also causes the underlying, preserved, sediments to decompact by a greater amount than if they had been decompacted without allowance for Tertiary uplift. Eocene/Oligocene uplift has been treated this way in the decompaction of the post-Cimmerian sequence in wells 86/17-1, 87/12-1, 87/14-1 and 87/16-1 (Chapter 6).

3.6.2 Uplift of Greater or Equal Magnitude to Later Subsidence

Figure 3.8 shows the decompaction of well 72/10-1 with (dashed) and without (dotted) allowance for the 600m of Tertiary uplift. Unlike well 86/17-1, however, subsidence recommenced following uplift, and 500m of post-uplift sediments were deposited. Since Tertiary uplift was of greater magnitude than later subsidence the pre-uplift (Eocene and earlier) units will not have compacted during deposition of the post-uplift sequence. The uplift unconformity can thus be treated as decompaction basement during decompaction of the post-uplift (Oligocene and later) sequence, as shown by the dashed line. The pre-Eocene sediments are decompacted as a separate

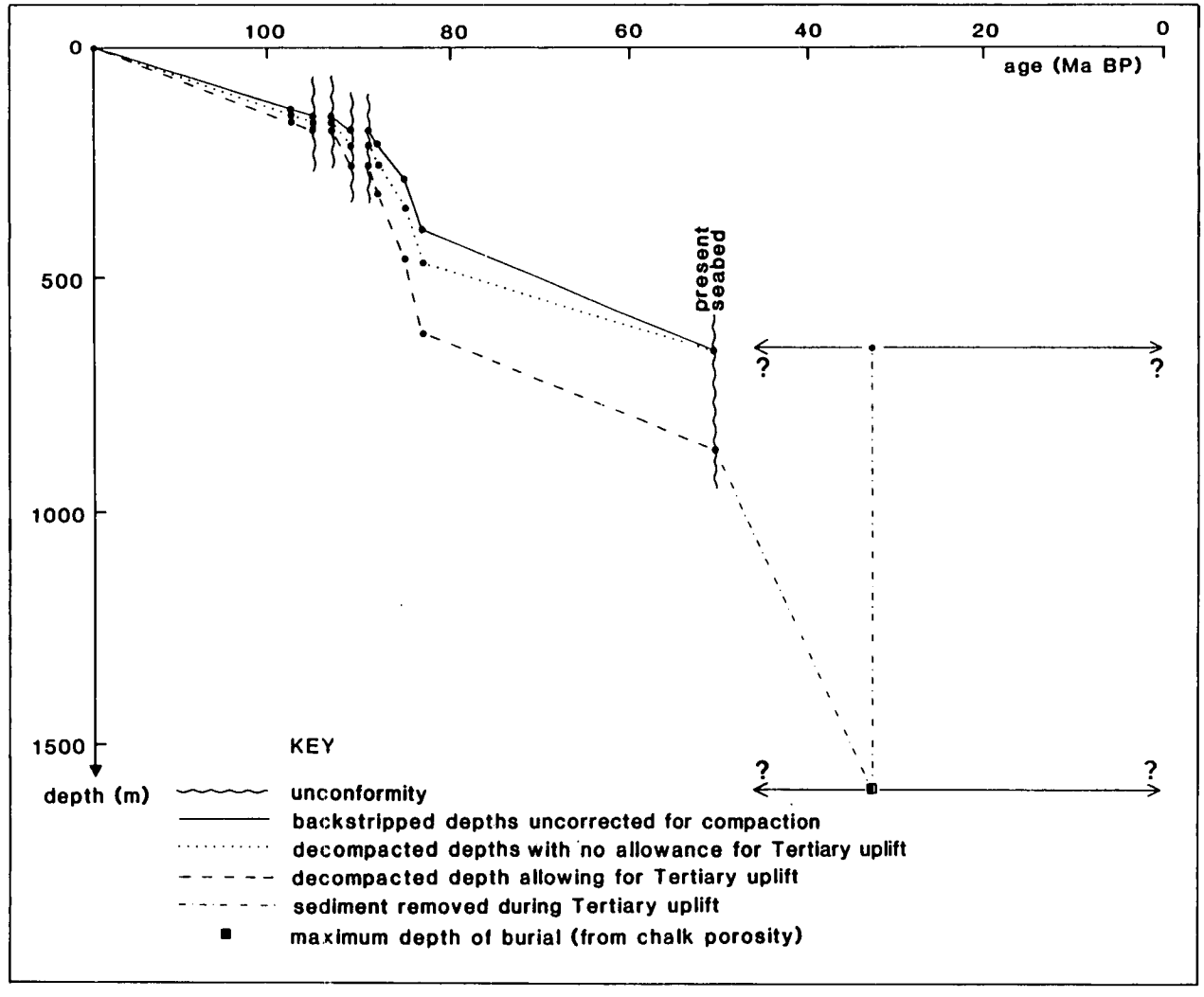

Figure 3.7 Decompacted depths to Cimmerian unconformity with and without allowance for Tertiary uplift, well 86/17-1. See text for discussion.

sequence, with the insertion of a topmost unit 600m thick removed during uplift, the dot-dash line between 42 and 36Ma.

Eocene/Oligocene uplift has been treated in this way in the decompaction of the post-Cimmerian sequence in all wells other than those cited in Section 3.6.1. Cimmerian uplift has also been implicitly treated in this way in the post-Cimmerian subsidence curves of Chapter 6, where Cimmerian basement has been taken as decompaction basement. The magnitude of Cimmerian uplift, although difficult to estimate, is believed to be of similar magnitude to post Cimmerian subsidence (Section 5.2.3).

3.6.3 Uplift of Lesser Magnitude Than Later Subsidence

If uplift is of lesser magnitude than later subsidence, then the pre-uplift sequence will not initially compact during the deposition of the post-uplift sediments, but will again start to compact once it has been buried beyond its previous greatest depth of burial.

No wells have been specifically treated in this way. It is in fact a drawback of uplift estimation from porosities that uplift of lesser magnitude than later subsidence can not be "seen" (Section 7.4). Such Tertiary uplift probably did occur in wells 73/1-1, 73/12-1 and 73/13-1. Their chalk porosities lie on the normal compaction trend (Figure 7.1), and hence they are at their greatest depth of burial. However, uplift is observed in the surrounding wells, and it is probable that wells 73/1-1, 73/12-1 and 73/13-1 were also uplifted, but by a smaller amount than later subsidence. Hence the true case for these wells probably lies between the extremes of no, and maximum Tertiary uplift shown in Figure 6.7, but its exact definition is not possible.

3.6.4 Uplift and Sediment Densities

Although pre- and post-uplift sequences can be decompacted separately, the density of the entire sequence must be considered when calculating the effect of sediment loading on subsidence (Section 3.7). Figure 3.8 shows the evolution of the average density of the sediment column in well 72/10-1. The pre-uplift units in well 72/10-1 attained an average density of $2.06 gcm^{-3}$ immediately prior to uplift. Following uplift, with removal of the

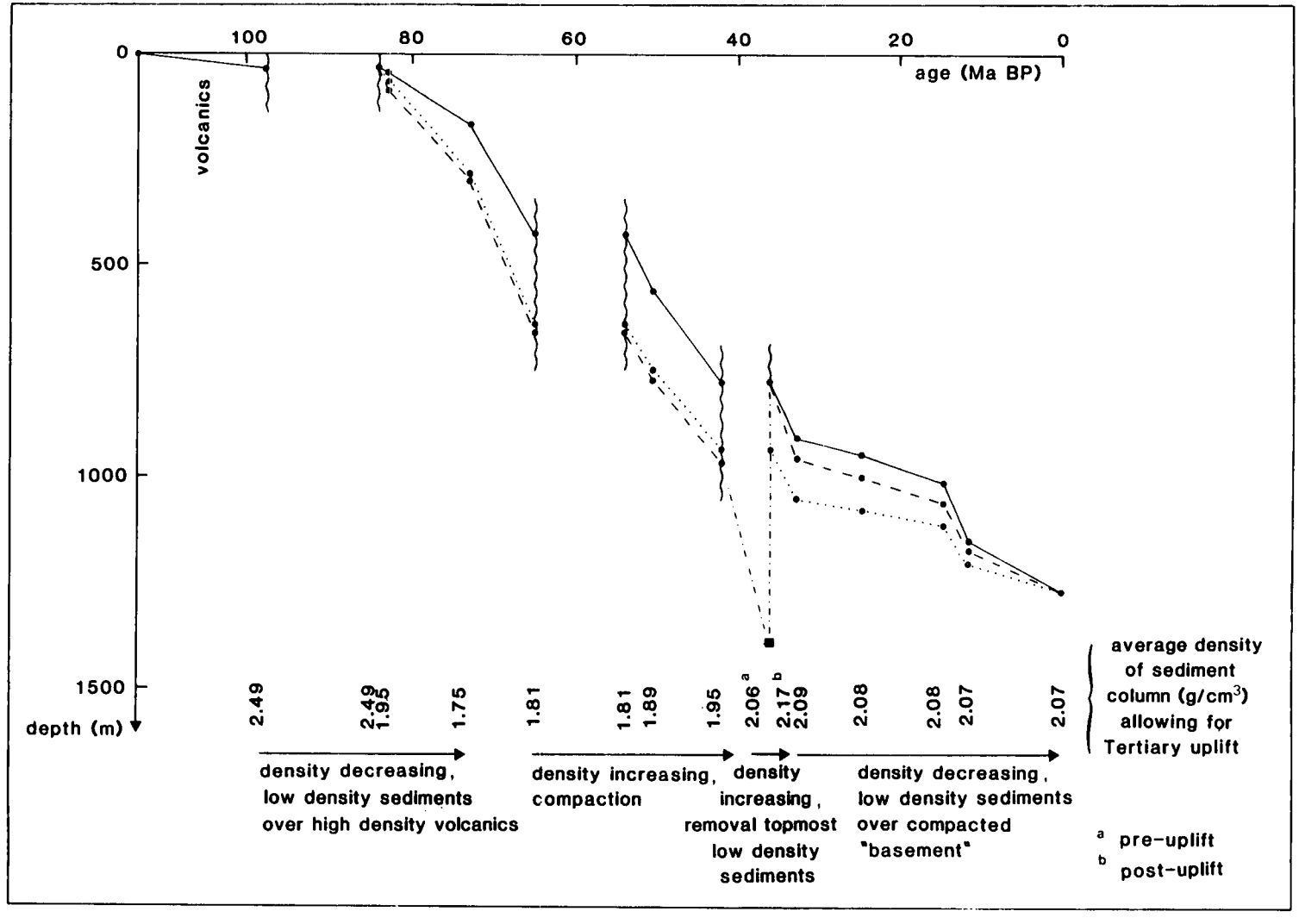

Figure 3.8 Decompacted depths to Cimmerian unconformity with and without allowance for Tertiary uplift, well 72/10-1. Key as Figure 3.7, see text for discussion.

top 600m of sediments, the average density increased to 2.17gcm^{-3}. Low density sediments deposited following uplift reduced the average density of the sediment column to 2.09gcm^{-3}. In this way a "density discontinuity" is created across the uplift unconformity.

Extra compaction and density variations associated with uplift can be readily accommodated in standard sediment decompaction programs, and, as shown by Figures 3.7 and 3.8, have a significant effect on the calculated subsidence history of a well.

3.7 CALCULATION OF TECTONIC SUBSIDENCE

In order to isolate the driving force, or tectonic element, of basin subsidence it is necessary to remove the loading effect of sediment deposited in response to that driving force, and of any overlying water column (Section 1.4.1.1). The aim is to calculate the depth to basement through time in the absence of surface loads, or assuming a constant water load. This quantity, tectonic subsidence, can be readily compared with predictions from geophysical models of basin subsidence.

3.7.1 Sediment Loading

Under a load the lithosphere may attain isostatic equilibrium either by Airy-type (local) or flexural compensation. Following the discussion in Section 1.4.1.2) and previous subsidence studies (e.g. LePichon and Sibuet, 1981; Bond and Kominz, 1984; Karner et al, 1987; Hegarty et al, 1988) local Airy-type compensation has been assumed. Thus the tectonic subsidence of water-loaded basement (T) is related to decompacted sediment thickness (S), water depth during deposition (W_d) and eustatic sea-level change (ΔSL) according to Steckler and Watt's (1978) equation.

$$T=S\{(\rho_m-\rho_s)/(\rho_m-\rho_w)\}+W_d-\Delta SL\{\rho_m/(\rho_m-\rho_w)\} \qquad (5)$$

where ρ_m, ρ_s and ρ_w are the densities of the mantle (3.33gcm^{-3}), sediment (Sclater and Christie (1980) and Section 3.6.4) and water (1.03gcm^{-3}) respectively

3.7.2 Palaeobathymetry

Water depth during sediment deposition must be added to the unloaded subsidence. For example, a sudden subsidence pulse may result in the creation of a depression that takes some time to fill with sediment. Figure 3.9 shows the palaeobathymetric limits for the Mesozoic sequence of the Western Approaches Trough. It has been compiled from a number of biostratigraphic well reports. Sub-aerial sediments have been arbitrarily assigned zero water depth. Vertical error limits on the subsidence plots in Chapters 5 and 6 represent the error limits of palaeobathymetric resolution.

3.7.3 Eustatic Sea-Level Change

Eustatic sea-level change must also be allowed for in the calculation of tectonic subsidence. During a sea-level highstand the excess water acts as a load on the basement and depresses it. There have been major disagreements between published global sea-level models, these are briefly discussed and the choice of sea-level curves in this study justified. However, the particular choice remains very much a matter of personal scientific preference (Falvey and Deighton, 1982).

Vail et al (1977) produced a relative sea-level curve from the late Triassic to the present using a modal average of correlative regional cycles derived from seismic stratigraphic studies. However, it has been argued that many of the sea-level changes recognised by Vail et al (1977) represent widespread tectonic phases (e.g. Bally, 1980; Watts et al, 1982).

In spite of criticism of the Vail et al (1977) curve there is agreement on the occurrence of long-term (first order) sea-level changes. The late Cretaceous highstand, associated with the submergence of most land areas and chalk deposition, is such a first order sea-level change. Considering changes in the volume of mid ocean crests, Pitman (1978) suggested that the late Cretaceous highstand was some 350m above present sea-level. Falvey and Deighton (1982) showed that errors in the magnetic time scale and spreading rates could reduce this maxima to 220m. This lower estimate is in broad agreement with that of Watts and Steckler (1979) based on well data off the US Atlantic margin and those of Wise (1974) and Bond (1978) based

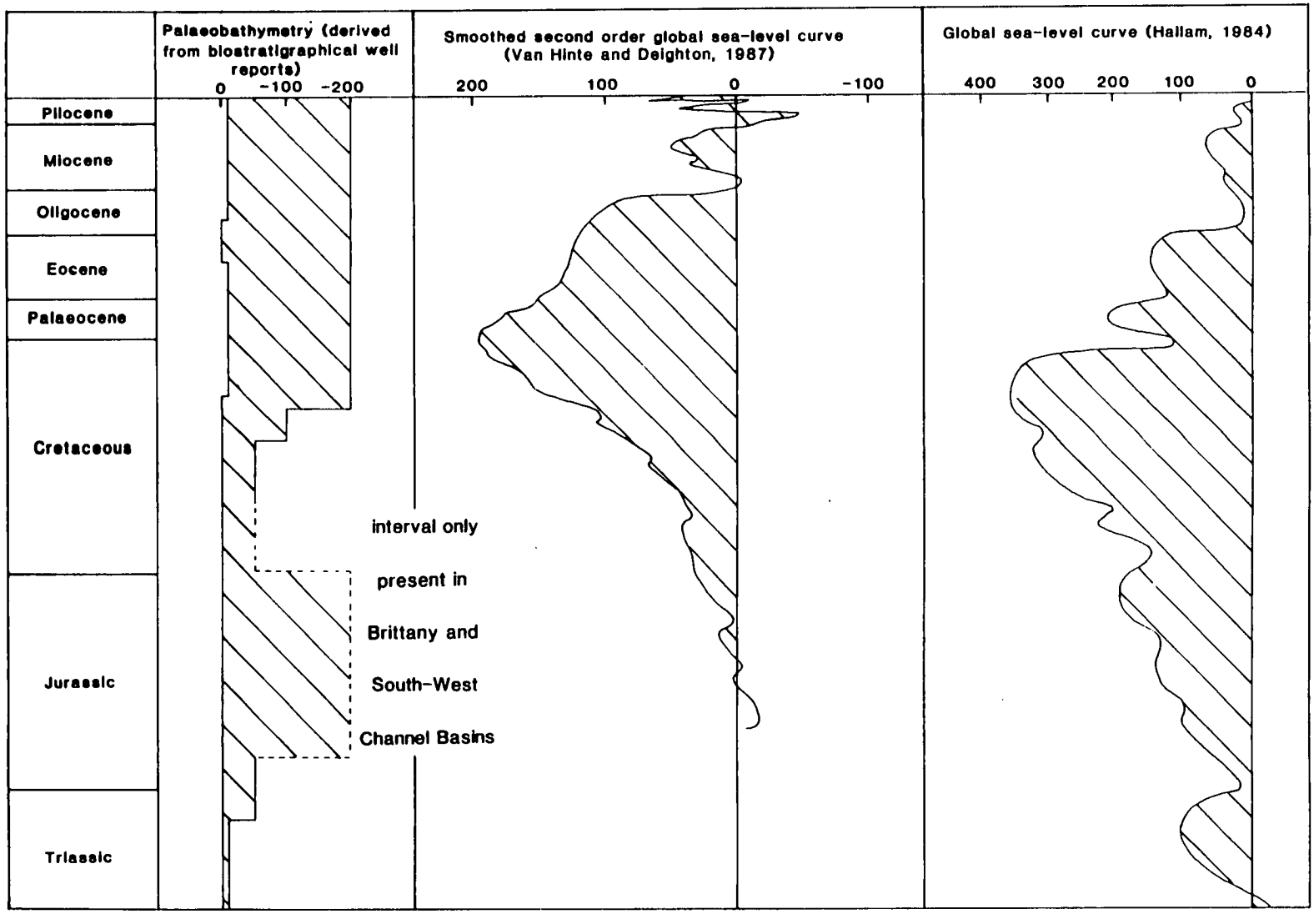

Figure 3.9 Palaeobathymetric and eustatic variations used in tectonic subsidence calculations

on continental flooding. The sea-level curve chosen is essentially a first and second order Vail et al (1977) curve calibrated with a 200m late Cretaceous highstand (Figure 3.9). The sea-level curve of Haq et al (1987) is an update of the Vail et al (1977) curve, and the long term (first order) component of this curve would also be suitable for subsidence studies. For comparison, the post-Cimmerian subsidence plots of Chapter 6 have also been corrected following the Hallam (1984) eustatic sea-level curve which has a 360m late Cretaceous highstand (Figure 3.9).

In spite of debate on the form of the global sea-level curve its influence on subsidence should not be discounted, particularly when, as in this study, reasonable palaeobathymetric control is available (cf. Chadwick, 1986; Karner et al, 1987). For example, consider the average post-Cimmerian sediment thickness of 1.5km in the Melville Basin. At a typical sediment density of $2.2gcm^{-3}$ this is equivalent to approximately 0.74km of water-loaded subsidence. During the deposition of this sequence the water depth has increased from 0m to approximately 160m, and sea-level has dropped from a highstand of 200-360m above present sea-level. The post-Cimmerian tectonic subsidence corrected for changes in the height of the overlying water column thus becomes 1.19-1.42km (equation 5).

Eustatic sea-level change is not included in subsidence curves for the sub-aerial Permo-Triassic sequence (Chapter 5).

3.7.4 Chronological Calibration

The horizontal axis of a geohistory plot is calibrated in time. This is subject to errors in biostratigraphical, lithostratigraphical and occasionally radiometric dating. In this study the biostratigraphical time periods given in well logs and reports have been chronologically calibrated according to the time scale of Harland et al (1982). The time scales of Berggren et al (1985) and Kent and Gradstein (1985) are very similar to that of Harland et al (1982), but those of Van Hinte (1976a, 1976b) and Odin et al (1982) assign consistently younger ages to the Cretaceous and Jurassic stages. This variation is, however, systematic and does not significantly affect geophysical modelling of basin subsidence. Hence error bars of chronological calibration are only shown for boundaries whose stage

position is uncertain. This only applies to the pre-Rhaetian continental red-beds of the Permo-Triassic (Section 5.2.1).

Sea-bed ages are not given in the well reports and these have been taken from the nearest available BGS offshore micropalaeontological sites (Warrington and Owens, 1977; Wilkinson and Halliwell, 1980). Dating of the top and bottom of unconformities has been estimated by extrapolating known sedimentation rates into the area of uncertainty (Van Hinte, 1978).

CHAPTER 4

VARISCAN STRUCTURES AND THEIR EFFECT ON SUBSEQUENT TECTONIC PHASES

4.1 INTRODUCTION

During the Variscan orogeny a set of ENE-WSW (060-070°N) striking, SSE-dipping thrusts and steeper, NNW-SSE (150-160°N) striking wrench faults were created (Section 2.3). These have been mapped across the Western Approaches Basin using seismic and gravity data (Figure 4.1).

Many studies have suggested that zones of weakness presented by pre-existing faults, most commonly thrusts, are reactivated during later extension (e.g. Brewer and Smythe, 1984; Wernicke, 1985; Beach, 1987). Localization of extension across a pre-existing thrust produces a sedimentary basin in the vacated hanging wall. Renewed compression along the basement fault will cause uplift of the sedimentary basin (positive inversion). Alternatively, successive extensional phases result in basins following basins (successor basins). The aim of this chapter is to discuss the role of the Variscan structures during subsequent tectonic phases in the Western Approaches Trough.

4.2. THE WESTERN APPROACHES BASIN BASEMENT STRUCTURE MAP

This section discusses the basement structure map of the Western Approaches Basin (Figure 4.1). Basement events apparent on reflection seismic profiles were originally mapped from the Petty-Ray dataset and checked, where possible, on the less extensive GECO (Geophysical Company of Norway) dataset (Appendix A). The events generally occur as packets of reflectors around one second's two-way-time (TWT) thickness with individual reflections continuous for only a few kilometres. The amplitude of the reflections is comparable to that of the overlying higher amplitude sedimentary reflections, although this may be due more to interference, tuning and multiple effects rather than individual acoustic impedance contrasts. Similarly the high reflection frequency

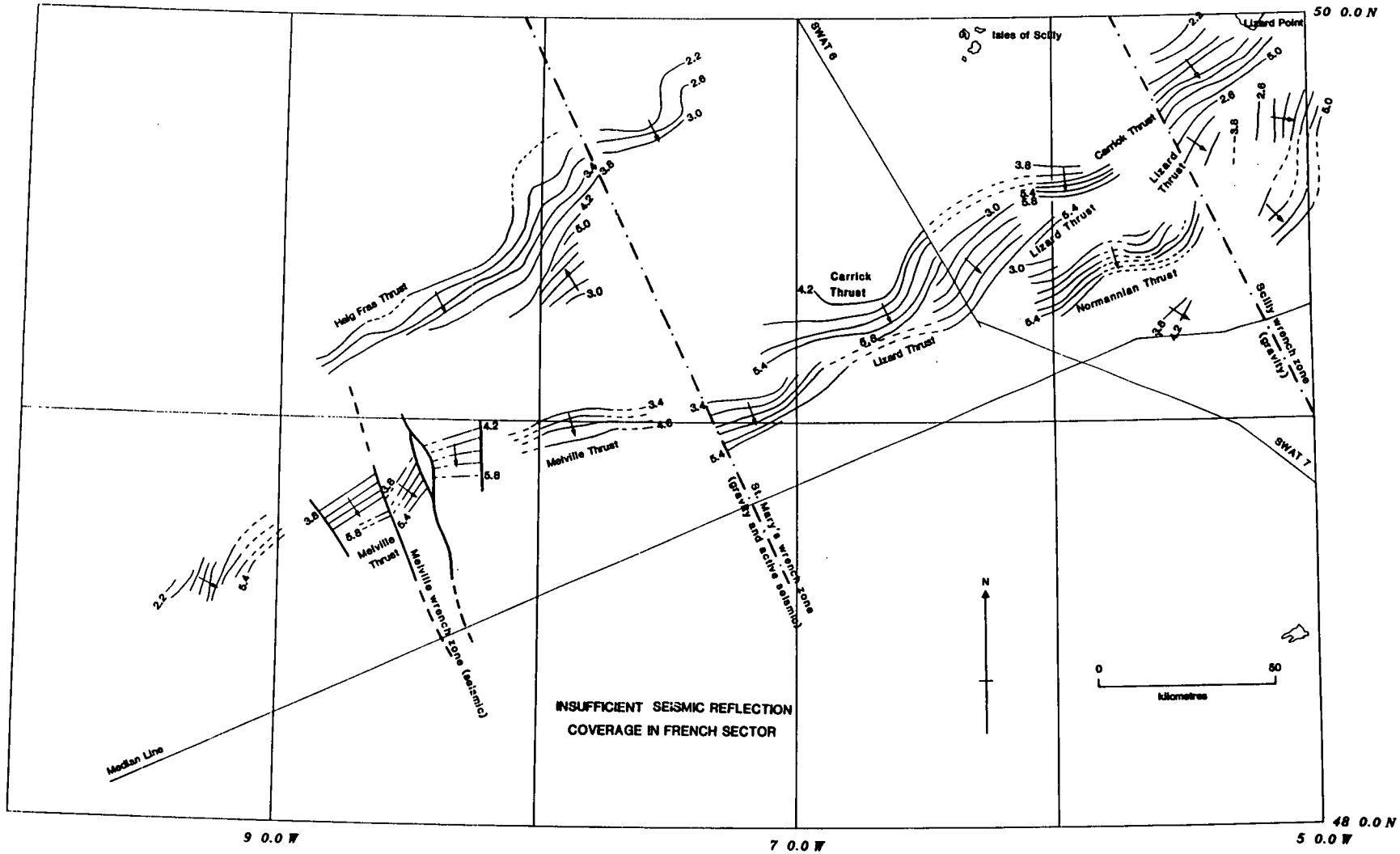

Figure 4.1 Simplified pre-Permian structural map of the Western Approaches Basin. Contours are in TWT (0.4s interval) to intra-Variscan basement events.

within the reflector packages is a function both of "real earth" spacing and the seismic response to that spacing.

The basement events strike approximately 060-070°N and on depth conversion are typically planar with dips of 25-30° to the SSE. Two major events can be traced continually from Cornwall to the western end of the St. Mary's Basin between 7° and 8°W. The lower, northern event correlates with the Carrick Thrust as seen onshore south Cornwall (Leveridge et al, 1984; Holder and Leveridge, 1986 and Figure 2.5(b)), and the upper, southern event correlates with the Lizard Thrust. Although shown as single events in Figure 4.1 they are broad zones of deformation (one second's thickness in TWT at basement velocities corresponds to 2½-3km) and probably comprise complex imbricate fans and duplexes.

The Lizard Thrust is imaged on SWAT 6 (Figure 4.3) where it has also been termed the Scilly Isles Fault System (BIRPS and ECORS, 1986). It can be traced from a highly diffractive mid crust at 4s TWT (approximately 10km depth) to near the base of the St. Mary's Basin (4-5km deep) and appears to comprise two discrete reflector packages each around 0.3-0.5s TWT thickness and a similar distance apart. This may be analogous to the Lizard/Dodman imbricate fan branches described by Holder and Leveridge (1986 and Figure 2.5(b)). The separate branches are also apparent on a commercial line adjacent to SWAT 6 (Figure 4.11) but elsewhere on the commercial data only one broader zone is resolved.

The Carrick Thrust is imaged between 4 and 5½s TWT on SWAT 6, where it has the appearance of a deep thrust duplex (Figure 4.3). Immediately east of SWAT 6, on the commercial lines, the Carrick Thrust is well defined as a broad zone of high amplitude convex-upwards reflectors between 4 and 6s TWT. This may correspond to the upper branch of the duplex as seen on SWAT 6 (Figure 4.3).

A third event lies to the south and above the Lizard Thrust between 5°20' and 6°00'W. This event is termed the Normannian Thrust after the uppermost thrust in the model of Holder and Levridge (1986 and Figure 2.5(b)), but unlike the Carrick and Lizard Thrusts, can not be demonstrably linked with a structure to the east.

The broad zones of deformation mapped as the Carrick, Lizard and Normannian Thrusts may combine at depth (? possibly along a

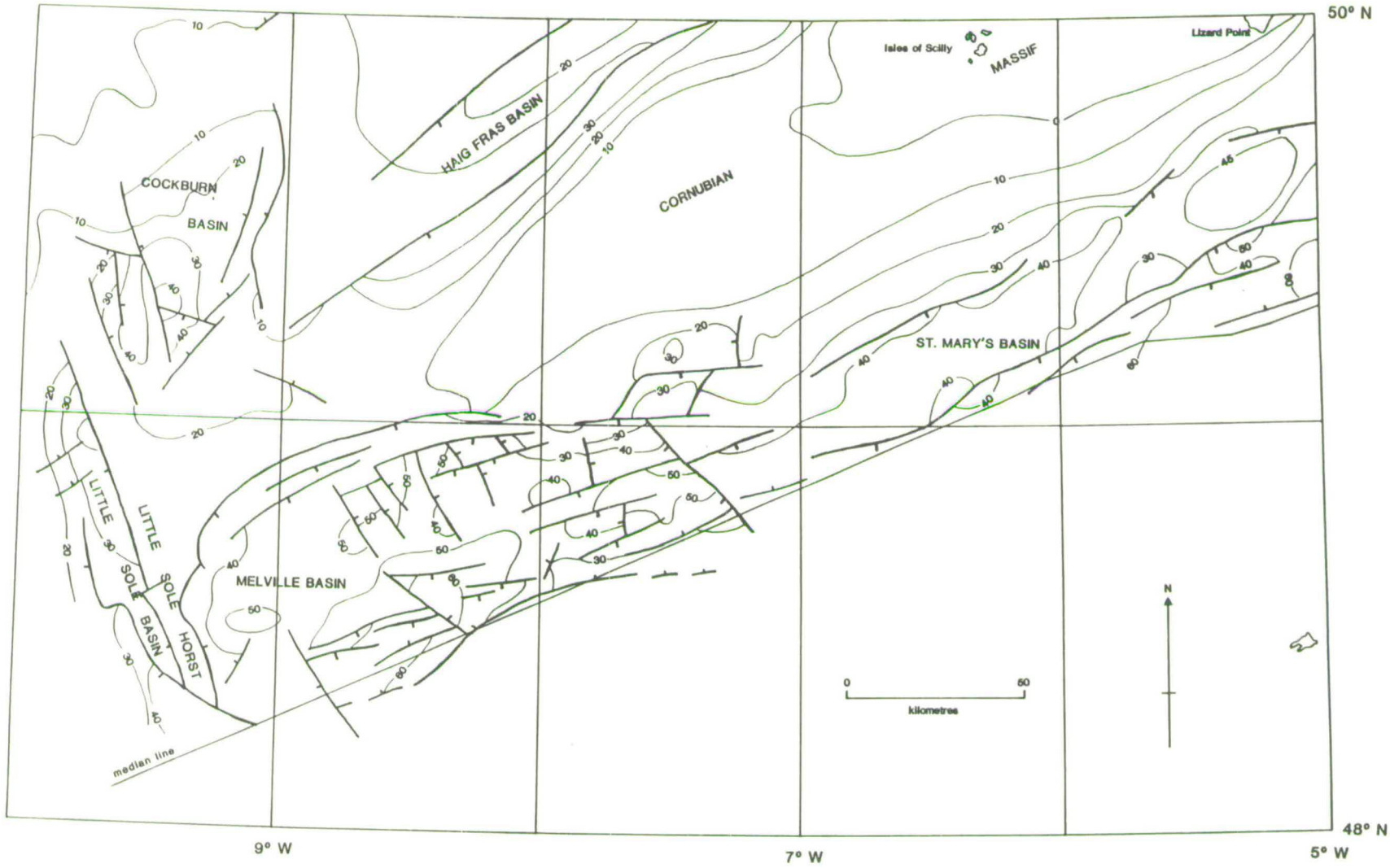

Figure 4.2 Simplified post-Carboniferous structural map of the Western Approaches Basin. Contours are in hundreds of metres to top Variscan basement (Chapman, in press).

rheological detachment at the top of the reflective lower crust) to form a complex imbricate thrust fan of crustal scale.

A major basement event, the Haig Fras Thrust, is associated with the Haig Fras Basin between approximately 7½ and 9°W (Figures 4.1 and 4.2). There is no direct "ground truthing" of this event, but by analogy with the events in the St. Mary's Basin it is interpreted as a Variscan thrust. Around 8°W, this event is associated with a NNW-dipping event which is interpreted as a back thrust as described onshore south-west England (Coward and Smallwood, 1984).

In the Melville Basin only one major SSE-dipping basement event is apparent on the reflection seismic data. Since the Melville Basin is separated from the St. Mary's Basin by a major discontinuity it is not possible to correlate this event with any specific thrust to the east and it is termed the Melville Thrust.

The discontinuity between the Melville and St. Mary's Basins is apparent as a line truncating the gravity lows associated with the Cornubian and Haig Fras Batholiths (Figure 2.7). No coherent event is apparent in the reflection seismic data, although a strong top basement reflector in the St. Mary' Basin becomes disrupted and broadly downthrown passing over this zone into the Melville Basin. A marked change in structural style also occurs over the discontinuity (Figure 4.2). Such a major discontinuity, not directly imaged on reflection seismic data, is likely to be a vertical or near vertical structure, and it is interpreted as a major wrench fault in the NNW-SSE Variscan system and termed the St. Mary's wrench zone. Interestingly, although epicentre resolution of offshore events by the land-based seismograph station network is not good, present-day earthquake activity is observed along the St. Mary's wrench zone (Walker, 1987). The trend of the St. Mary's wrench zone (150°N), as defined by the gravity data, is sub-parallel to the Sticklepath-Lustleigh fault zone onshore south-west England (140°N). Other faults in this set occur just west of Land's End (gravity data), termed the Scilly wrench zone, and within the Melville Basin (major set of NNW-SSE trending cover faults apparent on reflection seismic data), termed the Melville wrench zone.

Anomalous, broadly north-south striking events are observed at the eastern and western limits of the Western Approaches Basin, just west

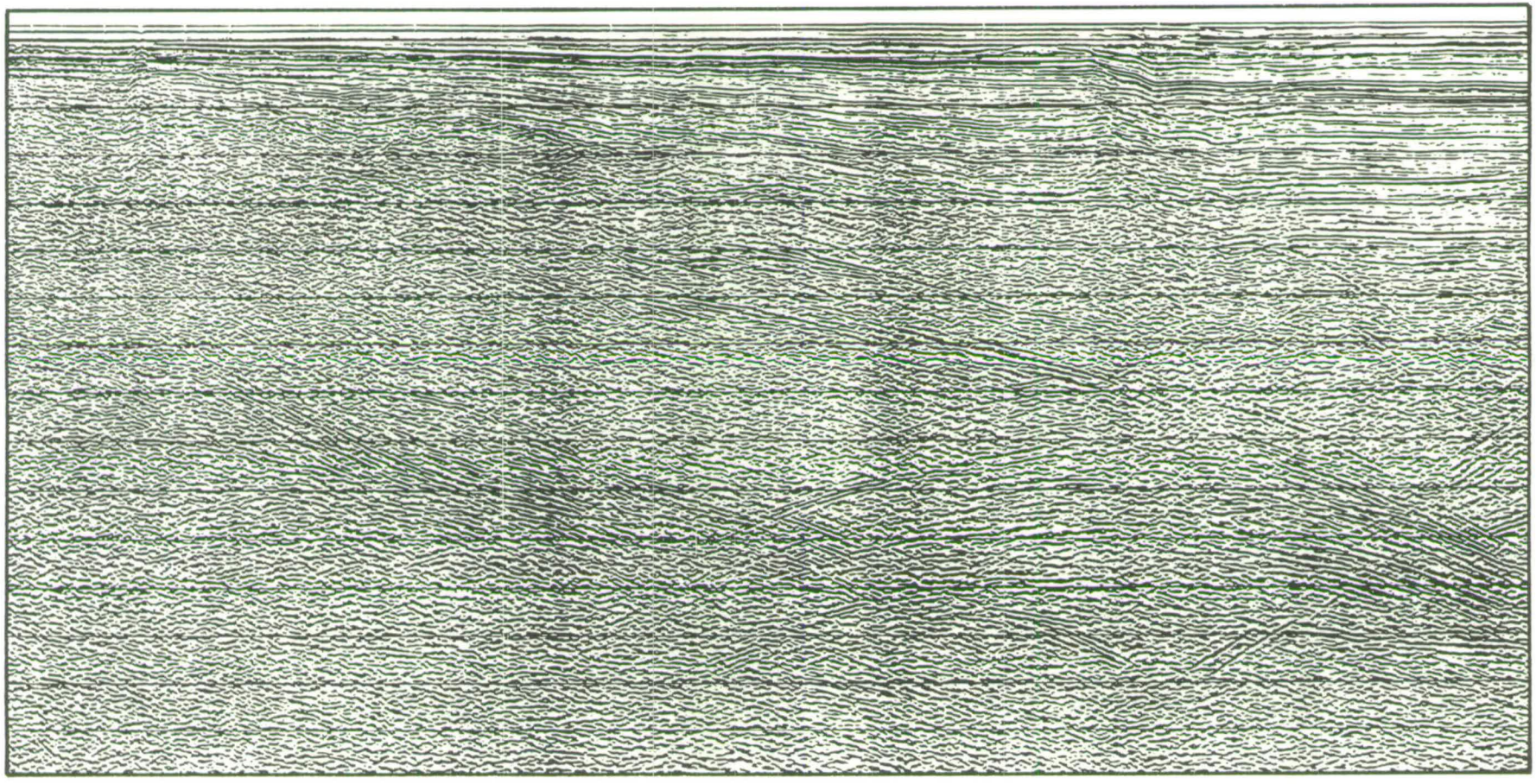

Figure 4.3(a) BIRPS SWAT 6 showing Lizard and Carrick Thrusts beneath the northern flank of St. Mary's Basin (interpretation on following page).

Figure 4.3(b) Interpretation of BIRPS SWAT 6 across the northern flank of St. Mary's Basin.

of 5 and 9°W respectively. On the seismic data they appear similar to the Variscan thrusts (Figure 4.9), however, in orientation they are closer to the steeper wrench faults. They are speculatively interpreted as oblique/lateral ramps to the NNW-moving thrusts (Figure 4.10(a)).

Data coverage over the French sector is not sufficient to extend the basement map into the Brittany and South-West Channel Basins. No coherent events of the type shown in Figure 4.1 are apparent on SWAT 7 under the eastern Brittany Basin.

4.3 BASEMENT FAULT REACTIVATION AND BASIN STYLE: REVIEW

The reactivation of basement structures has been widely recognized as an important control on basin evolution (e.g. Brewer and Smythe, 1984; Wernicke, 1985; Beach 1987). This section briefly outlines the techniques used in this study to analyse such reactivation. Particular attention is paid to dating reactivation with respect to the preserved sediments (c.f. Kirton and Hitchen, 1987) and the distinction between demonstrable deep-seated fault reactivation and that which is inferred from "spatial coincidence".

Figure 4.4 shows half-graben-type sedimentary basins controlled by faults which have propagated from basement fault zones. The sediment layers dip towards, and are controlled by, the reactivated fault. If fault activity was syn-depositional then the sedimentary layers diverge towards the controlling fault (Figure 4.4(a)), if it was post-depositional they are parallel (Figure 4.4(b)). Later compressional reactivation will invert the basin reducing the dip of the sedimentary layers towards the controlling fault (Figure 4.4(c) and (d)). Superposition of these simple styles can lead to a great variety of basin morphologies.

The above rules hold whether or not the half-graben controlling faults continue at depth and basement reactivation cannot be inferred from the mere existence of a half-graben. A basement fault which propagates upwards into the half-graben-bounding fault must be imaged. The Bristol Channel Basin is a good example of a half-graben controlled by a deep-seated fault zone. Early Cretaceous reactivation of the

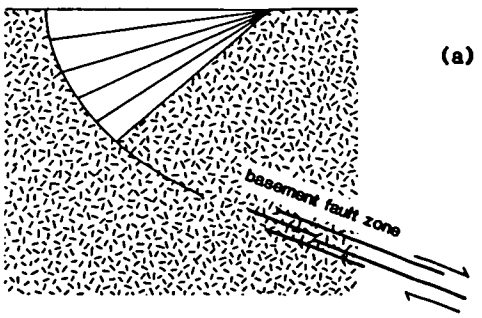

(a) Sediment wedges dip towards controlling fault. Syn-depositional extensional reactivation of basement fault.

(b) Parallel sediment layers dip towards controlling fault. Post-depositional extensional reactivation of basement fault.

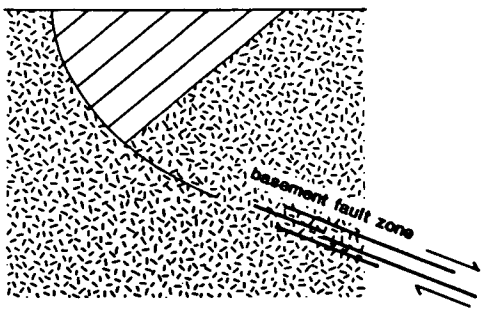

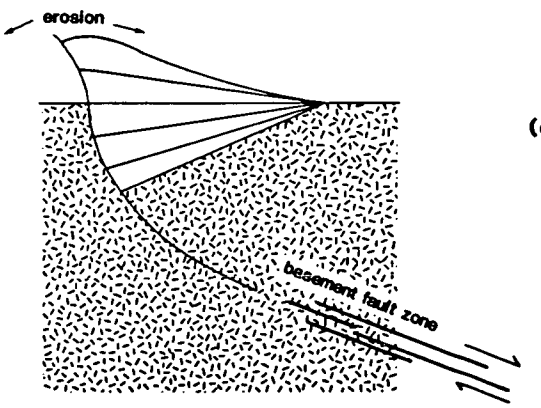

(c) Sediment wedges fanning towards controlling fault. Compressional reactivation of extensional (syn-depositional) fault.

(d) Parallel sediment layers gently dipping towards controlling fault. Compressional reactivation of extensional (post-depositional) fault.

Following erosion of uplifted material compression may be recognized by deposition on the flanks of the inverted basin accompanying its erosion and by changes of throw on basinal faults (the effects of extension reducing upwards and changing to the effects of compression)

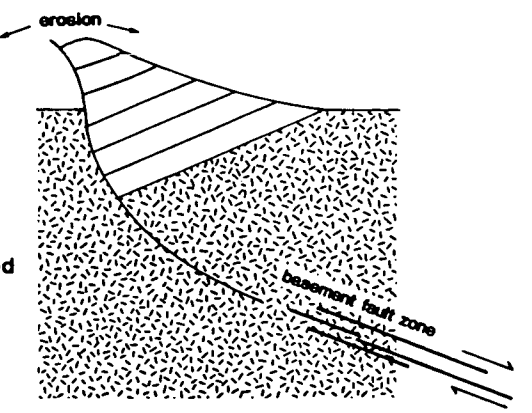

Figure 4.4 Schematic half-grabens controlled by basement fault reactivation (no synthetics or antithetics to the half-graben controlling fault shown). Half-grabens controlled by planar faults will have a different form, but syndepositional "fanning" will still occur.

Bristol Channel Fault Zone, a former Variscan thrust, preserved a half-graben containing Triassic and Jurassic strata (Brooks et al, 1988). Basement fault reactivation (Brewer and Smythe, 1984) also occurred both during and following sedimentation in the late Palaeozoic-Mesozoic basins of the north-west British continental shelf (Kirton and Hitchen, 1987). The Murre Fault, which bounds the west side of the southern Jeanne D'Arc Basin on the Canadian Atlantic margin, again overlies a prominent zone of basement reflectors and was periodically active during the deposition of a thick syn-rift section of Triassic-early Cretaceous sediments (Keen et al, 1987).

Symmetrical, rather than half-graben-type, basins also overlie basement faults (Figure 4.5). In these basins the control of the basement fault is not always so readily demonstrated. BIRPS and ECORS (1986) and Beach (1987), interpreted the broadly symmetrical North Celtic Sea Basin as being controlled by extensional reactivation of the underlying Variscan thrust (Variscan Front). However, Pinet et al (1987) pointed out that after migration the underlying thrust is not coincident with the basin floor and that the distribution of depocentres is not consistent with simple reactivation of the thrust. Difficulties such as these may be reconciled with basement fault reactivation if instead of fault propagation from the tip of the thrust as shown in Figure 4.4 there is a more complex pattern of back- or forward-stepping basinal faults soling out deeper in the detachment (Figure 4.5(a)). This is the favoured interpetation of the relationship between the North Celtic Sea Basin and the Variscan Front. When basinal faults can not be shown to be linked to the deeper fault, then reactivation remains a tentative hypothesis based on "spatial coincidence" (Figure 4.5(b), for example the possible reactivation of the basement fault under the Plymouth Bay Basin imaged on SWAT 8 and 9). If a basinal fault demonstrably cuts the detachment then its control on that fault is probably minimal (Figure 4.5(c)).

The above classification is designed to help determine to what extent and at what time a basement fault controls overlying sediment distribution. Like most classifications, however, it is somewhat arbitary and gradations between the different types of basins are observed.

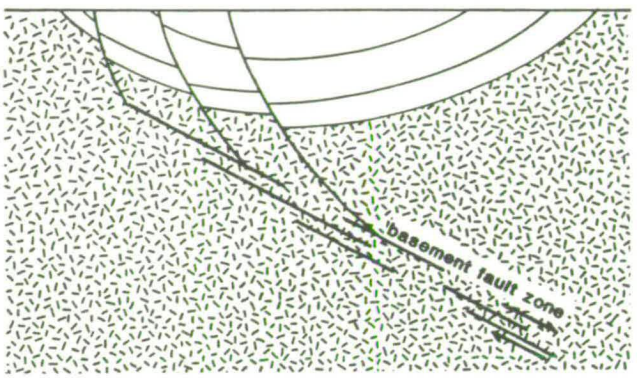

(a) Basin controlled by faults soling out into reactivated basement fault zone.

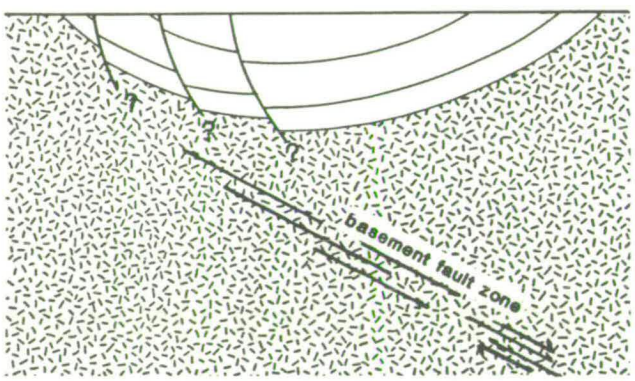

(b) No demonstrable relation between basin controlling faults and basement fault zone.

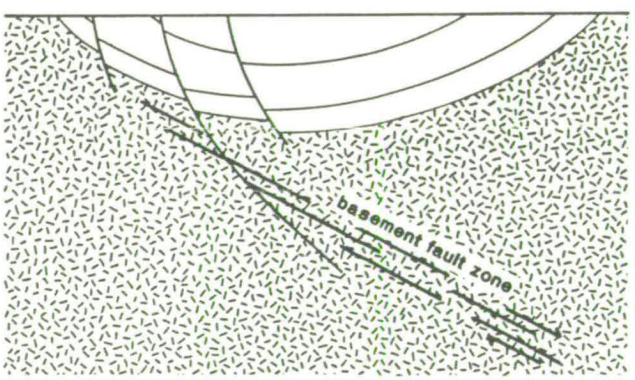

(c) Basin controlling faults cut basement fault zone, which has not been reactivated.

Figure 4.5 Schematic symmetrical basins overlying basement fault zones.

4.4 BASEMENT FAULT REACTIVATION AND BASIN STYLE: THE WESTERN APPROACHES BASIN

4.4.1 The Melville Basin

Although the Permian Aylesbeare Group and underlying volcanics and volcaniclastics thicken to the south individual units do not and reflections remain parallel (Figures 2.9 and 4.6). Hence, if the position of the Aylesbeare Group was controlled by extensional faulting it was post-depositional movement on a north-dipping structure in the French sector of the basin. Such a fault may occur but is not apparent in the limited dataset over the French sector. It is postulated that late Variscan topography, rather than extensional faulting, was the principal control on the deposition of the Permian sequence (Sections 2.5.4, 5.3.2 and 5.3.3).

The Sherwood Sandstone and Mercia Mudstone Groups appear to thicken dramatically into the north-dipping half-graben above the Melville Thrust, however, much of this is due to later halokinesis (Figure 4.6). Taking the post-Aylesbeare Group/pre-salt (i.e. Sherwood Sandstone and base of Mercia Mudstone Groups) interval there is only slight syndepositonal thickening. The Jurassic (Liassic) sediments show no evidence of syndepositional fault control (Figure 4.7).

The style of the preserved half-grabens of Triassic and Jurassic sediments is essentially parallel bedded and dipping towards the controlling faults (Figure 4.6 and 4.7). Extensional reactivation of the Melville Thrust was thus post-depositional but clearly pre-dates the deposition of the Chalk and thin early Cretaceous sequence. Like movement on the Bristol Channel Fault Zone (Brooks et al, 1988) and in South Celtic Sea Basin (Van Hoorn, 1987) it is assigned to the late Jurassic/early Cretaceous, Cimmerian period of tectonism (Section 2.7 and Chapter 6).

The Melville wrench zone was also extensionally reactivated during the Cimmerian (Figure 4.8). This late Jurassic/early Cretaceous reactivation of an orthogonal fault set (the Melville Thrust and wrench zone) has led to the preservation of what might be termed "quarter-

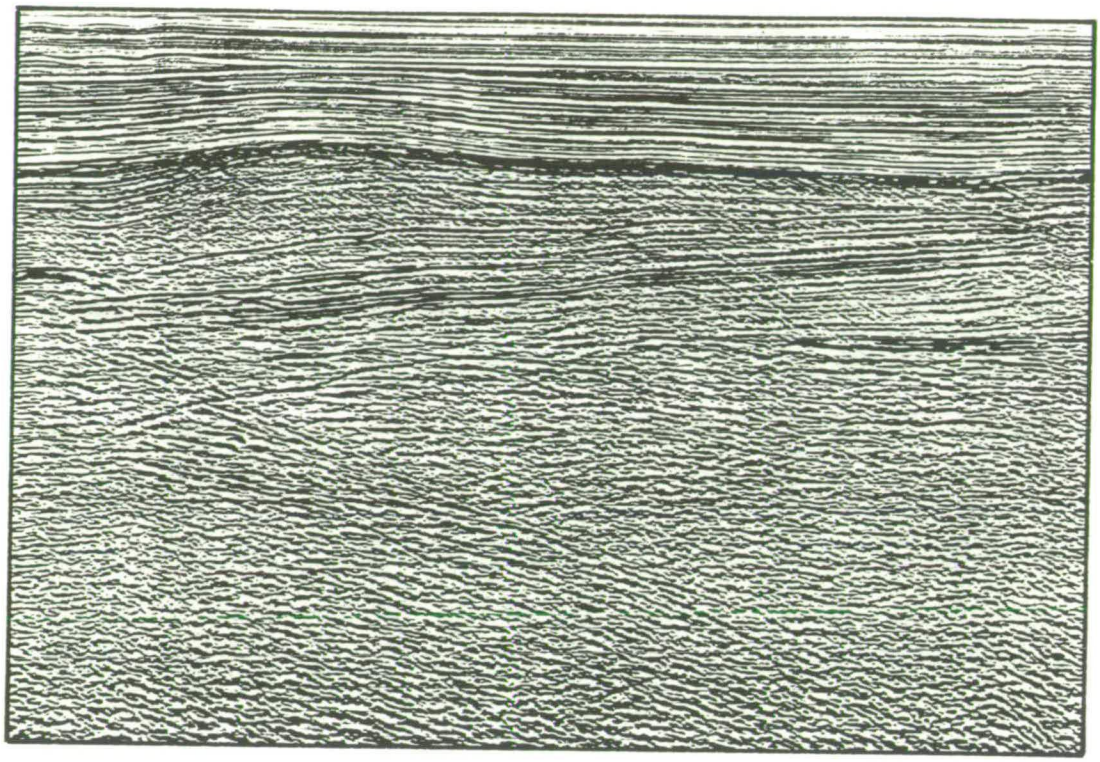

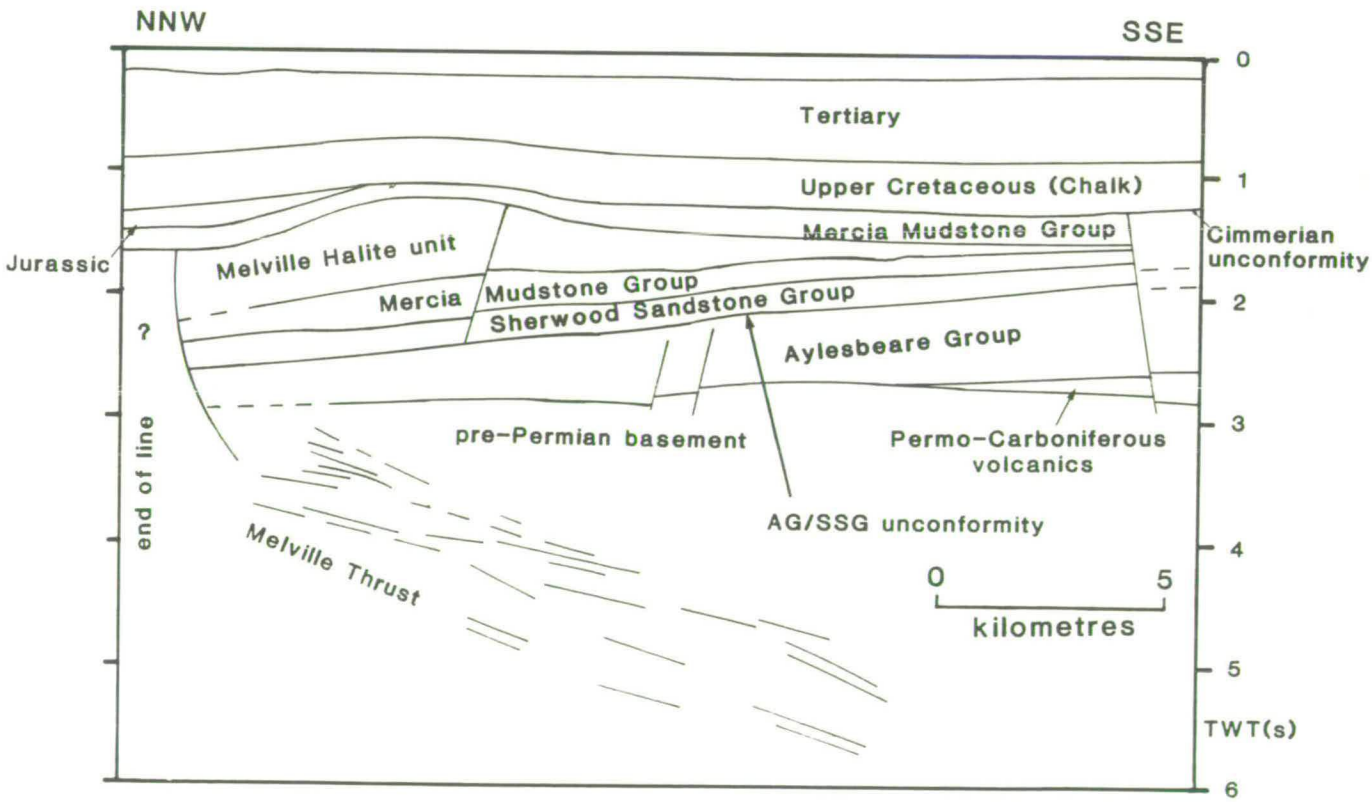

Figure 4.6 GECO line across Melville Basin showing Melville Thrust and overlying Triassic half-graben.

(a)

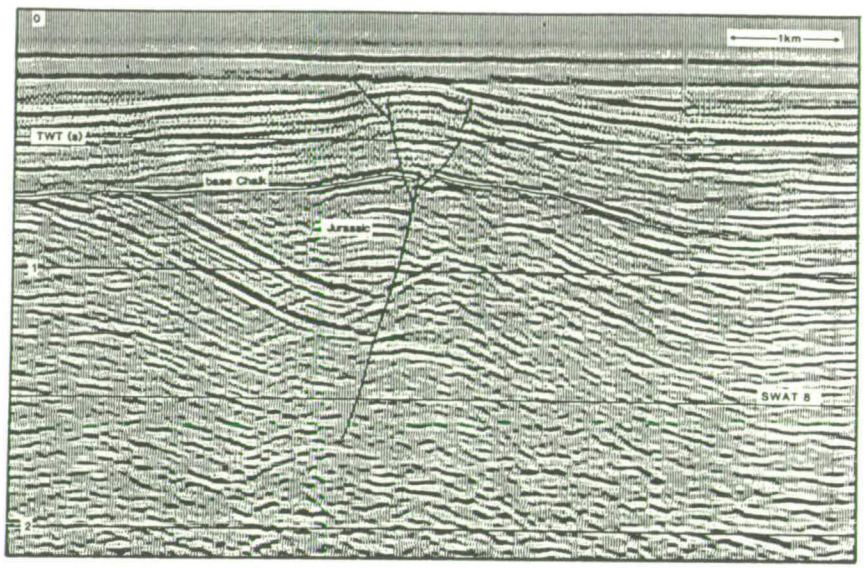

(b)

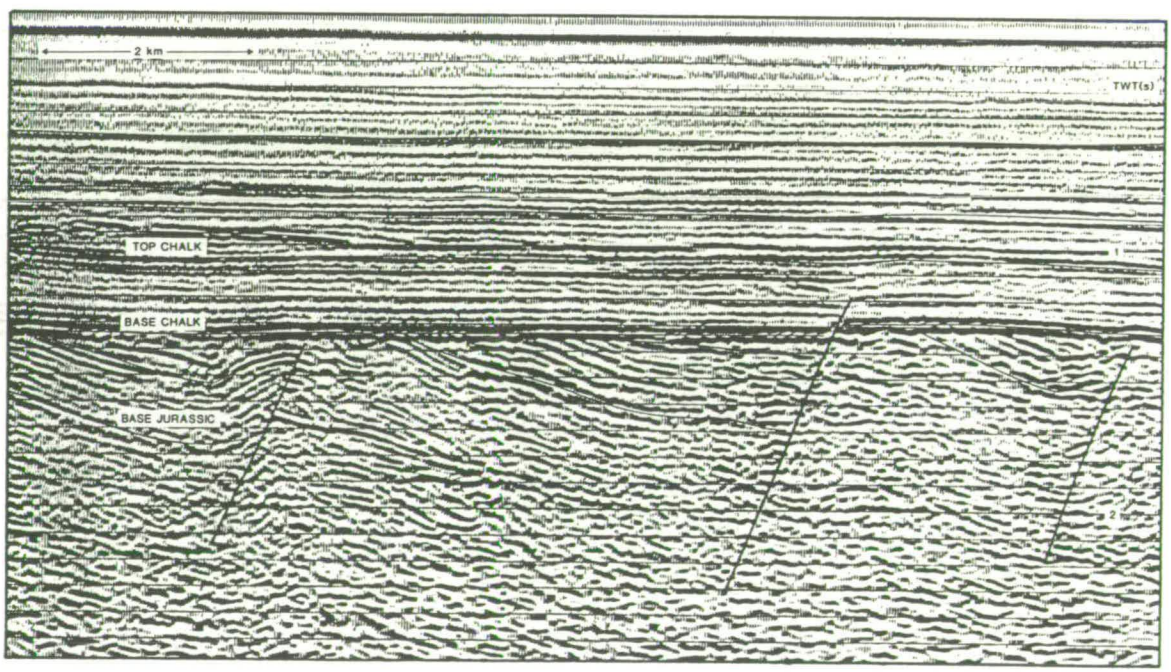

Figure 4.7 Post-depositionally faulted Jurassic half-grabens (a) BIRPS SWAT line 8 northern South-West Channel Basin. Note the change in throw and bifurcating branches of the fault in the Chalk, typical of a "flower structure". (b) southern Melville Basin.

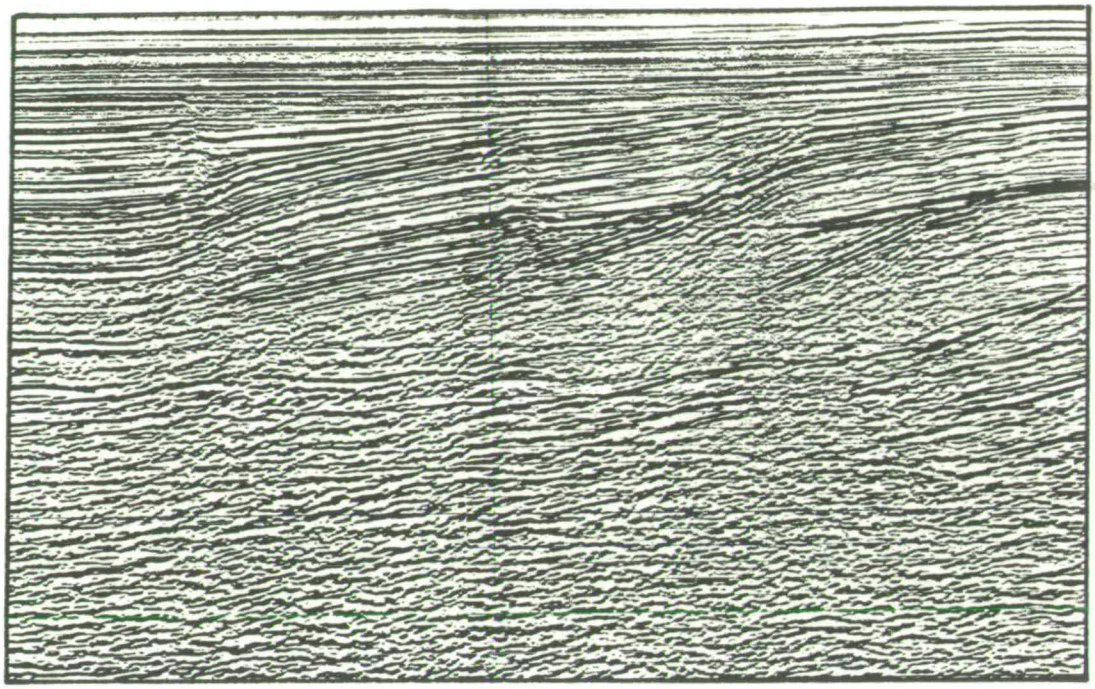

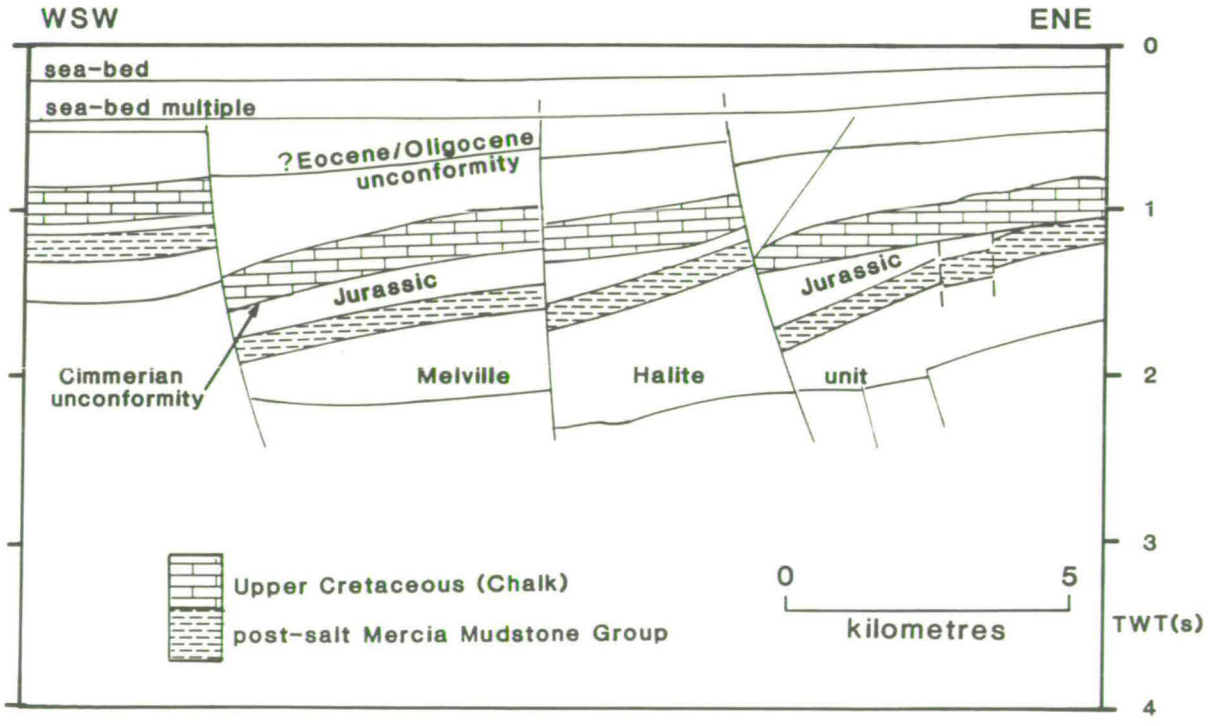

Figure 4.8 GECO line across Melville wrench zone showing Cimmerian and Tertiary reactivation of NNW-SSE trending structures.

Pre-Melville Halite reflectors not picked.

grabens" (Chapman, in press), fault bounded both to the NNW and to the WSW (Figure 4.2).

Although regional Cimmerian Atlantic-related shelf uplift removed 1-2km of Permian-Jurassic sediments (Sections 2.7 and 6.2) it was locally counteracted by the extension-driven subsidence associated with basement fault reactivation. In the Melville Basin rather than syn-rift (late Jurassic/early Cretaceous) sediments accumulating in fault-bounded lows, extension acted to reduce the magnitude of Cimmerian erosion and locally preserve Triassic and early Jurassic sediments in the isolated "quarter-grabens".

The Melville Thrust was not reactivated during the deposition of the post-Cimmerian sequence or its Eocene-Oligocene uplift. However, significant Tertiary extension, possibly in association with salt dissolution (T.J.C. Chapman, personal communication, 1988), occurred across the Melville wrench zone (Figure 4.8). The Tertiary saw major uplift and inversion of the Western Approaches Trough and surrounding areas through compression transmitted northwards from the Alpine foldbelt. In the Melville Basin uplift was concentrated during the Eocene-Oligocene hiatus (Section 2.9.3). The orientation of compressional structures in the Brittany Basin and the continental slope and the tectonics of Alpine/Pyrenean collision suggest that regional compression was in a NNW-SSE direction. Hence, the extensional reactivation of the Melville wrench zone at this time is interpreted as a local transtensional feature. Similar transtensional Tertiary reactivation of the Sticklepath-Lustleigh fault zone, a major Variscan wrench fault onshore south-west England, produced the Eocene-Oligocene Bovey and Petrockstow Basins of south-west England (Holloway and Chadwick, 1986). Holloway and Chadwick (1986) argued that the Sticklepath-Lustleigh fault zone had been reactivated in a sinistral sense. Sinistral reactivation is also tentatively proposed for the Melville wrench zone, although detailed analysis of fault and extension trends is required to test this hypothesis.

On the western flank of the Melville Basin, at its junction with the Little Sole Horst, progressively older, parallel-bedded sediments are truncated by the Cimmerian unconformity (Figure 4.9). Underlying

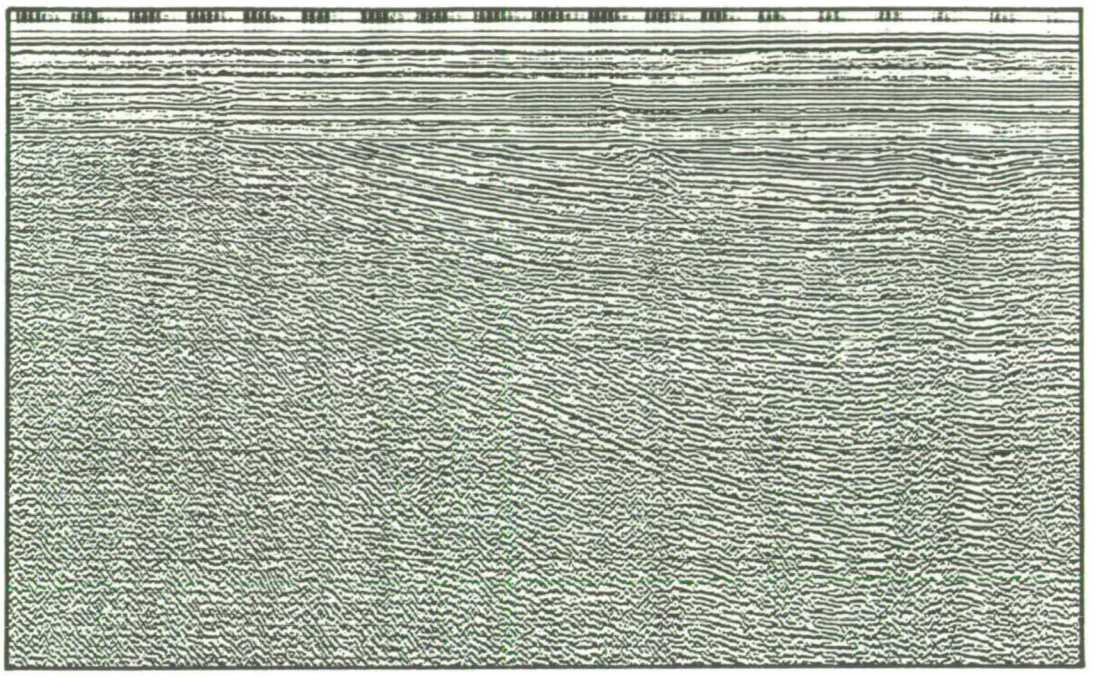

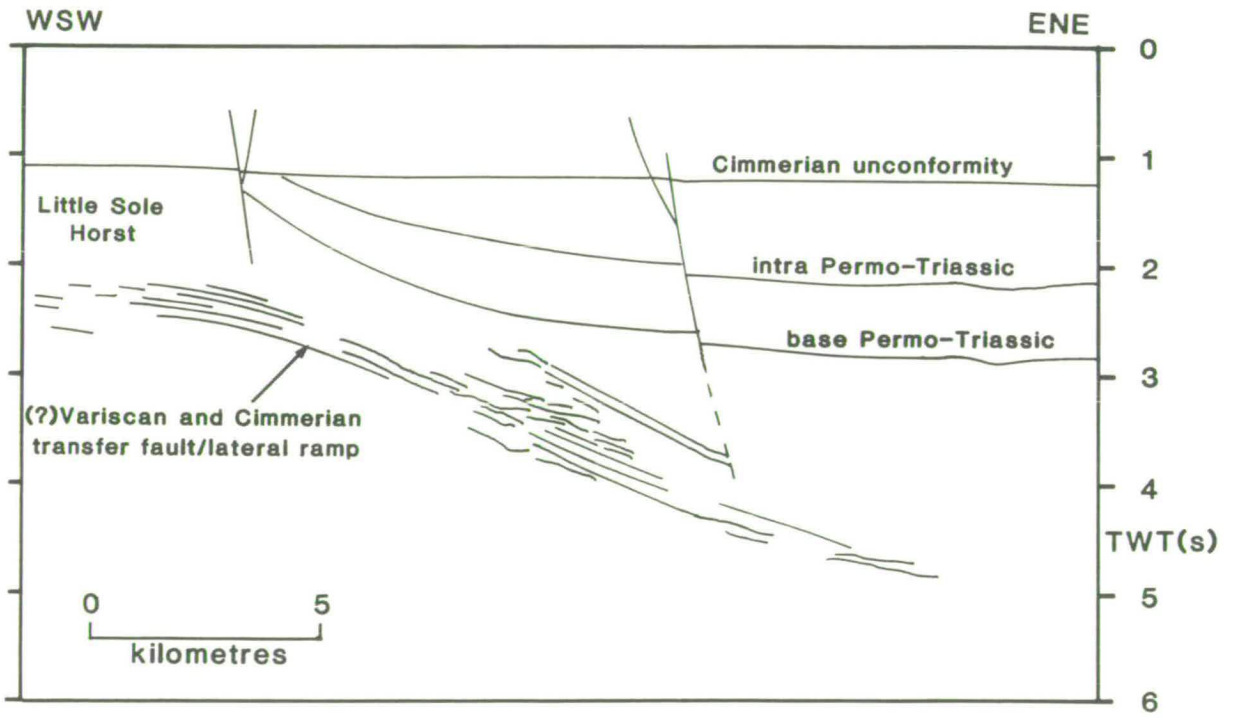

Figure 4.9 Petty-Ray line across western Melville Basin/Little Sole Horst. Basement event is interpreted as a Variscan lateral ramp reactivated in the Cimmerian. See text and Figure 4.10 for details.

basement reflections have been tentatively interpreted as an oblique/lateral ramp to the Melville Thrust. It is tempting to interpret Figure 4.9 in terms of ENE-WSW compression across the observed ramp. Such compression must be Cimmerian since it post-dates the preserved sediments (no syn-depositional thinning towards the structure) but pre-dates the undisturbed base Chalk. However, Cimmerian extension occurred across the similarly orientated Melville wrench zone and no compressional faulting or folding is observed in the preserved sediments. An alternative explanation is that this structure behaved as an oblique/lateral ramp to the Melville Thrust during Cimmerian extension (Figure 4.10(b)). Moving from the frontal ramp of the Melville Thrust across the oblique ramp the extension, and hence subsidence, which counteracted Cimmerian regional thermal uplift, is progressively transferred to the south (?out of the mapped area) and the magnitude of Cimmerian erosion increases (Figure 4.10(b)).

The Little Sole Horst separates the Melville Basin from the Little Sole Basin (Figure 4.2), the most inbound of the tilted early Cretaceous half-grabens of the continental slope. The Little Sole Horst is hence the boundary between the early Mesozoic shelf basin extensional domain (here the Western Approaches Basin) and the late Mesozoic Atlantic extensional domain which cut the former. It is interesting to speculate whether, through its control on the position of the Little Sole Horst, the possible ramp to the Melville Thrust determined the position of Atlantic rifting in the area.

4.4.2 The St. Mary's Basin

It is proposed that, like the Melville Basin along strike, the distribution of the thick Permian sequence in the central St. Mary's Basin (Figure 1.2(b)) was controlled by end Variscan topography rather than extensional faulting. Two Triassic sub-basins are preserved in the northern and southern St. Mary's Basin (Figure 1.2(b)). In the intervening central St. Mary's Basin the Triassic is thin or absent. Both the preserved Triassic sub-basins have a symmetrical rather than half-graben form. The northern sub-basin lies along strike from the northern Melville Basin half-graben, and the southern sub-basin lies

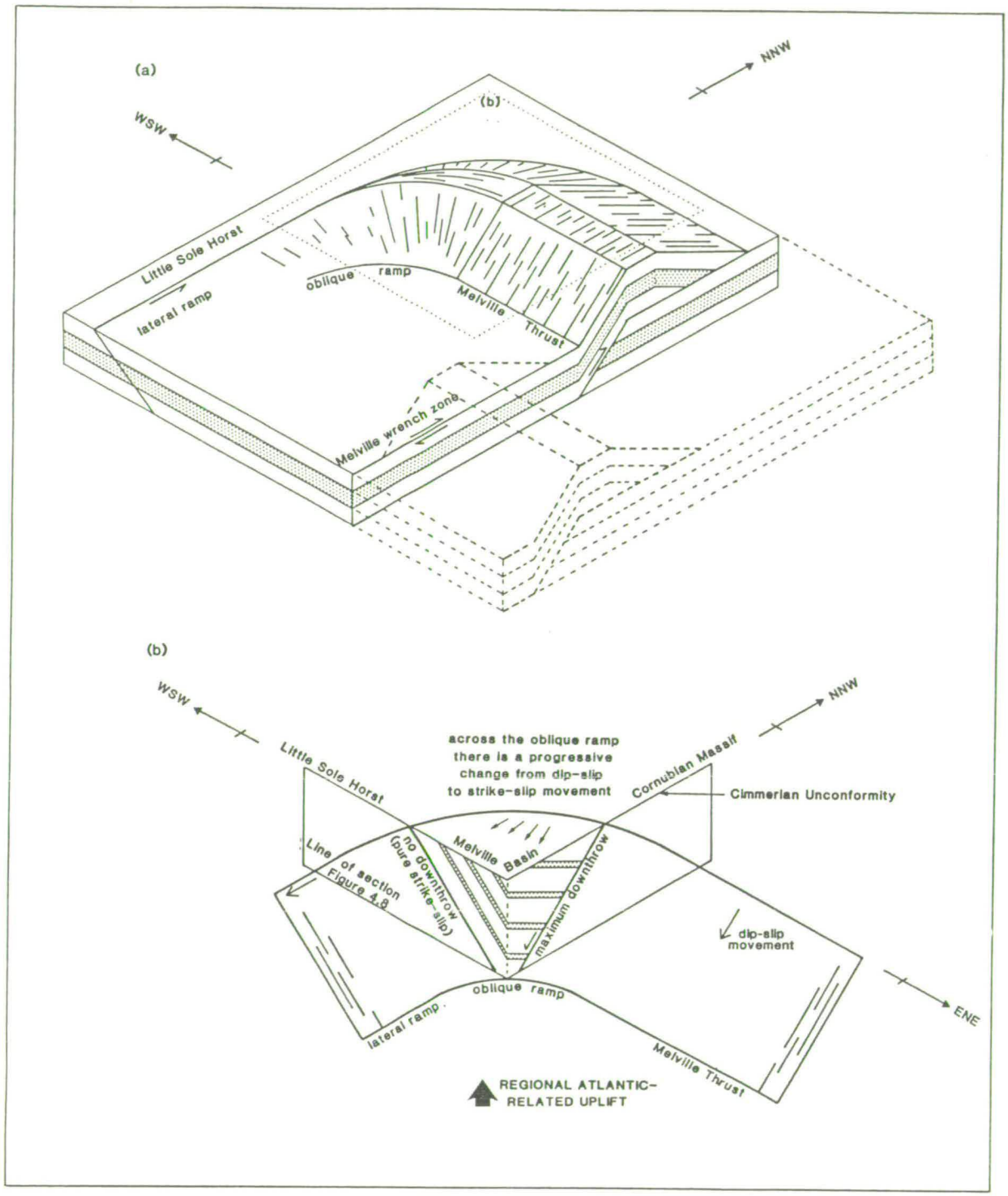

Figure 4.10 (a) Schematic Variscan tectonics of the Melville Basin between the Melville wrench zone and the Little Sole Horst.
(b) Schematic Cimmerian extensional tectonics of the oblique ramp at the northwestern margin of the Melville Basin, covering dotted area of upper diagram.

along strike from the southern Melville Basin Jurassic outlier which has been more deeply eroded to the east, in the St. Mary's Basin.

The basement of the St. Mary's Basin comprises a series of stacked thrusts. The deepest of these is the Carrick Thrust which does not subcrop in the Permo-Triassic but lies entirely within the basement. No reactivation of this structure is apparent (Figure 4.3). The Lizard Thrust underlies the northern flank of the St. Mary's Basin but there is little evidence of basinal faults being linked to it (Figures 4.3 and 4.11). Indeed, even allowing for velocity push down, a basinal fault appears to cut the Lizard Thrust in the vicinity of SWAT 6 (Figure 4.11). Similarly, the Normannian Thrust shows no evidence of reactivation nor does the possible lateral ramp structure at the eastern limit of the St. Mary's Basin have any demonstrable influence on the overlying sediments.

Two factors are believed to be responsible for the lack of apparent reactivation of the Variscan thrusts. The majority of the sequence in the St. Mary's Basin was deposited during the Permian denudational phase. Subsidence at this time was more through sagging due to sediment loading of pre-existing lows than due to extension, with possible reactivation of basement faults (Sections 5.3.2 and 5.3.3). Furthermore, the strongly faulted basement of the St. Mary's Basin accommodated such (dominantly Triassic and later) extension as there was over many faults. Unlike the Melville Basin, stresses were not sufficiently concentrated across a single structure to produce a "basin in the hanging wall".

In spite of the lack of apparent reactivation of basement faults there is a marked parallelism between the trend of the St. Mary's Basin and that of the underlying Variscan thrusts (Figures 4.1 and 4.2). The distribution of Permian sediments was controlled by end Variscan topography, in the case of the St. Mary' Basin the Cornubian Massif was probably the dominant sediment source area. The trend of the Cornubian Massif is parallel to that of the Variscan thrusts, and the Cornubian Batholith, at the heart of the Cornubian Massif, may have utilized these thrusts as zones of weakness during its emplacement. Thus the parallelism between the Permian basin and the Variscan thrusts owes more to orogenesis than to extensional tectonics. The Triassic sub-

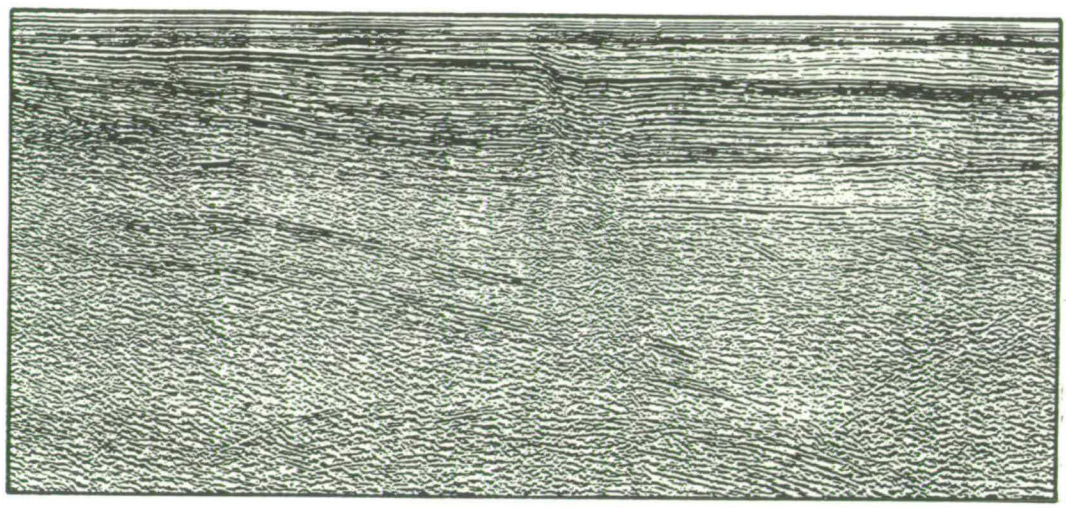

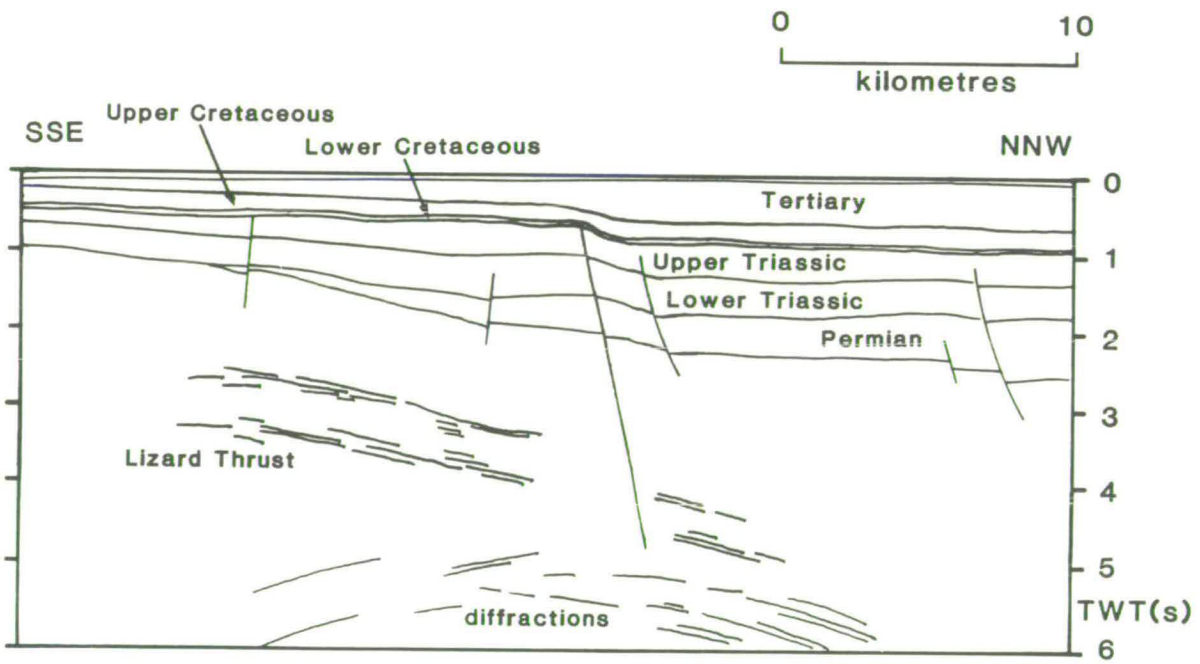

Figure 4.11 GECO line adjacent to BIRPS SWAT 6 showing Lizard Thrust beneath the northern St. Mary's Basin cut by major basinal fault. The thrust comprises two discrete branches. At a basement velocity of 6kms^{-1} and a velocity of 4kms^{-1} at the base of the sediments the top basement downthrow of 0.35s across the fault zone and resultant velocity push down of 0.12s does not account for the displacement of the Lizard Thrust at depth.

basins may follow the same trend due to a subtle control exercised by the pervasive ENE-WSW basement grain on later extensional faulting which is not resolved in the seismic data. Alternatively, the ENE-WSW fault trend may simply be the response to the Triassic extensional stress field in the absence of a controlling inherited structural grain.

4.4.3 The Haig Fras Basin

The Haig Fras Basin has been shown as a single (Smith, 1985) and a double (Chapman, in press) half-graben. Although at its eastern end, where crossed by SWAT 6, it appears as a double half-graben, 30km east at the southern end of SWAT 5, only a single broadly symmetrical basin is imaged. In general there are insufficient seismic data over the Haig Fras Basin to map these lateral variations. However, the symmetrical form shown by SWAT 5 and commercial data further west (Figure 1.2(a)) and also by Ziegler's (1982) regional cross-sections and the BGS Haig Fras map sheet (Fletcher and Evans, 1987) is believed to be the dominant basin morphology.

Although not well imaged in the seismic data, a Variscan thrust can be traced along the length of the shallow Haig Fras Basin (Figures 4.1 and 4.12). The thrust terminates at the southern flank of the Haig Fras Basin (Figure 4.12). The lack of basinal faults soling into the thrust combined with the overall relation between the thrust and basin suggest that reactivation of the Haig Fras Thrust did not control later basin evolution.

Shallow BGS wells in the north-east of the Haig Fras Basin have proven undifferentiated Permo-Triassic subcropping directly beneath the Cimmerian unconformity. It is suggested that the pre-Cimmerian of the Haig Fras Basin is dominantly Permian in age and was deposited when the area was a sub-aerial low between the late Variscan massifs of Cornubia and Haig Fras. Like the St. Mary's Basin, the parallelism between the Haig Fras Basin and Thrust is believed to be due to the control of Variscan structure on end Variscan topography rather than its control on later extension.

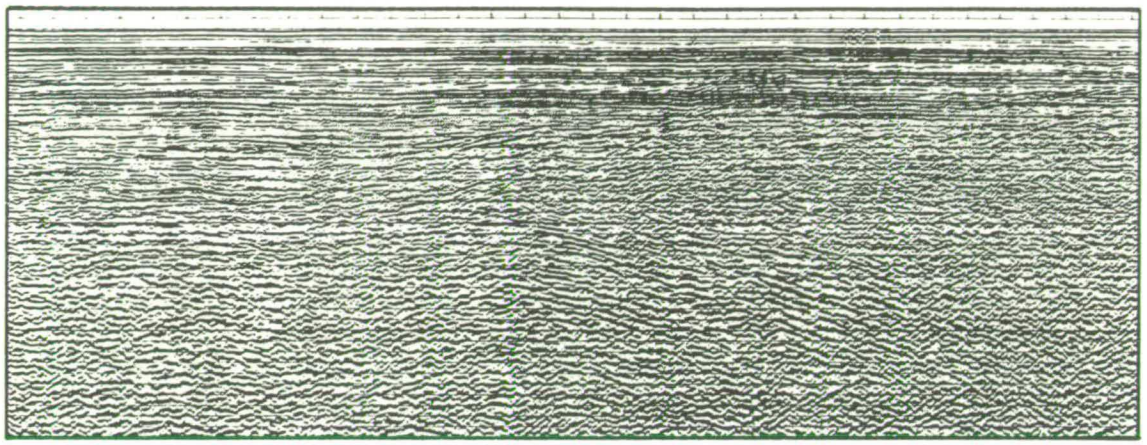

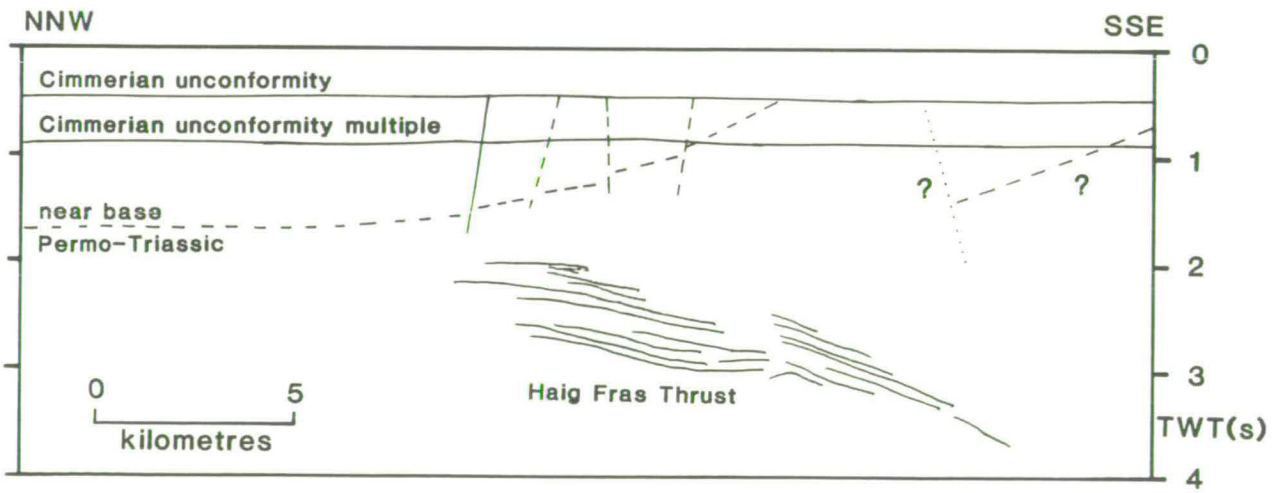

Figure 4.12 Petty-Ray line across Haig Fras Basin, underlying Haig Fras Thrust has no demonstrable control on basin development.

4.5 IMPLICATIONS FOR BASIN MODELS

The ENE-WSW Variscan structural trend mapped in the Western Approaches and Haig Fras Basins and the Cornubian Massif parallels that in northern Armorica (Figure 2.4). Hence from northern Armorica to the southern flanks of the South Celtic Sea Basin, contrary to Ziegler (1987a; 1987c), the Variscan structural trend is parallel to that of the superposed basins. Thrust reactivation can not be discounted *per se* as a control on basin distribution and geometry. Notwithstanding this, Variscan thrust reactivation can only be shown to have controlled the position of later extensional faulting in the Triassic-Jurassic of the Melville Basin. In the St. Mary's and Haig Fras Basins the parallelism of basement fault and basin trends reflects a more subtle control on Permian sediment source areas and possibly on Triassic extensional faulting.

No basin-controlling faults in the Western Approaches Trough can be shown to displace the Moho (SWAT 6 and 7), hence whole crustal simple shear models (Wernicke and Burchfiel, 1982; Wernicke, 1985; Beach, 1987) are not supported. However, formation of the Triassic-Jurassic sequence in the Melville Basin may be modelled by mid-upper crustal simple shear across the Melville Thrust. This may have been accommodated by pure shear in the more ductile lower crust and upper mantle (cf. Kusznir et al, 1987; Klemperer, 1988; Section 1.4.3.4). Extension in the Triassic of the St. Mary's Basin, which does not show the strong asymmetry typical of simple shear basins, may be broadly described as a pure shear phenomenon, although individual faults will of course deform by simple shear.

4.6 CONCLUSIONS

(i) The basement of the Western Approaches Basin comprises a set of ENE-WSW striking, SSE-dipping thrusts with oblique/lateral ramps that can be mapped over a wide area using commercial reflection seismic data. Steeper, NNW-SSE striking wrench faults are more readily observed on the gravity data.

(ii) Permian sediment accumulations are not significantly controlled by the extensional reactivation of these structures. Late Variscan topography is a more important control. The parallelism of the Permian basins and the Variscan thrusts reflects the broad control of similarly oriented structures on Variscan topography and not their reactivation during extension (cf. Brewer and Smythe, 1984; Allmendinger et al,1986; Beach, 1987; Keen et al, 1987; Brooks et al, 1988).

(iii) Half- and locally "quarter-"grabens of Triassic and early Jurassic sediments were preserved in the northern Melville Basin during regional Atlantic-related uplift by the Cimmerian (late Jurassic/early Cretaceous) extensional reactivation of an underlying Variscan thrust (Melville Thrust) and wrench zone (Melville wrench zone).

(iv) The probable Variscan lateral ramp at the western end of the Melville Thrust also acted as a ramp during Cimmerian extension. It hence determined the boundary between the Melville Basin and the Little Sole Horst, and possibly even the position of Atlantic rifting in the area.

(v) The Melville wrench zone was transtensionally reactivated during Tertiary compression across the Melville Basin. The Melville Thrust was not reactivated during this period.

(vi) The preserved Triassic of the St. Mary's Basin is symmetrical in form with several underlying thrusts. No single thrust significantly controlled sediment accumulation and extension was accommodated along many basement faults. The parallelism between the preserved Triassic and the basement faults may illustrate subtle control by the pervasive basement grain on later deformation or may simply be due to a coincidence between the orientations of Variscan compressional and Mesozoic extensional forces.

(vii) The Triassic and late Jurassic/early Cretaceous extension phases in the Melville Basin may be modelled as mid-upper crustal simple shear, whereas in the St. Mary's Basin extension may be broadly thought

of as pure shear. There is no evidence of whole crustal simple shear in the Western Approaches Trough.

CHAPTER 5

PERMIAN-JURASSIC TECTONIC EVOLUTION: EARLY BASIN DEVELOPMENT

5.1 INTRODUCTION

During the Permo-Triassic a thick sequence of dominantly continental red-beds, the New Red Sandstone, was deposited in the Western Approaches Trough. At the end of the Triassic, following eustatic sea-level rise and regional subsidence, shallow marine conditions were established. Shelf shales and limestones persisted until Callovian/Oxfordian regression resulted in an unconformity overlain by late Jurassic shallow/marginal marine and continental deposits. Late Jurassic shallowing was a prelude to the Cimmerian uplift of the Western Approaches Basin which led to the removal of all but isolated outliers of Jurassic rocks and locally cut back as far as the Permian.

The aim of this chapter is to elucidate the mechanisms of basin subsidence which accommodated the deposition of the Permian-Jurassic sequence. The exceptional magnitude of Cimmerian erosion combined with the lack of palaeontological age data for the New Red Sandstone complicates this. However, seismic, gravity and borehole subsidence data are combined with our knowledge of the geology of the period to interpret early basin development.

5.2 PERMIAN-JURASSIC TECTONIC SUBSIDENCE CURVES

Tectonic subsidence plots for the Permian-Jurassic of wells 72/10-1, 73/1-1 and 73/13-1 in the Melville Basin and the Jurassic of the wells in the French sector (Figures 5.1, 5.2 and 5.3) were constructed as outlined in Chapter 3. Difficulties specific to calculating and analysing subsidence plots for this sequence are briefly discussed below.

5.2.1 Chronological Calibration

Wells 72/10-1, 73/1-1 and 73/13-1 were selected because the Rhaetian/early Jurassic sediments eroded elsewhere in the Western Approaches Basin have been biostratigraphically dated (Section 3.7.4). The horizontal error bars on points for the underlying sequence represent the confidence limits of chronological calibration. The pre-Rhaetian of the Mercia Mudstone Group is constrained by palynological data to the Carnian-Norian. Limited palynological data suggest the Sherwood Sandstone Group may be as young as Carnian (Evans et al, in press) but by analogy with onshore south-west England it may extend to the beginning of the Triassic. There are no biostratigraphical data on the age of the base of the Permo-Triassic in wells 72/10-1, 73/1-1 and 73/13-1 and it has been shown as pre-Mercia Mudstone Group and post-Carboniferous.

5.2.2 Depth to Basement

The depth to the base of the Permo-Triassic (not penetrated in wells 72/10-1, 73/1-1 or 73/13-1) has been determined by depth converting reflection seismic data between well terminal depth and picked basement (using velocities extrapolated from the base of the well and stacking velocities). In well 73/13-1, considering the range of reasonable velocities, the error limits of the depth conversion are ±0.5km (±0.2km of tectonic subsidence at a sediment density of $2.41 gcm^{-3}$). In wells 72/10-1 and 73/1-1, where the base of the Permo-Triassic is much shallower, the error is ±0.1km (±0.04km of tectonic subsidence). This error is not significant in comparison with the very large potential dating error of this horizon.

The base of the Permo-Triassic, as determined by seismic data, has been taken as decompaction basement in wells 72/10-1, 73/1-1 and 73/13-1.

5.2.3 Magnitude of Cimmerian Erosion

In order to obtain an indication of the total magnitude of Permian-Jurassic subsidence in the Western Approaches Basin the thickness of the interval removed during Cimmerian uplift must be estimated.

If the magnitude of Cimmerian uplift was greater than the magnitude of post-Cimmerian subsidence (corrected for Tertiary uplift, Chapter 7) then the porosity-depth plots of Figure 3.3 should show a sharp drop across the Cimmerian unconformity due to overcompaction. This drop must be independent of lithological variation across the unconformity. Similar lithologies occur on either side of the Cimmerian unconformity in wells 73/8-1, 74/1-1, 83/24-1, 85/28-1, 86/17-1 and 86/18-1. There is a slight porosity drop across the unconformity in these wells (Figure 3.3) which suggests that the magnitude of Cimmerian erosion is similar to, or slightly greater than, the magnitude of post-Cimmerian subsidence. 1.4km of post-Cimmerian subsidence is observed in wells 72/10-1 and 73/1-1 and 1.5km in well 73/13-1. These values are in broad agreement with the thickness of the preserved Jurassic in the Brittany Basin and unpublished estimates of the amount of Cimmerian erosion based on maturation modelling. An error of ±0.2km (±0.1km of tectonic subsidence at a sediment density of 2.18gcm^{-3}) has been added to the palaeobathymetric/eustatic error limits for the top Jurassic horizon due to the uncertainty of this estimate.

5.2.4 Halokinesis

Wells 72/10-1 and 73/1-1 are both located over salt swells. Since most of the salt was emplaced post-depositionally during Cimmerian and Tertiary halokinesis its thickness was subtracted from sub-salt well depths.

5.2.5 French Wells

The Jurassic subsidence history of the Brittany and South-West Channel Basins is particularly important as post-Sinemurian Jurassic

sediments have only been recovered in wells Brezell-1, Lennket-1 and Lizenn-1.

Well Lennket-1 penetrated Armorican-type basement. However, wells Brezell-1 and Lizenn-1 terminated within the sedimentary sequence and no seismic data were available to extrapolate to basement. In well Brezell-1 Permian sandstone, unconformably underlying the base of the Jurassic (Figure 2.1), provides a reasonable decompaction basement. However, in well Lizenn-1 terminal depth was taken as decompaction basement. Since deposition of the basal units recovered in well Lizenn-1 will have been partially accommodated by compaction of the underlying sequence the true decompacted subsidence rate for those basal units will lie between the undecompacted and decompacted rates as shown on Figure 5.3(b).

5.3 PERMO-TRIASSIC TECTONIC EVOLUTION

5.3.1 Two-Stage Subsidence

The subsidence plots of Figures 5.1 and 5.2 exhibit rapid Permo-Triassic subsidence followed by slower Jurassic subsidence. From the subsidence plots alone it is not possible to distinguish whether Permo-Triassic subsidence occurred as a single pulse commencing at the base of the sequence (Figure 5.1) or as two or more discrete pulses (Figure 5.2). However, as discussed in Section 2.5.4, geological evidence defines two distinct phases of Permo-Triassic sedimentation. The first commenced with the basal Permo-Triassic breccio-conglomerates and sandstones and passed up into the shaly sandstones and shales of the Aylesbeare Group (henceforth referred to as the Permian sequence although it may extend into the early Triassic). The second commenced with the locally conglomeratic base of the Sherwood Sandstone Group and passed up into the Mercia Mudstone Group (the Triassic sequence). A minor unconformity, apparent on seismic reflection data, separates the sediments deposited during the Triassic phase from those of the Permian phase (Figure 2.9).

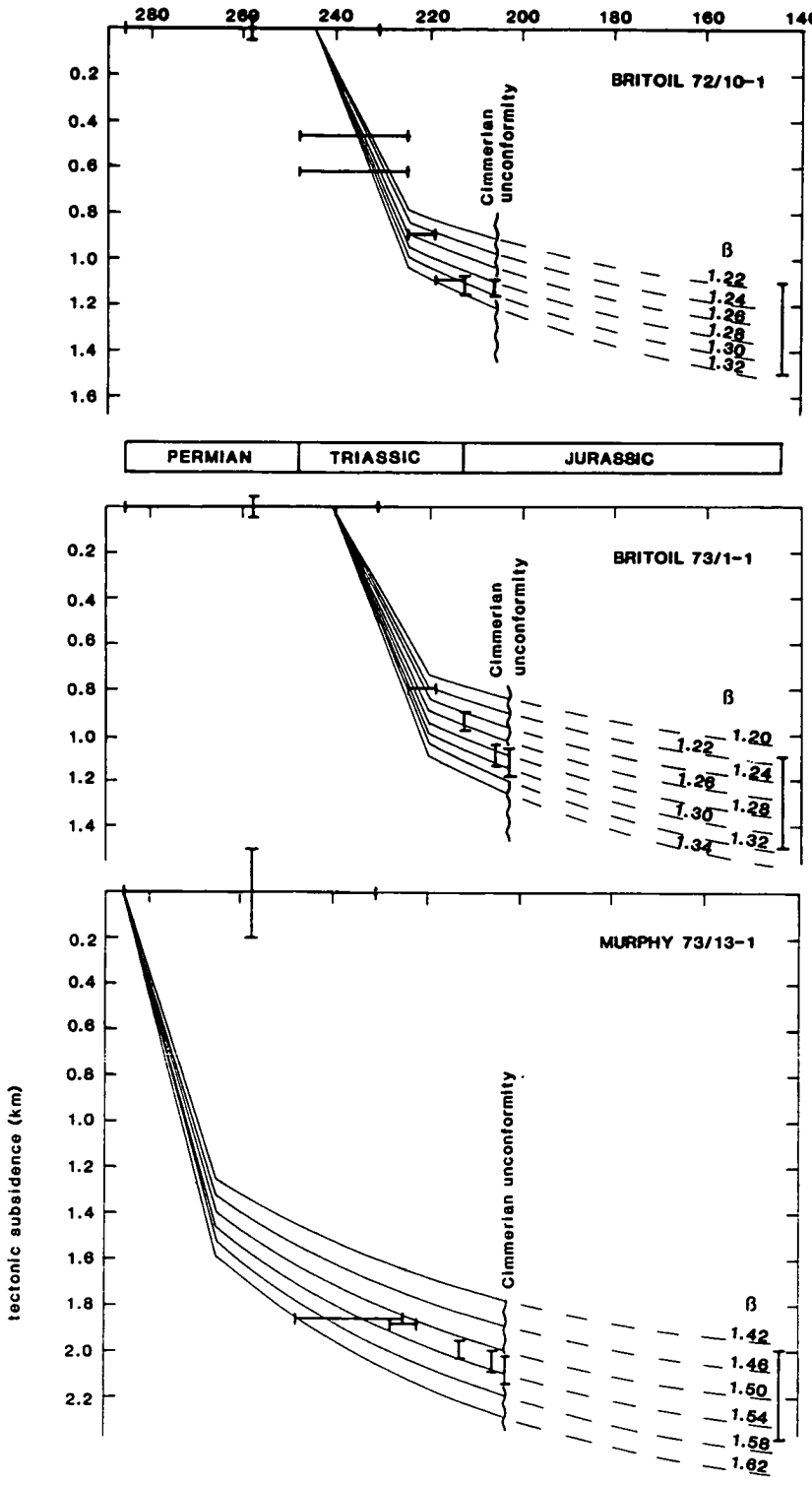

Subsidence data are corrected for sediment compaction and loading and changes in the height of the overlying water column (marine Jurassic sediments only).

All points are from the given well except the top basement horizon which was picked from reflection seismic data. The vertical error bars on this point represent the accuracy of depth conversion. Vertical error bars on early Jurassic data represent the accuracy of the palaeobathymetric and eustatic corrections. The position of the top Jurassic point was estimated from porosity data. The horizontal error bars in the Permo-Triassic are due to the difficulty of chronologically calibrating the continental red-beds of this period.

Model subsidence curves assume homogeneous extension with a rift pulse of duration 20Ma. Thermal subsidence during rifting was added to the fault-controlled subsidence. Pre-rift crustal thickness was taken as 30km, other parameters as Chadwick (1985a).

Figure 5.1 Permian-Jurassic subsidence in the Melville Basin modelled as a single extension-driven phase. See text for details.

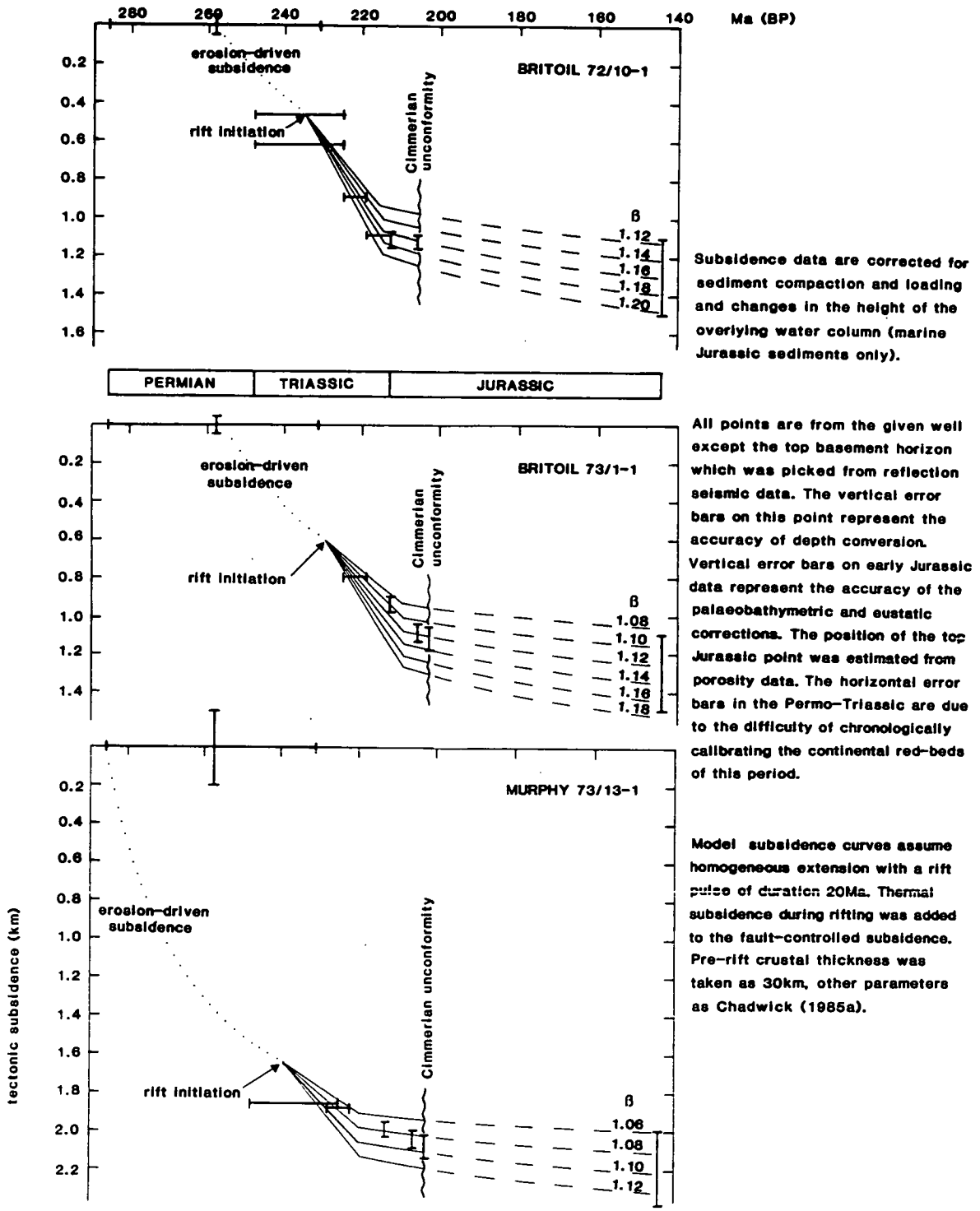

Subsidence data are corrected for sediment compaction and loading and changes in the height of the overlying water column (marine Jurassic sediments only).

All points are from the given well except the top basement horizon which was picked from reflection seismic data. The vertical error bars on this point represent the accuracy of depth conversion. Vertical error bars on early Jurassic data represent the accuracy of the palaeobathymetric and eustatic corrections. The position of the top Jurassic point was estimated from porosity data. The horizontal error bars in the Permo-Triassic are due to the difficulty of chronologically calibrating the continental red-beds of this period.

Model subsidence curves assume homogeneous extension with a rift pulse of duration 20Ma. Thermal subsidence during rifting was added to the fault-controlled subsidence. Pre-rift crustal thickness was taken as 30km, other parameters as Chadwick (1985a).

Figure 5.2 Permian-Jurassic subsidence in the Melville Basin modelled as a Permian erosion-driven phase followed by a Triassic extension-driven phase. See text for details.

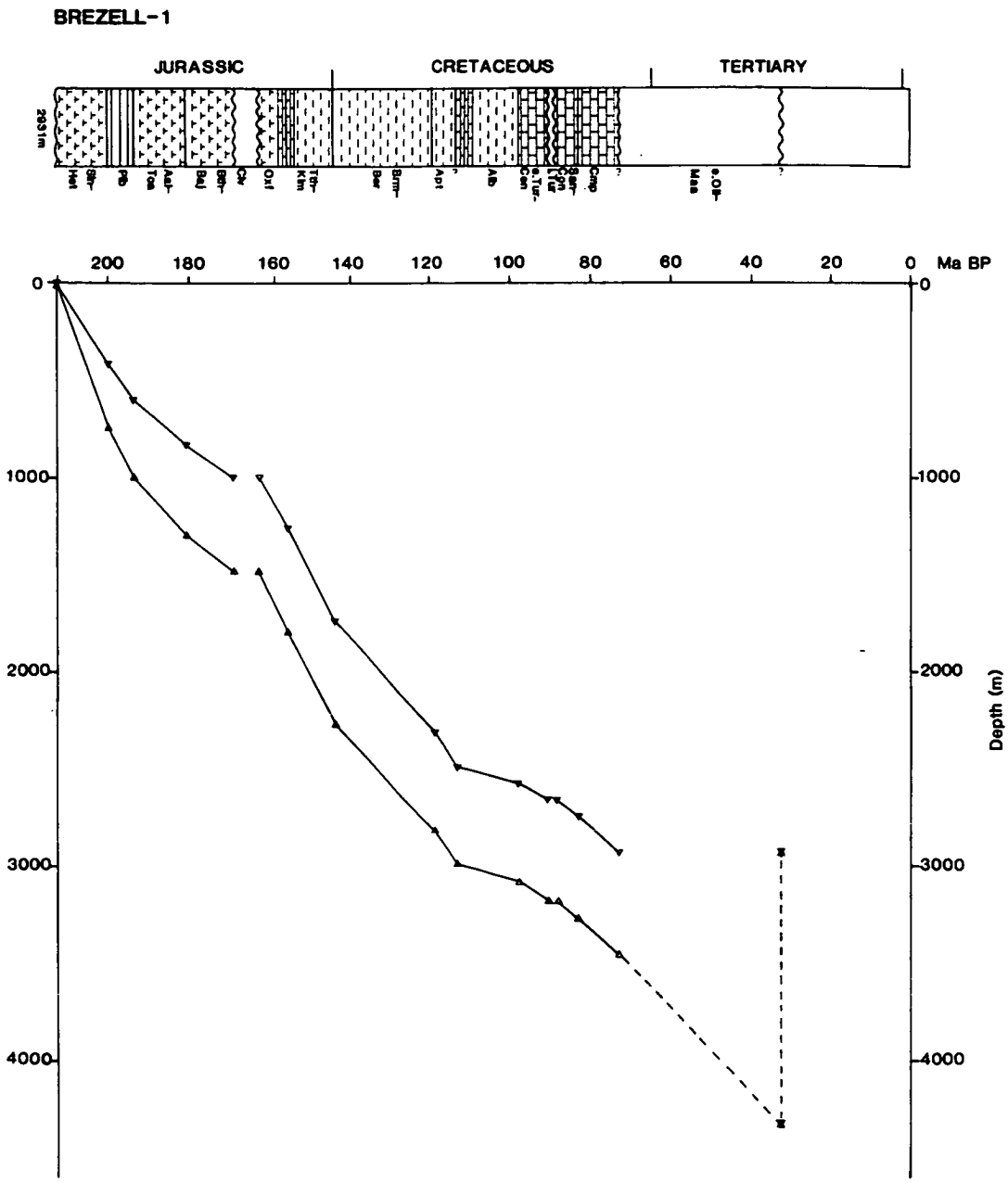

Figure 5.3 (a) Summary litholog for well Brezell-1 with observed and decompacted (lower plot) thicknesses above basement.

BREZELL-1 (cont.)

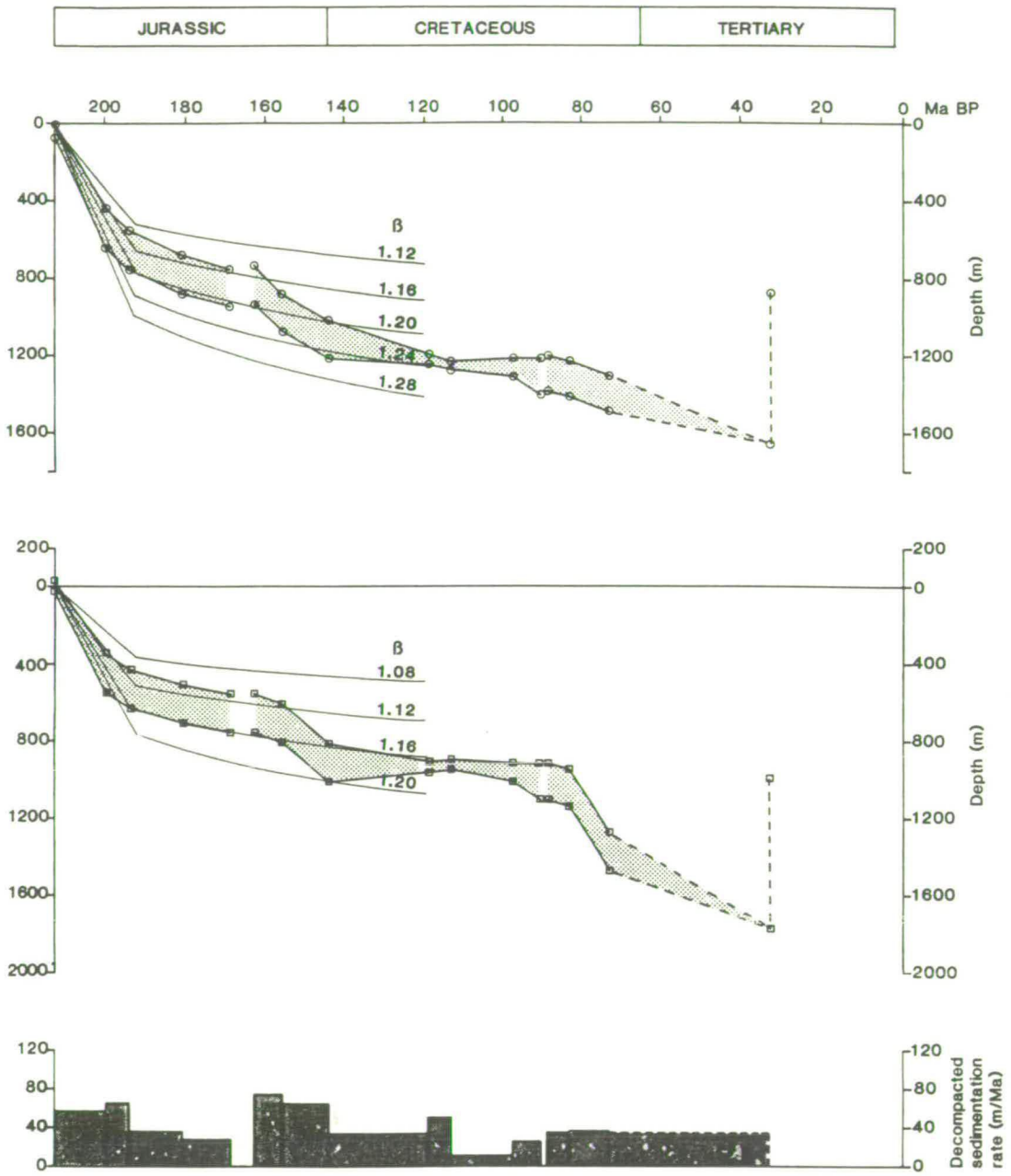

Figure 5.3 (a) (cont.) Tectonic subsidence plots for well Brezell-1 (corrected for sediment compaction and loading and changes in the height of the overlying water column). Upper plot corrected after Falvey and Deighton (1982) sea-level curve, lower after Hallam (1984). Dotted area represents error limits of palaeobathymetric correction. Model subsidence curves as Figure 5.1, rift duration 20Ma. Tertiary uplift estimated from chalk porosities (Chapter 7).

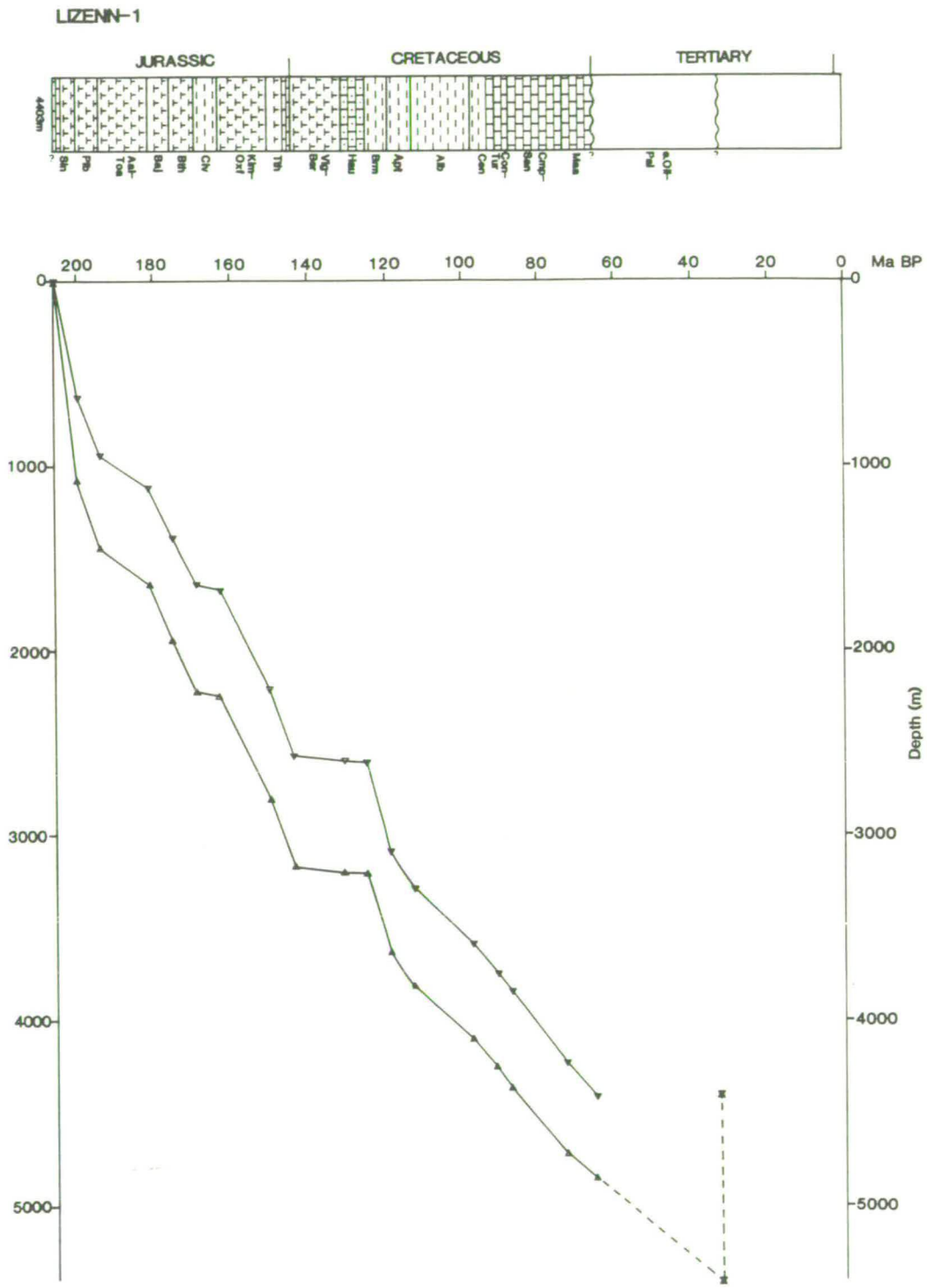

Figure 5.3 (b) Summary litholog for well Lizenn-1 with observed and decompacted (lower plot) thicknesses above basement.

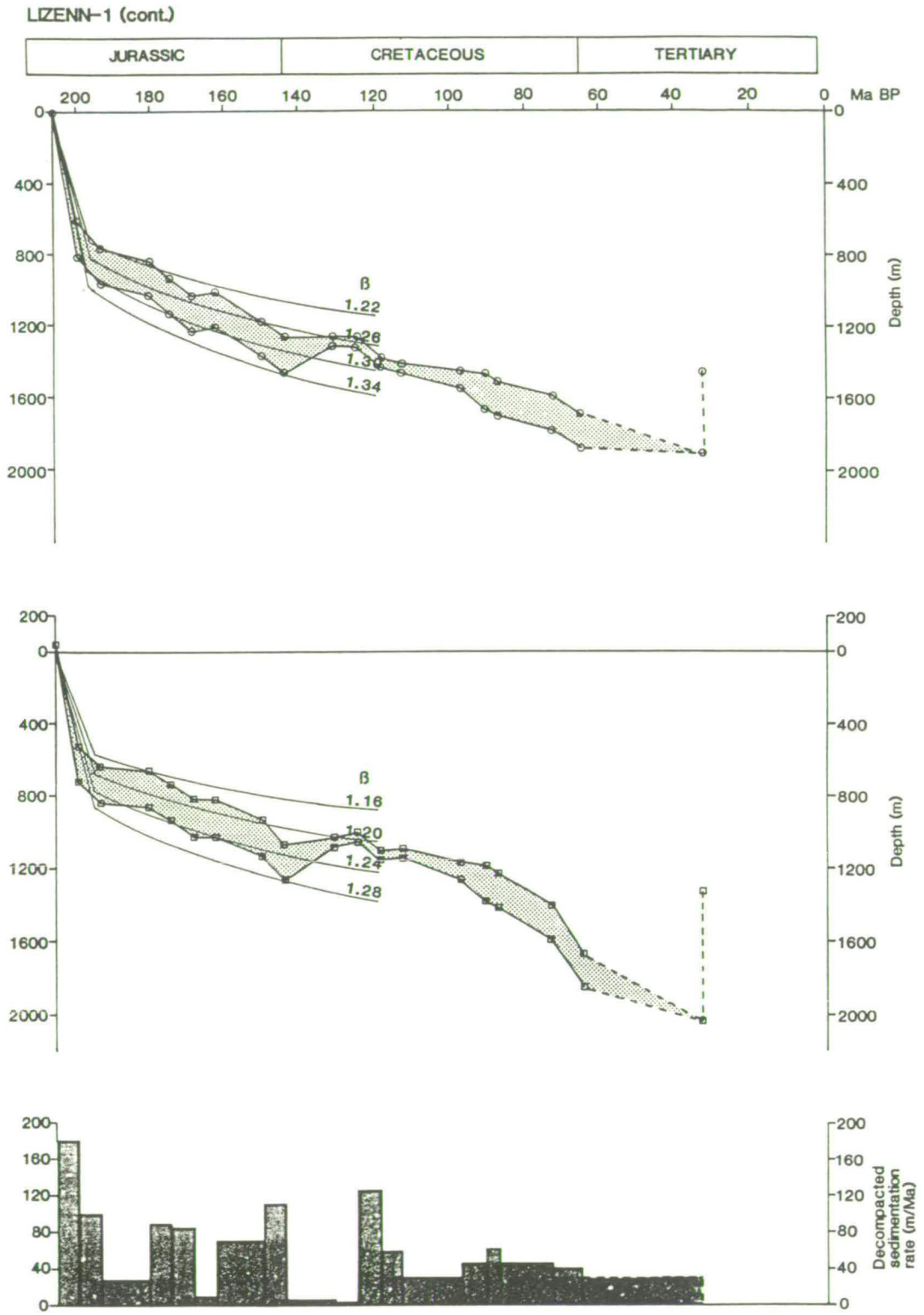

Figure 5.3 (b) (cont.) Tectonic subsidence plots for well Lizenn-1 (corrected for sediment compaction and loading and changes in the height of the overlying water column). Upper plot corrected after Falvey and Deighton (1982) sea-level curve, lower after Hallam (1984). Dotted area represents error limits of palaeobathymetric correction. Model subsidence curves as Figure 5.1, rift duration 10Ma. Tertiary uplift estimated from chalk porosities (Chapter 7).

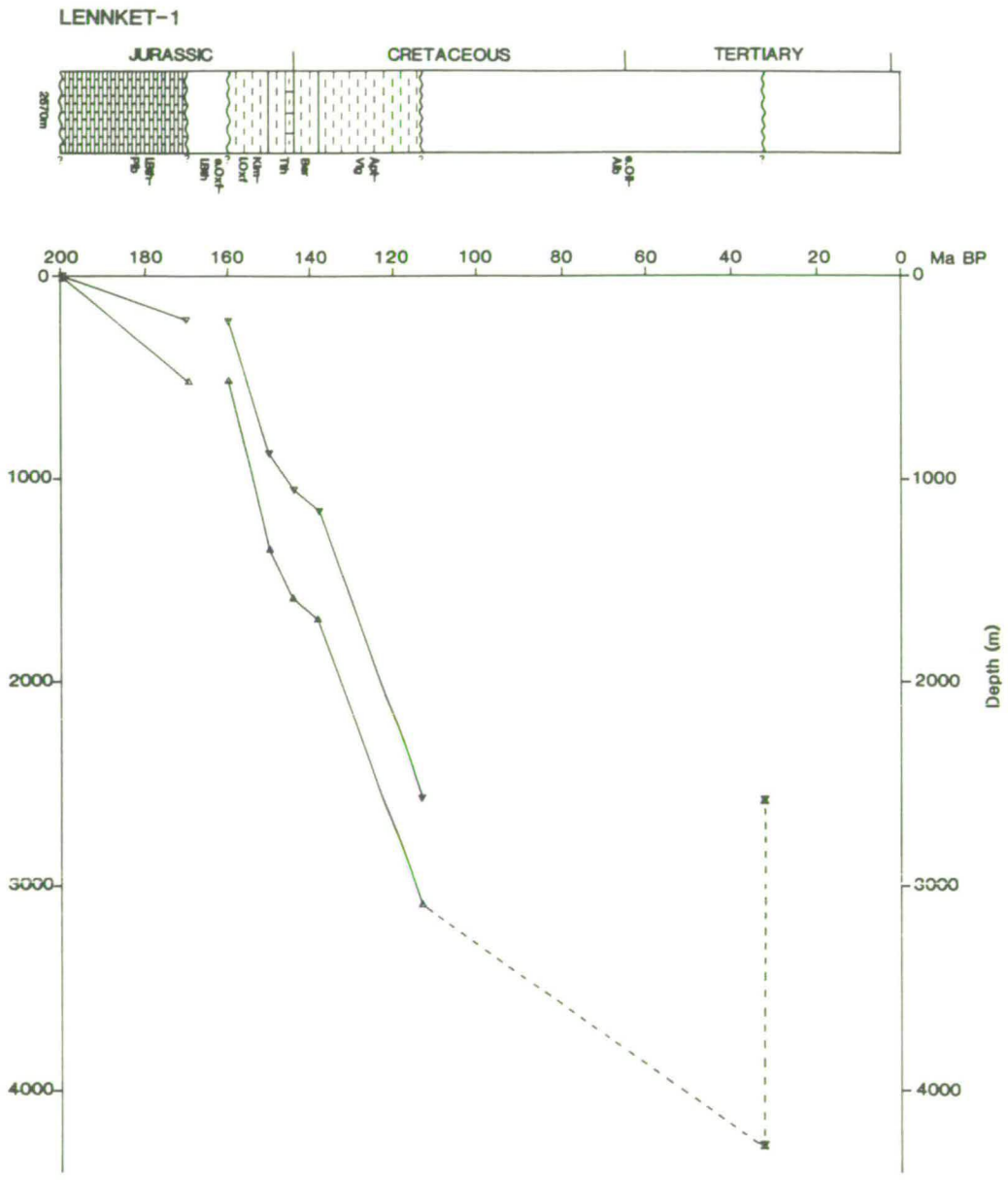

Figure 5.3 (c) Summary litholog for well Lennket-1 with observed and decompacted (lower plot) thicknesses above basement.

LENNKET-1 (cont.)

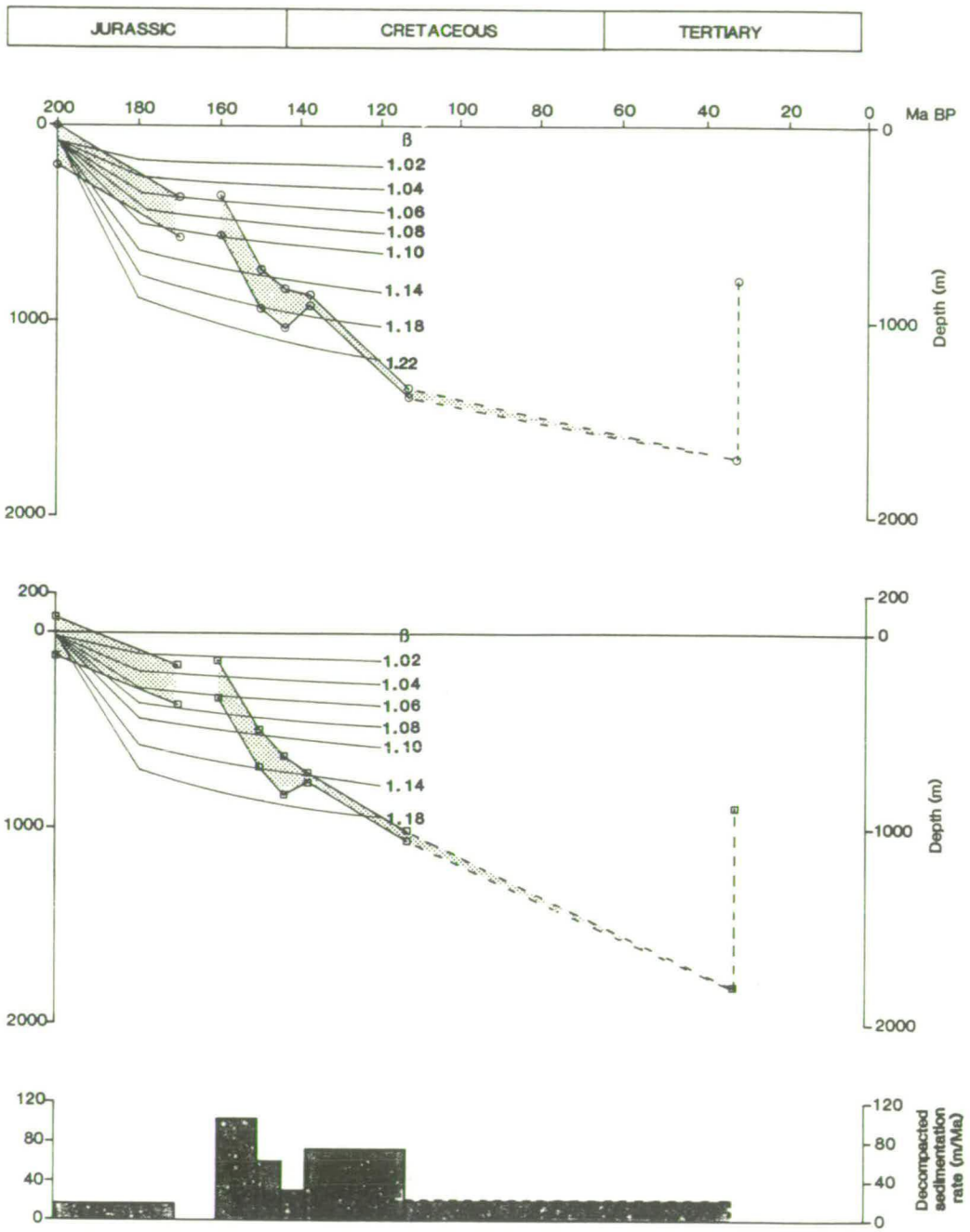

Figure 5.3 (c) (cont.) Tectonic subsidence plots for well Lennket-1 (corrected for sediment compaction and loading and changes in the height of the overlying water column). Upper plot corrected after Falvey and Deighton (1982) sea-level curve, lower after Hallam (1984). Dotted area represents error limits of palaeobathymetric correction. Model subsidence curves as Figure 5.1, rift duration 20Ma. Tertiary uplift estimated from chalk porosities (Chapter 7).

5.3.2. The Extension Problem

Chadwick (1985c, 1986) proposed a similar two-stage subsidence path for the Permo-Triassic of the Worcester and Wessex Basins and argued that both these phases were driven by lithospheric extension. Rapid subsidence during and immediately after rifting led to the deposition of the arenaceous units while the finer-grained Aylesbeare and Mercia Mudstone Groups were deposited during the slower thermal subsidence phases.

The model curves of Figures 5.1 and 5.2 assume homogeneous extension with a rift duration of 20Ma. Early thermal subsidence during rifting is added to the fault-controlled subsidence. This is a simplification of the effects of finite rifting (Jarvis and McKenzie, 1980; Cochran, 1983) but is not significant within the error limits of the subsidence data. Furthermore, the extension may be heterogeneous, but again this cannot be resolved in the subsidence data. The model curves simply illustrate the total magnitude of crustal stretching/thinning. This will be given by total subsidence (fault and thermal phases) regardless of the duration of extension or its possible heterogeneity or indeed lateral heat flow or any other modification of the lithospheric temperature distribution. These affect only the subsidence path and not its overall magnitude (Figure 5.4). Similarly, total subsidence is independent of the number of re-rifting events and is controlled only by the combined crustal thinning caused by these events (Figure 5.4).

If, like the Worcester and Wessex Basins (Chadwick, 1985c; 1986), this sequence was deposited in response to lithospheric extension then the observed total magnitude of Permian-Jurassic subsidence requires crustal thinning with a β-factor of approximately 1.5 in well 73/13-1 and 1.3 in wells 72/10-1 and 73/1-1 (Figure 5.1). The β-factor for extension across the Permian fault set measured from the published sections of Chapman (in press) across the Melville Basin is 1.02. Combining this with the β-factor of 1.05 for Triassic extension (Chapman, in press) gives a total Permo-Triassic extension of only 1.07.

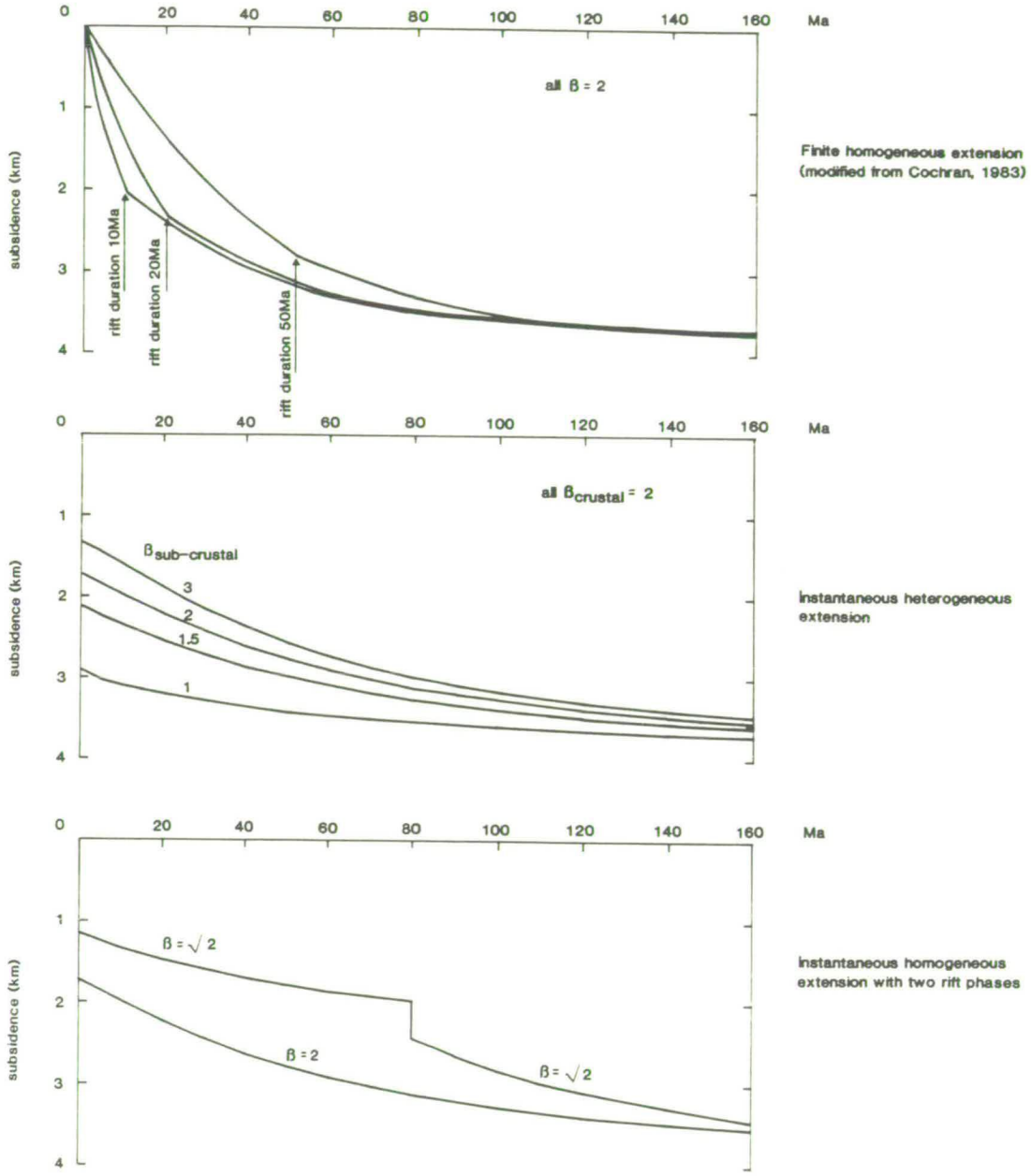

Figure 5.4 Model subsidence curves (normalized for water-loading) for extension and thinning of the crust by a factor of 2. Lithospheric physical parameters after Cochran (1983). Total subsidence is dependent only on the amount of crustal thinning and is independent of the response of the sub-crustal lithosphere to extension.

This discrepancy may be due to the limited resolution of the seismic data and/or the geometrical simplicity of "summing the heave"-type estimates of extension (Section 1.4.3.3). In this study "whole crustal" extension values, derived from gravity and deep seismic data, are preferred to estimates of crustal thinning based on the extension of the cover as apparent on seismic reflection data because of the inaccuracy of the latter (Section 8.4). Gravity and seismic modelling of crustal thickness are in close agreement and suggest an essentially flat Moho from the flanks to the centre of the St.Mary's Basin under up to 7km of sediment (Figures 8.14 and 8.15). Hence there is insufficient crustal thinning to account for the observed sediment thickness. Chapter 8 discusses whole crustal thinning and the thickness of the sedimentary sequence in the Western Approaches Trough in more detail.

The depth converted interpretation of SWAT lines 6 and 7 (Figure 8.15) suggests a slight shallowing of the reflection Moho (by approximately 1km) under the eastern Brittany Basin. This is consistent with the increase in Triassic-Jurassic subsidence from the St. Mary's to the Brittany Basin (Figure 1.2). However, assuming there was no wholesale crustal simple shear, if Permian subsidence had been extensionally-driven then the thinnest crust would be anticipated under the southern St. Mary's Basin where the post-Carboniferous sedimentary sequence is thickest.

If there is an irreconcilable excess of subsidence over extension in the Western Approaches Trough can an alternative or more probably additional driving mechanism of basin subsidence account for this excess?

5.3.3 Permian Subsidence: Variscan Denudation

The downlap of the Permian onto Variscan basement (Figure 2.9) is due to northward tilting of the Melville Basin during the Triassic and Cimmerian. In the Permian sediments gradually onlapped a high in the northern Melville Basin (Figure 5.5(a)). This high was created by a combination of Variscan reverse movement along the Melville Thrust (Figure 4.10(a)) and intrusion of the Cornubian Batholith, from which the Permian sequence was in part shed (clasts in the basal

conglomeratic horizons in well 72/10-1 are derived from the Cornubian Batholith). It is proposed that the Permian of the Western Approaches Trough is a post-orogenic intermontane molasse-type sequence and that basin subsidence was primarily driven not by extension but by denudation of the adjacent massif (Figure 5.5(a)). This accounts for the discrepancy between extension and subsidence.

Isostatic adjustment due to the infilling of a sub-aerial topographic low will increase the magnitude of that initial low (Figure 5.6). For sediments with an average density of $2.3gcm^{-3}$ the entire Permian sequence of well 73/13-1 represents the infilling of approximately 1km of topography (Figure 5.6).

The pre-Cimmerian sequence recovered in well 73/2-1, overlying the Melville Thrust in the northern Melville Basin, provides support for the denudational model. Allochthonous Armorican-type basement penetrated at the base of the well is directly overlain by the Sherwood Sandstone Group (Figure 5.5(b)). Variscan compression on the Melville Thrust drove the allochthonous basement northwards generating a high from which sediments were sourced into the southern Melville Basin during the Permian (Figure 5.5(a)). It remained a high until Triassic extension and reactivation of the Melville Thrust caused active subsidence of the now peneplained northern Melville Basin. Hence in well 73/2-1 the Sherwood Sandstone Group directly overlies allochthonous Armorican basement with no intervening Permian sediments (Figure 5.5(b)).

The Permian sequence varies from 5-6km thick in the southern Western Approaches Basin to absent in the northern Western Approaches Basin over only 25km laterally. This exceptionally rapid lateral thickness variation supports a denudational model and is in contrast with the Permian of the Worcester Basin which is of comparatively even thickness (Chadwick 1985c Figure 4).

The Permo-Triassic sequence thins southwards under the Brittany and South-West Channel Basins. Although sufficient seismic data were not available to extend the basement map of Figure 4.1 into the French sector of the Western Approaches Trough Variscan thrusts are observed in the area (J.P. Lefort, personal communication, 1987). It is proposed that Variscan thrusting and granite intrusion combined to produce a Permian high in the Brittany Basin/South-West Channel Basin/Armorican

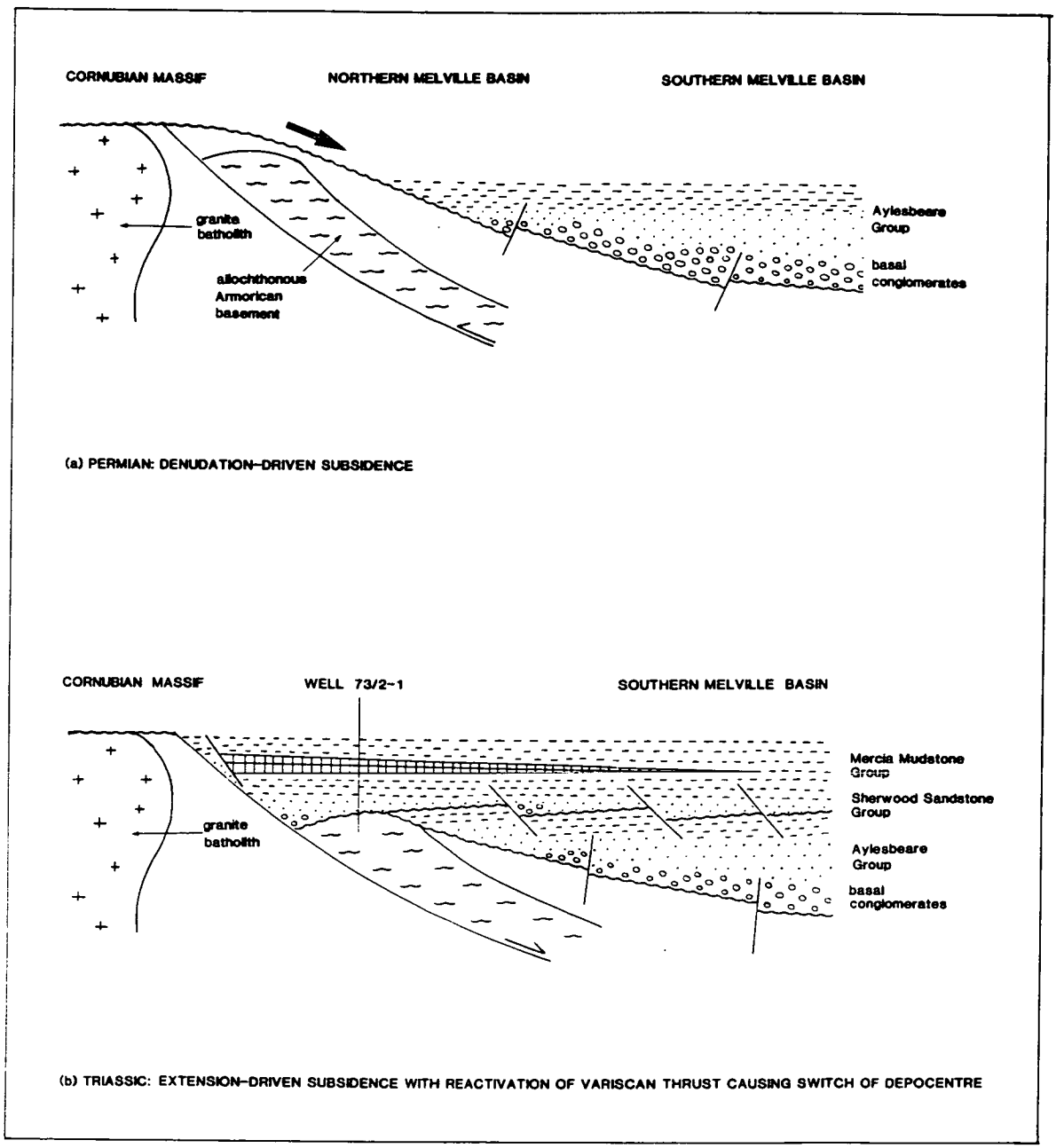

Figure 5.5 Schematic illustration of the (a) Permian and (b) Triassic subsidence phases in the Melville Basin.

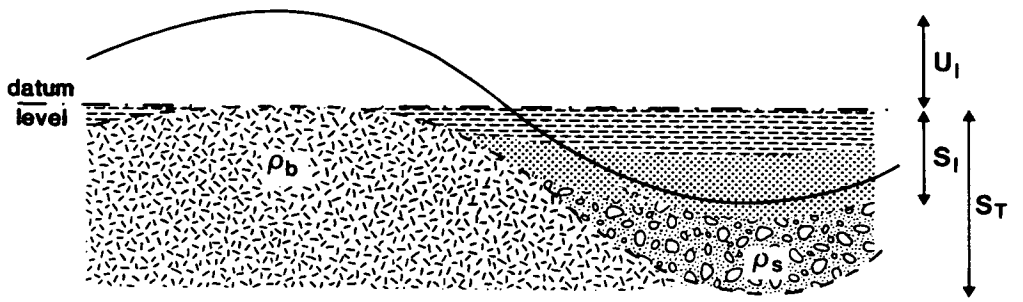

Unloading of high by erosion amplifies uplift:

$$U_T = U_I\left[\frac{\rho_m}{\rho_m - \rho_b}\right]$$

Loading of low by sedimentation amplifies subsidence:

$$S_T = S_I\left[\frac{\rho_m}{\rho_m - \rho_s}\right]$$

for $\rho_m = 3.33 gcm^{-3}$, $\rho_b = 2.8 gcm^{-3}$ and $\rho_s = 2.3 gcm^{-3}$:

$$U_T = 6.28\ U_I$$

$$S_T = 3.23\ S_I$$

High never attains U_T magnitude, erosion is contemporaneous with isostatic uplift. U_T is total thickness of material eroded from the high.

Figure 5.6 Isostatic response to post-orogenic peneplanation (local Airy isostasy assumed). Solid line is post-orogenic topography, dashed line is depth to basement following peneplanation. Ornamentation shows end peneplanation geology.

Massif as they did in the northern Western Approaches Basin/Cornubian Massif.

5.3.4 Triassic Subsidence: The Onset of Extensional Tectonics

Unlike the Permian of the Melville Basin the Triassic is demonstrably fault-controlled. Both the Sherwood Sandstone Group and the Mercia Mudstone Group thicken syndepositionally into ENE-WSW and NNW-SSE trending normal faults (Section 4.4.1 and Figures 4.6 and 4.8). However, the lack of fault control on the preserved Liassic sediments of the Melville Basin (Figure 4.7) suggests rifting in the Western Approaches Basin was complete by the end of the Triassic. It is proposed that Triassic extension and rapid fault-controlled subsidence followed by Liassic thermal relaxation was responsible for the second phase of basin subsidence in the Western Approaches Basin (Figure 5.5(b)).

Again there is a discrepancy between the magnitude of measured Triassic-Jurassic extension and subsidence. Well 72/10-1 requires homogeneous extension with a β-factor of 1.12-1.20, well 73/1-1, 1.09-1.17 and well 73/13-1, 1.06-1.13 (Figure 5.2), while the measured extension of the Triassic rifting is only 1.05 (Chapman, in press). This discrepancy is probably the result of inaccuracies in the estimation of extension from seismic data (Section 1.4.3.3) and of "hidden" extension in the now eroded post-Sinemurian Jurassic sequence.

The magnitude of Triassic-Jurassic subsidence and extension, as measured from well and seismic data, is lower in the southern than in the northern Melville Basin. This is consistent with the observed syn-depositional thickening of the sequence. The change in driving mechanism of basin subsidence led to the switch in depocentre from the southern Melville Basin in the Permian to the northern Melville Basin in the Triassic (Figure 5.5).

The absence of Triassic sediments from well Brezell-1 (Figure 2.1) suggests that the decrease in Triassic extension and subsidence continued into the Brittany Basin. The Armorican source of the Sherwood Sandstone Group in the Wessex Basin (P.W. Hawkes, conference communication, 1988) further supports this hypothesis.

5.4 JURASSIC TECTONIC EVOLUTION

In the Western Approaches Basin the preserved Liassic (Hettangian-Sinemurian) sediments show no syn-depositional fault control (Figure 4.7) and subsidence rates were generally low. Although well 73/1-1 shows a minor early Jurassic subsidence pulse (Figure 5.2) it was essentially a time of quiescent thermal subsidence following Triassic extension and rapid subsidence.

In contrast the Hettangian-Sinemurian subsidence rate in wells Brezell-1 and Lizenn-1 (Figures 5.3(a) and (b)) is very rapid, even allowing for possible decompaction errors, and fits subsidence following earliest Jurassic rifting. Hence extensional stresses persisted from the Triassic into the Jurassic, with the focus of rifting migrating southwards from the northern Melville Basin to the Brittany Basin.

The magnitude of early-mid Jurassic subsidence is less in the South-West Channel Basin (Figure 5.3(c)) than in the Brittany Basin. However, the basal carbonate unit is simply assigned an undifferentiated Liassic-Dogger age and rift timing can not be constrained. Well Lennket-1 does, however, show a pronounced Oxfordian-Tithonian subsidence kick following the mid/late Jurassic unconformity (Figure 5.3(c)). A smaller subsidence kick can be seen in the Oxfordian-Tithonian of well Brezell-1 (Figure 5.3(a)), but is not apparent within error limits of well Lizenn-1 (Figure 5.3(b)). This late Jurassic subsidence pulse may also have occurred in the Western Approaches Basin, but any evidence of it has been removed by Cimmerian erosion.

5.5 COMPARISON OF RIFT TIMINGS WITH THE WESSEX BASIN

Published studies of basin subsidence in the southern UK are restricted to the Wessex Basin (Chadwick, 1986; Karner et al, 1987). Chadwick (1986) identified the following rift pulses: Permian, early-mid Triassic, late Triassic/early Jurassic and late Jurassic (Figure 5.7). These can be correlated with the Permian, Triassic, early Jurassic and

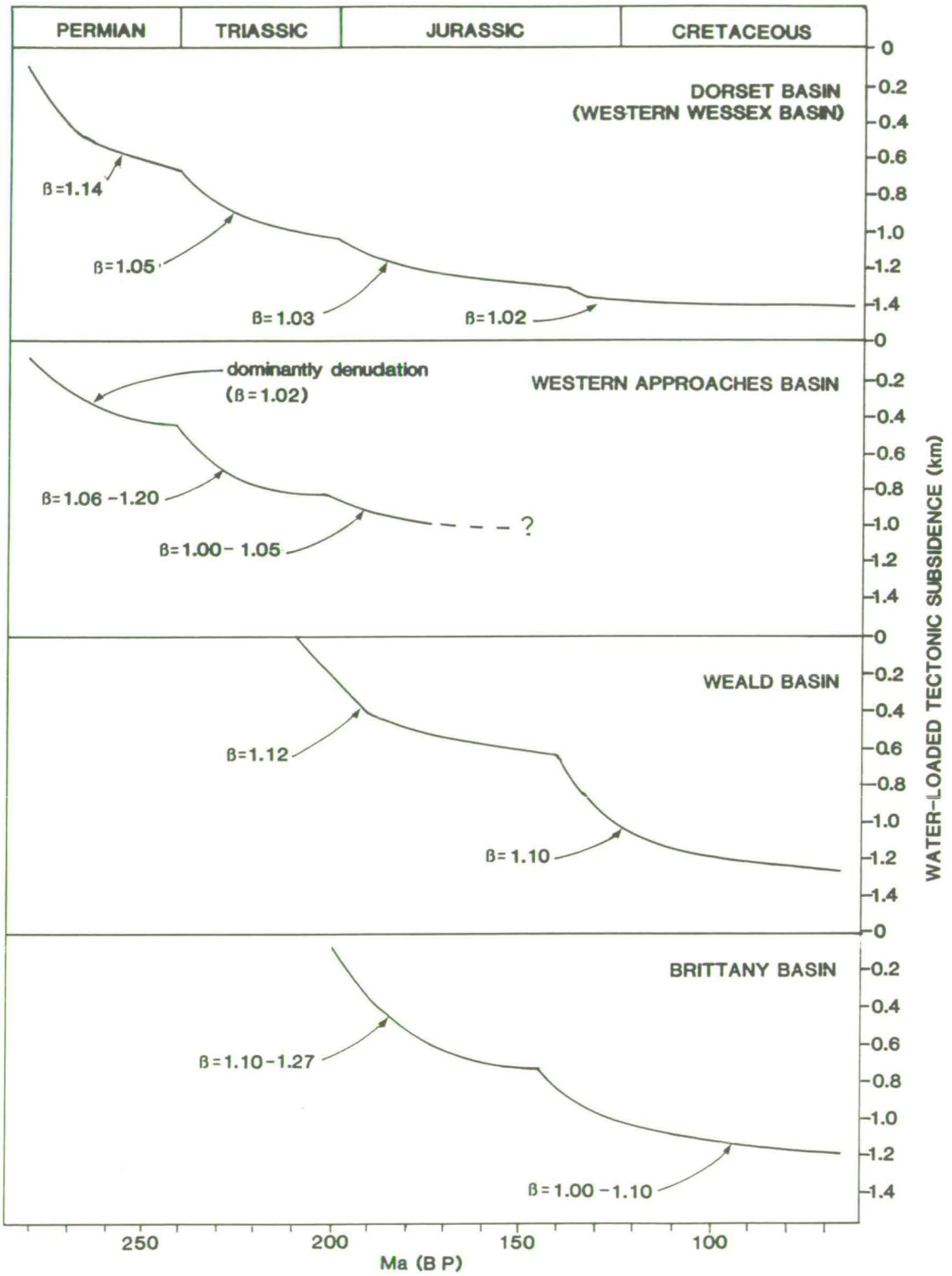

Figure 5.7 Comparison of tectonic subsidence curves for the Western Approaches Trough to the Wessex Basin. Wessex Basin curves (Dorset and Weald Basins) are from Chadwick (1986). Western Approaches Trough curves are simplified from this Chapter. Note the similarity of the Western Approaches Basin to the Dorset Basin and the Brittany Basin to the Weald Basin.

late Jurassic subsidence pulses in the Western Approaches Trough, although it has been argued above that the first of these was denudation-driven in the Western Approaches Basin.

There is further similarity in the spatial migration of the different rift pulses (Figure 5.7). In the western Wessex Basin (e.g. Dorset Basin) subsidence commenced in the Permian and there were subsequent rift pulses in the Triassic, early Jurassic and late Jurassic (Chadwick, 1986). However, in the eastern Wessex Basin (Weald Basin) subsidence did not commence until the early Jurassic, but this rift pulse is of very much greater magnitude than in the west (Figure 5.7). The late Jurassic rift pulse is also of very much greater magnitude in the east than the west (Figure 5.7). Hence the Permian-Jurassic subsidence history of the Weald Basin appears to be analogous to that of the Brittany and South-West Channel Basins, while the western Wessex Basin is more similar to the Western Approaches Basin. No detailed study of the causes of this "rift migration" has been made but it is tentatively suggested that it reflects the orientation of pre-existing basement fault zones with respect to the extensional stresses responsible for rifting.

Regionally, Triassic-early Jurassic rift development in the Western Approaches Trough was part of a formerly coherent northeast-trending rift system covering Iberia, and the western European and eastern Canadian continental shelves (Masson and Miles, 1986). The Triassic-Jurassic extensional stresses responsible for rifting were related to the break up of Pangea, and more specifically crustal extension in the Arctic North Atlantic and the opening of the Tethys Ocean in southern Europe (Ziegler, 1982).

5.6 CONCLUSIONS

(i) The early basin development of the Western Approaches Trough may be split into a Permian denudational phase and Triassic, early Jurassic and late Jurassic extensional pulses. Individual events can not all be recognised throughout the basin. Although this is in part due to

the poor resolution of fully corrected subsidence data, "rift migration" is clearly demonstrated.

(ii) The lack of observed extension may be reconciled with the magnitude of subsidence if the Permian subsidence phase was driven principally by Variscan denudation rather than extension. This hypothesis is consistent with the observed facies and distribution of Permian sediments.

(iii) During the Triassic, at the unconformity between the Aylesbeare and Sherwood Sandstone Groups (early-early late Triassic), the depocentre switched from the southern Western Approaches Basin to the northern Western Approaches Basin. This reflects a switch in driving mechanism of basin subsidence from denudation to extension with reactivation of Variscan basement structures in the Melville Basin.

(iv) Triassic rifting and subsidence was not well developed in the Brittany Basin where extension and rapid subsidence commenced in the early Jurassic. This subsidence pulse is less well developed in the South-West Channel Basin. A minor early Jurassic rift event may also have occurred in the Western Approaches Basin, but it is not well resolved in the subsidence data.

(v) A late Jurassic subsidence pulse occurred in the South-West Channel Basin and to a lesser extent in the Brittany Basin. The Western Approaches Basin may also have seen increased subsidence at this time, although evidence of the post-Sinemurian Jurassic tectonics of the Western Approaches Basin has been removed by later erosion.

(vi) The timing of rift pulses correlates with the Wessex Basin and more regionally with the development of a formerly coherent rift system in the North Atlantic domain.

CHAPTER 6

LATE JURASSIC-CRETACEOUS TECTONIC EVOLUTION: CIMMERIAN UPLIFT, RIFT/WRENCH MOVEMENTS AND LATE CRETACEOUS REGIONAL SUBSIDENCE

6.1 INTRODUCTION

During the late Jurassic-early Cretaceous the sub-basins of the Western Approaches Trough exhibited contrasting tectonic histories. Subsidence in the Brittany and South-West Channel Basins accommodated the deposition of up to 2.5km of late Jurassic-early Cretaceous sediments. However, uplift in the Western Approaches Basin at this time led to the erosion of 1-2km of Jurassic-Permian sediments. In the late Cretaceous regional subsidence throughout the Western Approaches Trough, combined with eustatic sea-level rise (Haq et al, 1987), led to the transgression of the Chalk sea.

The aim of this chapter is to elucidate the counteracting mechanisms of basin subsidence and uplift responsible for the differing late Jurassic-early Cretaceous evolution of the sub-basins and the cause of the widespread late Cretaceous subsidence.

6.2 CIMMERIAN UPLIFT

Late Jurassic-early Cretaceous uplift and deformation occurred in the Western Approaches and South Celtic Sea Basins, the Cornubian Massif and across southern England. It has been widely linked to the synchronous Biscay/Atlantic rifting which preceded the separation of Europe and North America (e.g. Hallam and Sellwood, 1976; Kamerling, 1979; Ziegler, 1982). This causal link, the driving mechanism of which was not discussed by the above authors, implies rift flank uplift of unusually wide extent and large magnitude (i.e. the entire south-west British continental shelf). This section investigates the possible driving mechanism(s) of this uplift in more detail.

The degree to which uplift is associated with rifting depends on the prior thermal state of the lithosphere. This is constrained by two end members of rift mechanisms. In active rifting crustal extension is a response to thermal upwelling of the asthenosphere. In passive rifting extension is a response to a remotely induced extensional stress field and there is no dynamic heat input/hotspot activity (Morgan and Ramberg, 1987).

The absence of significant volcanic material (White et al, 1987) and the lack of evidence of an axial rift dome (Montadert et al, 1979) over the north Biscay margin during rifting indicate that continental rifting and eventual separation in this area was extensionally-driven without significant dynamic heat input. This hypothesis is further supported by the absence of high velocity, highly intruded or metamorphosed lower crutal layers beneath the present continental slope (Ginzburg et al, 1985).

In passive rifting significant regional uplift is not generally observed (Kazmin, 1987). However, passive continental separation at the south-west British margin resulted in a widespread uplift. This may have been caused by "lateral thermal processes". Heterogeneous extension and conductive and convective heat flow are discussed below.

Rheological considerations suggest that extension of the brittle crust will tend to be localized within a rift axis, while extension of the ductile sub-crustal lithosphere will be more widely distributed, affecting the rift flanks (Rowley and Sahagian, 1986; Kusznir et al, 1987). On the rift flanks, in the absence of crustal extension, any extension of the sub-crustal lithosphere will generate uplift (Figure 1.4). Neither the magnitude of uplift in the Western Approaches Basin nor the effect of ductility of the sub-crustal lithosphere on the distribution of extension are sufficiently well constrained to quantitatively model this process. However, areas of excess sub-crustal stretching on the rift flanks must be balanced by areas of excess crustal stretching in the rift axis if volume is to be conserved in the two layers (White and McKenzie, 1988).

Conductive lateral heat flow may act in combination with heterogeneous extension. This may contribute a few hundred metres of flank uplift up to 50km away from active extension (Cochran, 1983).

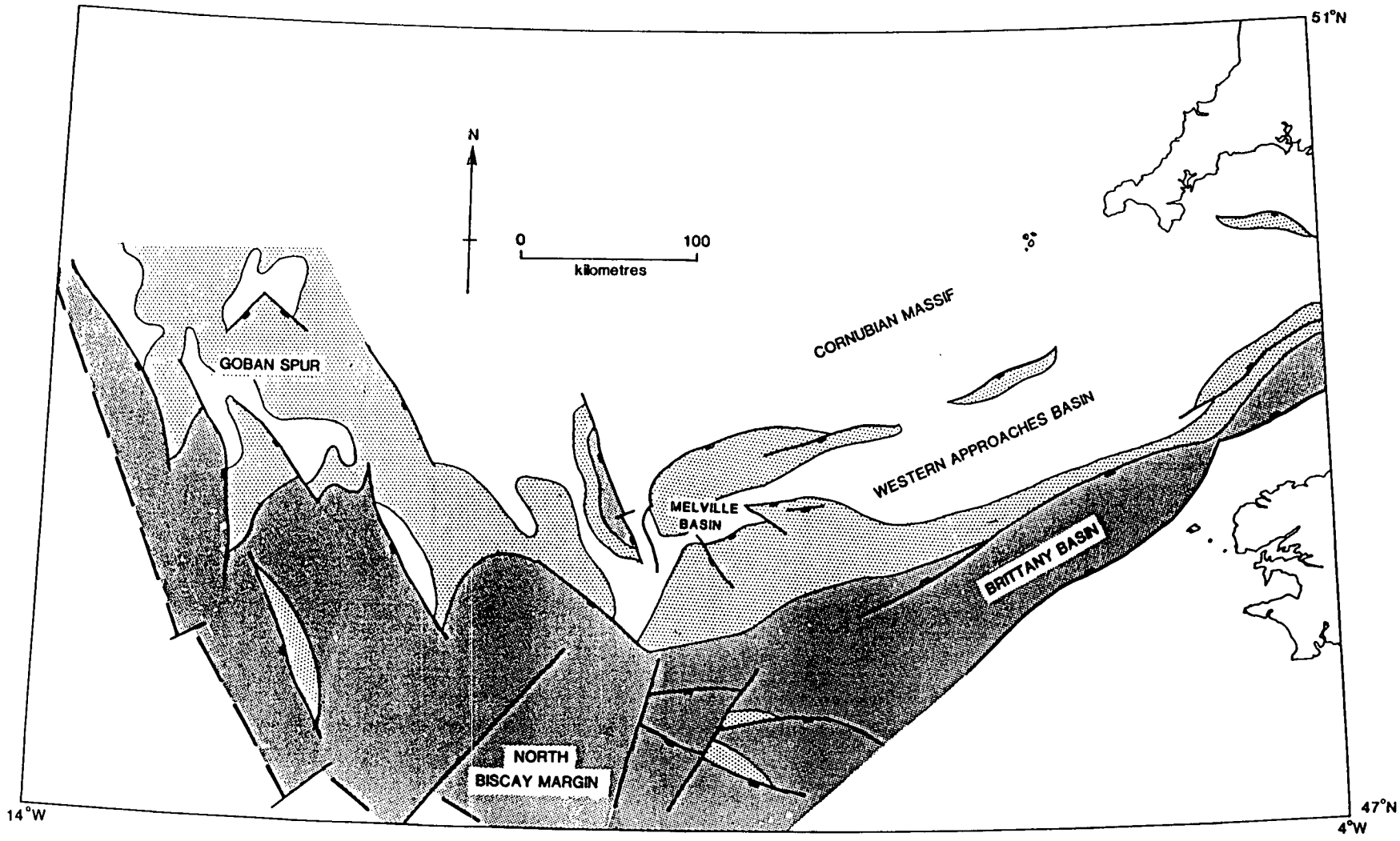

Figure 6.1 Distribution of late Jurassic–early Cretaceous uplift and erosion (highly simplified). Blank areas subject to most severe erosion, Variscan basement–Trias subcrops under Cimmerian unconformity. In areas of lighter shading Jurassic–Triassic subcrops. Darker shading represents areas where a complete or near complete late Jurassic–early Cretaceous sequence was deposited.

Alternatively, Steckler (1985) invoked convective flow in the mantle induced by the horizontal temperature gradients at the edges of the rift zone to generate the 1.3-1.4km of, now partially eroded, syn-rift flank uplift in the Gulf of Suez. In this mechanism lateral heat flow is enhanced by convection and, as in heterogeneous extension and conductive lateral heat flow, uplift is due to the increased temperature, hence decreased density, of the lithosphere in the absence of crustal stretching.

Organic maturation data, which indicate an increased palaeo-geothermal gradient in the shelf basins during the late Jurassic-early Cretaceous (Kamerling, 1979; unpublished data), suggest that "lateral thermal processes" were active. Lateral thermal processes generate increased geothermal gradients without a dynamic heat input due to the relaxation of uplifted isotherms under the rift flanks by heat conduction to the surface.

Mechanical flexure (Watts et al, 1982) may also have caused uplift of the rift flanks. However, estimates of the elastic thickness of the lithosphere of the British continental shelf suggest that it is sufficiently low for flexural effects to be negligible (Section 1.4.1.2), particularly during the increased temperatures associated with rifting. Neither isostatic (Jackson and McKenzie, 1983) nor geometric (Barr, 1987) footwall rebound can account for the observed magnitude and spatial extent of Cimmerian uplift.

Although it is not possible to determine the relative importance of the various lateral thermal and mechanical mechanisms it is instructive to note the regional symmetry of late Jurassic-early Cretaceous uplift across the Cornubian Massif. Both the South Celtic Sea (Kamerling, 1979; Van Hoorn, 1987) and Western Approaches Basins were subjected to major uplift and erosion at this time, while no unconformity can be traced throughout the North Celtic Sea (Tucker and and Arter, 1987) or Brittany Basins. Whatever the principal mechanism(s), late Jurassic-early Cretaceous uplift appears to have been focused by the presence of the low density granitic material comprising the Cornubian and Haig Fras Batholiths.

As would be anticipated the magnitude of late Jurassic-early Cretaceous erosion decreases eastwards away from the rift axis across

southern England (Hallam, 1971). Furthermore, the "late Cimmerian" unconformity of the North Sea is not a single basin-wide event, but rather refers to several unconformities, generally restricted to structural highs, which are controlled by eustasy and local tectonic effects such as footwall uplift (Fyfe et al, 1981; Rawson and Riley, 1982; Badley, 1988).

Regional uplift was counteracted by fault-controlled subsidence on the north Biscay margin (Montadert et al, 1979) and in the Brittany Basin (Figures 6.2 and 6.3) where a complete late Jurassic-early Cretaceous sequence was deposited (Figure 6.1). In the Melville Basin the post-depositional downthrow of the preserved Liassic is also ascribed to this period (Figure 4.7). However, unlike the north Biscay margin and the Brittany Basin, the magnitude of fault-controlled subsidence in the Melville Basin was not sufficient to fully counteract regional uplift. Faulting only locally reduced uplift, preserving Liassic sediments in isolated topographic lows (Figure 6.1). In areas where fault activity was absent uplift and erosion reached a maximum, cutting back as far as the Permian (Figure 6.1).

In addition to any possible focusing of "lateral thermal processes" the stable block of the Cornubian Massif may have inhibited the counteracting fault-controlled subsidence in its proximity, hence concentrating uplift in the Western Approaches and South Celtic Sea Basins.

6.3 LATE JURASSIC-EARLY CRETACEOUS FAULT STYLE

The fault-controlled subsidence which counteracted early Cretaceous uplift is of crucial importance to the preservation and depth of burial, hence maturity, of potential Liassic hydrocarbon source rocks. The distribution and maturity of Liassic source rocks is, in turn, probably the controlling factor on the prospectivity of the Western Approaches Basin (Appendix B). Hence, late Jurassic-early Cretaceous fault style merits detailed attention.

Figures 6.2 and 6.3 show the southern end of the BIRPS SWAT lines 7 and 8 across the eastern Brittany and South-West Channel Basins

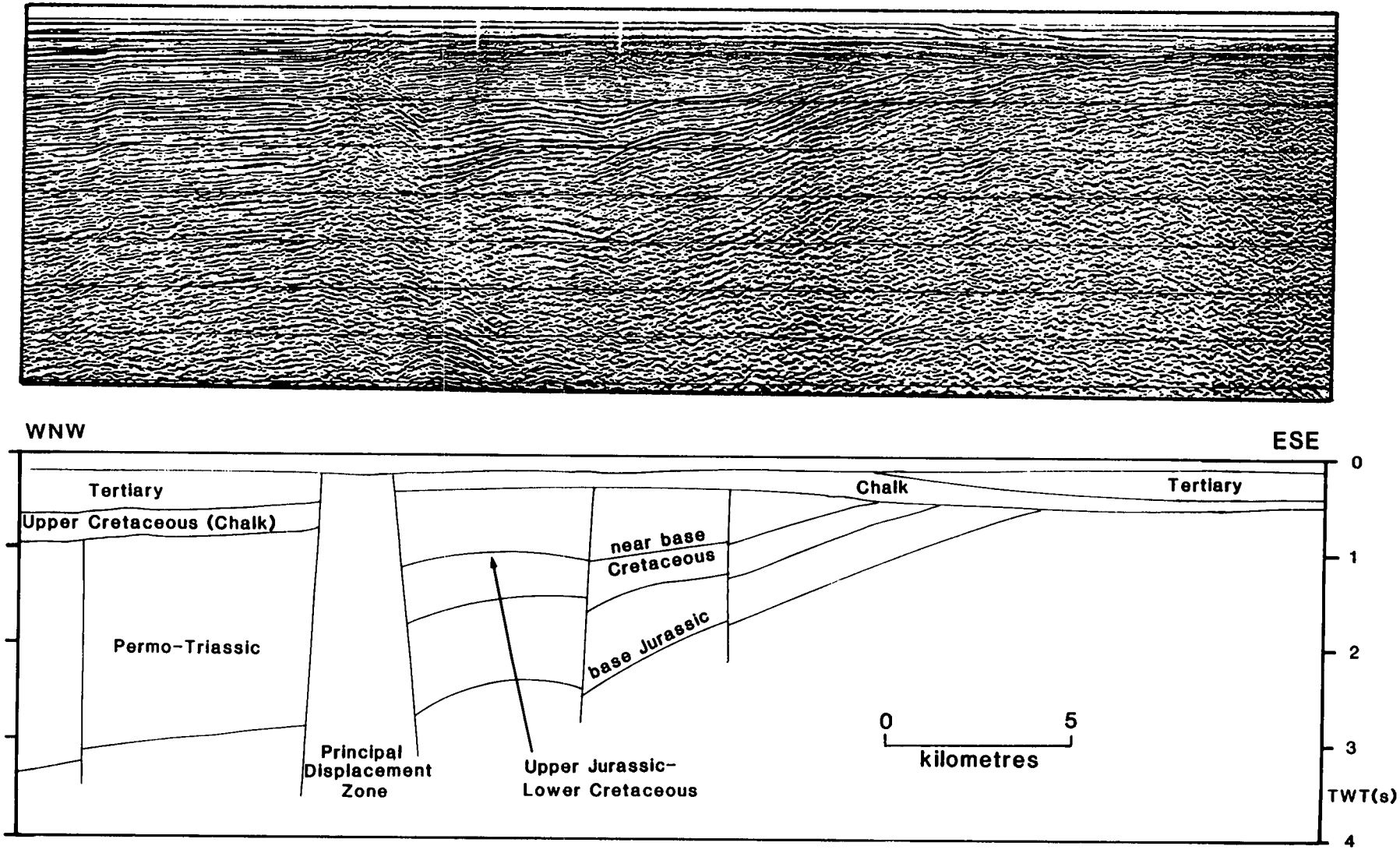

Figure 6.2 BIRPS SWAT 7 across eastern Brittany Basin. PDZ downthrows Upper Jurassic-Lower Cretaceous to the south. Note also the Tertiary inversion of the Upper Jurassic-Lower Cretaceous depocentre. See Figure 6.4 for location.

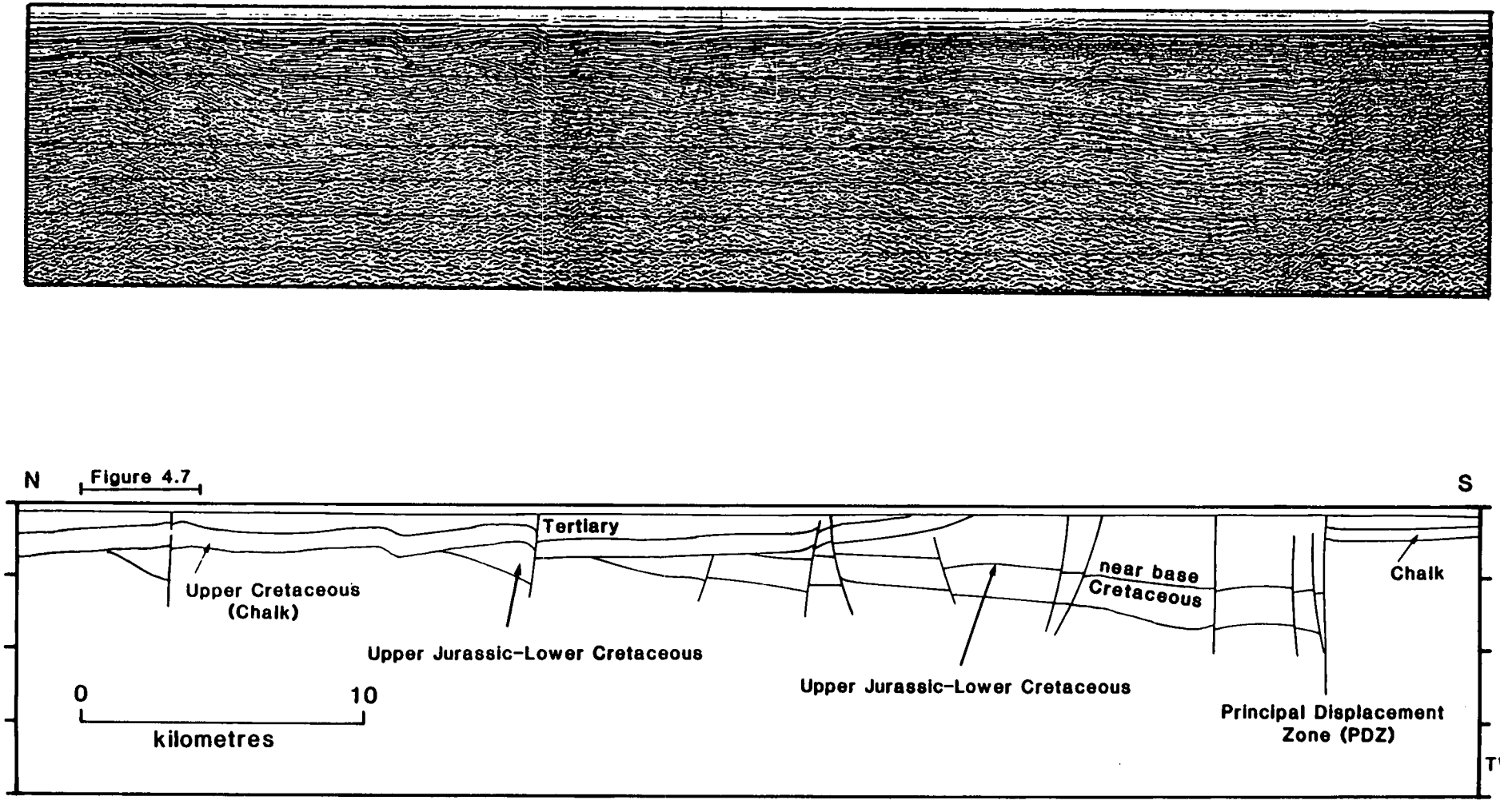

Figure 6.3 BIRPS SWAT 8 across South-West Channel Basin. PDZ downthrows Upper Jurassic-Lower Cretaceous to the north. Note also Tertiary inversion of late Jurassic- early Cretaceous depocentres. See Figure 6.4 for location.

respectively. On SWAT line 7 the late Jurassic-early Cretaceous downthrow of the principal displacement zone (PDZ) separating the Brittany and Western Approaches Basins is to the south. On SWAT line 8 there is no major fault zone between the South-West Channel and Western Approaches Basins. Here the PDZ forms the southern margin of the South-West Channel Basin, and downthrows to the north in the late Jurassic-early Cretaceous. Figure 6.4 shows the positions of the BIRPS SWAT lines 7 and 8 and the major faults in the area. Sinistral strike-slip movement on the PDZ would, due to its curvilinear trace, generate releasing bends, hence transtensional basin formation, to its south and north on SWAT lines 7 and 8 respectively. Near the shelf edge the polarity of the PDZ reverses (Figure 1.2(a)), returning to the style observed in the South-West Channel Basin. This is again consistent with local transtensional movement in a sinistral strike-slip setting. The rapid late Jurassic/early Cretaceous subsidence of well Lennket-1 (Figure 5.3(c)) which lies immediately north of the PDZ in the South-West Channel Basin is consistent with this hypothesis.

The steepness and associated wide zone of incoherent reflections exhibited by the PDZ are typical of the seismic expression of a major strike-slip fault (Figures 6.2, 6.3 and 6.5). The difficulty of correlating reflections across the fault is also distinctive, as is the "flower structure" in the northern South-West Channel Basin (Figure 4.7(a)). The deep, narrow form of the early Cretaceous transtensional basin associated with the PDZ is indicative of "trapdoor"-type pull apart basins generated within strike-slip settings.

Independent support for the sinistral strike-slip model is provided by Chapman (in press) who showed that the pattern of compressional folds within the preserved Liassic of the Melville Basin fitted transpression during sinistral strike-slip movement.

It is postulated that the PDZ continues westwards onto the continental slope at Shamrock Canyon, the northern margin of Meriadzek Terrace, where it separates the gently sloping, highly canyoned continental slope of Goban Spur from the steeper, less incised north Biscay margin. Eastwards it passes into the Hurd Deep Fault zone.

It is unlikely that the late Jurassic-early Cretaeous deformation involved pure sinistral strike-slip motion because of the excess of

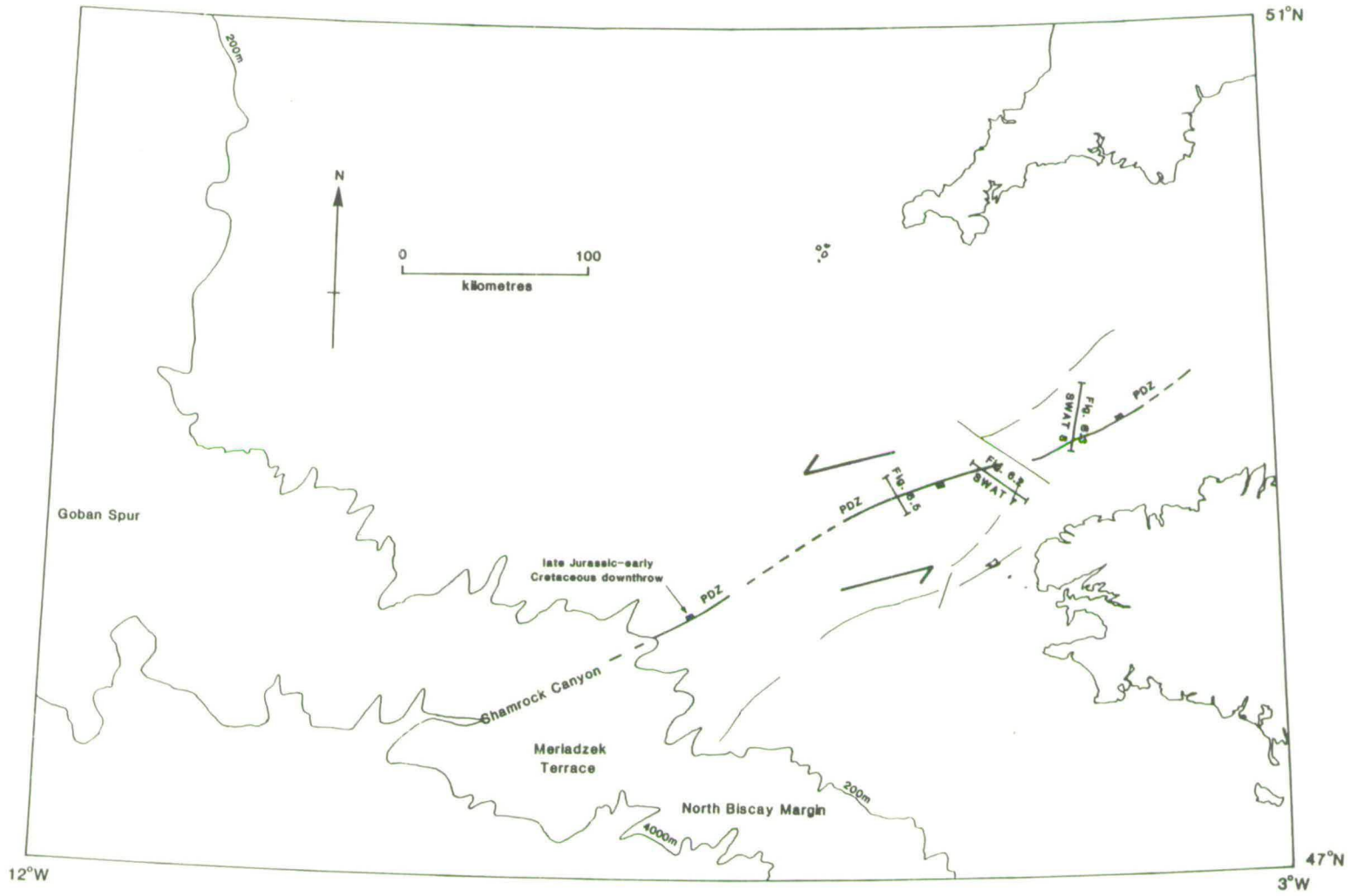

Figure 6.4 Late Jurassic-early Cretaceous displacements on the principal displacement zone (PDZ) through the Brittany and South-West Channel Basins. The changes in downthrow direction are consistent with transtension in a sinistral strike-slip regime. The lack of transpressional features indicates that strike-slip movements were accompanied by extension. Sinistral movements may have accommodated rifting/separation on North Biscay margin which pre-dated that on Goban Spur.

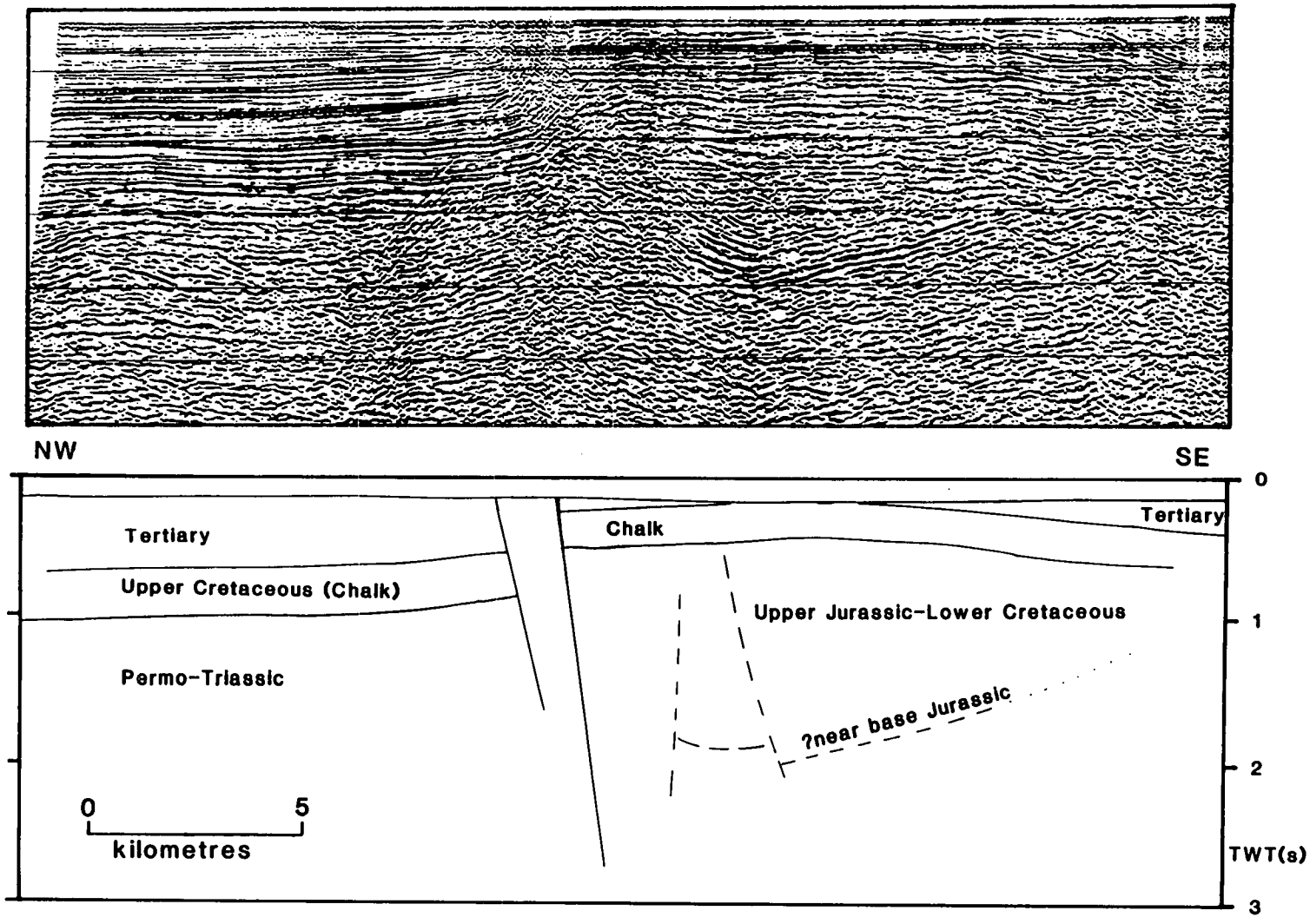

Figure 6.5 Commercial line over the PDZ between the Brittany and St. Mary's Basins. The steepness of the PDZ and its associated wide zone of incoherent reflections and the difficulty of correlating reflectors across the fault zone are all typical of a major strike-slip fault. No data were available to tie reflectors on this line.

transtensional over transpressional features (observed faulting is almost entirely extensional). Hence, it appears that the Western Approaches Trough underwent a period of sinistral rift/wrench movements.

The change from Triassic-Jurassic extension in the Western Approaches Trough to the extensional/sinistral strike-slip movements of the early Cretaceous may have accommodated rifting of the Bay of Biscay (Figure 6.4), which predated opening further north at Goban Spur. However, it may also reflect a more fundamental change in plate kinematics between Eurasia and Africa/Iberia as described by Savostin et al (1986 and Figure 6.6). The change in the relative motion of Eurasia/Africa during the early Cretaceous is consistent with the development of sinistral strike-slip movements within the European plate along ENE-WSW zones such as the PDZ of Figure 6.4.

6.4 POST-CIMMERIAN SUBSIDENCE

Following Cimmerian uplift the Western Approaches Basin was diachronously transgressed. Sedimentation generally commenced in Barremian-Albian times (Figures 2.11(b) and (c)). However, latest Jurassic and a condensed early Cretaceous sequence overlie the Cimmerian unconformity in the eastern St. Mary's Basin (well 87/12-1), and on the shelf edge (wells 72/10-1, 73/1-1 and 73/12-1) late Santonian-Campanian chalks are only separated from the Cimmerian unconformity by an Apto-Albian volcanic/volcaniclastic unit (Section 2.7).

The absence of pre-Chalk Cretaceous sediments from most of the Melville Basin suggests the area did not subside below sea-level until the transgression of the Chalk sea. In wells, generally further east, where a significant early Cretaceous sequence is preserved (73/5-1, 73/7-1, 74/1-1, 85/28-1, 86/17-1, 86/18-1, 87/12-1) the sediments are continental or marginal or shallow marine and highly condensed (e.g. the Berriasian-Barremian of well 87/12-1 is only 43.5m thick). The condensed nature of the pre-Chalk Cretaceous and its absence from much of the Melville Basin strongly suggests that post-Cimmerian subsidence

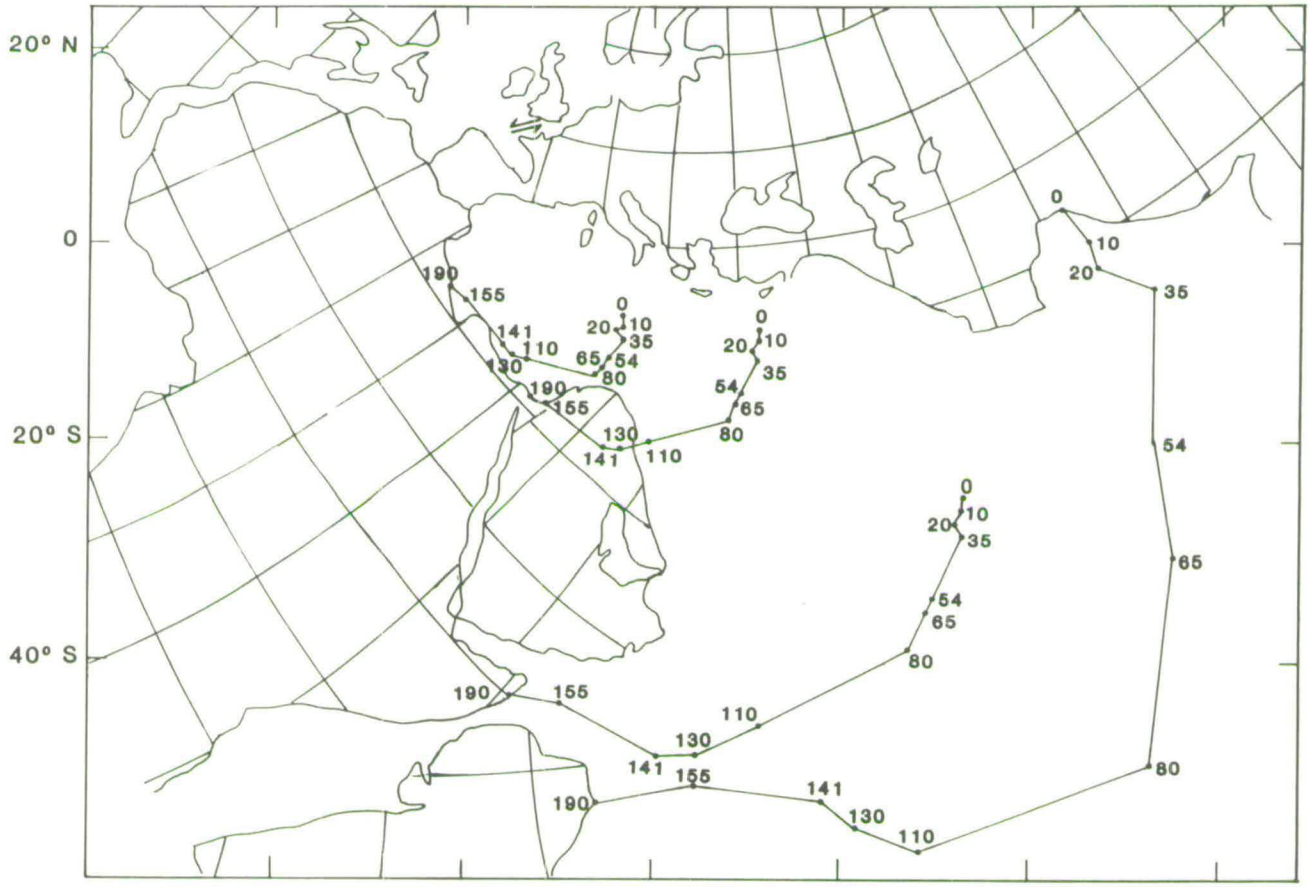

Figure 6.6 Relative motion history of Africa, Iberia, Arabia and India with respect to Eurasia from early Jurassic to Present from Savostin et al (1986). Olique Mercator projection with the north pole at 50° N, 155° W, present latitudes and longitudes every 10° on continents, ages in Ma. Change in relative motion during the late Jurassic-early Cretaceous is consistent with sinistral strike-slip motion in the Western Approaches Trough as indicated.

did not commence immediately following uplift. In the Western Approaches Basin the Barremian-Aptian was a period of basement stability following regional uplift and prior to the onset of regional subsidence in the late Albian-Campanian (Figure 6.7). It is postulated that the interaction between eustatic sea-level rise and end Cimmerian topography controlled sediment distribution at the time.

In the St. Mary's Basin post-Cimmerian subsidence began in the late Albian-Turonian, 90-100Ma (Figure 6.7) whereas to the west in the Melville Basin subsidence commenced in the late Cenomanian-Campanian, 80-94Ma (Figure 6.7). Similarly, subsidence commenced earlier in well Lizenn-1 than further west in Brezell-1 (Figures 5.3(a) and (b)). The mechanisms of post-Cimmerian subsidence are intimately linked to the late Jurassic-early Cretaceous tectonic history of the Western Approaches Trough, which in turn was related to Atlantic/Biscay rifting. Hence the relationship between the time of onset of subsidence and position relative to the shelf edge.

The principal driving mechanisms of post-Cimmerian subsidence in the Western Approaches Basin were cooling and isostatic readjustment following thermally driven uplift and erosion, combined with cooling following extension (Figure 6.7). The exponentially decaying rate of post-Cimmerian subsidence (Figure 6.7) and the lack of faulting is typical of subsidence due to cooling of heated lithosphere. The heating was caused by the "lateral thermal processes" which drove Cimmerian uplift, and the extension was associated with the fault-controlled preservation of the Lias.

The model curves of Figure 6.7 assume subsidence following heterogeneous stretching with a crustal β-factor of 1.05 and a varying sub-crustal β-factor. The crustal β-factor was taken from Chapman's (in press) estimation of Cimmerian extension which was based on extrapolation of the preserved sequence into the interval eroded by Cimmerian uplift (T.J.C. Chapman, personal communication, 1988). This is only a rough approximation but, other than during the early stages of subsidence, the model curves are not highly sensitive to variation of the crustal β-factor due to the excess of sub-crustal extension. Crustal thinning due to erosion was included in the curves and assumed to have

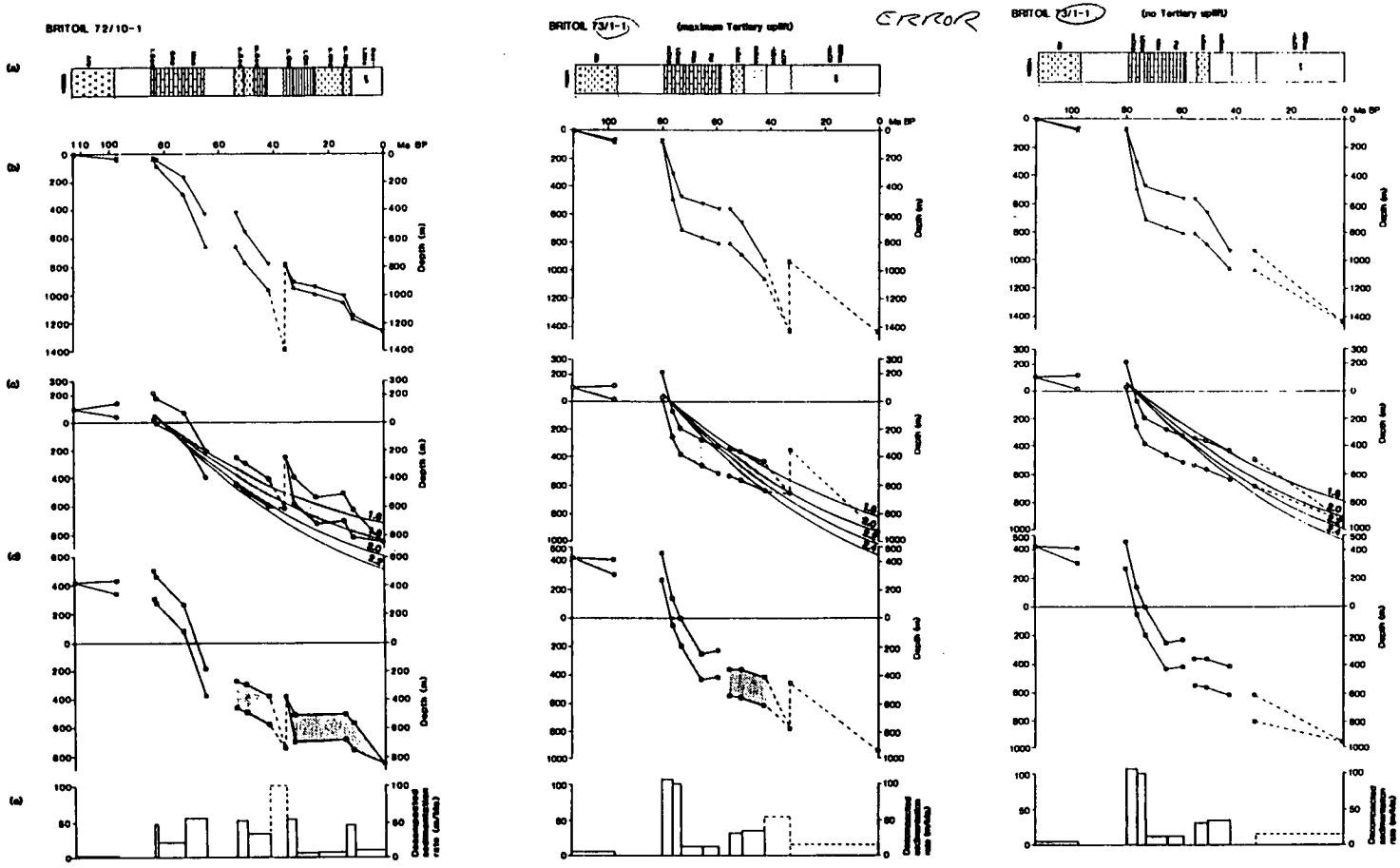

Figure 6.7 Post-Cimmerian subsidence plots for the Western Approaches Basin. (a) Simplified litholog with horizontal axis in time. (b) Present and decompacted (lower plot) thicknesses above basement. (c) and (d) "Tectonic subsidence" corrected for sediment loading and changes in the height of the overlying water column, (c) corrected after Falvey and Deighton (1982) sea-level curve, (d) after Hallam (1984) sea-level curve. In both cases shaded area represents resolution of palaeobathymetric data. (e) Decompacted sedimentation rate.

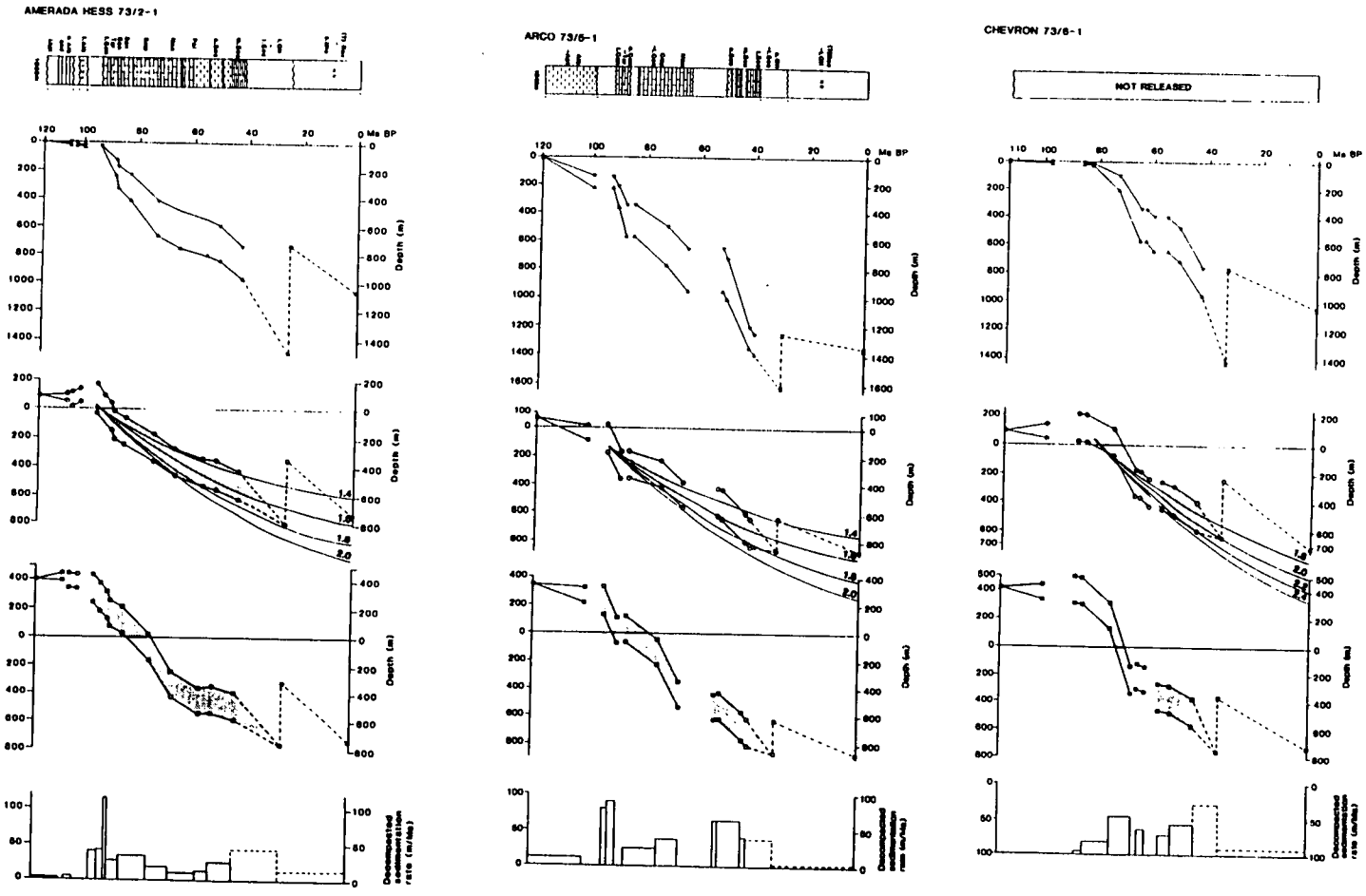

Figure 6.7 (continued) Model subsidence curves for subsidence following heterogeneous stretching with a crustal B-factor of 1.05 and sub-crustal B-factor as indicated. Initial crustal thickness 27km, other parameters as Chadwick (1985a). Crustal thinning due to erosion was included in the curves and assumed to have kept pace with uplift, thus maximising erosional thinning. Only plots corrected after Falvey and Deighton (1982) sea-level curve modelled, plots corrected after Hallam (1984) sea-level curve with 360m late Cretaceous highstand are shown for comparison.

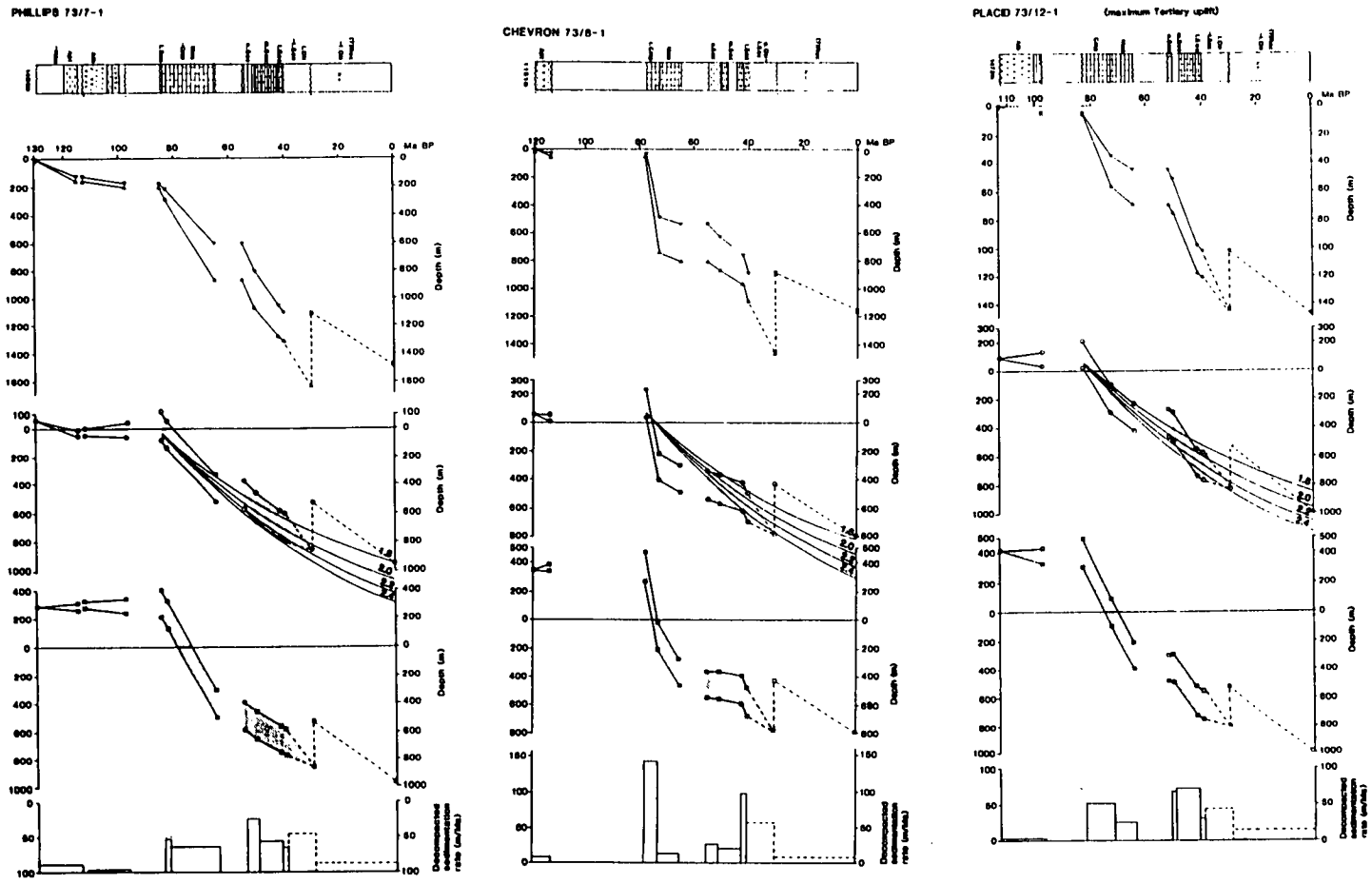

Figure 6.7 (continued)

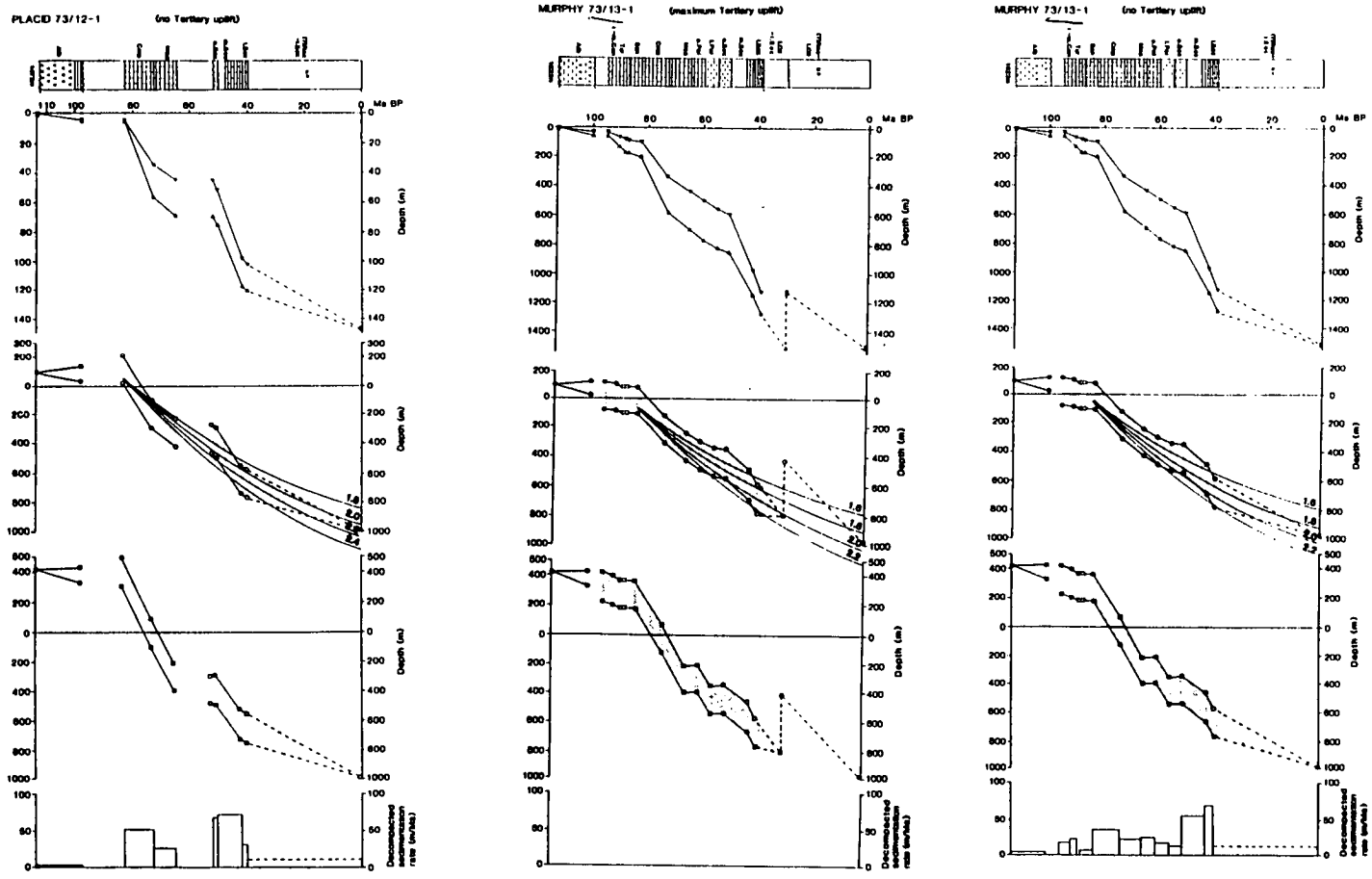

Figure 6.7 (continued)

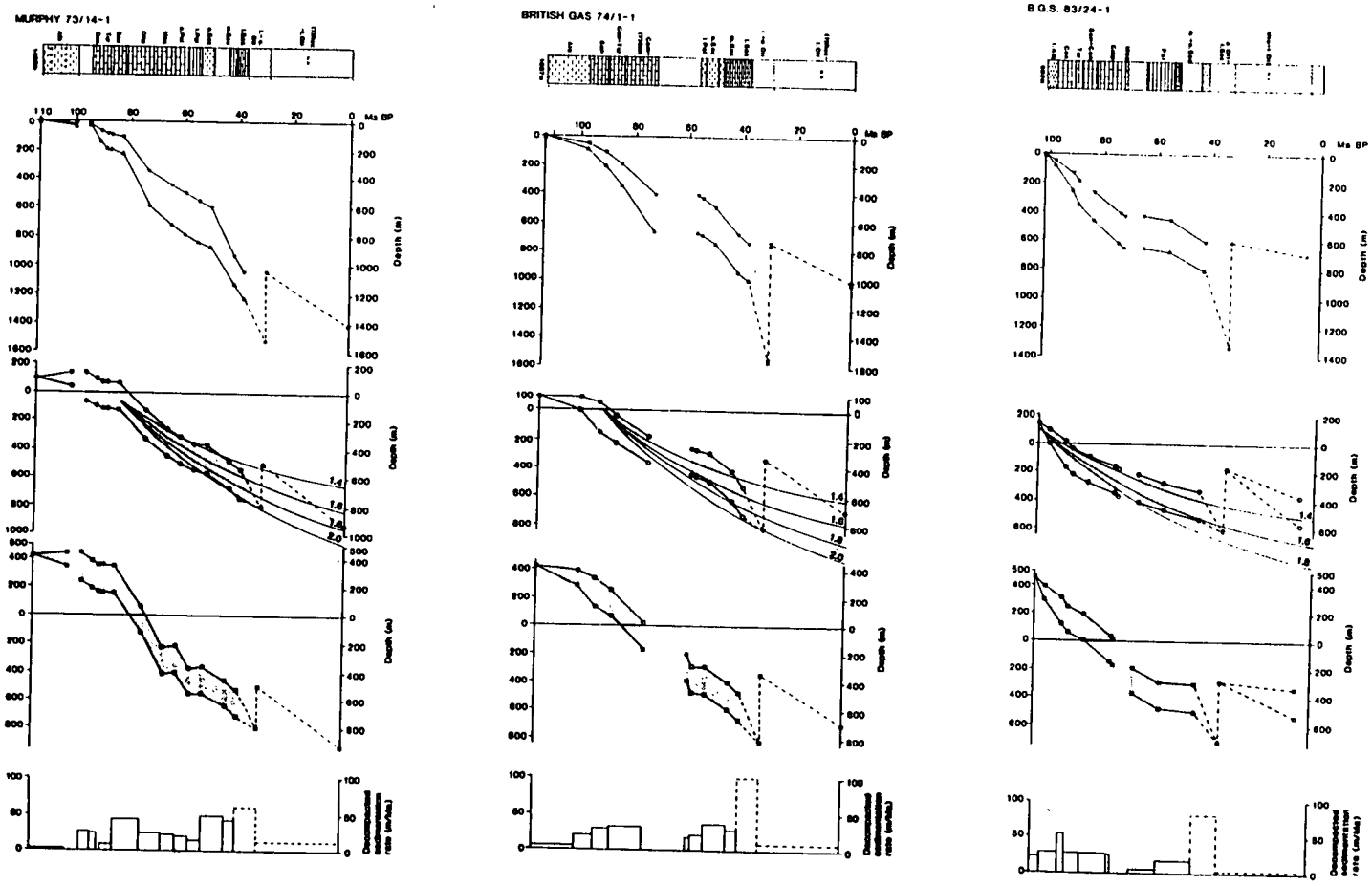

Figure 6.7 (continued)

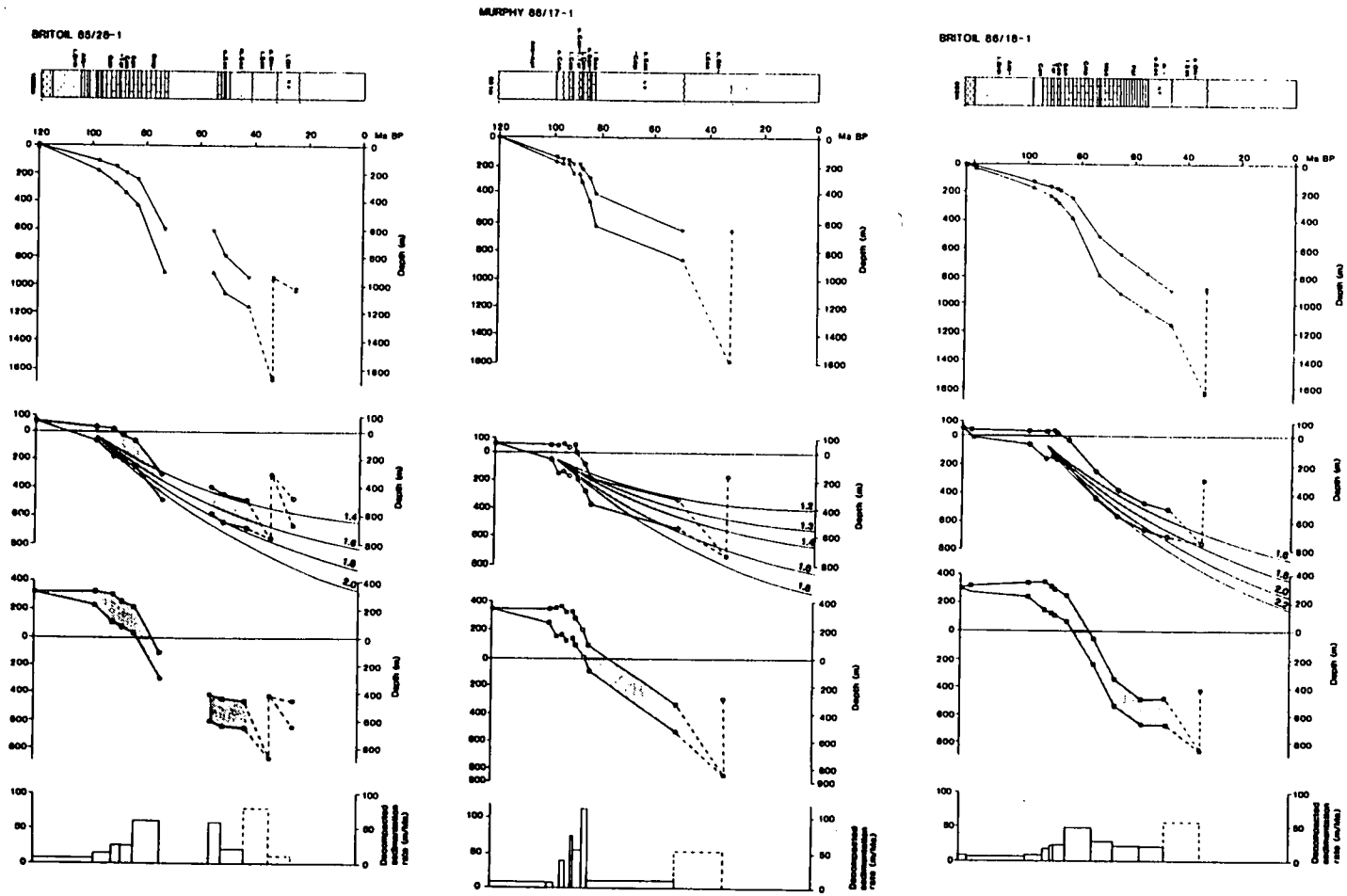

Figure 6.7 (continued)

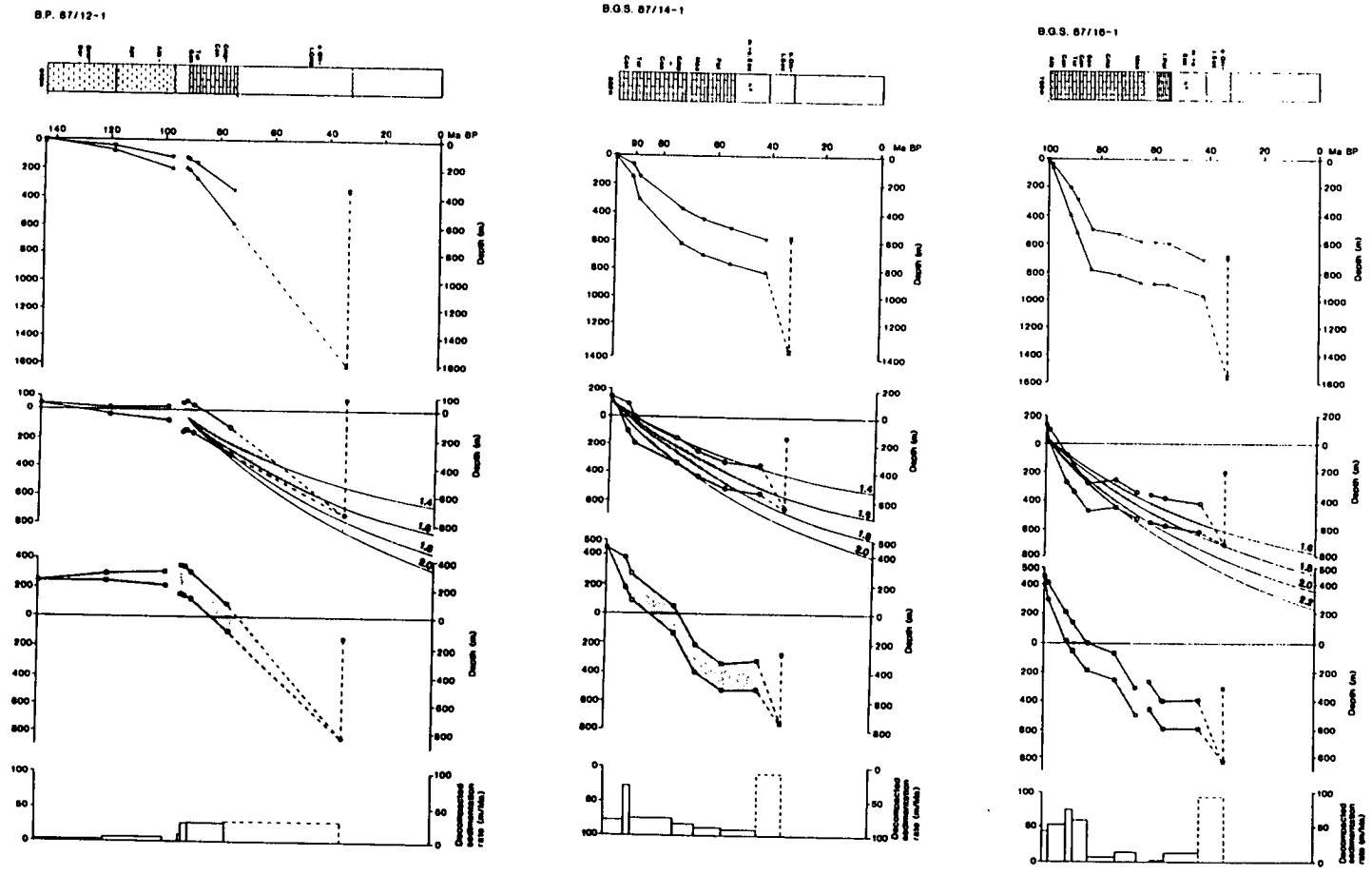

Figure 6.7 (continued)

kept pace with uplift. This maximises erosional thinning (Hellinger and Sclater, 1983).

McKenzie (1978) criticised heating of the continental lithosphere, uplift and erosion as a subsidence mechanism in the North Sea rifts due to the lack of evidence of the required erosion. However, this is not the case in the Western Approaches Basin. The relationship between the magnitudes of erosion and consequent subsidence is controlled by the densities of the eroded material and that which is deposited during later subsidence (Figure 6.8). In the Western Approaches Basin the Permian-Jurassic sediments removed would have been of similar density, when eroded, to the post-Cimmerian sediments deposited following uplift. In this case the magnitude of erosion and subsidence are the same, as observed in the Western Approaches Basin (Figure 6.8).

In contrast to the Western Approaches Basin, subsidence in the Brittany and South-West Channel Basins, where there was no Cimmerian erosion, was driven by cooling following extension of the lithosphere. The thermal subsidence phase in the Brittany and South-West Channel Basins demonstrates that there was a component of lithospheric extension in addition to the sinistral strike-slip movements described above. In narrow, transtensional "trapdoor"-type basins lateral heat loss is very rapid and no long-term thermal subsidence phase occurs (Pitman and Andrews, 1985). The post-Cimmerian subsidence of the French wells can not be modelled due to Tertiary inversion and erosion. However, it is postulated that a preserved sequence would fit subsidence following heterogeneous stretching with a higher crustal β-factor than in the Western Approaches Basin.

Post-rift subsidence of the continental slope was driven dominantly by cooling following extension, although there was also some erosion of the crests of tilted half-grabens, paticularly on Goban Spur. Conversely, post-Cimmerian subsidence of the unfaulted Cornubian Massif was driven by cooling following thermally driven uplift and erosion. The lack of localization of regional thermal subsidence, particularly after correction for Tertiary uplift, in comparison to the distribution of earlier fault-controlled subsidence, illustrates the heterogeneity of lithospheric extension.

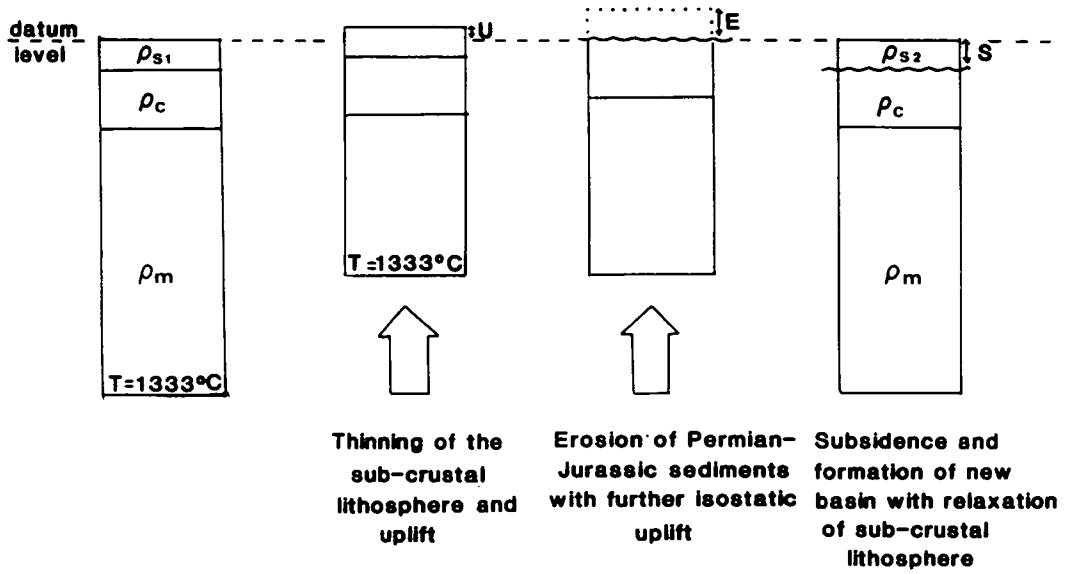

$$E = \left(\frac{\rho_m}{\rho_m - \rho_{s1}} \right) \times U$$

(erosion maximized by assuming all uplift is eroded)

$$S = \left(\frac{\rho_m - \rho_{s1}}{\rho_m - \rho_{s2}} \right) \times E$$

If $\rho_m = 3.33 gcm^{-3}$ and $\rho_{s1} = \rho_{s2} = 2.3 gcm^{-3}$, then:

$$E \simeq 3.2 \times U \quad \& \quad S = E$$

Figure 6.8 Relationships between initial uplift due to sub-crustal thinning, amount of erosion allowing for isostatic unloading, and subsidence following cooling of the sub-crustal lithosphere.

The Cimmerian unconformity of the south-west British continental shelf is directly comparable to the Avalon unconformity of the eastern Canadian continental shelf which juxtaposed the south-west British margin prior to continental separation (Masson and Miles, 1986). Keen et al (1987) argued, on similar grounds, that relaxation following heterogeneous extension drove the post-Avalon unconformity subsidence of the eastern Canadian continental shelf.

The cause of the time lag between the initiation of ocean spreading, Aptian on the north Biscay margin (Montadert et al, 1979) and mid Albian on Goban Spur (Masson et al, 1985), and the onset of post-Cimmerian subsidence on the shelf is not clear. Since the delay is most pronounced on the outer shelf (wells 72/10-1, 73/1-1, 73/6-1 and 73/12-1) it is proposed that even with the initiation of ocean spreading "lateral thermal processes" were still sufficiently active to buoy up the continental shelf. As the passive margin moved away, relatively, from the spreading centre these processes decayed, first on the inner shelf and laterally on the outer shelf.

Although chalk sedimentation on the outer shelf did not commence until the late Santonian-Campanian the thickness of the the Chalk is similar throughout the shelf (approximately 500m), hence the very rapid late Santonian-Maastrichtian subsidence rates on the outer shelf (Figure 6.7, wells 72/10-1, 73/1-1, 73/6-1 and 73/12-1). Within the erosion/extension model presented these subsidence rates imply either a shorter thermal time constant for the lithosphere under the outer shelf, or a crustal β-factor of greater than that of 1.05 which was used to model all the wells. The latter hypothesis is preferred.

It is also possible that while the extension/erosion model fits post-Cimmerian subsidence to a first order the rapid early subsidence of the outer shelf may be a second order variation superimposed on this pattern. This may be due to less readily tested subsidence mechanisms such as lower crustal (Bott, 1980) or asthenospheric creep (Sloss and Speed, 1974) from the continental shelf towards the ocean basin (Section 1.4.6).

Flexure is not considered to have been a major control on post-Cimmerian subsidence. Although the continental slope adjacent to the Western Approaches Trough was sediment starved, a flexural component

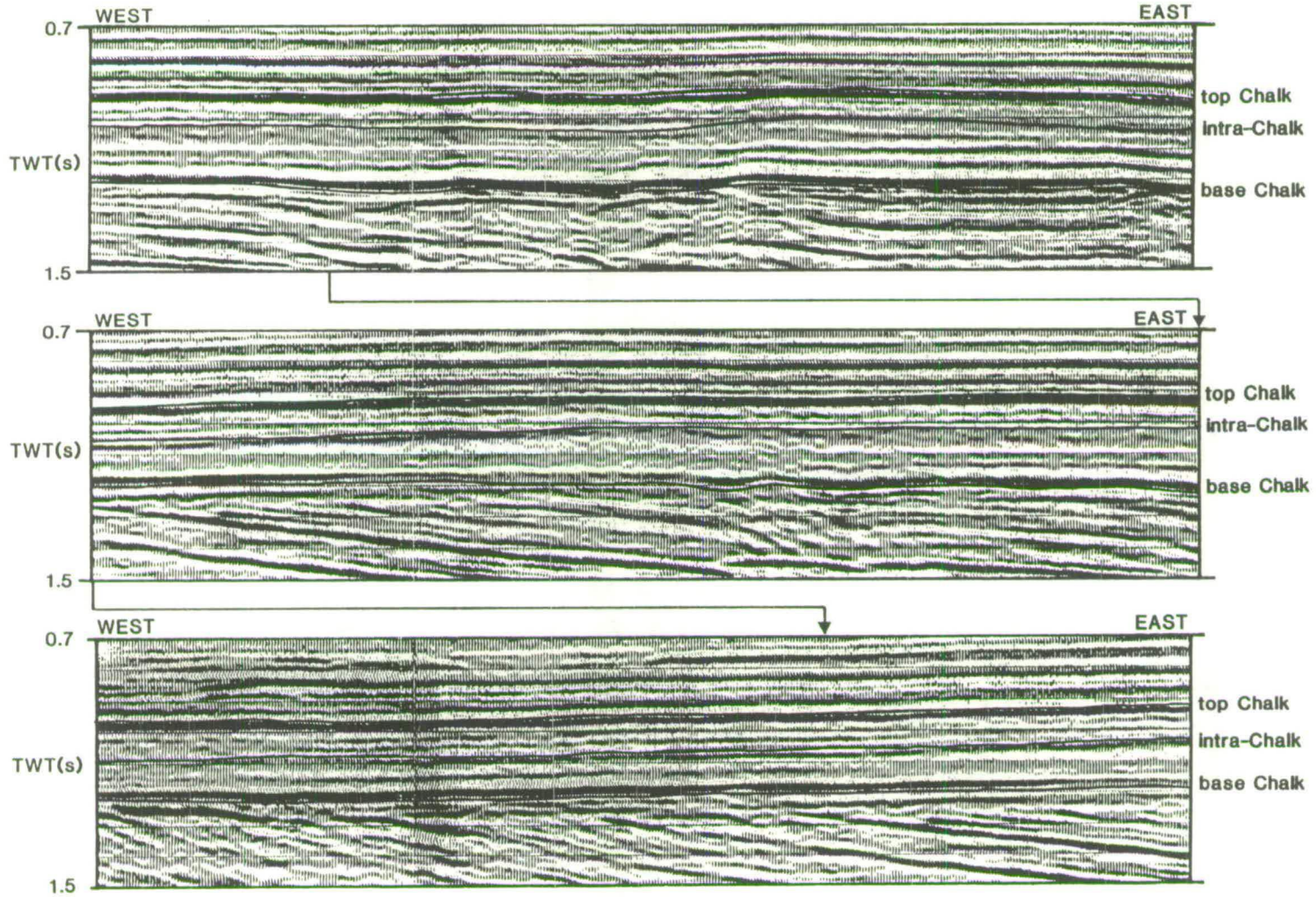

Figure 6.9 Westward thinning of Chalk and gentle downlap of intra-Chalk reflectors near shelf edge indicate that flexure related to Biscay/Atlantic spreading and cooling did not control post-Cimmerian subsidence. On the outer shelf the base of the Chalk is separated from the Cimmerian unconformity only by a thin volcanic/volcaniclatic unit.

of subsidence could have been caused by cooling, and consequent density increase, of the adjacent oceanic lithosphere. However, the pattern of westward post-Cimmmerian onlap (downlap with later subsidence), towards the shelf edge (Figure 6.9) is the opposite of that which would result from flexural subsidence due to cooling of the oceanic lithosphere (Watts et al, 1982). Furthermore, the degree of mechanical coupling between oceanic and continental lithosphere has not been demonstrated, and such estimates of the elastic thickness of the continental lithosphere of the British continental shelf that have been made suggest that it remains sufficiently low, even in the post-rift phase, for local isostasy to be a reasonable assumption (Section 1.4.1.2).

6.5 CONCLUSIONS

(i) Flank uplift associated with passive late Jurassic-early Cretaceous Biscay/Atlantic rifting appears to have been driven by "lateral thermal processes" (heterogeneous stretching and conductive and convective heat flow). Mechanical processes (footwall uplift and flexure) are considered to have been subsidiary.

(ii) Uplift was of greatest magnitude over the Cornubian Massif and the adjacent Western Approaches (and South Celtic Sea) Basin. The "lateral thermal processes" may have been focused by the low density granites of the Cornubian Massif. Alternatively the rift/wrench movements which counteracted subsidence (iii) may have been inhibited by the massif.

(iii) In the Brittany (and North Celtic Sea) Basin there is no regional late Jurassic-early Cretaceous unconformity. Sinistral rift/wrench movements and consequent subsidence, consistent with the relative plate motions of Eurasia and Africa, counteracted regional Cimmerian uplift.

(iv) Following Barremian-Aptian stability regional post-Cimmerian subsidence commenced in the late Albian (on the inner shelf)-Campanian (on the outer shelf).

(v) The lack of regional variation in the magnitude of post-Cimmerian subsidence, with respect to the distribution of late Jurassic-early Cretaceous sediments, illustrates the heterogeneity of late Jurasssic-early Cretaceous lithospheric extension:

(a) Subsidence of the Cornubian Massif was driven by cooling following uplift and erosion due to extension of the sub-crustal lithosphere without crustal stretching/faulting

(b) Subsidence of the Western Approaches Basin was driven dominantly by post-erosional cooling but had an additional component of crustal stretching.

(c) Subsidence of the Brittany Basin and the continental slope was driven by cooling following lithospheric extension without significant supracrustal erosion.

CHAPTER 7

TERTIARY TECTONIC EVOLUTION: BASIN UPLIFT

7.1 INTRODUCTION

Porosity-depth plots were originally prepared for the wells in the Western Approaches Trough in order to determine the normal compaction trends of the major lithologies (Chapter 3). It became apparent, however, that porosity-depth relations were irregular in a fashion not simply attributable to normal compaction (Figures 3.3 and 3.4). The causes of this variation are most readily studied in the lithologically homogeneous chalk.

Possible petrological and diagenetic causes of the porosity-depth relations in the Chalk are discussed in the first part of the chapter. However, it is concluded that Tertiary uplift is the most plausible explanation. This explanation is also considered to apply to porosity-depth relationships in the clastic sequences. However, in clastic sequences the effects of uplift are more difficult to isolate from those of lithological variation (particularly shale content). The second part of the chapter discusses the geodynamic mechanisms respon sible for the Tertiary uplift of the Western Approaches Trough.

7.2 POROSITY-DEPTH RELATIONS IN THE CHALK

Figure 7.1 shows chalk porosity-depth plots, derived as outlined in Chapter 3, for ten of the wells in the Western Approaches Trough. The apparent lack of correlation between porosity and depth can be resolved by considering individual wells. All the chalk sequences, regardless of their present depth of burial, show a relatively consistent porosity reduction with depth, but have widely differing surface intercept values. The steady, depth-controlled decrease in porosity with depth is clearly apparent in the sonic, density and neutron logs of well 87/16-1 (Figure 7.2).

Least-squares regression lines have been calculated for the available wells for both linear porosity-linear depth and natural log porosity-linear

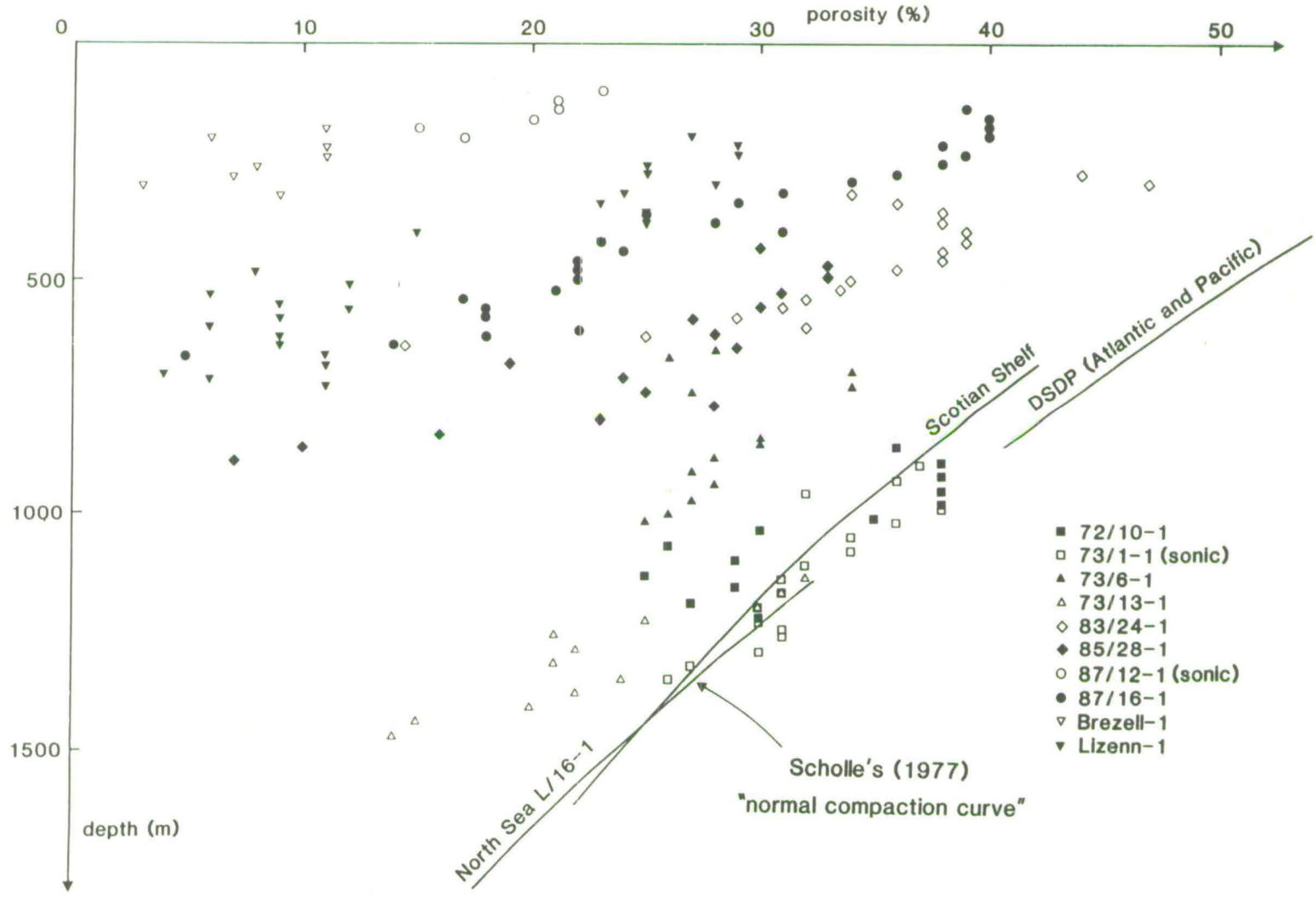

Figure 7.1 Chalk porosity–depth plots for ten wells in the Western Approaches Trough. Porosites are from neutron–density crossplot unless otherwise stated.

depth (Table 7.1). The correlation co-efficient between chalk porosity and depth has been calculated for each well, and most wells show a good fit (greater than 0.8) for both linear and log plots (Table 7.1). Correlation co-efficients tend to be marginally higher for the linear relations. Such linear relations are unlikely to be valid for a chalk throughout its burial history (Scholle, 1977; Davis, 1987), but appear to be valid over the interval seen in any individual well, typically 350-550m for a complete section.

Minor variations are locally superimposed on the first order decrease in porosity with depth, particularly in wells with lower correlation co-efficients. For example, unusually low porosities occur in the younger, upper chalks of well 73/6-1 (Figure 7.1). Rapid porosity loss with depth also occurs at the base of the Chalk, for example in wells 85/28-1 and 87/16-1 (Figures 7.1 and 7.2). The causes of these second order variations are discussed in Section 7.3.2.

Extrapolated surface porosities from the linear relationships of Table 7.1 vary from 15 to 93% with a mean of 58%. Published estimates of typical original surface porosities for chalks also vary, but Schlanger and Douglas (1974) suggested around 80% for a variety of DSDP chalks, while D'Heur (1984) and Taylor and Lapre (1987) suggested ≥70% and 75% respectively for North Sea chalks. Comparison between these figures and the data in Table 7.1 suggests that, while wells towards the upper limits in Table 7.1 have reasonable extrapolated surface porosities, porosities in the other wells have been significantly reduced beyond that which is indicated by their present porosity-depth relation. The diagenetic hardening of chalk is discussed in the next section, with particular reference to the porosity-depth relations of the Western Approaches Trough.

7.3 CHALK DIAGENESIS AND INTERPRETATION OF THE POROSITY-DEPTH DATA

7.3.1 Normal Diagenesis

Chalk diagenesis has been widely reviewed in the literature (e.g. Mapstone, 1975; Bathurst, 1975; Scholle, 1977; Garrison, 1981; Taylor and Lapre, 1987), and only a brief review of the consensus is presented here.

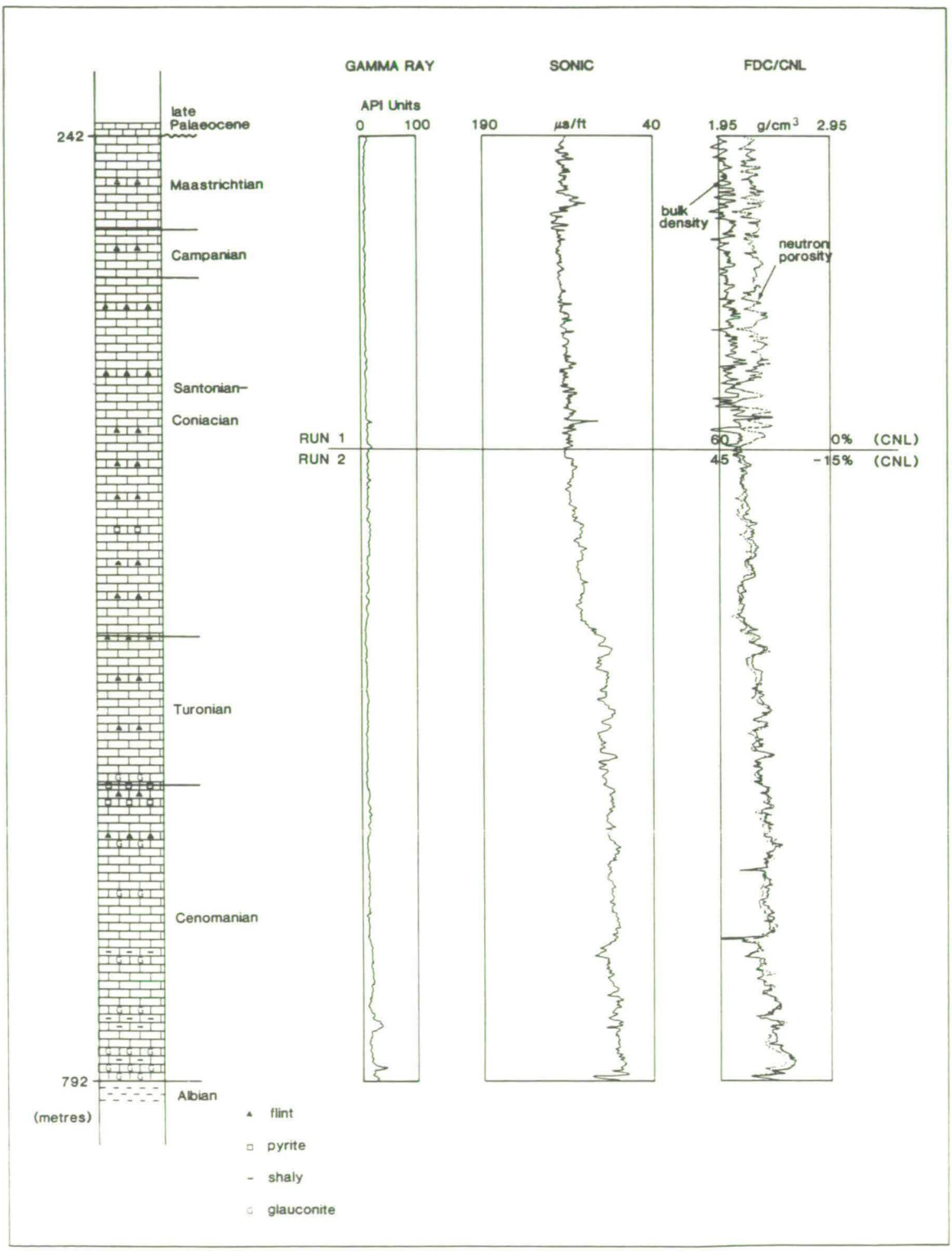

Figure 7.2 Well logs over the chalk of 87/16–1.

Table 7.1 Least-squares regression lines (porosity on depth) and correlation co-efficients for chalk neutron-density porosity-depth data (porosity in % and depth in km). * represents sonic-derived porosity (for wells where no density-neutron logs run through the chalk).

well	number of data	linear/linear least squares line	linear/linear corr. co-ef.	natural log/linear least squares line	natural log/linear corr. co-ef.
72/10-1	13	ϕ=68.3-34.8z	0.820	ϕ=4.58-1.077z	0.809
73/1-1	17	ϕ=55.6-20.7z	0.890	ϕ=4.20-0.649z	0.890
73/2-1	19	ϕ=73.5-56.7z	0.905	ϕ=5.09-2.280z	0.853
*73/5-1	15	ϕ=77.5-51.8z	0.921	ϕ=5.30-2.122z	0.853
73/6-1	13	ϕ=37.3-10.6z	0.480	ϕ=3.64-0.359z	0.482
*73/7-1	14	ϕ=65.0-34.8z	0.866	ϕ=4.78-1.380z	0.876
*73/8-1	17	ϕ=92.7-71.0z	0.952	ϕ=5.90-2.938z	0.868
73/12-1	11	ϕ=54.6-21.8z	0.657	ϕ=4.29-0.790z	0.659
73/13-1	12	ϕ=85.7-48.1z	0.920	ϕ=5.91-2.151z	0.912
73/14-1	13	ϕ=91.8-56.8z	0.883	ϕ=6.66-2.968z	0.847
74/1-1	12	ϕ=75.8-67.1z	0.883	ϕ=5.88-3.596z	0.845
83/24-1	19	ϕ=57.9-51.7z	0.825	ϕ=4.30-1.726z	0.759
85/28-1	16	ϕ=54.7-45.7z	0.848	ϕ=4.71-2.398z	0.788
86/17-1	9	ϕ=51.8-73.6z	0.835	ϕ=4.51-3.673z	0.808
86/18-1	11	ϕ=36.6-22.1z	0.463	ϕ=3.82-1.166z	0.503
*87/12-1	6	ϕ=30.2-70.0z	0.888	ϕ=3.52-3.671z	0.866
87/14-1	23	ϕ=49.3-53.6z	0.915	ϕ=4.04-1.887z	0.899
87/16-1	27	ϕ=50.2-57.7z	0.960	ϕ=4.20-2.463z	0.870
Brezell-1	8	ϕ=14.8-25.6z	0.443	ϕ=3.01-3.802z	0.427
Lizenn-1	26	ϕ=37.8-45.9z	0.906	ϕ=4.07-3.070z	0.867

Chalk is a micritic (fine-grained) limestone, comprising mostly debris from the minute skeletons of coccoliths (planktonic algae). Lesser contributions come from other skeletal material and clay minerals. Coccoliths are composed of low-magnesian calcite, hence chalk has great chemical stability at surface temperatures and pressures. This chemical stability, resulting in resistance to dissolution and reprecipitaion in pore spaces, is the basic cause of its high primary porosity in comparison with high-magnesian calcite and aragonite carbonates.

There are three broad depth zones into which chalk diagenesis may be split; early diagenesis (surface or near surface processes), physical compaction and chemical compaction.

Early diagenesis is generally far less important in chalks than in shallow water limestones due to its chemical stability and also its relatively deep water setting. Such early diagenesis as does occur is influenced by bioturbation, which reduces porosity by physically rearranging the grains, hence dewatering the sediment. Bioturbation also allows better advection of ionic species in the interstitial waters of the sediment ooze than occurs by diffusion alone, hence enhancing cement precipitation. Porosities are probably in the range 60-70% following early diagenesis.

Physical compaction becomes important when the overburden weight is sufficiently great to cause mechanical rearrangement of the grains. Grains are moved closer together by reorientation, repacking and breakage with the concurrent expulsion of pore fluids. Physical compaction is probably important from a depth of a few metres to about 1km and may reduce porosities to around 40%.

At depths of around 1km for chalks with pore fluids of normal marine composition, the overburden pressure becomes sufficiently large to overcome the chemical stability of the chalk and chemical compaction occurs. Calcium carbonate is dissolved, preferentially at grain contacts, where external pressure is greatest. The dissolved calcium and carbonate ions migrate into nearby sites with lower external pressure, such as pore spaces, where precipitation occurs due to the pressure drop. The concurrent expulsion of pore fluids leads to porosity reduction. Such chemical compaction will usually result in reduction of porosities to near zero, after burial to 2-4km.

Chalks undergoing the above "normal diagenetic" sequence will have porosities which approximately follow Scholle's (1977) "normal compaction" trend as defined by North Sea, Scotian Shelf and DSDP data and replotted on Figure 7.1. Hence, wells 73/1-1, 73/12-1 and 73/13-1 appear to have undergone "normal diagenesis", while the remainder of the chalks have been "abnormally hardened".

7.3.2 Additional Processes

There are many reasons for chalk porosities not following the "normal compaction" trend, and these are discussed below, with reference to their ability to generate the low porosities seen in the Western Approaches Trough.

7.3.2.1 Sedimentation Rate

Rapid sedimentation rates preclude total infaunal bioturbation hence reducing the advection of ionic species and consequent early cementation. This will result in high porosities. Conversely, extremely low sedimentation rates are probably at least partially responsible for the low porosity chalk hardgrounds (Bathurst, 1975). However, there is no evidence of unusually slow sedimentation rates, when corrected for compaction, in the low porosity wells of the Western Approaches Trough. For example, the decompacted average sedimentation rate for the Maastrichtian of the low porosity well Lizenn-1 is 39 m/Ma, whereas in the high porosity well 73/13-1 it is 23 m/Ma. The relatively low porosities in the older, lower chalks may, however, be partially associated with sedimentation rate, where the abundance of glauconite (Figure 7.2) may indicate intervals of very slow or non-deposition (Odin and Matter, 1981).

7.3.2.2 Mass Flow

Many authors have recognized the importance of mass flow deposits on the distribution of good reservoir quality in the chalk of the Central Graben (e.g. Kennedy, 1987; D'Heur, 1984). Sediment mass movement destroys any early cements and porosity reduction caused by early grain repacking.

Allochthonous chalks are very rapidly re-deposited and, if sufficiently thick, only bioturbated at their tops. Hence prior to burial they have higher porosities than autochthonous chalks.

In order to explain the porosity-depth relations of Figure 7.1, the high porosity wells must be entirely allochthonous, and the low porosity wells entirely autochthonous, with a gradation between. However, the rather monotonous decrease in porosity with depth in most wells suggests that allochthonous chalks are rare in the area (cf. Kennedy, 1987 Figure 4; D'Heur, 1984 Figures 5 and 6). Furthermore, otherwise normally compacted autochthonous chalks would not have the very low porosities seen in the Western Approaches Trough.

7.3.2.3 Test Composition and Morphology

The precise skeletal composition of chalk components will influence the diagenetic history. High-magnesian calcite and aragonite tend to dissolve and reprecipitate during early diagenesis. Test size also influences the rate of chemical compaction. Pressure solution is more effective at small grain sizes due to the short transport distance between areas of solution and reprecipitation. Furthermore, the increased surface area available for reaction of small and/or rough grains renders them more liable to dissolution. Walter (1985) suggested this can be a more important factor than mineralogy.

The Danian "Chalk" of well 73/6-1 contains more diverse bioclastic debris than the underlying Maastrichtian. Furthermore, the Danian coccoliths tend to be of smaller grain size than those of the Maastrichtian (Gartner and Keany, 1978). These factors may be responsible for the low porosities in the Danian as observed in well 73/6-1. However, it is unlikely that there would be systematic grain size and mineralogy variation between concurrently deposited planktonic shelf sediments in wells only a few tens of kilometres apart such as would be required to explain the porosity-depth distributions of the Western Approaches Trough.

7.3.2.4 Shale Content

The presence of clay minerals will have an influence on both mechanical and chemical compaction. Clay minerals reduce the sorting of the chalk, and hence during mechanical compaction pore space in a dirty chalk will be reduced beyond that in a clean chalk. During chemical compaction clay minerals can absorb magnesium ions which would otherwise inhibit cementation (D'Heur, 1984).

The presence of clay minerals, along with low sedimentation rate, is responsible for the low porosities in the lower, older chalks of the Western Approaches Trough, as shown by the gamma ray log reponses of Figure 7.2 which are indicative of increasing clay content in the Cenomanian Chalk. Similar gamma ray log increases are seen in the majority of wells with Cenomanian Chalks. There is not, however, a systematic variation of clay content between different wells through the entire chalk sequence as would be required to explain the porosity-depth relations of Figure 7.1.

7.3.2.5 Pore Fluid Composition

Neugebauer (1974) showed that the magnesium content of the pore fluid is a crucial factor in diagenesis. If magnesium concentration is above 0.01M ($240mgl^{-1}$) then magnesium ions "poison" the calcite lattice, and further precipitation is retarded. Conversely if chalks are flushed extensively with magnesium-poor fluids, such as typical groundwaters, cementation may be rapid (Scholle, 1977). Such flushing must occur prior to major burial, before the permeability of the very fine-grained chalk inhibits the passage of waters. The relatively high permeability of buried chalks, such as in many North Sea chalk reservoirs, is due to fracturing (Watts, 1983). The passage of groundwater through such fractures does not cause extensive flushing of pore waters.

No sub-aerial exposure occurred during chalk deposition in the Western Approaches Trough, and the only possibility for meteoric water flushing was at the time of the Cretaceous/Tertiary boundary, immediately following its deposition. While there may have been local sub-aerial exposure at this time (Section 2.9.1), it can not be consistently correlated with chalk porosity.

The chalk of well 73/2-1 (Figure 3.3, not shown on Figure 7.1) has porosities on average approximately 5% lower than 73/6-1 at the same depth, yet has an overlying conformable marine Palaeocene. Conversely, the Palaeocene is absent in the high porosity well 72/10-1. Furthermore, flushing would be more effective in the younger, upper chalks than in the older, lower chalks, because lower chalks will already have lost permeability and porosity under the weight of the overlying chalk. With the exception of the relatively rare Danian Chalk, anomalously low porosities are not seen in the upper chalks. For these reasons major removal of magnesium ions from the pore fluids by groundwater flushing is not thought to be the cause of anomalously low porosities in the chalk of the Western Approaches Trough.

7.3.2.6 Heat Flow

Hancock (1976) suggested that the hardness of the onshore chalk of Northern Ireland was caused by high heatflow in the region, as witnessed by the Tertiary volcanism. Such a heat source may have existed in the Western Approaches Trough with Atlantic opening to the west during the Albian, and may have been maintained during the late Cretaceous. There is, however, no correlation betweeen distance from this potential heat source and porosity. Compare, for example, the porosity-depth relations of well 72/10-1, approximately 40km from the shelf edge, and well 87/12-1, some 450km distant (Figure 7.1).

7.3.2.7 Tectonism

Tectonism may both reduce and increase porosity. Mimran (1977) studied chalks on the Purbeck monocline at Dorset and the Isle of Wight, where density increases with increasing dip. Enhanced mechanical compression and pressure solution due to the tectonic stress cause the density increase, however, in Dorset localized shearing may have further enhanced these processes. Dips in the chalk of the Western Approaches Trough are very seldom greater than 5° and usually less than 1°, and would not be associated with significant hardening. Localized shearing, such as seen in Dorset, can not explain the regional porosity-depth variations seen in the

area. Watts (1983) and Mimran (1985) considered the effect of fracturing on chalk porosity and permeability. Watts (1983) suggested that movement associated with underlying salt diapirism in the Albuskjell field of the Ekofisk complex generated fractures. While this process will significantly increase permeability, it is doubtful as to whether wholesale porosity increase could be caused. Such secondary fracture porosity, detected by neutron and density logs, will not be seen by the sonic log. Even in the unconsolidated chalks the correlation between sonic and nuclear porosities indicates that secondary fracture porosity is not responsible for the observed inter-well variations. Mimran (1985) showed that enhanced groundwater flushing of fractured chalks in Israel dissolved calcium carbonate in the fault zone and reprecipitated it in nearby unfaulted chalks which were consequently hardened. Again this process is too localized to explain the low porosities of the Western Approaches Trough.

7.3.2.8 Overpressure and Hydrocarbons

Both overpressuring and the entry of hydrocarbons into pore spaces have been shown to have a profound effect on chalk porosity (e.g. Scholle, 1977; Munns, 1984). However, they result in porosities higher than that predicted by the "normal compaction" curve, and are not discussed here.

7.3.2.9 Uplift

The reduction of chalk porosity by "normal diagenesis" is a largely non-reversible process. If overburden is removed calcite cement in pore spaces will not return to the matrix grains, nor will the matrix grains re-arrange themselves with greater spacing. Hence, if chalk is uplifted following burial it will, excepting any secondary porosity created, retain the lowest porosity attained. The arguments cited above against any diagenetic mechanism, combined with regional evidence of Tertiary uplift, make the latter the most plausible cause of the low porosity chalks of the Western Approaches Trough.

This interpretation of the chalk porosity-depth relations is essentially consistent with many workers who believe that burial depth is the primary control on chalk porosity. For example, Scholle (1977) stated that

"secondary factors such as pore-fluid pressure, tectonic stresses, pore-water chemistry, and possibly thermal gradient influence rates and patterns of porosity loss, but all of these are subordinate, on a regional scale, to burial depth".

Tertiary uplift occurred throughout the Western Approaches Trough and its adjacent continental slope (Section 2.9.3). Late Oligicene-Miocene compressional deformations in the Brittany and South-West Channel Basins resulted in the develoment of a major anticline (Ziegler, 1987a; Figure 1.2) and the chalk of wells Brezell-1 and Lizenn-1 has a correspondingly low porosity (Figure 7.1). Chalk is absent from well Lennket-1 which presumably underwent even greater uplift than wells Brezell-1 and Lizenn-1. Earlier, Palaeocene, uplift has been recognised in the Celtic Sea and Cardigan Bay Basins (Tucker and Arter, 1987) and also in the Fastnet Basin (Robinson et al, 1981). In the Wessex Basin uplift took place initially during the Maastrichtian to Palaeocene and culminated in Oligocene to Miocene times (Lake and Karner, 1987).

The lack of evidence of compressional deformations on seismic data over the Western Approaches Basin has led to little attention being paid to Tertiary uplift in the area, in spite of sedimentary hiatuses both in the Palaeocene and the Eocene-Oligocene (Section 2.9.3). The main uplift in the Melville Basin is ascribed to the widespread Eocene-Oligocene unconformity which is associated with compressional movements on the adjacent continental slope (Masson and Parson, 1983). Further east in the basin uplift may have been somewhat later, in the Oligocene-Miocene, as proposed by Ziegler (1987a) for the Brittany Basin.

In the Western Approaches Basin well log data is more sensitive to uplift than seismic data. Any uplift achieved without deformation, whose expression is a disconformity, will require resolution by well rather than seismic data.

7.4 QUANTIFICATION OF THE UPLIFT

Magara (1976) has shown that the amount of greater burial than that which is now observed in an uplifted shale sequence may be calculated by comparing the sonic log with wells which have not been uplifted. A modified

version of this technique has been applied to the chalk porosity data from the Western Approaches Trough. It is assumed that all chalks follow the "normal compaction" trend on burial and that porosity loss is non-reversible. Porosity variations caused by processes other than "normal diagenesis" and porosity increases during uplift may result in errors in the calculated uplift magnitude. The wells with the highest porosity for their given depth of burial, 73/1-1, 73/12-1 and 73/13-1, are assumed not to have been uplifted. This is probably reasonable since their porosities lie on the "normal compaction" trend of Scholle (1977) (Figure 7.1).

Figure 7.3 shows the evolution of chalk porosity in a well during initial burial (A), post-burial uplift (B), and later post-uplift burial (C-E). The amount of uplift, Δd, of well B in Figure 7.3 is simply the vertical displacement between its porosity-depth plot and that of the "normally compacting" well A, 500m in this case. In practice this was determined by calculating vertical displacement of the average porosity-depth gradient ($46\%km^{-1}$) between the mean porosity-depth value of well 73/1-1 and the well under consideration. This value is shown as apparent uplift in Figure 7.4(a). If there is no post-uplift subsidence, then this will be the true uplift magnitude. However, if further subsidence occurs the magnitude of the apparent uplift is reduced by the amount of post-uplift subsidence. This is illustrated in wells C and D of Figure 7.3. Overburden weight following uplift does not cause any further porosity loss until the chalk re-attains its previous greatest depth of burial, although the apparent uplift becomes smaller as the chalk is progressively buried. In well C the apparent uplift is 250m, and to obtain the true value of 500m the 250m of post-uplift subsidence must be added to the apparent uplift. In well D the chalk has returned to its original burial depth of well A, and no porosity anomaly is observed. With the addition of yet more overburden the chalk will once again begin to follow its "normal compaction" trend as shown by well E. Hence, although we can be confident that wells 73/1-1, 73/12-1 and 73/13-1 are on or near the "normal compaction" trend, and can be used as reference wells, they may have been subject to Eocene/Oligocene uplift of equal or lesser magnitude than the thickness of Oligocene and later sediments. Uplift values corrected for the amount of Oligocene and later sedimentation are shown in Figure 7.4(b).

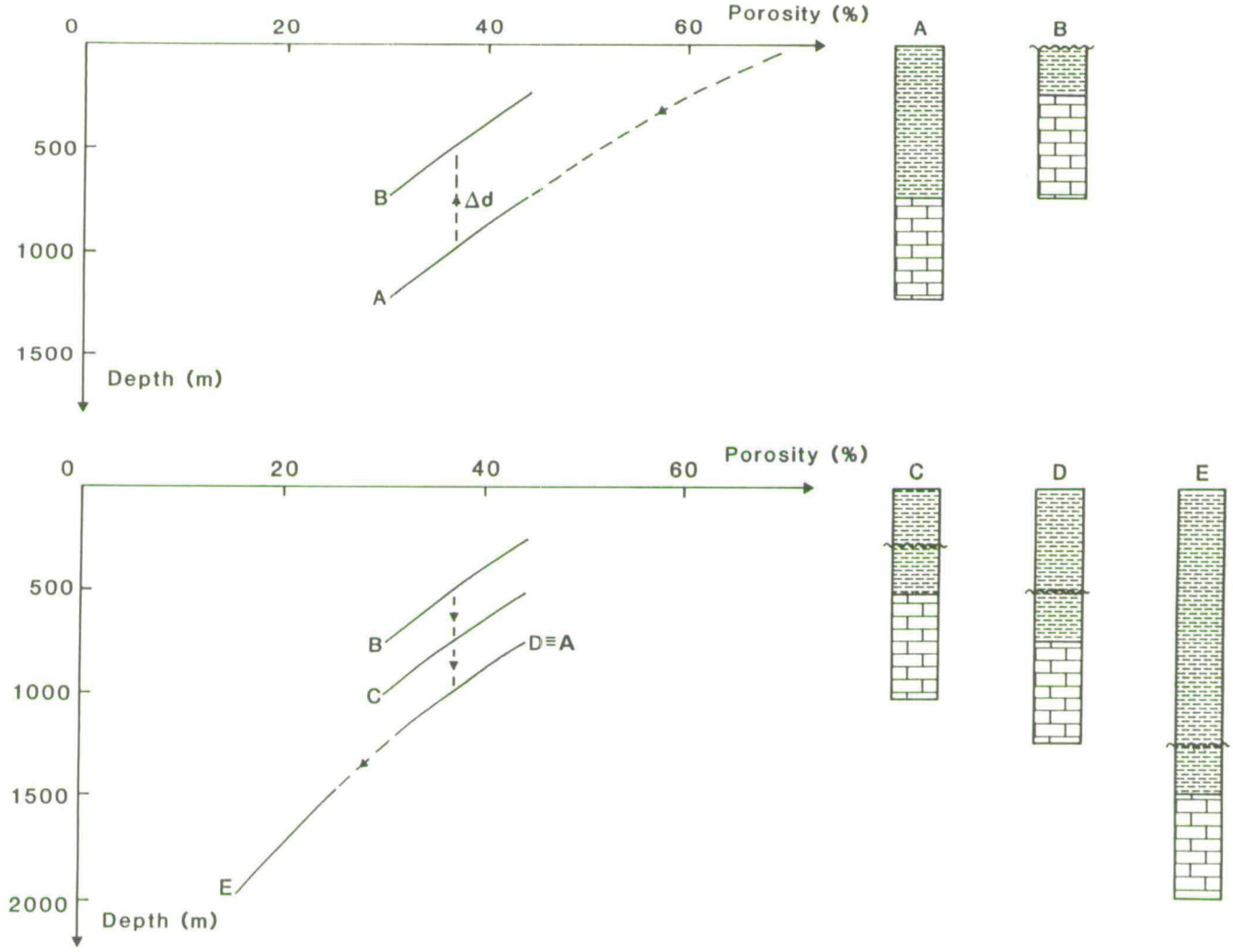

Figure 7.3 Chalk porosity evolution in an uplifted well, see text for discussion.

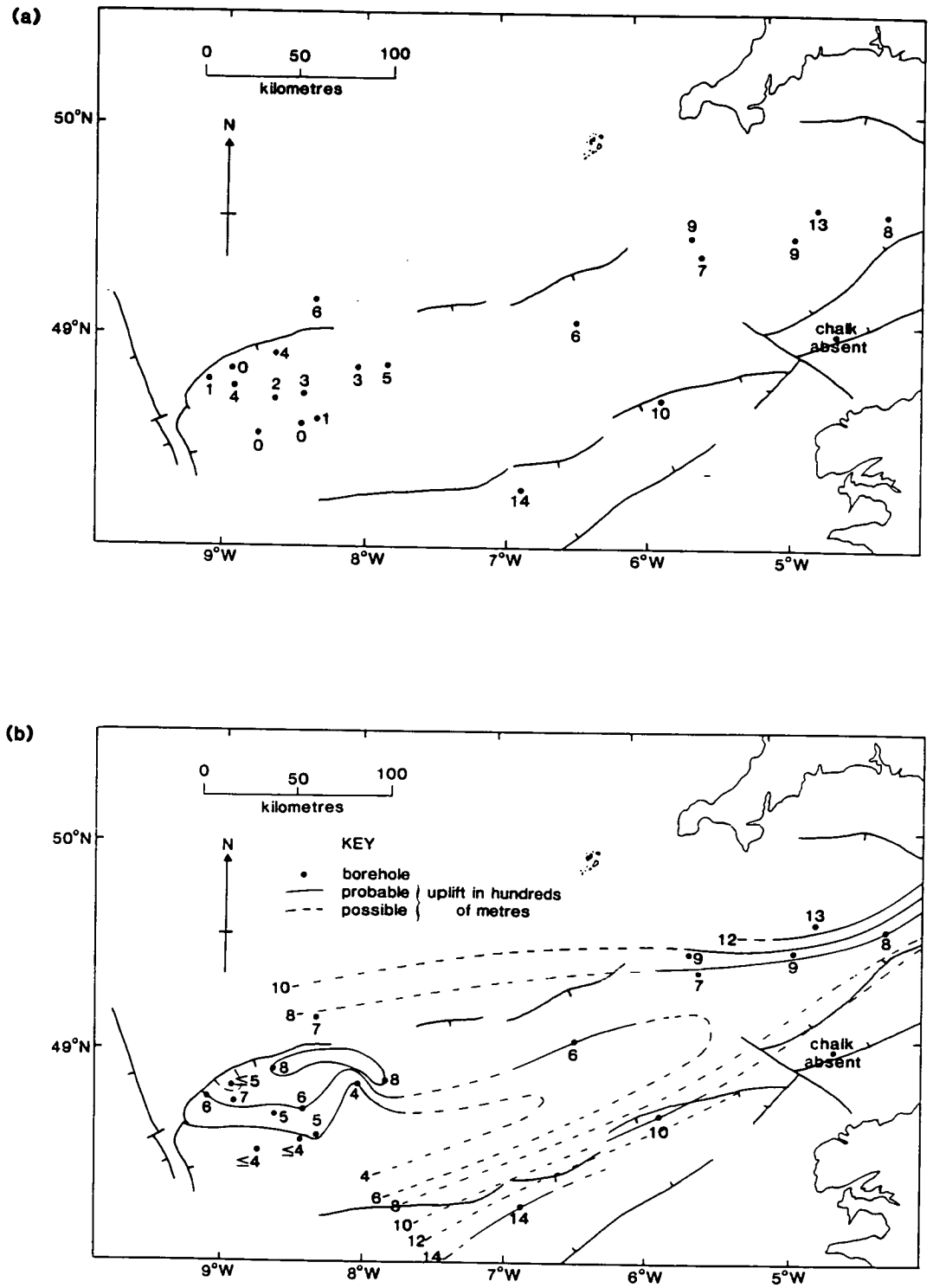

Figure 7.4 Uplift in hundreds of metres as calculated from chalk porosity data for wells in the Western Approaches Trough (a) apparent uplift, point values (b) true uplift corrected for post-uplift subsidence, point values with approximate contours at 200m intervals.

An attempt has been made to contour the uplift data of Figure 7.4(b). Uplift was greatest in the Brittany Basin, and drops sharply passing north into the Melville Basin. Further east, from the eastern Brittany Basin into the St. Mary's Basin, and the South-West Channel Basin to the Plymouth Bay Basin the drop is less pronounced, and significant uplifts are recorded in east of the Western Approaches Basin. Uplift values increase again moving north from the sub-basins of the Western Approaches Basin onto the Cornubian Massif.

7.5 MECHANISMS OF TERTIARY UPLIFT

Although Tertiary compressional movement, with its associated uplift, has been widely described in the surrounding areas (Section 7.3.2.9) it has not previously been reported in the Western Approaches Basin. Tertiary uplift in the Western Approaches Basin was accommodated without the upper crustal compression which accompanies uplift in the surrounding basins. This contrast in structural styles is illustrated by the BIRPS SWAT lines 7 and 8 (Figures 6.2 and 6.3) where a major anticline developed in the post-mid Cretaceous sediments of the Brittany and South-West Channel Basins has no expression in the Western Approaches Basin.

At this point the distinction between uplift and inversion should be clarified. Uplift is simply taken to be upward vertical movement of the crust and implies no genetic mechanism or specific geometry. In keeping with Lake and Karner (1987), inversion implies the change in structural relief from a basinal area into a structural high (positive inversion) or a structural high into a basin (negative inversion).

7.5.1 Pure Shear Compression

The Tertiary inversion of the sedimentary basins of southern England and Wales, has been explained in terms of compressional tectonics by Chadwick (1985a). The lithospheric section of Figure 7.5(a) is subjected to compressive stress which results in shortening by a factor β. Both the crust and the sub-crustal lithosphere are thickened by a factor 1/B which causes an isostatically driven initial uplift (U_I) due to replacement at

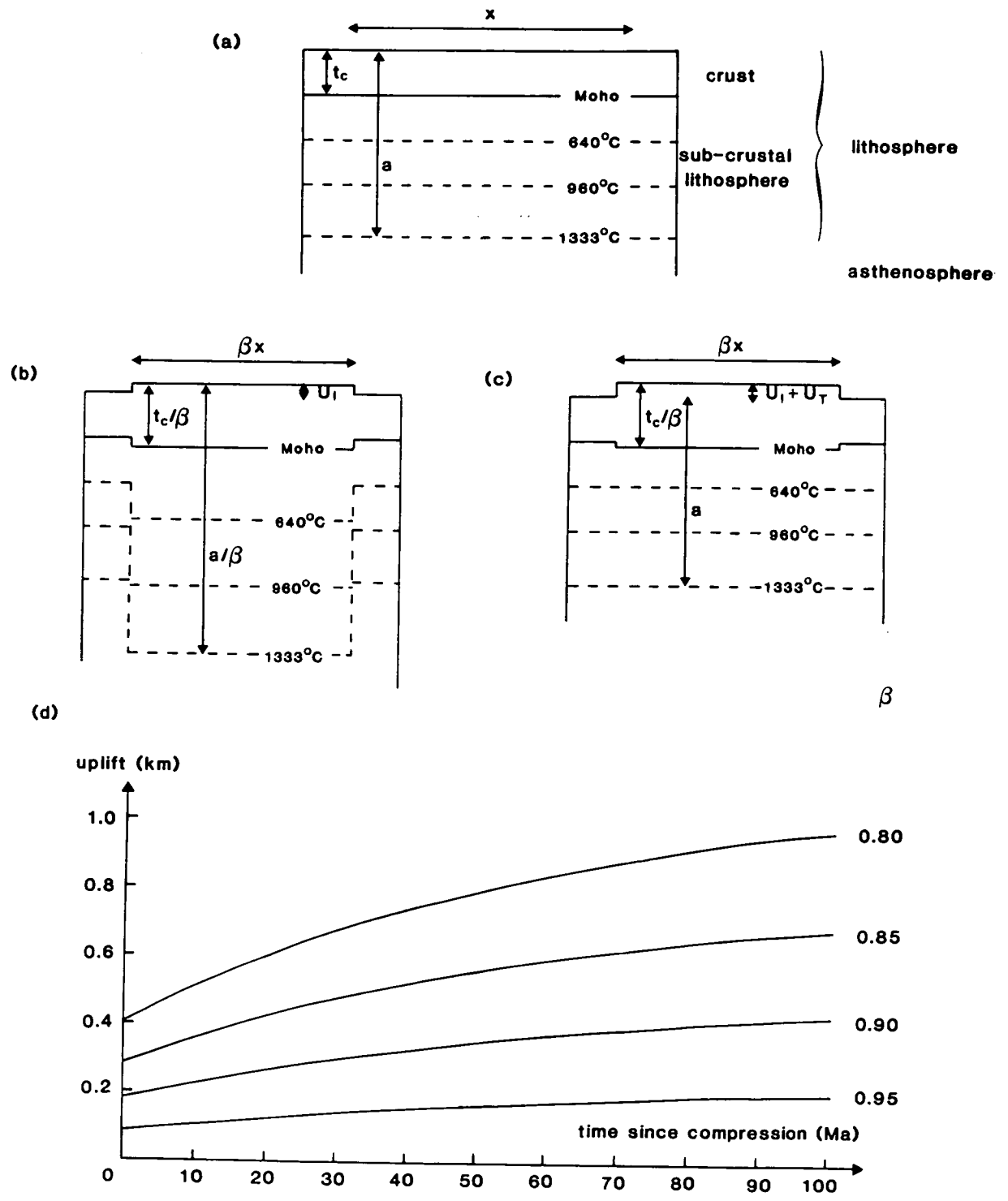

Figure 7.5 The effect of instantaneous homogeneous pure shear compression on a lithospheric section assuming local Airy isostasy; (a) pre-shortening, (b) immediately after shortening pulse, (c) after thermal re-equilibration, (d) uplift against time for air-loaded lithosphere. Pre-compressional crustal thickness 27km, other parameters after Chadwick 1985a.

depth of dense mantle material by lighter crustal material (Figure 7.5(b)). A subsequent, thermal relaxation uplift (U_T) is caused by heating of the relatively cold lithospheric material pushed down into the hot asthenosphere (Figure 7.5(c)). This process is, of course, analogous to McKenzie's (1978) model for subsidence following extension of the lithosphere.

The change from regional post-Cimmerian subsidence to Tertiary uplift reflects a fundamental change in plate kinematics between Iberia/Africa and Eurasia (Figure 6.6). Compression was driven by collisions in the Alpine foldbelt with the compressional stresses which uplifted the Western Approaches Trough probably transmitted from the Pyrenees.

Such compression, if it uplifted all the surrounding areas, must also have acted across the Western Approaches Basin. Hence, compressional structures such as folding and reverse reactivation of normal faults, would be anticipated. They do not occur, although the area has clearly been uplifted. This is in contradiction of the homogeneous pure shear compression model outlined above.

7.5.2 Simple Shear Compression

The absence of Tertiary compressional deformation in the Western Approaches Basin may be due to the localization of deformation over the Alpine foreland by the reactivation of basement faults (simple shear). In Figure 7.6 the entire crust of the hanging wall of the major crustal detachment is under compression, although related structures are only developed above ramps in the detachment. Hence, following the model of Beach (1987), the pattern of deformation observed could be explained if the Western Approaches Basin lay above a flat, while the Brittany Basin (and the other inverted basins) lay above a crustal ramp. However, this explanation is at odds with the known crustal struture of the Western Approaches Basin which is underlain by a series of dipping Variscan thrusts (Chapter 4), equating to ramps in any major crustal discontinuities. If a Beach-type (1987) active ramp, which is not imaged in the seismic data, controls Tertiary deformation in the Brittany Basin it is difficult to account for the absence of reactivation of the Melville, Carrick, Lizard and Normannian Thrusts.

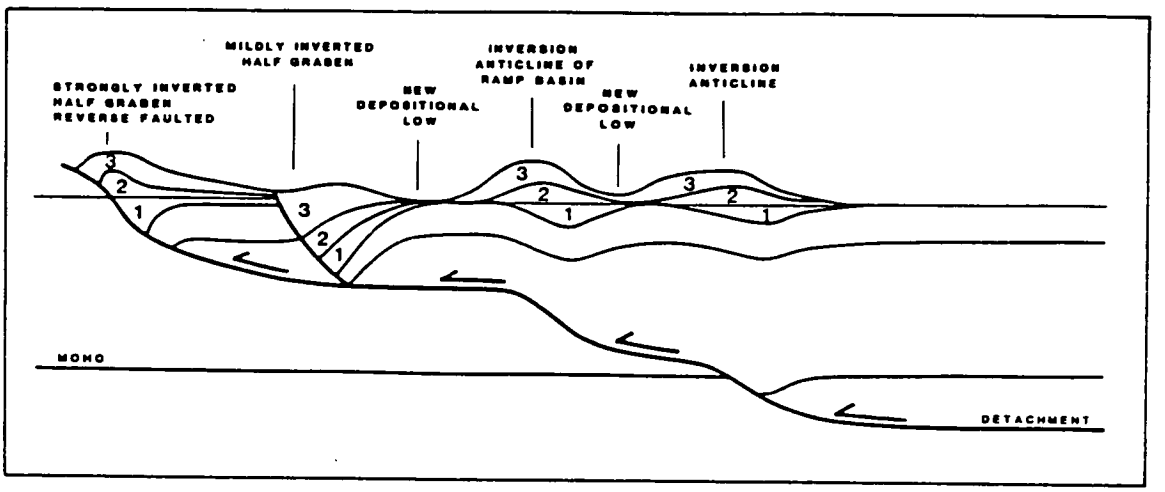

Figure 7.6 Simple shear compression above a crustal detachment, note compressional structures are only developed above ramps in the detachment (from Beach, 1987).

7.5.3 Inversion Progradation

In spite of the presence of basement faults the upper crust of the Western Approaches Basin was sufficiently strong to transmit Alpine compressive stresses further to the north without itself deforming. Ziegler (1987b) described this process as "inversion progradation", and cited the transmission of Alpine compressive stresses through the relatively undeformed West Netherlands-Broad Fourteens Basin into the deformed Sole Pit Basin.

Ziegler (1987b) suggested that the early Cretaceous/Tertiary inversion of the Fastnet-Celtic Sea Basin was also caused by inversion progradation, through the Western Approaches Trough. With time, however, stresses built up sufficiently to invert the Western Approaches Trough. This process he termed "inversion retrogradation". The situation is, however, more complex. Inversion progradation may apply to the Fastnet-Celtic Sea Basin, and inversion retrogradation may apply to the Brittany and South-West Channel Basins. However, the Western Approaches Basin, which has not been deformed, comprises a distinct structural unit. During the Tertiary, as during its earlier tectonic evolution, the Western Approaches Trough can not be considered as a single structural entity and must be analysed in terms of its component sub-basins.

Ziegler (1987b) suggested that inverted basins overlay thinner crust than those which transmitted stress without themselves being deformed. The depth converted interpretation of BIRPS SWAT lines 6 and 7 (Figure 8.15) suggests 1-2km of crustal thinning under the eastern Brittany Basin with respect to the St. Mary's Basin. Prior to Tertiary compression and deformation in the Brittany Basin this thinning would have been more pronounced. It is proposed that inversion pro- and retro-gradation better account for the differential behaviour of the Brittany, Western Approaches and Celtic Sea-Fastnet Basins than simple shear, however, this does not preclude the action of simple shear within individual basins.

7.5.4 Heterogeneous Compression

Sclater et al (1980), Royden and Keen (1980), Hellinger and Sclater (1983) and Rowley and Sahagian (1986) argued that differential stretching of the crust and sub-crustal lithosphere could explain the subsidence histories of sedimentary basins and continental margins not satisfactorily described by the homogeneous extension model.

The process of heterogeneous compression can explain the uplift, without compressional deformation, observed in the Western Approaches Basin. While the upper crust of the Western Approaches Basin was able to transmit the Tertiary compressive stresses to the north without itself deforming, the more ductile sub-crustal lithosphere (and possibly the lower crust) did not have sufficient strength to do so, and consequently thickened. If the lithospheric section of Figure 7.7(a) is subjected to a pure heterogeneous compression with shortening restricted to the sub-crustal lithosphere then there is an initial isostatic subsidence (S_I) due to the replacement, in the sub-crustal lithosphere, of hot, low density mantle material by colder, heavier material (Figure 7.7(b)). As this material heats up there is an exponentially decaying thermal uplift (Figure 7.7(c)) with a time constant similar to that of thermal subsidence in a homogeneously extended basin. This mechanism can produce uplift in a compressive regime without accompanying upper crustal compressional deformation. The following sections discuss the quantification of heterogeneous compression and its applicability to the Western Approaches Trough and surrounding areas.

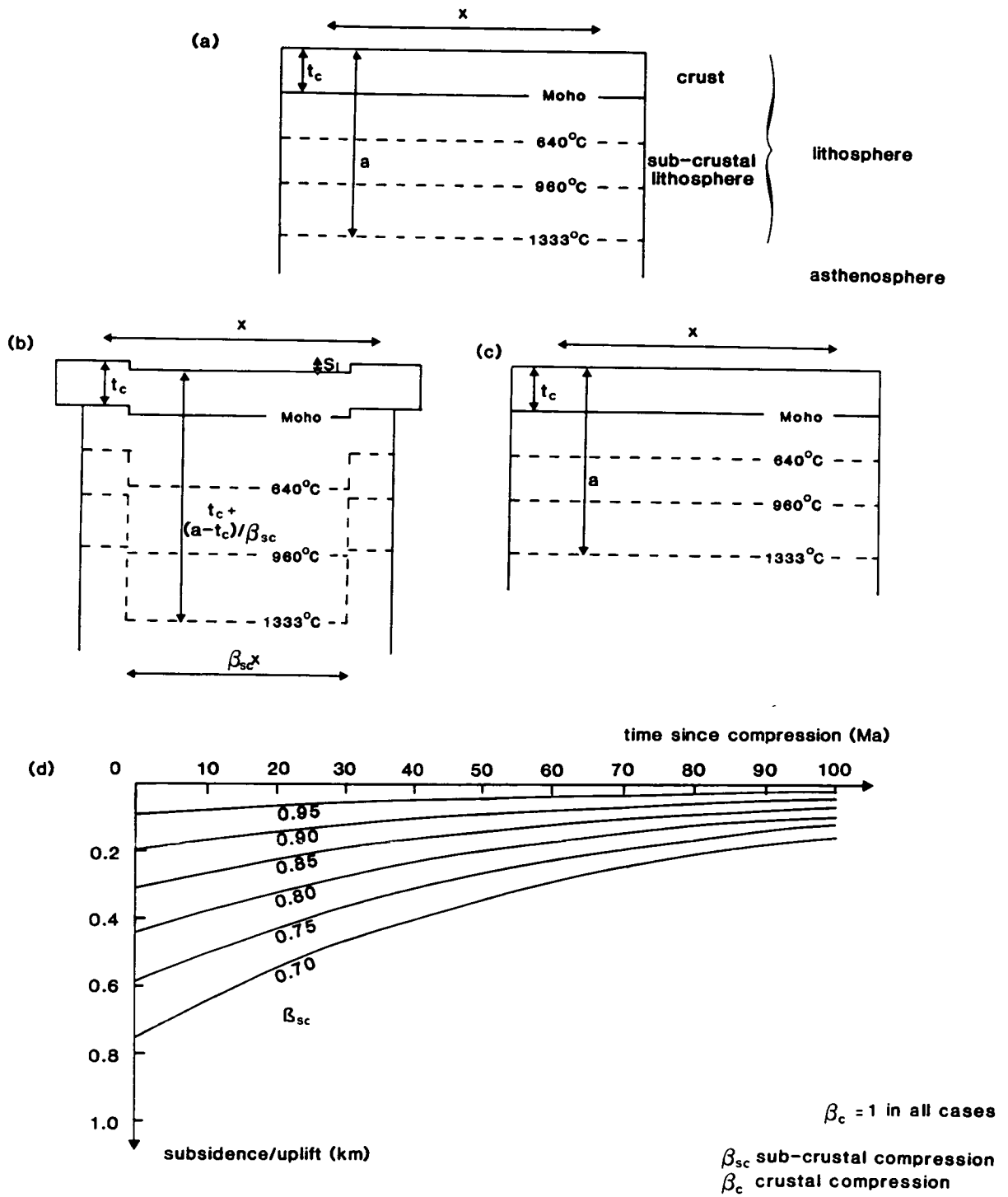

Figure 7.7 The effect of instantaneous heterogeneous pure shear compression on a lithospheric section assuming local Airy isostasy;(a) pre-shortening,(b) immediately after shortening pulse, (c) after thermal re-equilibration,(d) subsidence/uplift against time for air-loaded lithosphere. Pre-compressional crustal thickness 27km, other parameters after Chadwick 1985a.

7.5.4.1 Heterogeneous Compression: Quantification

The solution to the thermal subsidence of the lithosphere following heterogeneous extension (Hellinger and Sclater, 1983) as derived from Lubimova and Nikitina (1975) is,

$$e(t) \simeq p \sum_{k=0}^{\infty} (C_{2k+1}/2k+1)\exp[-(2k+1)^2 t/\tau] \qquad (1)$$

where

$$C_n = 2(-1)^{n+1}/n^2\pi^2[(\beta_c-\beta_{sc})\sin(n\pi t_c/a\beta_c)+\beta_{sc}\sin(n\pi/\beta_1)] \qquad (2)$$

and $e(t)$ is the elevation above which the lithosphere sinks to after time t, β_c, β_{sc} and β_1 are the crustal, sub-crustal and lithospheric stretching factors respectively, t_c and a are the crustal and lithospheric thicknesses respectively, τ is the thermal time constant of the lithosphere and p is a constant defined by the physical properties of the lithosphere

This is of the same form as the solution to the thermal subsidence of the lithosphere following homogeneous extension (McKenzie, 1978) but fails under compression (when $\beta<1$) because the $\sin(n\pi t_c/a\beta_c)$ and $\sin(n\pi/\beta_1)$ terms (equation 2) tend to zero when the $t_c/a\beta_c$ and $1/\beta_1$ terms tend to integer values. In extension, when $\beta>1$, these terms are between zero and one.

An alternative solution to the thermal uplift/subsidence of the lithosphere in response to heterogeneous compression was derived following a suggestion by R.A. Chadwick (personal communication, 1988). The initial (S_i) and final (S_∞) subsidence of the lithosphere following heterogeneous extension, as given by isostatically balanced lithospheric columns (Hellinger and Sclater, 1983), are, with a sign change, valid under compression. In the absence of surface loading,

$$S_i = \{[(\rho_m-\rho_c)t_c(1-\alpha T_m t_c/2a)-\alpha\rho_m T_m t_c/2](1-1/\beta_c) - [\alpha\rho_m T_m (a-t_c)/2](1-1/\beta_1))/[\rho_m(1-\alpha T_m)] \qquad (3)$$

$$S_\infty \simeq \{t_c(\rho_m-\rho_c)[1-\alpha T_m t_c/2a](1-1/\beta_c))/[\rho_m(1-\alpha T_m)] \qquad (4)$$

where the symbols are as equations (1) and (2) and ρ_m and ρ_c are the densities of the crust and mantle respectively, α is the thermal expansion co-efficient of the lithosphere and T_m is the temperature at the base of the lithosphere

The total thermal uplift/subsidence (S_t) is given by the difference between S_∞ and S_i and its value after time t, following LePichon and Sibuet (1981), is given by,

$$S_t(t) = S_t[1-\exp(-t/\tau)] \tag{5}$$

$$S_t = S_\infty - S_i = \{\alpha T_m[(1-1/\beta_c)t_c+(a-t_c)(1-1/\beta_i)]\}/2(1-\alpha T_m) \tag{6}$$

The relative magnitudes of the initial and thermal uplift/subsidence resulting from heterogeneous compression will be determined by the relative amounts of crustal and sub-crustal shortening. For crustal shortening greater than sub-crustal shortening the initial uplift will be of relatively greater magnitude than in homogeneous compression (Figure 7.8(a)). For sub-crustal shortening with progressively less crustal shortening the magnitude of the initial uplift is reduced until it becomes zero, and then is replaced by an initial subsidence (Figure 7.8(b)). Sub-crustal shortening with no crustal shortening is the end member of this series.

The initial subsidence caused by sub-crustal compression, in the absence of crustal compression, will be enhanced by sediment loading. Assuming local Airy isostasy the magnitude of sediment loaded subsidence (S_s), in comparison with air-loaded subsidence (S_a), is given by

$$S_s = S_a[\rho_m/(\rho_m-\rho_s)] \tag{7}$$

where ρ_m and ρ_s are mantle and sediment densities respectively

Similarly, the ensuing thermal uplift will be enhanced by erosion (sediment unloading). With complete re-equilibration of the sub-crustal lithosphere, in the absence of crustal deformation, a lithospheric section will re-attain its pre-compressional form, and isostatic level, prior to

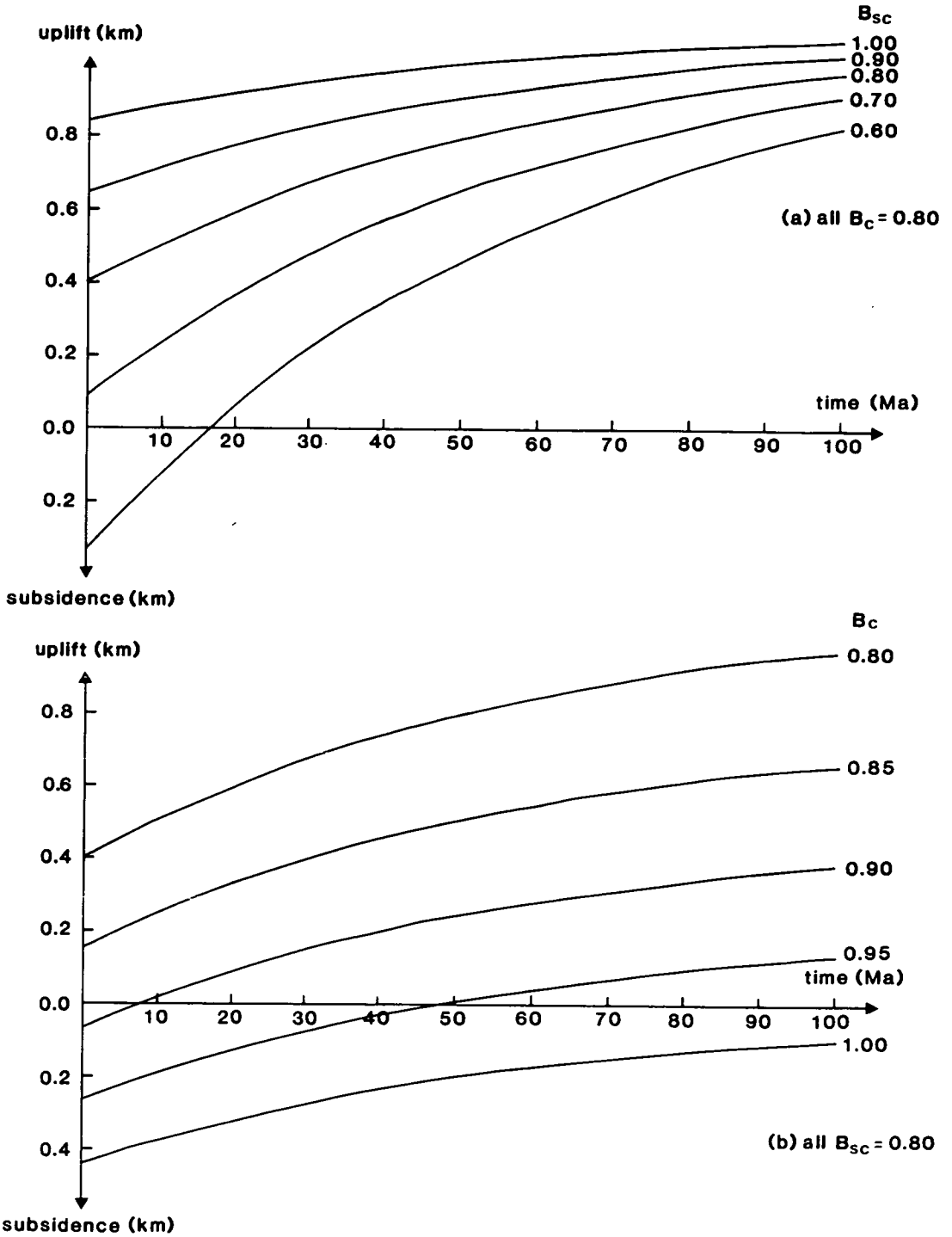

Figure 7.8 Sample curves for heterogeneous pure shear compression. Pre-compressional crustal thickness 27km, other parameters after Chadwick (1985a). (a) Constant crustal shortening (β_c) with variable sub-crustal shortening; (b) constant sub-crustal shortening (β_{sc}) with variable crustal shortening. All curves assume air-loaded lithosphere.

compression. Hence any sediments deposited as a response to heterogeneous lithospheric compression will tend to be eroded.

7.5.4.2 Heterogeneous Compression: Observations on the Tertiary Uplift of the Western Approaches Trough and Surrounding Areas

Erosion consequent upon the Tertiary uplift of the Western Approaches Basin did not significantly cut down into pre-compressional sediments. This is witnessed by the relatively short time gap of the uplift unconformity. The heterogeneous compression model predicts that sub-crustal compression without crustal compression leads to an initial subsidence followed by an uplift that will only cut down to the pre-compressional surface and not into pre-compressional sediments (Figure 7.7). The initiation of the pre-uplift rapid subsidence phase has been preserved immediately under the uplift unconformity in the Eocene of wells 73/8-1, 73/13-1, 73/14-1 and 74/1-1 (Figure 6.7).

In contrast, the crustal and sub-crustal shortening to which the Brittany Basin was subjected caused both an initial uplift and a thermal uplift (Figure 7.5). Hence, in the Brittany Basin the uplift cut down into the underlying sequence and chalk now outcrops over much of the seabed.

Figure 7.9 shows a possible schematic distribution of crustal and sub-crustal compression from north-west France to southern Ireland. Shortening of the sub-crustal lithosphere is assumed to decrease steadily with distance from the Alpine foldbelt (Figure 7.9(b)). Crustal, or upper crustal, shortening is shown to be zero in areas such as the Western Approaches Basin and Cornubian and Armorican Massifs where Tertiary compressional deformation is generally absent (Figure 7.9(c)). The broad pattern of uplift and crustal deformation over the sedimentary basins is reconciled by the simplified model, which also predicts the physiographic uplift of the Cornubian, Armorican and Irish Massifs. Balance of the shortening in the two layers is not implied by the diagram, but this question is discussed in the next section.

This model requires a regional detachment between the crust and the sub-crustal lithosphere, or possibly within the crust itself. A rheological boundary at top of, or within the reflective lower crust, or the Moho itself

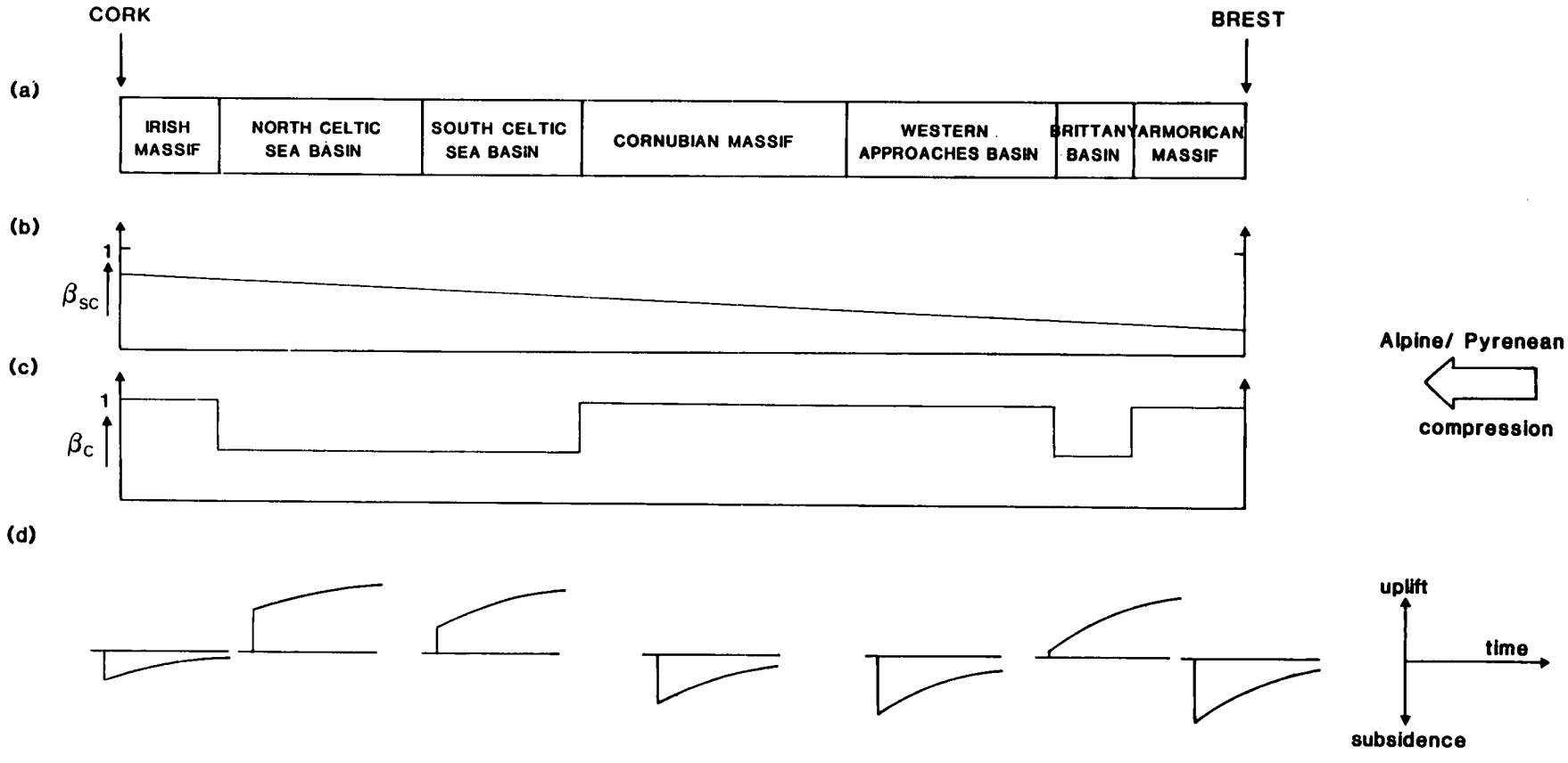

Figure 7.9 (a) Major structural elements between Brest and Cork showing schematic distribution of (b) sub-crustal and (c) crustal Tertiary compression with (d) resultant vertical movements. See text for discussion.

(Kusznir and Park, 1987; Kusznir et al, 1987) may facilitate such a detachment.

Although the variable timing of uplift across the south-west British continental shelf may be explained in terms of inversion pro- and retro-gradation this does not account for the relatively short time interval of erosion (Maastrichtian-Palaeocene, Eocene-Oligocene, Oligocene-Miocene etc.) recorded by the uplifted basins. For a lithospheric thermal time constant of 62.8Ma (Parsons and Sclater, 1977) uplift in the Melville Basin, which was concentrated during the Eocene-mid Oligocene hiatus, a period of some 15Ma, will only have attained 21% of its total magnitude (equation 5). The duration of erosion in an area is not, however, solely controlled by the duration of "tectonic uplift" in that area.

The magnitude of uplift in surrounding areas will have a crucial bearing on the relationship between the duration of tectonic uplift and the duration of erosion in any area. Since the Cornubian Massif and Brittany Basin were uplifted by a greater amount than the Melville Basin (Figure 7.4(b)) they may have sourced sediment into the Melville Basin thus causing subsidence while the sub-crustal lithosphere was still recovering from compression. Eustatic sea-level rise might also result in tectonic uplift not being expressed as an unconformity. It is proposed that interaction between the timing (controlled by inversion pro- and retro-gradation) and relative magnitudes of tectonic uplift, in addition to eustatic sea-level change, resulted in the variable timing and duration of Tertiary erosion across the sub-basins of the Western Approaches Trough, and surrounding areas.

It is interesting to note that (homogeneous) lithospheric compression of the highly extended north Biscay margin and North-East Atlantic Basin, as described by Masson and Parson (1983) (Section 2.9.3), will have caused an initial subsidence (Murrell, 1986). This phenomenon is analogous to the initial uplift produced by extension of already thin crust (Dewey, 1982). In both cases the response of the lithospheric section with thin crust is dominated by the behaviour of the sub-crustal lithosphere. Under compression thickening of the lithosphere promotes an "initial thermal subsidence" because of the downwarping of relatively low temperature isotherms (dense material) into the asthenosphere (Figure 7.5(b)). If "normal" thickness crust is compressed then the initial uplift associated with the replacement of dense mantle material by light crustal material

more than compensates for this "initial thermal subsidence". With complete thermal re-equilibration crustal thickening will, regardless of initial crustal thickness, result in a net uplift, and thinning will always cause net subsidence.

There are distinct similarities between the predicted behaviour of the homogeneously compressed thin crust of the shelf and that of the heterogeneously compressed (excess sub-crustal thickening) normal thickness crust of the Western Approaches Basin. In both cases the initial response (subsidence) is controlled by the downwarping of the lithospheric isotherms, and thermal re-equilibration causes uplift (Figure 7.7(d)).

7.5.4.3 Heterogeneous Compression: β-Factors and the Space Problem

In order to test the heterogeneous compression model it is necessary to investigate the amount of sub-crustal compression required to produce the the observed uplift in the Western Approaches Basin. Taking the present crustal thickness of 27km (from SWAT 7) and a lithospheric thickness of 100km (inherited late Jurassic-early Cretaceous thinning will not have fully re-equilibrated) and allowing for sediment unloading, a sub-crustal β-factor of 0.70, with no crustal compression, causes approximately 0.52km of air-loaded initial subsidence. At a sediment density of $2.3gcm^{-3}$ this is equivalent to a sediment-loaded subsidence of 1.68km (equation 7). Allowing erosion to have attained 21% of its total value, and ignoring changes in palaeobathymetry and eustatic sea-level (erosion is presumably sub-aerial) this produces 0.42km of uplift. Even this large sub-crustal shortening (30km of shortening over 100km) does not quite generate the observed magnitude of uplift (Figure 7.4(b)). It seems probable that there is a small amount of crustal compression not apparent on the seismic data. This will act to decrease the inital subsidence magnitude and increase the total uplift (Figure 7.8(b)).

To avoid a space problem the sub-crustal β-factors required to produce the observed uplift in the Western Approaches Basin must be balanced by excess crustal compression elsewhere. The Tertiary compressional anticline in the Brittany Basin has, unfortunately, been largely eroded (Figure 6.2), but extrapolation of the preseved part of the structure to Ziegler's (1987a) estimate of 3000m structural relief, and allowance for parasitic folding as

is observed on the preserved part of the anticline, gives a crustal B-factor of 0.98. Similarly, Chadwick (1985b) proposed a crustal β-factor of 0.98 for the Wessex Basin. These rough values indicate that the apparent crustal deformation of the surrounding basins can not balance the required sub-crustal shortening in the Western Approaches Basin. Indeed, a homogeneous compression with a β-factor of 0.98 can not produce the observed uplift in the Brittany Basin. Allowing for sediment unloading (ρ_m=2.3gcm^{-3}), with erosion in the Oligocene-Miocene (33Ma), and with crustal and lithospheric thicknesses of 27 and 100km respectively, such a compression produces only 0.2km of uplift. This is an average value across the anticline but is very much less than the values indicated by the chalk porosities (Figure 7.4(b)).

The contradictions between apparent crustal β-factors and uplift magnitudes parallel those often found when modelling subsidence by extension. Many sedimentary basins and continental slopes show less crustal extension than would be expected from their observed subsidence (e.g. Royden and Keen, 1980; Sclater et al, 1980; Chenet et al, 1982; Bessis, 1986; Hegarty et al, 1988). Although the above authors did not generally deal with the space problem introduced by excess sub-crustal stretching, three broad approaches to the problem, modified from those proposed in extensional regimes (cf. Section 1.4.3.3), are propsed.

In order to solve the space problem Rowley and Sahagian (1986) and White and McKenzie (1988) argued that stretching in the two layers may be distributed differently but should be of the same total magnitude over a sedimentary basin and its flanks. Similarly, but on a larger scale, if the Western Approaches Trough and surrounding areas, indeed possibly Alpine foreland as a whole, exhibit an excess of sub-crustal over crustal shortening then this may be compensated for by excess crustal shortening in the highly deformed internides of the Alpine foldbelt. This hypothesis can only remain speculative as sufficiently accurate comparison of β-factors and total uplift magnitude in mountain ranges is not feasible.

Alternatively, as discussed in Section 1.4.3.3, it has been argued that the extension apparent on seismic reflection data is a significant underestimate of true extension. Compressional β-factors may similarly be minimum estimates of shortening, and greater accuracy might allow more accurate prediction of uplift magnitudes across the south-west British

continental shelf. Accurate β-factors are, of course, difficult to obtain when the expression of uplift is an unconformity.

White (1988) argued that with detailed analysis of the fault geometry crustal extension in the Viking Graben and subsidence can be reconciled. However, Ziegler and Van Hoorn (in press) argued this was not the case and invoked additional subsidence driven by lower crustal attenuation through basification of the lower crust and consequent upward displacement of the Moho. Crustal and sub-crustal extension will not balance in the latter case. Similarly, if compressional β-factors can not explain the observed magnitude of uplift then additional, non-compressional, uplift mechanisms must have acted.

7.5.5 Non-Compressional Mechanisms

Uplift can, of course, be generated without lithospheric compression. McGetchin et al (1980) proposed fourteen uplift mechanisms, one of which was compression. These will not all be discussed as the majority are not applicable to the non-volcanic, non-plume, passive margin setting of the Western Approaches Trough in the Tertiary. Two non-compressional mechanisms may, however, have played a significant role in the Tertiary uplift of the area.

McGetchin et al (1980) suggested that uplift of the Colorado Plateau may be caused by its isolation from the faulted and extended areas surrounding it. Extension has occurred in the basins surrounding the Cornubian Massif while it has remained intact. In combination with the low density of the granite batholiths forming the core of the massif this explains its Mesozoic history as a structural high. Renewed uplift of the massif may have been triggered by Tertiary compression, hence Tertiary uplift was of greater magnitude on the Cornubian Masssif than in the Western Approaches Basin (Figure 7.4(b)).

Halokinesis also caused Tertiary uplift. Tertiary uplift of the salt domes of the northern Melville Basin is witnessed by the onlap of Tertiary sediments onto the domes (Figure 2.9). This may be responsible for the isolated uplift high in the northern Melville Basin (Figure 7.4(b)). Indeed, the salt domes have maintained a slight seabed expression to the present

day. Like uplift of the Cornubian Massif, halokinesis may have been triggered by Tertiary compression.

7.6 CONCLUSIONS

(i) Log-derived chalk porosities for twenty wells in the Western Approaches Trough show a consistent porosity decrease with depth (average 46%km^{-1}), but have widely differing extrapolated surface intercept values.

(ii) The highest porosity wells lie close to the "normal compaction trend" for chalks, the remaining wells are abnormally hardened.

(iii) Only Tertiary uplift can satisfactorily account for the abnormal hardening of the chalks. The magnitude of this uplift can be quantified using the porosity data.

(iv) In the Brittany and South-West Channel (and Celtic Sea and Wessex) Basins, and the adjacent continental slope, uplift was accompanied by compressional deformation transmitted from Alpine plate collisions to the south. Uplift in these basins may largely be explained in terms of homogeneous compressional tectonics.

(v) In the Western Approaches Basin no Tertiary deformation is observed and the crust must have been sufficiently strong to transmit compressive stresses without itself deforming.

(vi) In the undeformed Western Approaches Basin and Cornubian Massif Tertiary uplift may have been generated by compression of the sub-crustal lithosphere without compression of the crust.

(vii) In order to generate significant uplifts by heterogeneous lithospheric compression there must be a large excess of sub-crustal over crustal compression. This does not appear to be balanced by crustal shortening in the deformed basins which themselves require an excess of sub-crustal compression to generate the observed uplift; either

(a) Excess sub-crustal compression is balanced by excess crustal compression in the Alpine internides, or

(b) Estimation of crustal β-factors by comparison of deformed and undeformed bed lengths on seismic data gives a gross underestimate of the amount of crustal shortening, or

(c) Additional non-compressional mechanisms have been active

(viii) Tertiary compression may have triggered both renewed uplift of the Cornubian Massif due to the presence of the low density granite batholiths and renewed halokinetic uplift in the northern Melville Basin.

CHAPTER 8

"WHOLE CRUSTAL" THINNING: GRAVITY AND DEEP SEISMIC MODELLING

8.1 INTRODUCTION

A sedimentary basin of reasonable areal extent formed by crustal thinning (extension or sub- or supra-crustal erosion) which is in local isostatic equilibrium will exhibit a gravity anomaly only at its edges. High density upper mantle material which replaces attenuated crustal material at depth is compensated for by the low density sedimentary basin fill. Similarly, the Mohorovicic discontinuity (Moho) as imaged on seismic reflection data, in two-way-time (TWT), is largely independent of sediment thickness because the low velocity of basinal sediments counteracts the shorter travel distance through the thinned crust. Hence, in order to test crustal thinning as a basin-forming mechanism by investigating the level of the underlying Moho using gravity or deep seismic reflection data the effects of the basin fill must be removed.

Since exploration wells constrain sediment velocities simple two-dimensional unmigrated depth-conversion of the seismic Moho (the base of the reflective lower crust) is fairly straightforward. A more sophisticated three-dimensional gravity stripping process has been used to remove the effect of the sedimentary basin fill from the observed Bouguer gravity. "Backstripped" gravity may then be inverse modelled to define a gravity Moho (the position of the dominant crust/mantle density interface). Estimates of Moho depth from deep seismic reflection and gravity data can readily be used to determine the magnitude of "whole crustal" thinning (β-factor). Whole crustal β-factors may in turn be compared with the sediment thickness across the basin in order to assess the importance of crustal thinning (extension or sub- or supra-crustal erosion) as a basin-forming mechanism.

8.2 GRAVITY ANALYSIS

8.2.1. Bouguer Gravity Data

The gravity database used in this study comprises the surveys carried out by the Marine Geophysics Programme of the British Geological Survey (BGS) as part of its programme of offshore geophysical exploration (Dobinson, 1984; Appendix A). These and other surveys covering the entire UK continental shelf and land area were interpolated onto a 2km by 2km grid by Hunting Geology and Geophysics under contract to the BGS. Gridded Bouguer gravity data are the required input for the backstripping procedure. The gravity database does not extend significantly into the French sector of the Western Approaches Trough (Appendix A).

Available data on the thickness of the sedimentary basin fill, the 1:1000000 map of depth to the top of the pre-Permian surface published by the BGS (Smith, 1985; Figure 8.1) is also restricted to the British sector of the basin. Gravity analysis was thus, unfortunately, restricted to the British sector of the Western Approaches Trough (i.e. the Western Approaches Basin). It was, however, extended northwards to cover the entire Cornubian Massif up to the southern flanks of the South Celtic Sea Basin.

Figure 8.2 shows a contour map of the Bouguer gravity data and Figure 8.3 shows a mesh perspective of the same dataset. All contour maps and perspective views in this chapter were prepared using the Interactive Surface Modelling program available on the BGS Keyworth Vax Computer. The horizontal axes of the plots are UTM (Universal Transverse Mercator) positions based on a central meridian of 3°W (the central meridian for the entire UK gridded gravity dataset). The main features of the Bouguer gravity map are briefly discussed below

The prominent ENE-WSW trending low running from 4-8°W (labelled anomaly A) corresponds to the low density granitic Cornubian Batholith (Bott et al, 1970; Edwards, 1984a). The similarly trending low some 75km to the NNW (B) corresponds to the Haig Fras Batholith. The low in the northern Melville Basin (C) is at least in part due to the presence of salt (Section 2.5.1). The high in the extreme south-west (D),

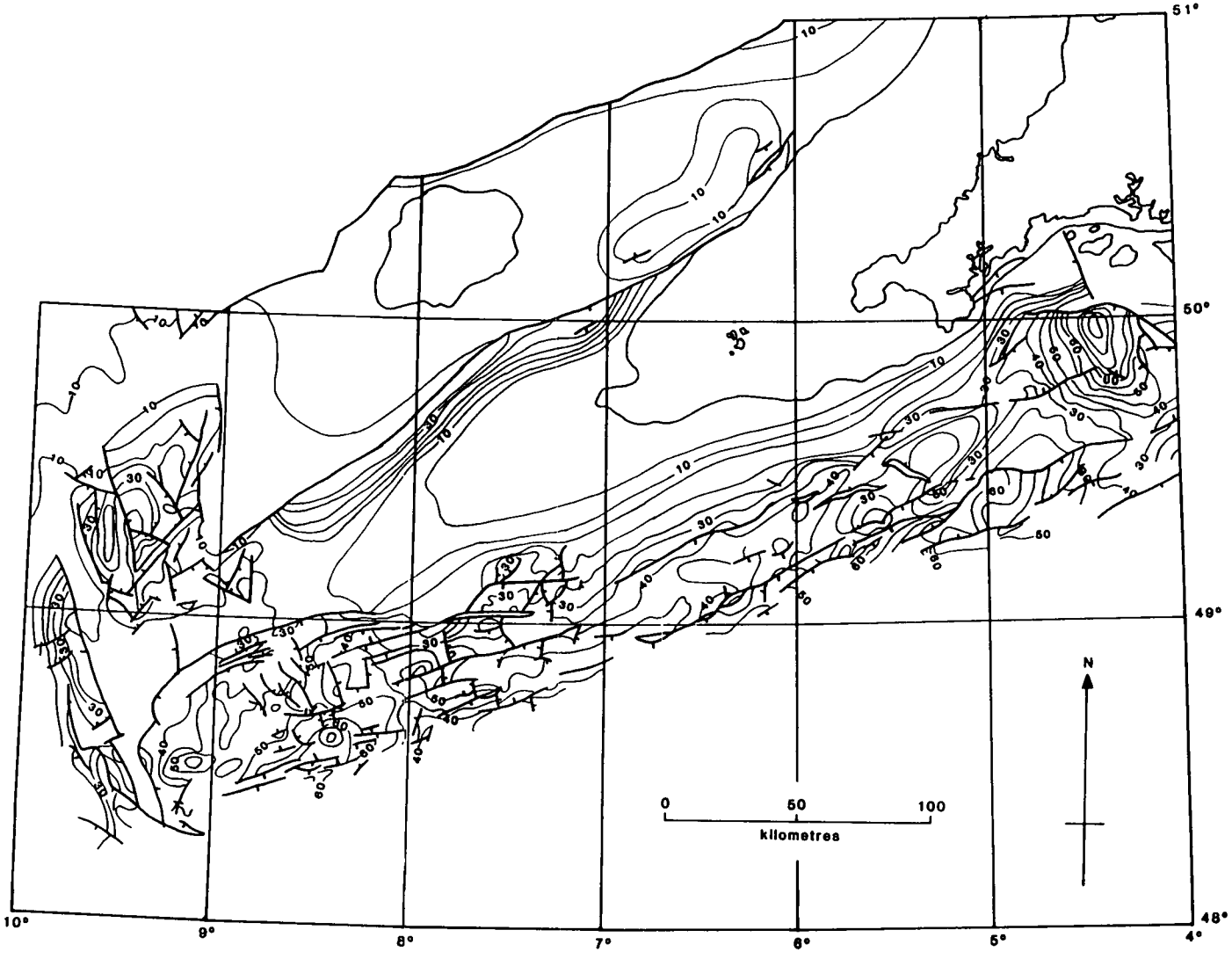

Figure 8.1 BGS map of depth to the top of the pre-Permian surface (Smith, 1985). Contours in hundreds of metres below sea-level, contour interval 500m.

prominent on the perspective plot, covers the top of the continental slope over which there is a large Bouguer gravity high due to the increasing water depth. A high (E), again prominent on the perspective plot, lies at the southern flank of the Cornubian Batholith near 7°W. This anomaly was named the Madura body by Edwards et al (1983) who interpreted it as a steep-sided pre-Chalk (?)basic igneous body, the surface of which comes to within 2km of the seabed. In addition to the local Madura body there is a slight high flanking the lows associated with the Cornubian and Haig Fras Batholiths. This decreases into the Western Approaches and Haig Fras Basins and is believed to be due to the relatively dense Variscan basement rocks which occur at or near the seabed on the basin flanks.

8.2.2 Backstripping the Effect of the Sediments from the Bouguer Gravity

Three-dimensional backstripping of the effect of the sediments from the Bouguer gravity was carried out using programs written as part of the PhD research of Genc (1988). Full acknowledgment and appreciation both for access to the programs and help in using them is expressed by the author to H.T. Genc. Program listings and a more detailed analysis of the backstripping procedure may be found in Genc (1988).

In order to evaluate the gravity effect of the low density sediments the morphology of the sedimentary basin and its density variation with depth must be known. These parameters are discussed (Sections 8.2.2.1 and 8.2.2.2) then the method of computation of the gravity effect is outlined (Sections 8.2.2.3, 8.2.2.4 and 8.2.2.5).

8.2.2.1 Morphology of the Sedimentary Basin

The morphology of the sedimentary basin was taken from the BGS 1:1000000 map of depth to the top of the pre-Permian surface, henceforth referred to as basement, of the United Kingdom (South) (Smith, 1985). This shows contours every 500m below sea-level (in the deeper part of some basins the interval is 1000m). The south-west part of this map (Figure 8.1) was digitized every 2km along each contour.

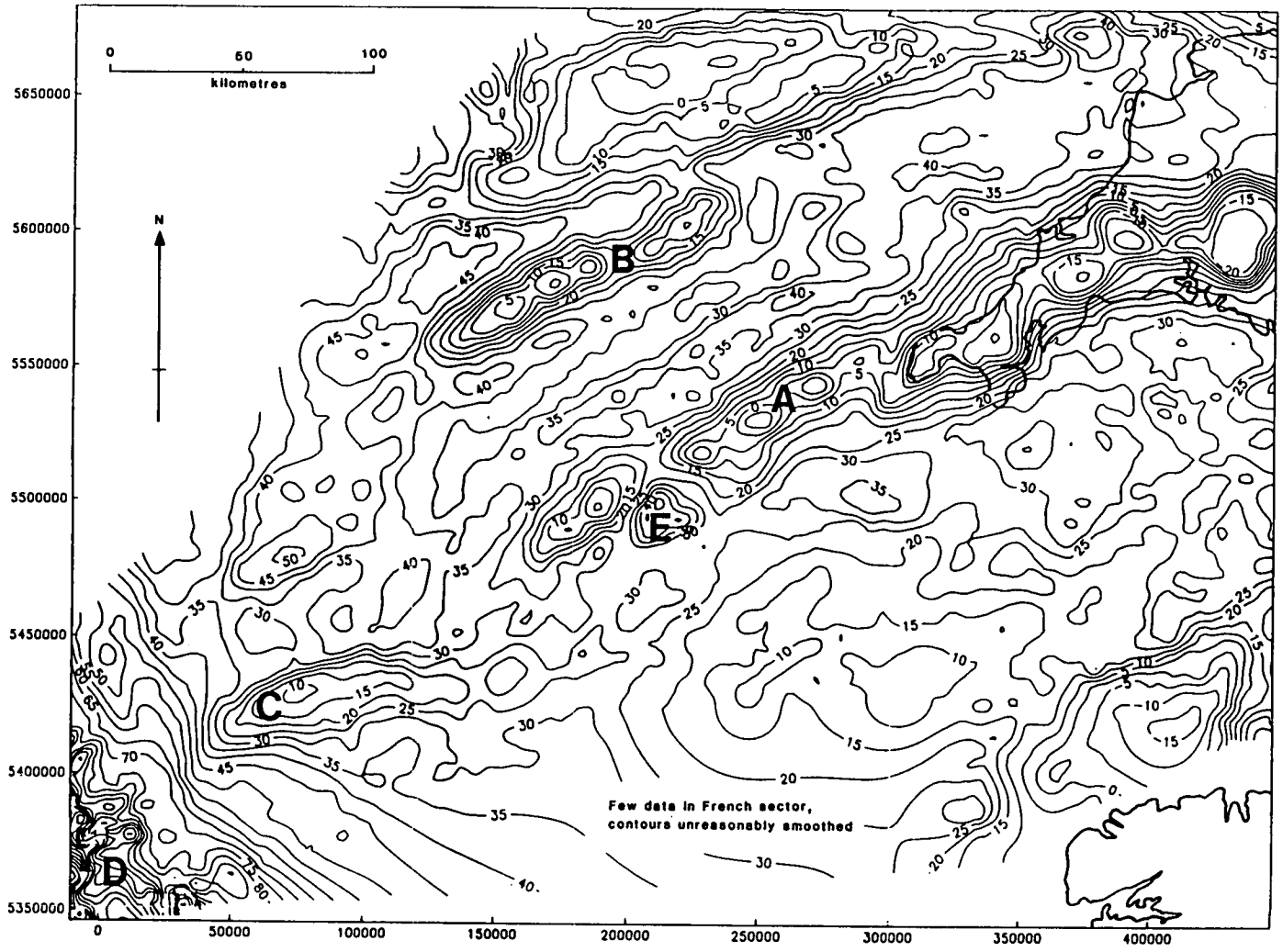

Figure 8.2 Observed Bouguer gravity data (contour interval 5 mgal). Horizontal axes are UTM positions based on central meridian at 3° W. Anomalies A and B are due to the Cornubian and Haig Fras Batholiths respectively, anomaly C is due to salt in the northern Melville Basin and possibly also a westward extension of the Cornubian Batholith. Anomaly D is due to the continental slope effect and anomaly E is the Madura body (Edwards et al, 1983).

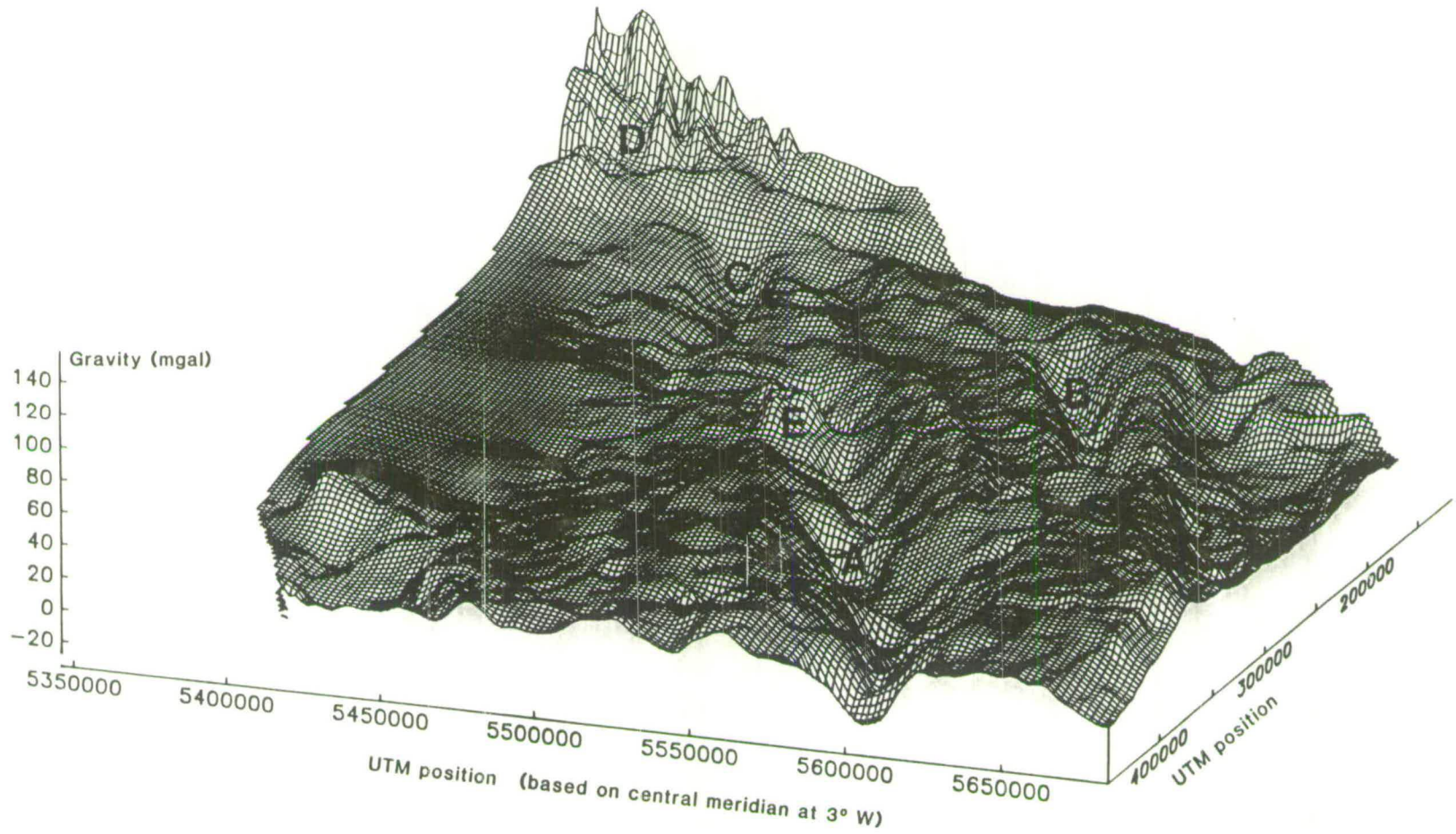

Figure 8.3 Mesh perspective view of the observed Bouguer gravity data. Viewing from an elevation of 15° and an azimuth of 110° N (down the axis of the Cornubian Batholith, towards the continental slope). Labelled anomalies as Figure 8.2.

Digitized contour data is the required input for the contour integration method which was used for computing the gravity effect of the sediments at depths greater than 500m below sea-level (Section 8.2.2.3). For the prism model, which was used to calculate the gravity effect of the sediments covering the top 500m below sea-level (Section 8.2.2.4), it was necessary to interpolate the 500m contour onto a regular (2km x 2km) grid.

The top basement contours are given relative to sea-level but the Bouguer gravity data have already been corrected for the effect of the water column. Hence when correcting the Bouguer gravity data for the effect of the sediments the water column should not be included. The relevant bathymetric data are in the BGS Oracle Offshore Database in the form of line data (Alexander and Fyfe, 1988). These data were interpolated onto the same grid as the 500m basement contour.

8.2.2.2 Sediment Densities

In two-dimensional gravity backstripping the shape of the polygons defining the sedimentary horizons (Tertiary, Upper Cretaceous etc.) is generally defined from reflection seismic data. These horizons are then assigned constant densities (e.g. Donato and Tully, 1981; Zervos, 1987; Holliger and Klemperer, in press). This is not, however, feasible in three-dimensional backstripping as the three dimensional form of each sedimentary horizon would require to be known. Not only are such data unavailable, but computation of the three-dimensional gravity effect of each sedimentary horizon would take a prohibitive amount of computer time.

For this study it has been assumed that sediment density changes only as a function of depth. This is not ideal as at a depth of say 1km the Tertiary will generally have a lower density than the Permian. However, the alternative density assumption generally made in two-dimensional stripping is also imperfect because Tertiary at surface will have a very much lower density than at 2km depth.

Figure 8.4 shows a plot of density against depth for the nineteen exploration wells in the Western Approaches Basin used in this study. The densities were originally derived from the FDC logs in order to

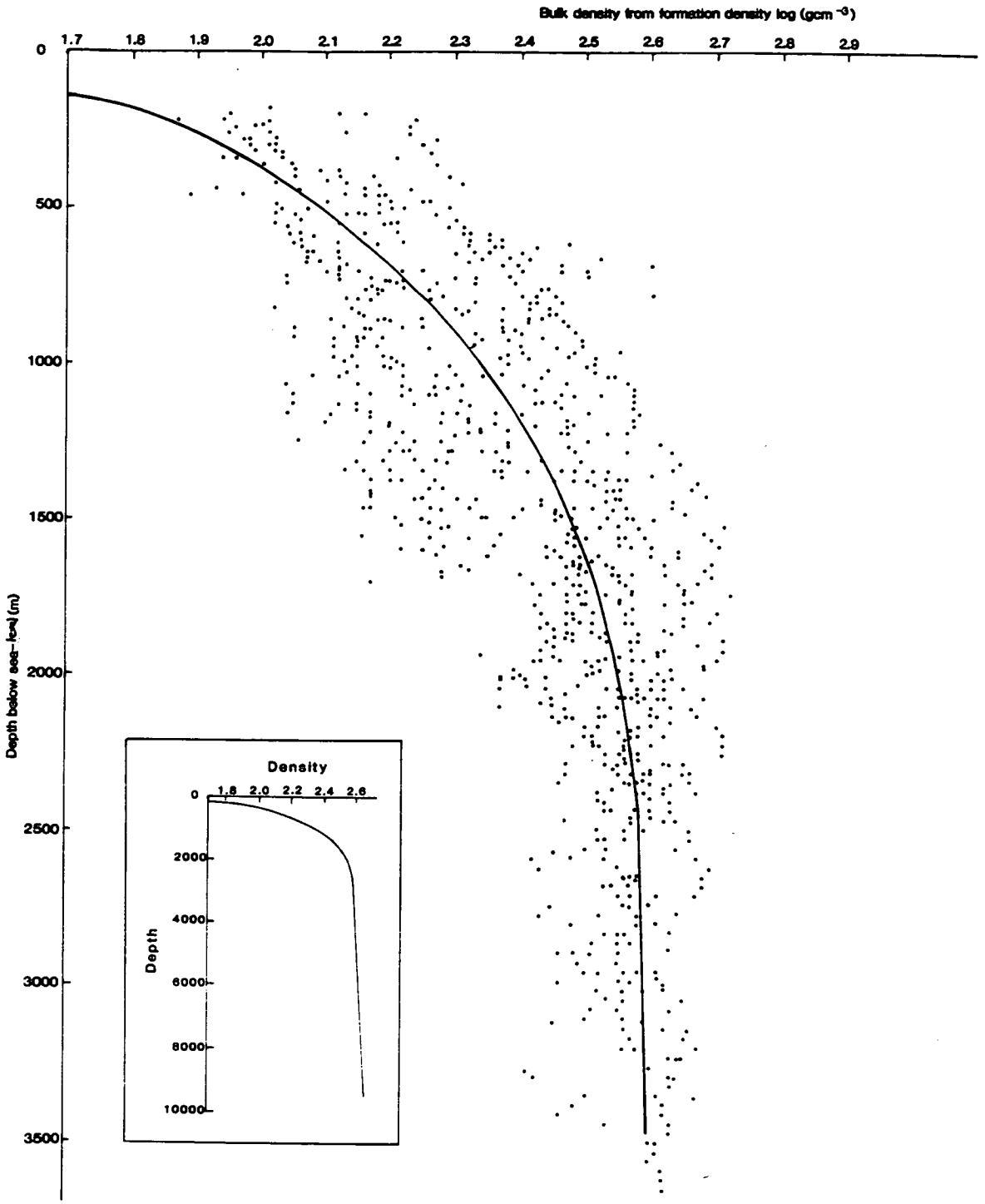

Figure 8.4 Density/depth data for the Western Approaches Basin derived from nineteen FDC (formation density) logs. Densities evaluated every 100ft over 40ft interval and every 20m over 10m interval in logs recorded in imperial and metric units respectively. Inset shows density/depth relationship extrapolated to 9.5km assuming a maximum sediment density of 2.67gcm^{-3} (the Bouguer density, and close to the grain density of most sedimentary rocks). Note the origin on the density axis is 1.7gcm^{-3}.

calculate formation porosities (Chapter 3). Each data point is the average density over a 10m or 40ft interval in wells recorded in metric and imperial units respectively. The seabed density value of 1.7gcm^{-3} was derived from an average grain density of 2.7gcm^{-3} and an average seabed porosity of 60% (Section 3.5 and Table 3.1). This was placed at an average seabed depth of 150m below sea-level. The maximum density was taken as 2.67gcm^{-3}, the Bouguer density, which is close to the grain density of most sedimentary rocks (Table 3.1). The fit of the density data to the chosen density/depth function (Figure 8.4) vindicates the use of depth alone to describe density variation.

In practice only the densities at the contoured top basement levels are used in the backstripping procedure as the program interpolates the gravity effect of the sediments between the contour levels. The relevant densities are shown on Table 8.1

Table 8.1 Sediment densities (ρ) used in gravity backstripping.

depth (km)	ρ (gcm^{-3})	depth (km)	ρ (gcm^{-3})	depth (km)	ρ (gcm^{-3})
0.5	2.100	4.0	2.610	7.0	2.645
1.0	2.340	4.5	2.620	7.5	2.650
1.5	2.480	5.0	2.625	8.0	2.655
2.0	2.550	5.5	2.630	8.5	2.660
2.5	2.580	6.0	2.635	9.0	2.665
3.0	2.590	6.5	2.640	9.5	2.670
3.5	2.600				

8.2.2.3 Computing the Gravity Attraction of the Sediments: Contour Integration Method

Following Genc (1988) the gravity effect of the sediments was evaluated using the contour integration method developed by Talwani and

Ewing (1960). An irregular body may be represented by a series of horizontal contours (Figure 8.5(a)). In this case a sedimentary basin is defined by contours to the top of the basement (Figure 8.1). The gravity anomaly per unit thickness (V(z)) at a reference point (P) associated with a given contour may be obtained by surface integration around that contour,

$$V(z) = G\Delta\rho(z)[\oint d\psi - \oint z/(r^2+z^2)^{1/2}d\psi] \qquad (1)$$

where G is the gravitational constant, $\Delta\rho(z)$ is the density contrast of the sediments in that contour and ψ, z and r are the cylindrical co-ordinates used to define the boundary of the contour

If the contour is approximated by an n-sided polygonal lamina (the digitized contour points) equation (1) can be rewritten with discrete values,

$$V(z) = G\Delta\rho(z)[\sum_{i=1}^{n}\{\psi_{i+1}-\psi_i-\arcsin[z\cos\theta_i/(p_i^2+z^2)^{1/2}] + \arcsin[z\cos\phi_i/(p_i^2+z^2)^{1/2}]\}] \qquad (2)$$

where the parameters of the equation are as shown in Figure 8.5(b)

The total gravity anomaly at P is the sum of the anomalies of all the laminae,

$$\Delta g = \oint V(z)dz \qquad (3)$$

Since we can only evaluate V(z) at each 500m contour interval equation (3) was approximated by cubic numerical interpolation.

The gravity effect of the sediments was calculated for reference points covering the same 2km x 2km grid as the Bouguer gravity data, some 25000 positions.

At shallow depth, however, the interpolation procedure required to evaluate equation (3) fails (Genc, 1988), hence between the sea-bed and the 500m contour level it was necessary to evaluate the gravity effect of the sediments using an alternative method, the sediment prism model.

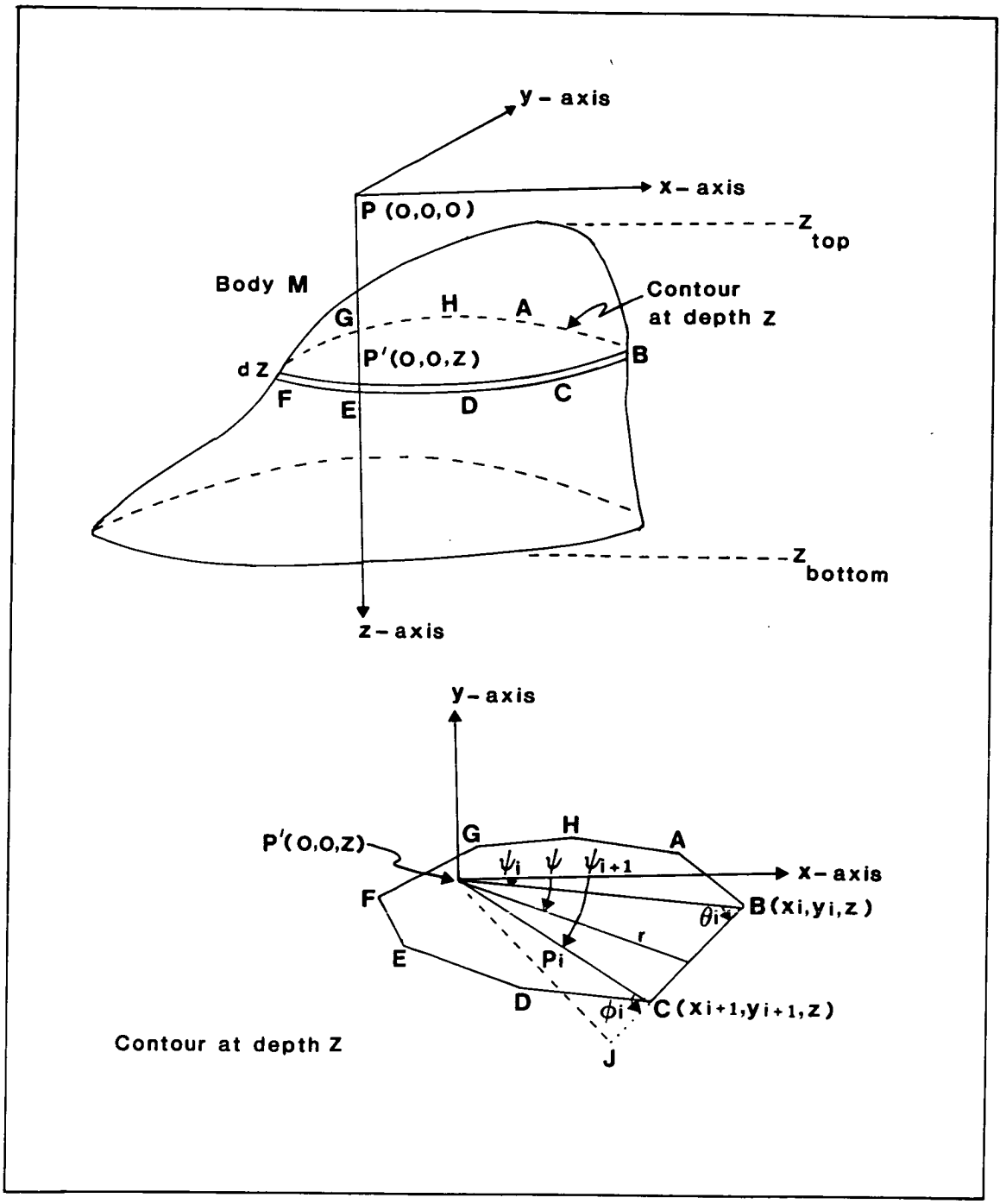

Figure 8.5 Geometrical elements involved in the computation of the gravity anomaly caused by a three-dimensional body (Talwani and Ewing, 1960).

8.2.2.4 Computing the Gravity Effect of the Sediments: Prism Model

Following Genc (1988) the top part of the sediments may be represented by a set of rectangular prisms. Individual prisms are defined by the 2km x 2km grid, the sea-bed and either the 500m contour level, or the base of the sediments where this is between sea-bed and the 500m contour level. The gravity effect of the top part of the sedimentary column can thus be calculated using the formula for the gravitational attraction of a prism,

$$\Delta g(x',y',0) = -G\Delta\rho[[[\{(x-x')\log(y-y')+R+(y-y')\log(x-x')+R) + z\tan^{-1}(zR/(x-x')(y-y'))]^{x_2}_{x_1}]^{y_2}_{y_1}]^{z_2}_{z_1} \quad (4)$$

where x' and y' are the field co-ordinates, x, y and z are to be replaced by x1, x2, y1, y2, z1 and z2 and $R = [(x-x')^2+(y-y')^2+z^2]^{1/2}$

The gravity effect of the sediments above 500m was added to the effect below 500m to give the total gravity effect of the sediments (Figures 8.6 and 8.7). Since the sediments have a low density compared to the basement their gravity effect must be added to the observed data in order to obtain the Bouguer gravity corrected for the effect of the sediments (Figures 8.8 and 8.9).

8.2.2.5 Computing the Gravity Effect of the Sediments: Salt

Late Triassic salt up to 1km thick, the Melville Halite unit, is present in the northern Melville Basin, typically at depths of 2-3km (Section 2.5.1). Salt has an anomaloulsy low density of around 2.15gcm^{-3} which is independent of burial depth. Considering Figure 8.4, in which salt was not included, and Table 8.1 there will be a density contrast of around 0.4gcm^{-3} between the salt and the density assumed for sediments at that depth. Hence an additional gravity backstripping procedure to remove the gravity effect of the salt from "average" density sediments was undertaken.

Maps of depth to the top and base of the salt were prepared by combining unpublished sources with seismic reflection data tied to the

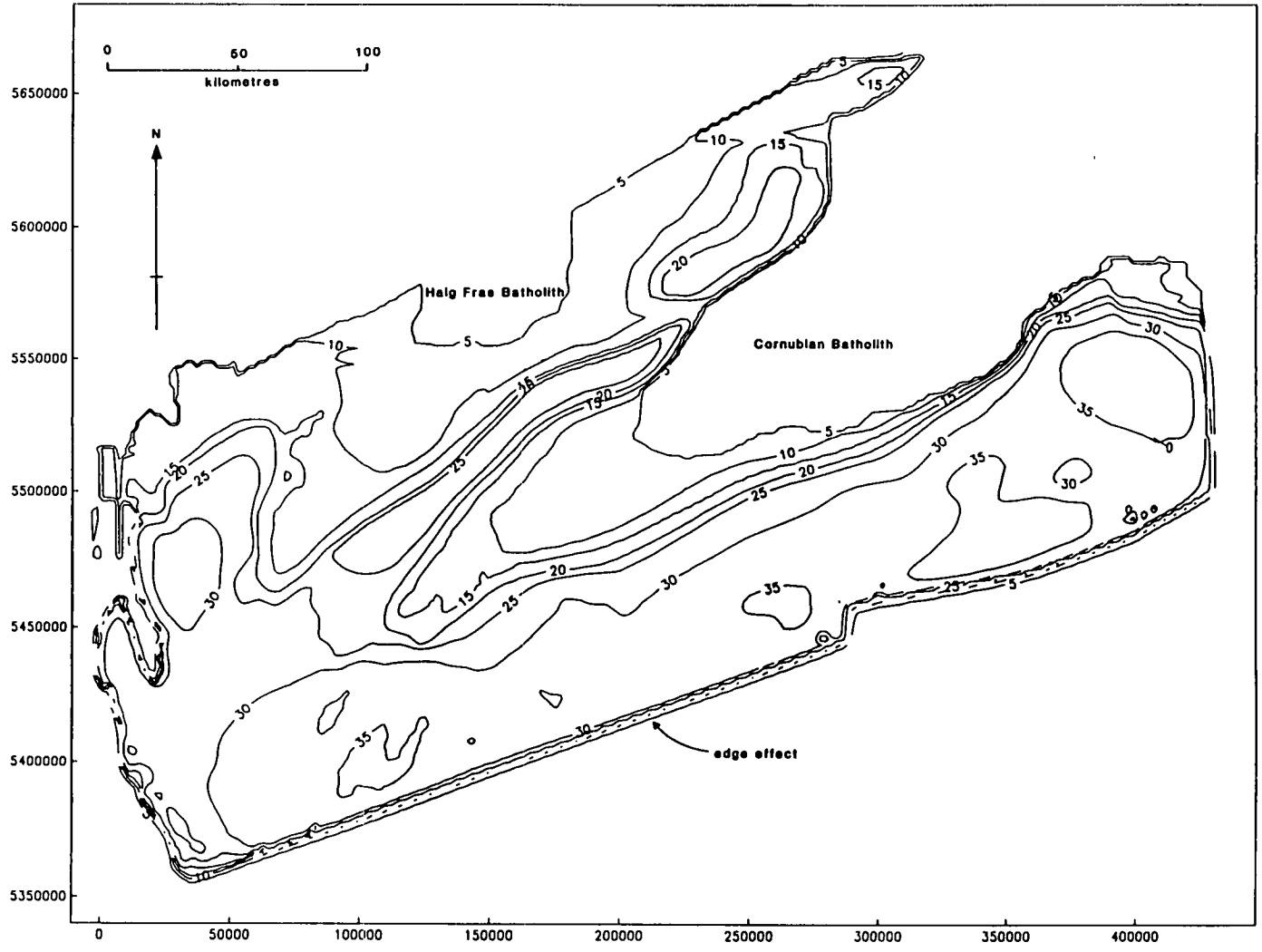

Figure 8.6 Gravity effect of the sediments with reference to the Bouguer density of 2.67gcm^{-3}(contour interval 5mgal).

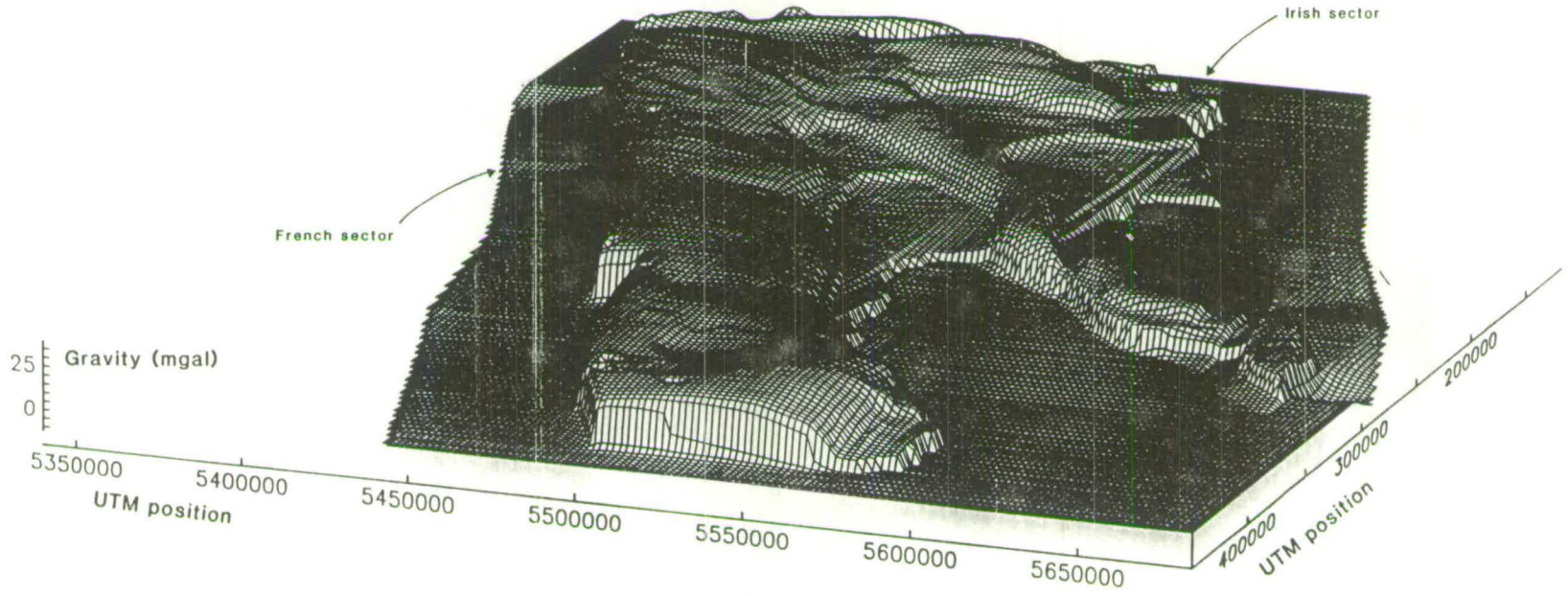

Figure 8.7 Mesh perspetive view of the gravity effect of the sediments (viewing as Figure 8.3).

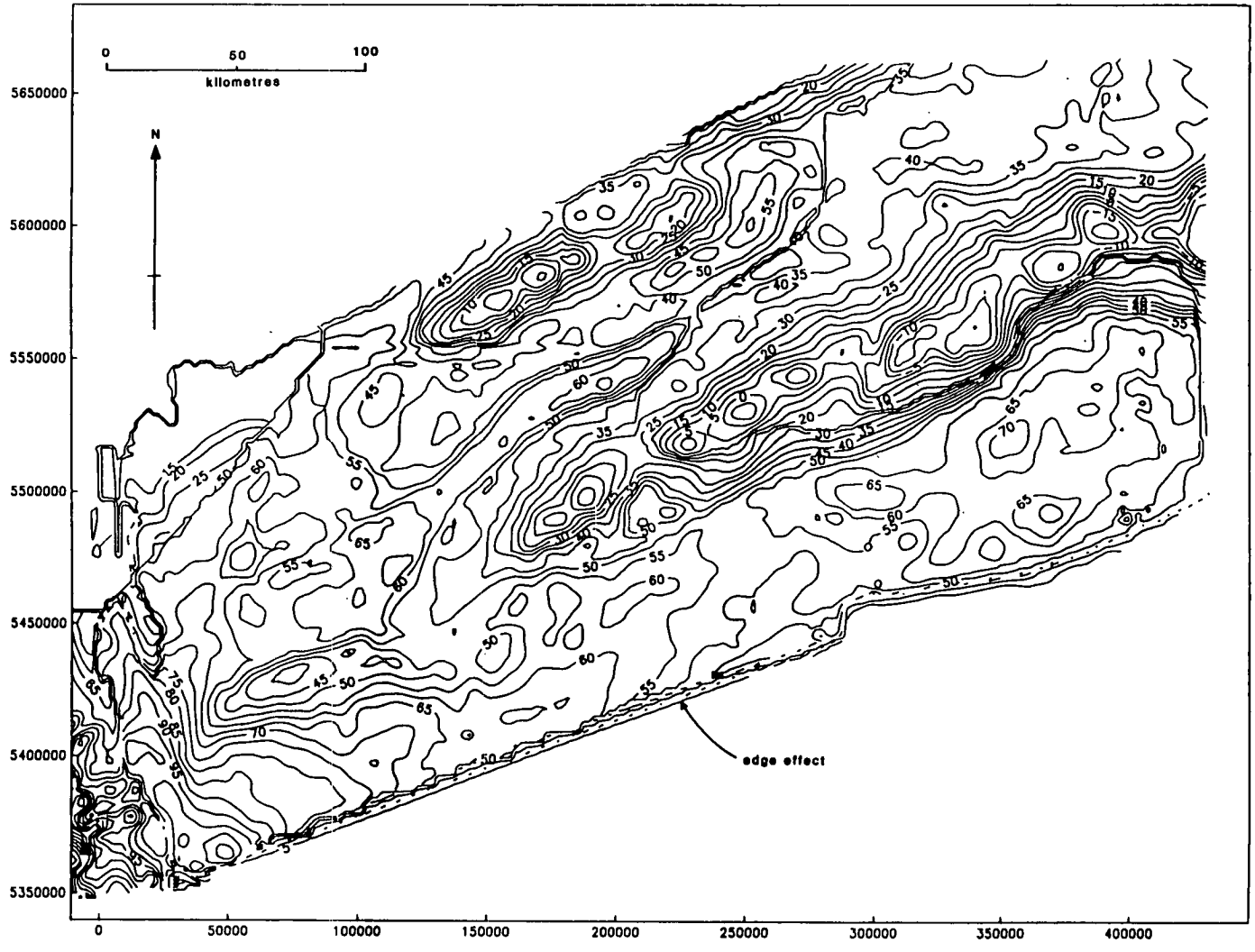

Figure 8.8 Sediment backstripped Bouguer gravity (contour interval 5mgal).

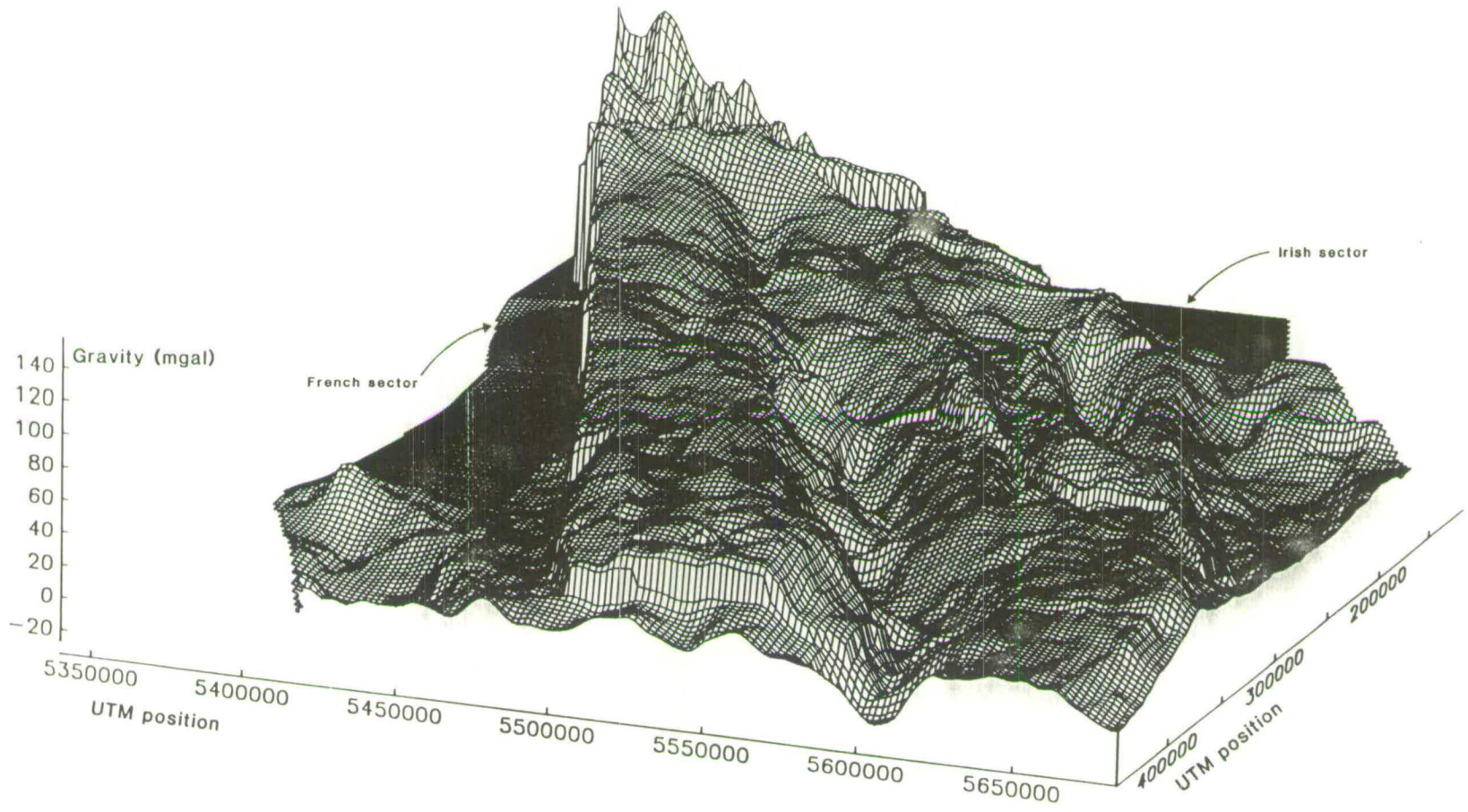

Figure 8.9 Mesh perspective view of the sediment backstripped Bouguer gravity (viewing as Figure 8.3).

five wells which penetrated the salt: 72/10-1, 73/1-1 (top salt only) 73/2-1, 73/5-1 and 73/6-1. The maps were depth converted using velocities derived from the above wells: 2.63kms^{-1} for the top salt, and 2.87kms^{-1} for the base salt (Figure 8.10).

The gravity effect of continuous salt of density 2.15gcm^{-3} between the digitzed base of the salt map and the 500m contour level was calculated using the contour integration method. This was repeated for the top salt horizon and the latter was subtracted from the former to give the gravity effect of the salt (Figure 8.11). The salt correction was added to the gravity effect of the "average" density sediments to give the gravity effect of the sedimentary basin corrected for the effect of the low density salt (Figures 8.12 and 8.13).

8.2.2.6 The Sediment Gravity Effect and Backstripped Gravity Maps

The gravity effect of the sedimentary fill of the Western Approaches Basin (Figure 8.6) increases rapidly across its flanks and remains relatively flat over its deeper parts. The 30mgal gravity effect contour closely corresponds to 2.5km sediment thickness. Hence, from 0 to 2.5km sediment thickness the gravity effect increases from 0 to 30mgal, whereas from 2.5km to the deepest parts of the basin it does not reach 40mgal. The minor contribution of the deeper sediments to the total gravity effect is due to their high density. At 9km depth (the base of the Plymouth Bay Basin) the sediments were assigned a density of 2.665gcm^{-3} (Table 8.1), a contrast of 0.005gcm^{-3} with the Bouguer density, hence integration of the gravity effect around this contour level adds a negligible amount to the total gravity effect of the basin.

The gravity effect of the sedimentary basin artificially becomes zero at the British/French median line (Figure 8.6). This is because the top basement map is limited to the British sector of the Western Approaches Trough (Figure 8.1) and basement was assumed to outcrop at seabed in the French sector. The gravity effect in the southern part of the British sector is also artificially reduced because there is no contribution from south of the median line (the "edge effect"). From Figure 8.6 it is apparent that the edge effect only extends approximately 10km into the British sector of the basin. This effect

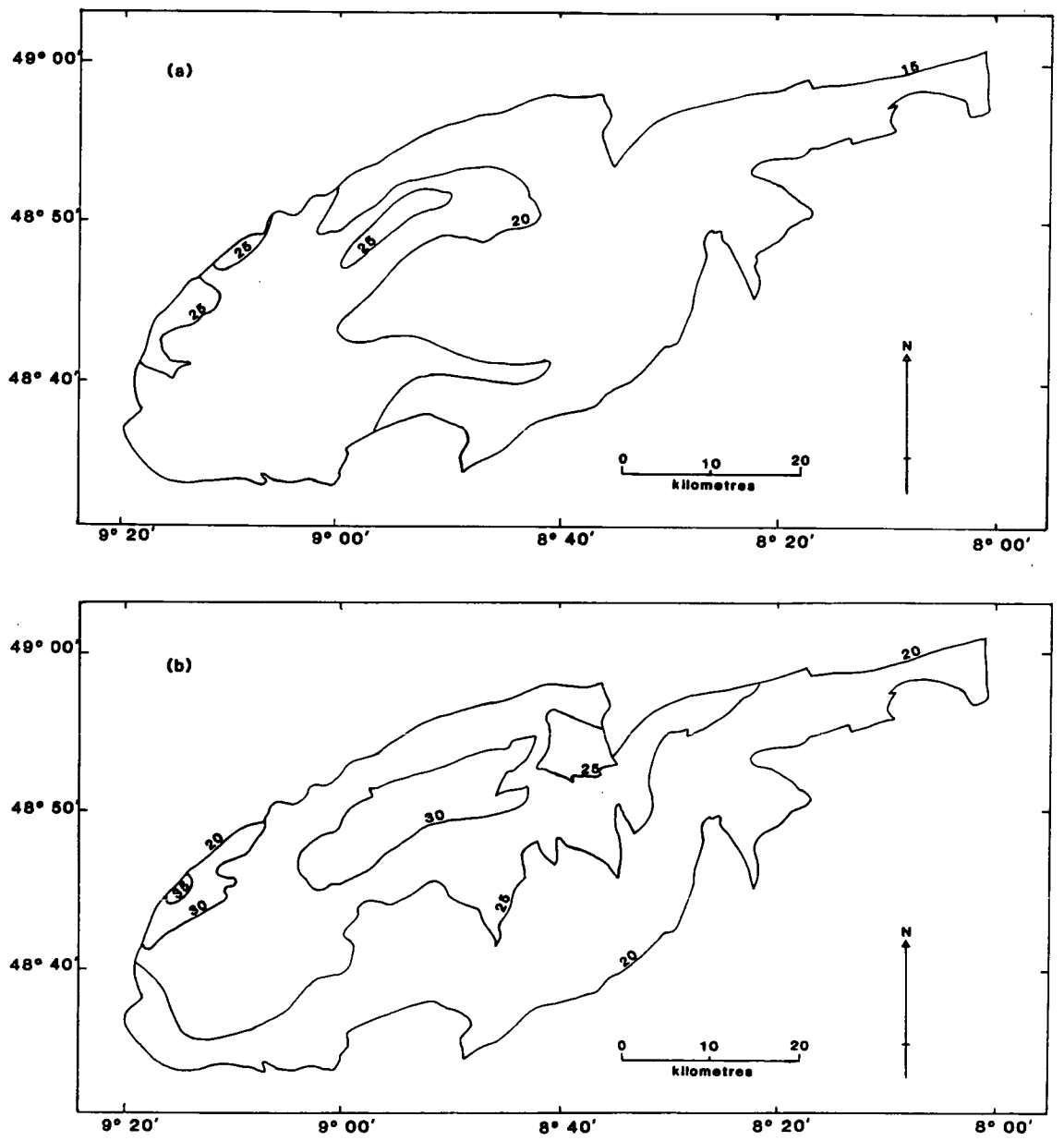

Figure 8.10 Depth to the (a) top and (b) base of the Melville Halite unit.

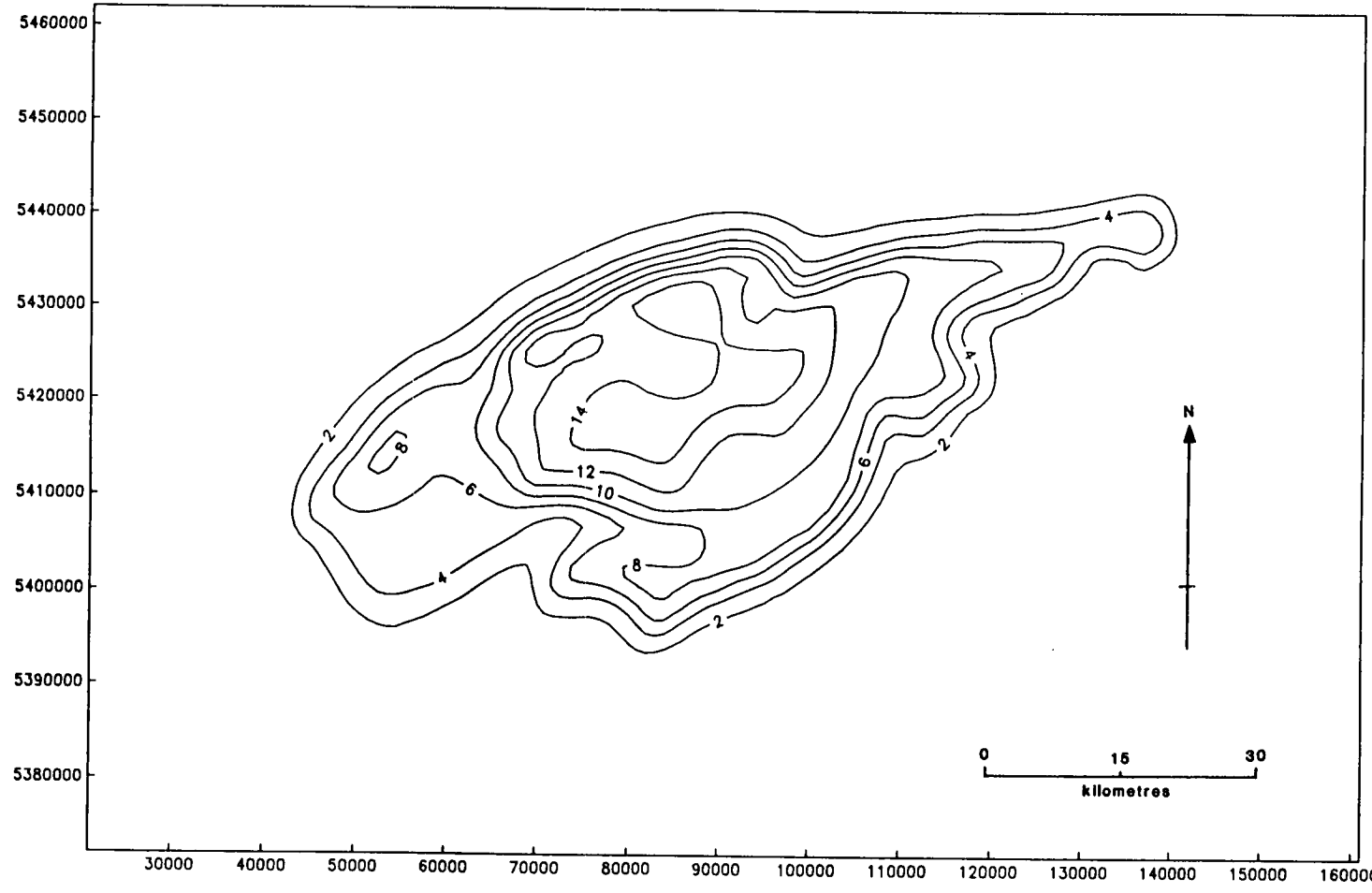

Figure 8.11 Gravity effect of the Melville Halite unit with reference to "normal density sediments" (contour interval 2mgal).

could be reduced by extrapolating the basement contours into the French sector. However, this would be an artificial procedure and the edge of the sedimentary basin was taken as the limit of the dataset in order that the magnitude of the edge effect could be realistically assessed.

Even after correction for the effect of the salt there is still a pronounced gravity low in the northern Melville Basin (Figures 8.12 and 8.13). The salt density of $2.15gcm^{-3}$ is not likely to be a major source of error. Hence if the gravity effect of the salt has been underestimated, the maps of depth to the top and base of the salt must underestimate its volume. The maximum magnitude of the salt correction is 15mgal, and the low present after the salt correction is still 15-20mgal. It seems unlikely that the maps to the top and base of the salt, calibrated by four wells which penetrate the entire salt sequence, could be responsible for such a large error. After correction for the effect of the salt the centre of the low is displaced somewhat to the north and closer to the trend of the Cornubian Batholith. It is hence proposed that the batholith actually extends to the north of the Melville Basin and is responsible for this residual gravity low.

The backstripped data picks out the granite batholiths even more clearly than the original Bouguer gravity data. The Cornubian and Haig Fras Batholiths either outcrop at seabed or have only a thin sediment cover. Hence, on the backstripped gravity data, their associated lows are amplified relative to the surrounding areas.

The backstripped gravity high in the southern Melville Basin (UTM eastings 50000-100000, northings 5350000-5400000) corresponds very closely to a prominent aeromagnetic anomaly (Figure 2.8, anomaly A). This anomaly was ascribed to the presence of volcanics at the base of the sedimentary column (but within the basin as defined by the top basement map). These volcanics will have a higher density than that predicted by Figure 8.4, hence they will have been over-corrected by the backstripping procedure. Although the presence of volcanics was postulated to be responsible for several other aeromagnetic anomalies (Section 2.4.2 and Figure 2.8) none of these are as volumetrically signifcant as the accumulation in the southern Melville Basin.

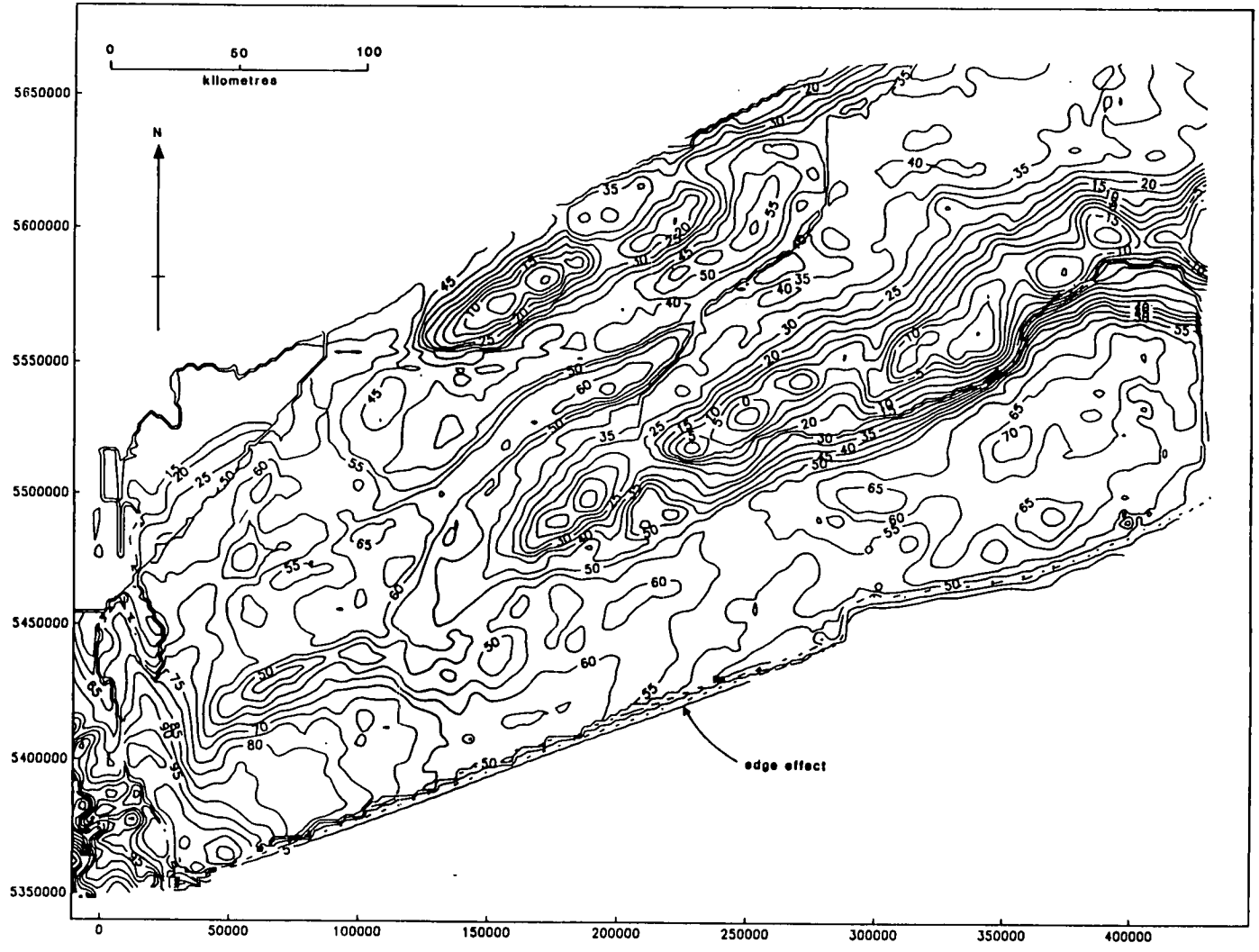

Figure 8.12 Sediment backstripped Bouguer gravity corrected for the effect of the Melville Halite unit (contour interval 5mgal).

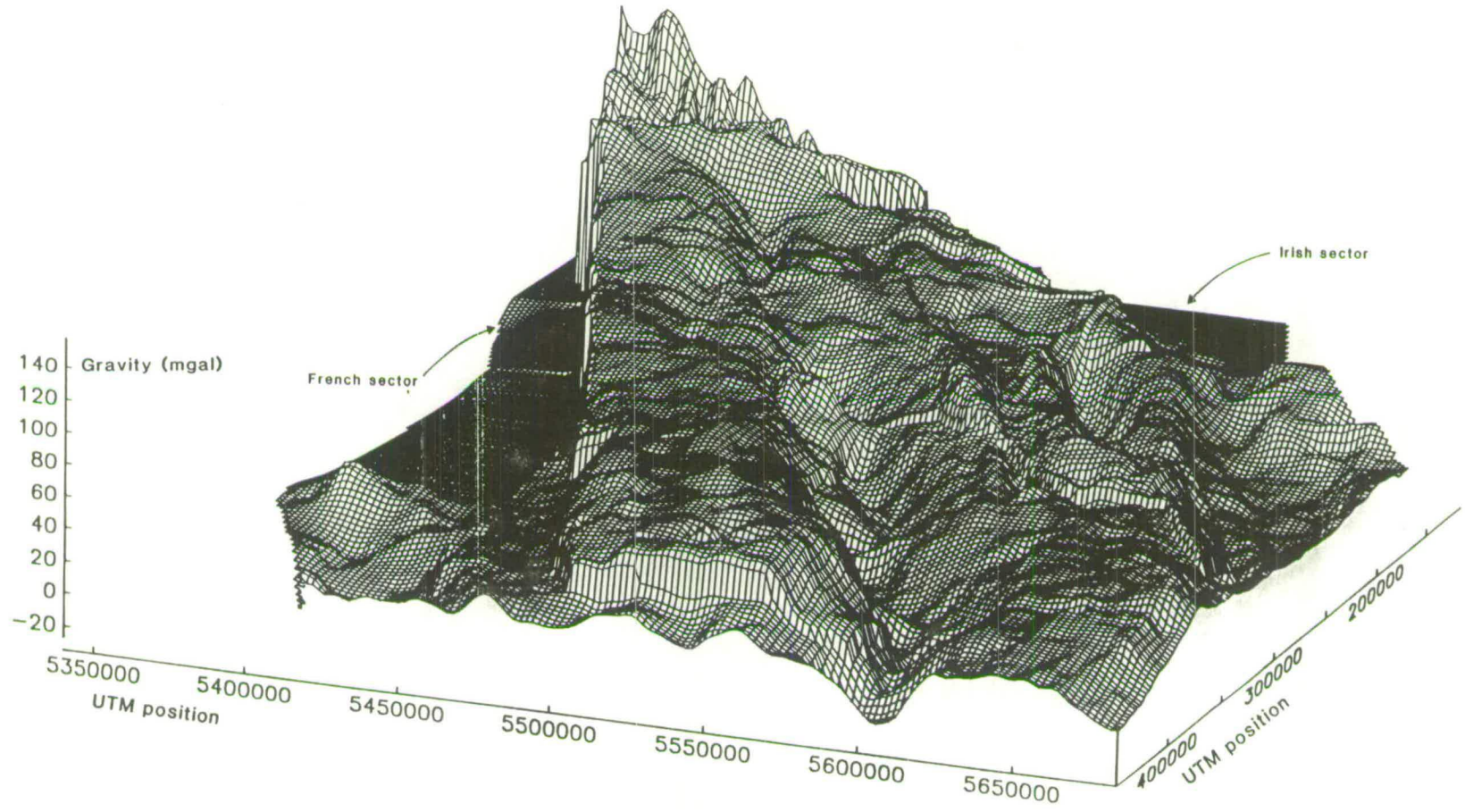

Figure 8.13 Mesh perspective view of the sediment backstripped Bouguer gravity corrected for the effect of the Melville Halite unit (viewing as Figure 8.3).

The Madura body (Edwards et al, 1983) compr ises anomalously high density material within the basement and is hence still apparent in the backstripped gravity map.

Any rise in the level of the Moho and consequent mantle upwelling under the Western Approaches Basin would result in a regional gravity increase in the backstripped gravity from the basin flanks to its centre. It is unfortunate that the effects of the Cornubian Batholith dominate at the basin margin, however, it is apparent that there is only a slight increase, of some 10-20mgal, in the backstripped gravity from the basin flanks to its centre. This is in marked contrast to the results of two-dimensional gravity modelling over the Viking Graben (Donato and Tully, 1981; Zervos, 1987; Holliger and Klemperer, in press) which have demonstrated the existence a positive backstripped gravity anomaly of some 100mgal in that area.

8.2.3 Modelling Moho Depth from the Backstripped Gravity Data

In order to investigate Moho topography in more detail a two-dimensional profile from the backstripped Bouguer gravity map was inversely modelled (Figure 8.14). A profile along the line of SWAT 6 and the north-western end of SWAT 7 was selected so that the results of the gravity modelling could be compared with the estimates of Moho depth from the deep seismic reflection data (Section 8.3). On this profile the entire sequence from sea-level to the top of the basement was assigned the backstripped density of 2.67gcm^{-3}. The density of the basement/lower crust was taken as 2.8gcm^{-3} and the mantle as 3.33gcm^{-3}. These values are close to those used by Donato and Tully (1981), Zervos (1987) and Holliger and Klemperer (in press) (2.75, 2.85 and 2.75gcm^{-3} for the lower crust and 3.25, 3.35 and 3.25gcm^{-3} for the mantle respectively). Since the effect of the Cornubian Batholith was not removed from the backstripped gravity data it must also be included in the inverse model. The granite batholith was assigned a density of 2.6gcm^{-3}. Modelling was carried out on the interactive 2½D (infinite strike length assumed, hence effectively 2-D) gravity and magnetic modelling program available on the BGS Murchison House Vax Computer (Busby, 1987).

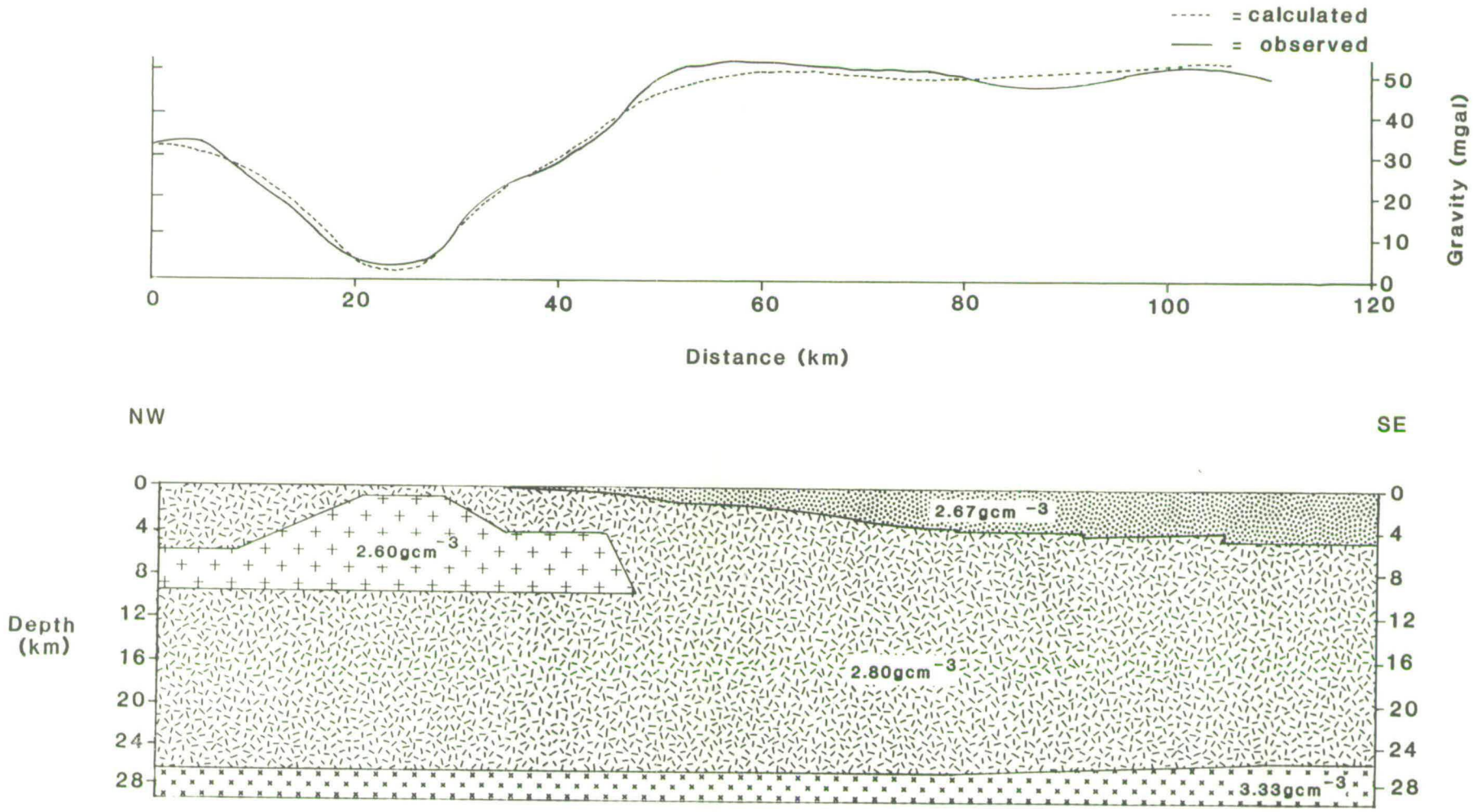

Figure 8.14 2-D model of backstripped gravity along line of SWAT 6 and north-west end SWAT 7. Calculated gravity values suggest maximum rise of 1km in Moho from the flanks to the centre of the St. Mary's Basin.

Although the backstripped gravity profile gives an indication of relative crustal thinning across the basin an external estimate of Moho depth is required at some point because of the non-uniqueness of inverse modelling. Bott et al's (1970) crustal refraction experiment along the axis of the Cornubian Batholith indicated a crustal thickness of between 23 and 30km, the best estimate being 27km. This value was used to control Moho depth at the northern end of SWAT 6. From Figure 8.14 it can be seen that the backstripped gravity data supports a maximum rise of 1km in the depth to the Moho from the flanks to the centre of the St. Mary's Basin. The modelled shape of the Cornubian Batholith is close to that suggested by Edwards et al (1983) from a gravity profile some 50km further west.

The two-dimensional gravity model of Figure 8.14 may be somewhat simplistic as it assumes a constant density of $2.8gcm^{-3}$ from the top of the basement to the base of the crust (cf. Hall, 1986; Meissner, 1986). However, the refraction data of Ginzburg et al (1985) suggest a P-wave velocity of $6.5kms^{-1}$ at the base of the crust underlying the outer shelf of the Western Approaches Trough. Following the relationship of Ludwig et al (1970) this is equivalent to a density of $2.8gcm^{-3}$. Combined with Rollin's (1988) mean density of $2.78gcm^{-3}$ for Devonian slates below 150m depth in mineral exploration boreholes onshore south-west England this supports a fairly constant basement/lower crustal density.

8.3 MODELLING MOHO DEPTH FROM THE DEEP SEISMIC DATA

Moho depths from refraction and wide angle reflection data on the British continental shelf and northern France have shown good agreement with the depth to the base of the reflective lower crust as imaged on normally incident deep seismic reflection data (Barton et al, 1984; Bois et al, 1986). Similarly, the base of the reflective lower crust under the Cornubian Batholith is, at 9s TWT (Figure 2.3), coincident with Bott et al's (1970) estimate of crustal thickness from refraction data taking an average crustal velocity of $6kms^{-1}$. Hence the

base of the reflective lower crust, which is well imaged along most of SWAT 6 and 7, was taken to represent the Moho.

The reflection Moho was digitized at 2km intervals. In TWT it is fairly flat at 10-10.5s under the St. Mary's Basin. It rises slightly to 9s under the Cornubian Batholith and the eastern Brittany Basin. In order to investigate the "real earth" shape of the Moho it is necessary to remove the velocity push down effect of the basinal sediments. Consequently, it was also necessary to pick and digitize the base of the sedimentary sequence (at the same 2km interval as the Moho). In the British sector of the Western Approaches Trough this horizon can be tied to commercial lines. In the French sector, where no tie lines were available, the picking of this horizon is less reliable, although the comments of C. Bois (personal communication, 1988) aided interpretation. As both the Moho and the base of sedimentary sequence are flat, or gently dipping in TWT errors due to non-normally incident reflections on the unmigrated data were ignored.

In order to remove the velocity push down effect of the basinal sediments the picked travel times to the Moho must be depth converted. The sediments were assigned a linear velocity/depth function derived from well data, with particular emphasis on wells which penetrated the top of the basement,

$$v_{s\langle average\rangle} \simeq 2.297+0.431TWT_s \qquad (5)$$

hence,

$$d_s \simeq 1.148TWT_s+0.216TWT_s^2 \qquad (6)$$

where the subscript 's' denotes a parameter measured to the base of the sedimentary sequence, $v_{s\langle average\rangle}$ is average velocity in kms^{-1}, TWT_s is the two-way-time in s and d_s is depth in km

Although the above linear relationship was found to fit the observed data better than an exponential function it should not be extrapolated to depth where unreasonably high velocities would be predicted. The

basement/lower crust was assigned a constant velocity of 6kms^{-1}, hence the depth to the Moho is given by,

$$d_m \simeq (1.148TWT_s+0.216TWT_s^2)+3(TWT_m-TWT_s) \quad (7)$$

where the subscript 'm' denotes a parameter measured to the Moho and symbols are as equation (6)

Figure 8.15(a) shows the depth to the base of the sedimentary sequence and to the underlying Moho along SWAT 6 and 7 after depth conversion. There is no rise in the Moho under the St. Mary's Basin but a small rise, of 1-2km, occurs under the eastern Brittany Basin. The Moho depths derived from the deep seismic reflection data (Figure 8.15(a)) show good agreement (±1.5km) with those derived from the gravity modelling (Figure 8.14).

8.4 WHOLE CRUSTAL THINNING, β-FACTORS AND SUBSIDENCE

The results of the two-dimensional modelling of Moho depth can be readily converted to magnitudes of whole crustal thinning across the Western Approaches Trough. These are expressed as β-factors where,

$$\beta_{whole\ crustal} = \text{original crustal thickness/ present crustal thickness} \quad (8)$$

Figure 8.15(b) shows whole crustal β-factors calculated for each of the digitized basement/Moho points taking the original crustal thickness as 27km (Moho depth at the basin flanks). Crustal thinning may be due to extension and/or sub- and/or supra-crustal erosion, hence whole crustal β-factors are not necessarily equivalent to extension values.

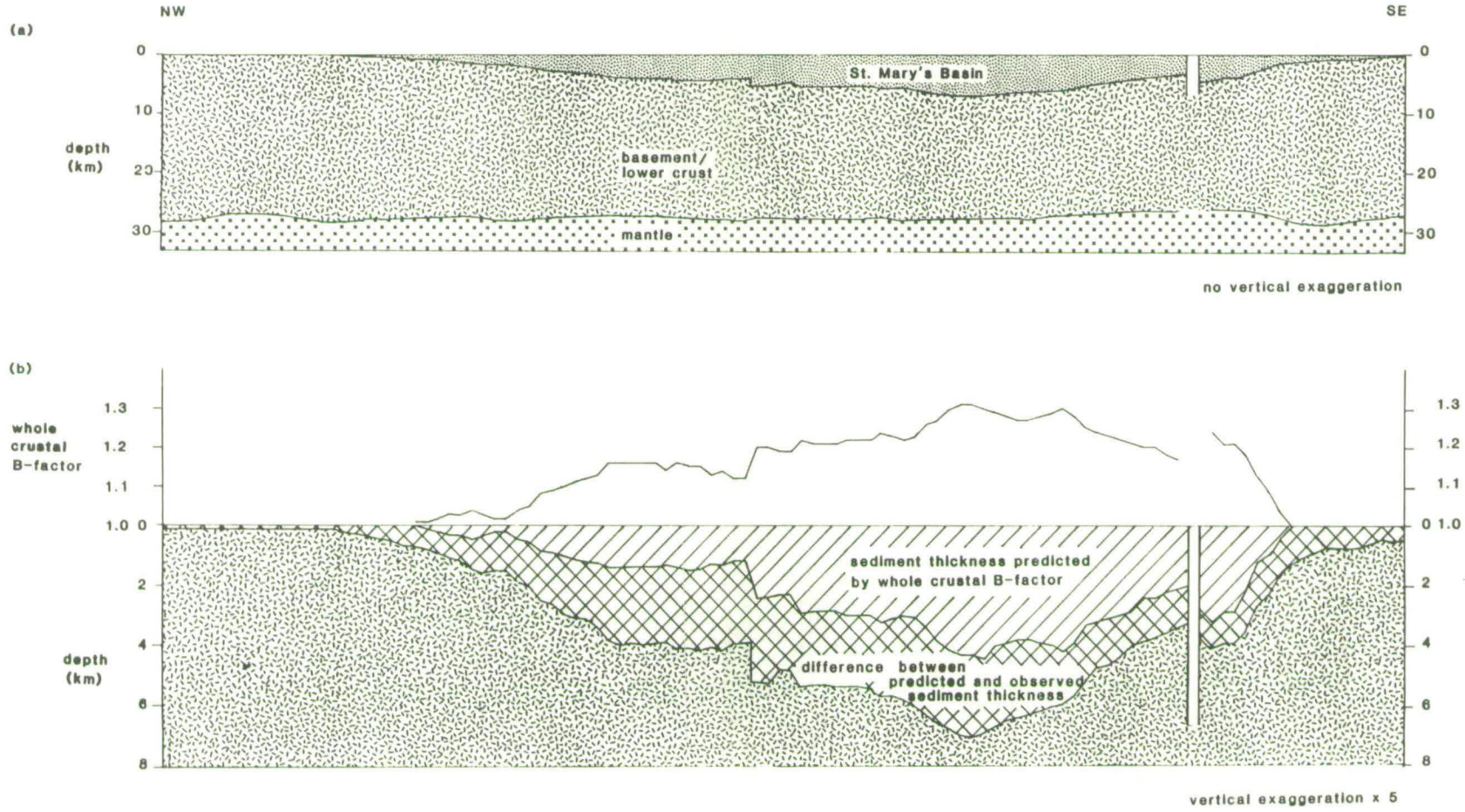

Figure 8.15 Modelling of SWAT 6 and 7 deep seismic reflection profiles. (a) Depth to the top of the basement and the Moho. (b) Whole crustal B-factors and predicted depth to top basement associated with that whole crustal B-factor. Observed depth to top basement also shown.

8.4.1 Reliability of Whole Crustal and Cover β-factors

Previous studies of sedimentary basins have concentrated on deriving and modelling the effects of β-factors based on estimates of the extension of the basinal sediments (e.g. LePichon and Sibuet, 1981; Chenet et al, 1982; Chadwick, 1985a; Hegarty et al, 1988; Badley et al, 1988). Whole crustal β-factors are preferred in this study because of the difficulty of estimating cover extension due to deformation at a scale not resolved by the seismic data, the "blanketting" seismic effect of salt (Shorey and Sclater, in press), extension out of the plane of section, pure shear of the sediments (bed thinning), non-vertical collapse of the hanging wall (White et al, 1986) and low angle faulting (Shorey and Sclater, in press).

Although "whole crustal" β-factors may be more reliable than those based on extension of the cover, if they are to be meaningfully compared with observed sediment thicknesses the Moho must not re-equilibrate after stretching. This assumption is supported by the preservation of Moho topography across the adjacent continent-ocean boundary (Ginzburg et al, 1985) and under sedimentary basins of similar age such as the Viking Graben (Donato and Tully, 1981; Zervos, 1987; Holliger and Klemperer, in press). Indeed it appears that while the crustal roots of mountain belts decay with time, ante-roots under sedimentary basins are "locked in" due to the higher lithospheric viscosities found at the relatively shallow level of basin ante-roots (N.J. Kusznir, conference communication, 1987).

8.4.2 Whole Crustal β-factors and Observed Subsidence in the Western Approaches Trough

From simple isostatic balance considerations whole crustal β-factors can, assuming local Airy isostasy, be readily converted to predicted total sediment thicknesses (S_∞) deposited in response to that crustal thinning (e.g. Hellinger and Sclater, 1983),

$$S_\infty \simeq \{t_c(\rho_m-\rho_c)(1-\alpha T_m t_c/2a)(1-1/\beta))/[\rho_m(1-\alpha T_m)-\rho_s] \qquad (9)$$

where t_c is the crustal thickness on the basin flanks, ρ_m, ρ_c and ρ_s are mantle, crustal and sediment densities respectively, α is the thermal expansion co-effecient of the lithosphere and T_m is the temperature at the base of the lithosphere

Taking the initial crustal thickness as 27km and assigning the other lithospheric physical properties as Chadwick (1985a) equation (9) may be simplified,

$$S_s \simeq 14.24(1-1/\beta)/(3.18-\rho_s) \qquad (10)$$

Hence in order to predict the thickness of a sedimentary sequence deposited in response to a given crustal thinning the average density of the sediment column must be known. Equation (10) is, in fact, sensitive to density; considering a β-factor of 1.3 total sediment thickness is 3.34km for a sediment density of $2.2gcm^{-3}$ and 4.19km for a sediment density of $2.4gcm^{-3}$.

The average density of the sedimentary sequence in the Western Approaches Basin was calculated to 1, 2, 3, 4, 5 and 6km depth from Figure 8.4 (Table 8.2). The thickness of the sedimentary sequence deposited in response to a given β-factor was then iteratively calculated using progressively increasing densities from Table 8.2. The predicted sediment thickness was accepted when it lay within 0.5km of the base of the interval of the assigned density (Table 8.2). For example, consider the total sediment thickness predicted by a β-factor of 1.25. At $1.94gcm^{-3}$ (the average density of 1km of sediments) this is 2.29km, hence $1.94gcm^{-3}$ is an unreasonably low density. At a density of $2.20gcm^{-3}$ it is 2.89km, still too low. The sediment thickness of 3.33km at a density of $2.33gcm^{-3}$ (the average sediment density of 3km of sediments) would be accepted.

Figure 8.15(b) shows the sediment thickness predicted by the observed whole crustal thinning at each of the digitized points along the profile derived as outlined above. It is clear from Figure 8.15(b) that the magnitude of whole crustal thinning does not satisfactorily account for the observed thickness of the sedimentary sequence in the St. Mary's Basin.

Table 8.2 Average density (ρ) of the sedimentary sequence over given depth intervals derived from Figure 8.4.

depth (km)	ρ (gcm^{-3})	depth (km)	ρ (gcm^{-3})	depth (km)	ρ (gcm^{-3})
0-1	1.94	0-3	2.33	0-5	2.44
0-2	2.20	0-4	2.40	0-6	2.47

The observed facies and distribution of the Permian sediments (Section 5.3.3) suggests they were deposited in response to denudation of the surrounding Variscan massifs rather than *in situ* crustal thinning. Therefore it is proposed that the discrepancy between crustal thinning and the thickness of the sedimentary sequence in the Western Approaches Trough is due to this denudational phase of sedimentation.

The discrepancy between predicted and observed sediment thicknesses is somewhat smaller in the extreme south of the St. Mary's Basin and the eastern Brittany Basin than in the northern and central St. Mary's Basin (Figure 8.15(b)). The thinness of the Permian sediments in the former area (Section 5.3.3) supports the hypothesis that the Permian sequence is responsible for the discrepancy. Furthermore, Bouguer gravity values are approximately 30mgal higher in the Brittany Basin than in the St. Mary's Basin (Lalaut et al, 1981). Hence it is tentatively proposed that backstripped gravity over the Brittany Basin might support a rise in the level of the underlying Moho with respect to the St. Mary's Basin.

The deep reflection seismic data provide only a two-dimensional picture of crustal thickness along a single profile. However, the backstripped gravity data of Figures 8.12 and 8.13 demonstrate that the Moho does not rise significantly away from the modelled profile.

Although not of direct relevance to this study it is noted that under the Permian and later depocentre of the Viking Graben, which lay north of the Variscan limit of deformation, the Moho rises by some 10km (Donato and Tully, 1981; Zervos, 1987; Holliger and Klemperer, in

press). It is tentatively proposed that whole crustal β-factors and total sediment thicknesses in the Viking Graben may be in reasonable agreement.

8.4.3 Whole Crustal β-factors and Subsidence Modelling

In any basin which has undergone a protracted tectonic history (almost 300Ma in the case of the Western Approaches Trough) it may reasonably be assumed that the present observed subsidence is close to the total subsidence. Present sediment thickness may thus be directly compared to crustal thinning as discussed above. Although the author did not himself follow this approach, it is retrospectively suggested that whole crustal studies provide a useful starting point in basin subsidence analysis. If crustal thinning satisfactorily explains the observed sediment thickness geological analysis should reveal whether extension or crustal erosion was the dominant process. If it was the former, complications introduced by rifting events of finite duration, heterogeneous extension, re-rifting events etc. may then be addressed with respect to individual rift phases (Figure 5.4). It should also be possible to distinguish broadly pure shear processes from those of crustal simple shear. In the latter case the total sediment volume predicted by whole-crustal β-factors will be in accord with the observed sediment volume. However, the location of the depocentre will be laterally displaced from that predicted by the whole crustal β-factors. The flexural strength of the lithosphere may also be investigated by the analysis of whole crustal β-factors in a basin demonstrably formed by crustal thinning (e.g. the Viking Graben?). The deposition of a basin margin sequence which is associated with no crustal thinning may be reasonably ascribed to flexure.

If crustal thinning can not explain the observed sediment thickness then denudation-driven subsidence or other mechanisms such as Sloss and Speed's (1974) asthenospheric creep or deep crustal metamorphism (Falvey and Middleton, 1981) and igneous activity (Beloussov, 1960; Royden et al, 1980) may be invoked. The effect of the latter two processes on the position of the Moho as defined by seismic and gravity data would, however, require careful consideration.

CHAPTER 9

THE GEOLOGICAL AND TECTONIC HISTORY OF THE WESTERN APPROACHES TROUGH: A SUMMARY

9.1 INTRODUCTION

This chapter presents a brief tectonic history of the Western Approaches Trough with reference to "typical" wells in the northern and southern Melville Basins and the Brittany Basin (Figures 9.1, 9.2 and 9.3). Its aim is to summarize the geological evolution of the Western Approaches Trough in terms of the controlling geodynamic processes decribed more fully in the preceding chapters.

9.2 SUMMARY

The structural style of the pre-Permian basement of the Western Approaches Trough was developed during the Variscan orogeny. Northward movement of Gondwanaland relative to northern Europe drove the northward emplacement of a series of nappes along south-dipping, ENE-WSW striking thrust faults. Movement on the thrust faults was linked by complementary movement on a series of steep NNW-SSE trending transfer faults. Together these structures impart a pronounced orthogonal structural grain to the resultant heterogeneous, allochthonous basement of the area.

The granitic Cornubian and Haig Fras Batholiths were emplaced at the end of the Variscan orogeny. They form the heart of the Cornubian Massif which remained as a high throughout the evolution of the adjacent Western Approaches Trough due to their low density and resistance to extensional deformation and its resultant subsidence. Extrusive igneous activity accompanied the intrusion of the batholiths with extensive outpourings of broadly andesitic volcanics in the southern Melville Basin.

Together the Melville Nappe and the Cornubian Massif formed an end Variscan to early Permian high covering the northern Melville Basin and

the adjacent massif. Coarse detritus shed from this high, and from the volcanics in the southern Melville Basin, fed proximal alluvial fans (Figure 9.2). The fans coalesced with time and passed upwards into the finer grained Aylesbeare Group, filling the intermontane depression in the southern Melville Basin and gradually onlapping the high to the north. Subsidence rates slowed with the progressive peneplanation of the Variscan massifs and there may have been a period of non-deposition prior to the onset of Triassic subsidence (Figure 9.2). Smaller scale fining up units within the broad fining up sequence of the basal Permian conglomerates and the overlying Aylesbeare Group represent individual fan and channel deposits.

The Melville Nappe remained as a high throughout the Permian and much of the northern Melville Basin did not receive any sediments until the Triassic subsidence phase (Figure 9.1). Permian sediments are likewise thin or absent in the Brittany and South-West Channel Basins (Figure 9.3) and these areas are also inferred to have formed end Variscan to early Permian highs.

The gravitational loading effect of the sediments amplified the initial magnitude of the topographic low in the southern Melville Basin by two to three times, accommodating the accumulation of up to 4km of Permian sediments. Extensional faulting did not strongly control the distribution of Permian sediments and extension-related subsidence was subsidiary to that driven by denudation. Subsidence driven by Permian denudation did not cause crustal thinning in the basinal areas. This accounts for the flatness of the Moho under the thick sedimentary sequence of the Western Approaches Trough.

In early-earliest late Triassic times (the age of the base of the Sherwood Sandstone Group) tensional stresses between Europe, Africa and North America (Masson and Miles, 1986) led to the extensional reactivation of the former Variscan thrusts and transfer faults in the Melville Basin and red-bed deposition throughout the Western Approaches Basin (Figures 9.1 and 9.2). The Triassic depocentre switched from the southern to the northern Melville Basin in response to the Triassic reactivation of the Melville Thrust and wrench zone. In the St. Mary's Basin there is no evidence of extensional reactivation of individual Variscan structures and the similarity of Variscan and Triassic trends

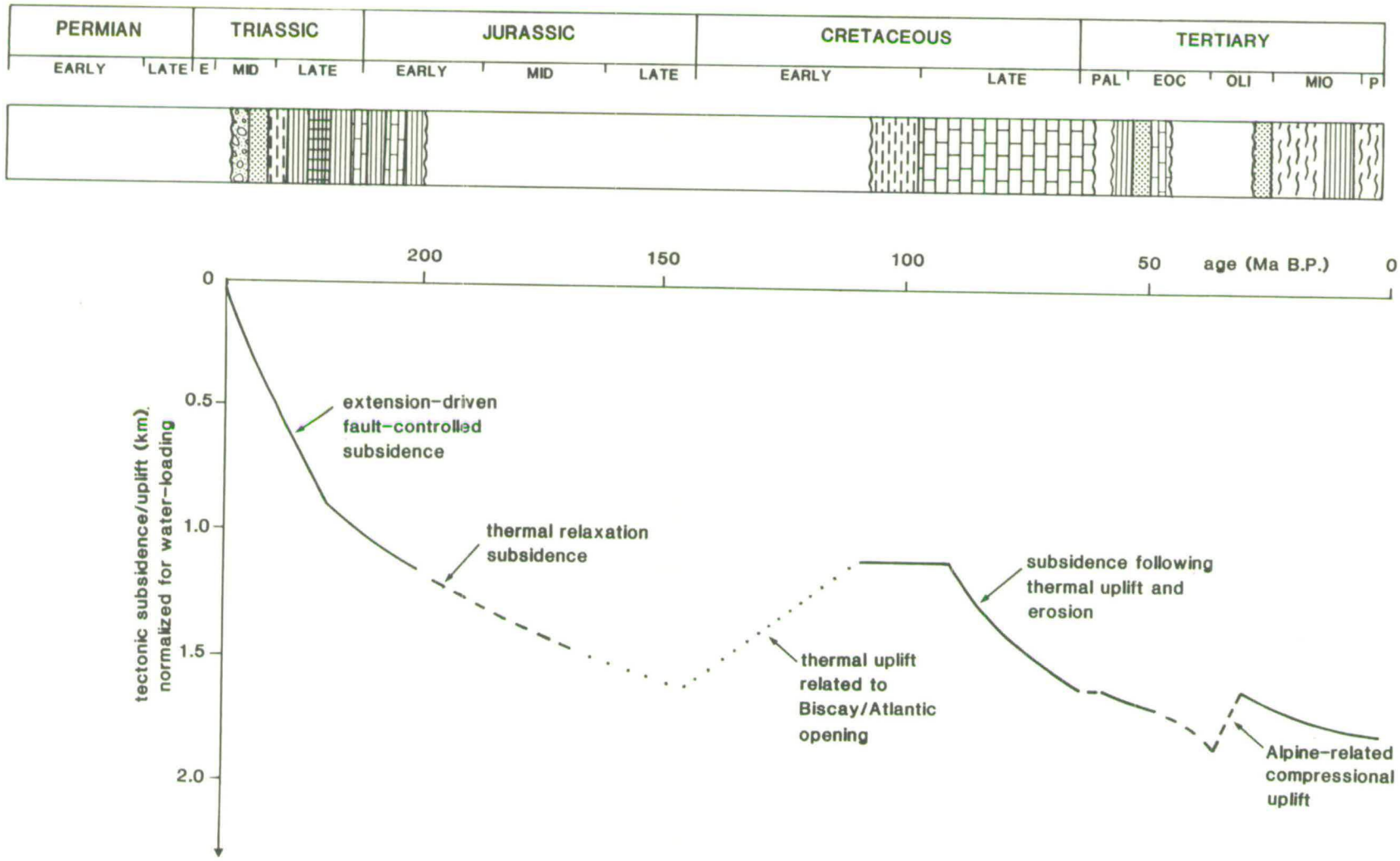

Figure 9.1 "Typical" subsidence history for the northern Melville Basin.

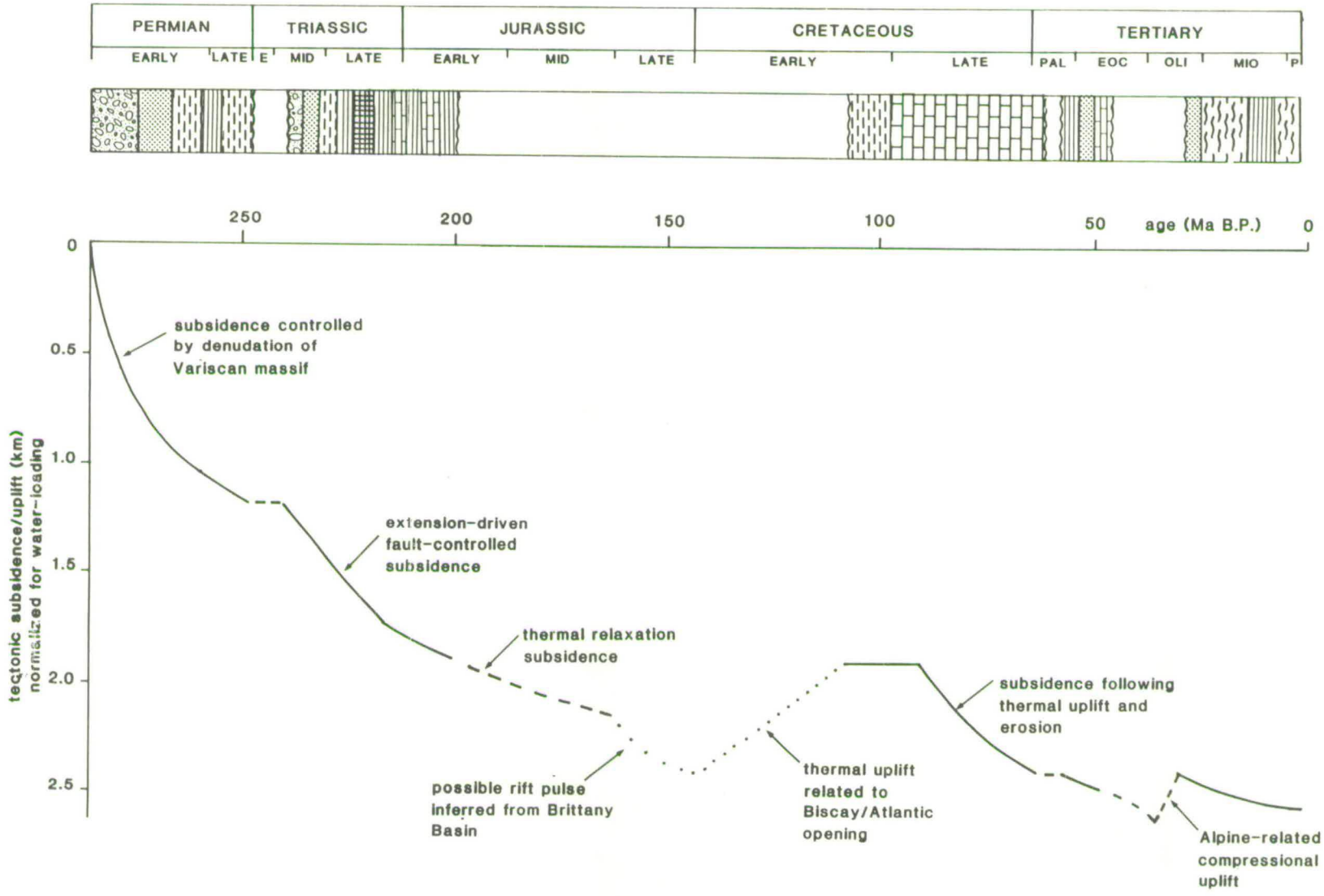

Figure 9.2 "Typical" subsidence history for the southern Melville Basin

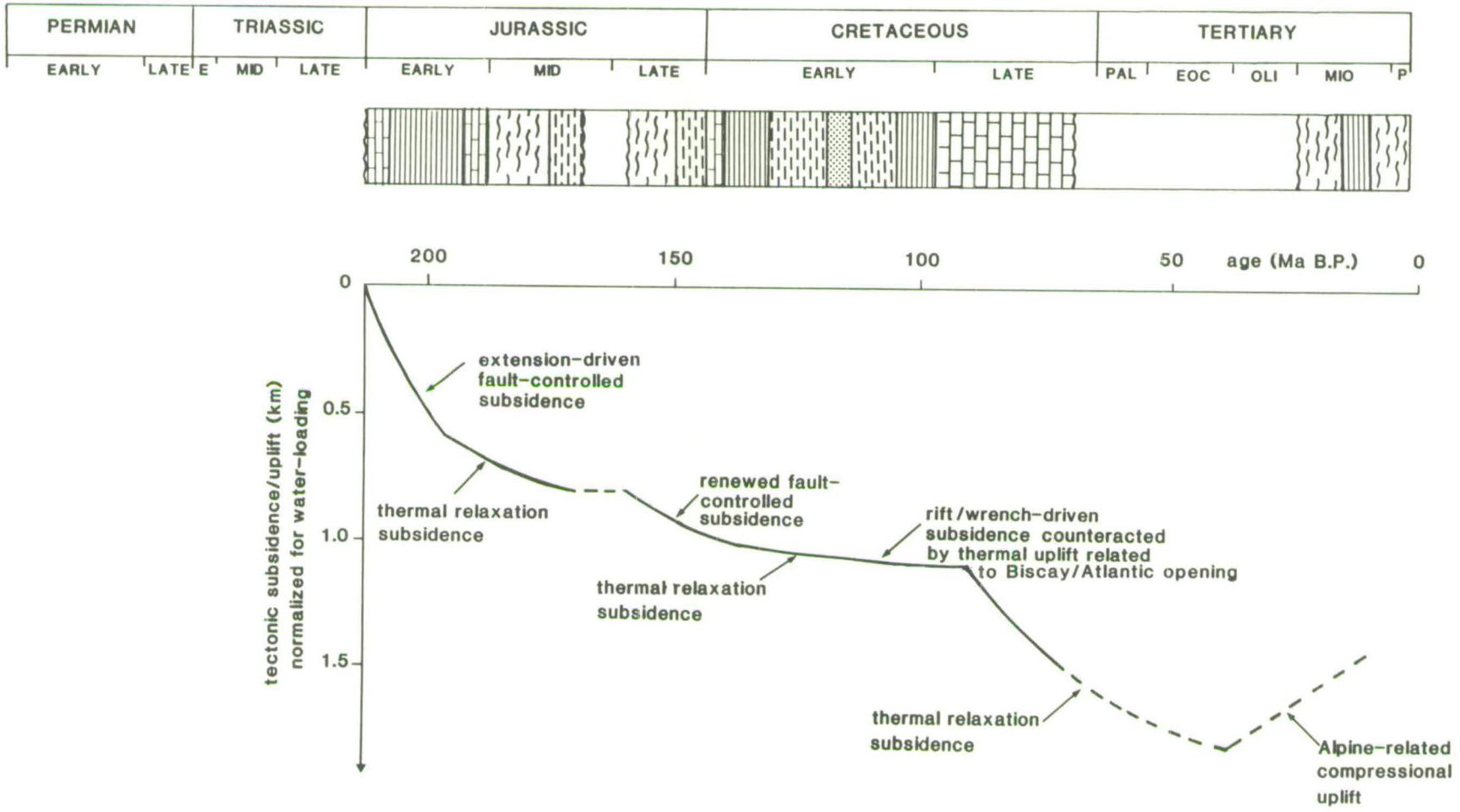

Figure 9.3 "Typical" subsidence history for the Brittany Basin.

may be due to a subtle basement control on later faulting or may be simply due to a coincidence between the directions of Variscan compression and Triassic extension.

The Sherwood Sandstone Group was deposited in response to the rejuvenation of topography along uplifted fault footwalls. It rests with a minor unconformity on thick Permian sediments in the southern Melville Basin (Figure 9.2) and directly on pre-Permian basement in the northern Melville Basin (Figure 9.1). Rapid fault-controlled subsidence continued during the deposition of the Mercia Mudstone Group and the decrease in grain size of the sediments from the Sherwood Sandstone Group is probably more due to a lack of proximal upstanding source areas than to decreasing subsidence rates. Faulting throughout the Melville Basin terminated towards the end of the Triassic. However, the onset of regional thermal subsidence combined with eustatic sea-level rise (Haq et al, 1987) led to marine transgression over the peneplained Rhaetian land surface. Shelf limestones and shales were deposited in the Western Approaches Basin during the thermal relaxation phase which continued into the Liassic. These originally covered a very much larger area than the outliers to which they are presently restricted and were probably deposited over a wider area than the Permo-Triassic red-beds (cf. Dewey's (1982) classic steer's head basin (Figure 1.3)).

Like the Permian, Triassic sediments are thin or absent in the Brittany and South-West Channel Basins (Figure 9.3). However, regional tensional stresses persisted in these basins following the end Triassic termination of faulting in the Melville Basin. These were accommodated by the initiation of extensional faulting in the Brittany Basin at the end of the Triassic/beginning of the Jurassic. Rapid fault-controlled subsidence persisted until Pliensbachian times resulting in the deposition of a thick sequence of Liassic rocks of similar facies to those found in the isolated outliers of the Melville Basin (Figure 9.3). The ensuing thermal subsidence continued until the Bathonian-Callovian with the deposition of thick calcareous mudstones (Figure 9.3). Regression at the end of the middle Jurassic is marked by a period of non-deposition. This event does not appear to have been associated with significant erosion or deformation and is attributed to a combination of low subsidence rates and eustatic sea-level fall.

Late Jurassic-early Cretaceous, Cimmerian erosion in the Western Approaches Basin removed up to 2km of Jurassic-Permian sediments. The youngest pre-Cimmerian rocks recovered from the Western Approaches Basin are Sinemurian in age, hence the geological history of the post-Sinemurian Jurassic is largely a matter for conjecture. However, in view of the observed spatial rift migration in Triassic-Jurassic times, direct comparison between the Jurassic of the Brittany Basin and the northern part of the Western Approaches Trough is unlikely to be valid.

The early-mid Jurassic subsidence phase in the Brittany Basin is not so well developed in the South-West Channel Basin where rapid subsidence only commenced following mid/late Jurassic non-deposition. Thick late Jurassic shallow and marginal marine calcareous shaly sandstones and shales pass upwards into early Cretaceous "Wealden" type clastics. Late Jurassic-early Cretaceous subsidence in the South-West Channel Basin was related to rift/wrench movements on the basin's southern bounding fault synchronous with rifting on the proto-slope (Montadert et al, 1979) and the conjugate Canadian Atlantic margin (Tankard and Welsink, 1987). In the Brittany Basin, away from the immediate vicinity of the principal late Jurassic-early Cretaceous displacement zone (PDZ) (wells Lizenn-1 and Brezell-1), the magnitude of late Jurassic-early Cretaceous subsidence was less than adjacent to the PDZ in the South-West Channel Basin (well Lennket-1). However, rift/wrench movements combined with eustatic sea-level rise (Haq et al, 1987) did result in the deposition of a complete late Jurassic-early Cretaceous sequence throughout the Brittany and South-West Channel Basins (Figure 9.3). Sinistral wrench movements in the Western Approaches Trough at this time may have accommodated rifting in the Bay of Biscay and appear to reflect a fundamental change in plate kinematics between Eurasia and Africa (Figure 6.6). Late Jurassic-early Cretaceous sediments in the Brittany Basin show slightly more marine influence than those of the South-West Channel Basin due to nearby incipient Biscay/Atlantic oceanic circulation.

In the Western Approaches Basin the late Jurassic-early Cretaceous was a time of major uplift resulting in the erosion of up to 2km of Permian-Jurassic sediments (Figures 9.1 and 9.2). Local subsidence due to rift/wrench movements (involving renewed reactivation of the former

Variscan thrusts and transfer faults) and salt withdrawal also occurred. However, this was subsidiary to the regional uplift and served only to locally reduce the magnitude of Cimmerian erosion, preserving isolated Liassic outliers surrounded by Permo-Triassic red-beds. The magnitude and extent of Cimmerian uplift is, mechanistically, the most enigmatic aspect of the post-Carboniferous tectonic evolution of the Western Approaches Trough. Although clearly related to Bisacy/Atlantic opening, uplift was concentrated over the Cornubian Massif. Considerable erosion occurred throughout the Western Approaches and South Celtic Sea Basins, however, no late Jurassic-early Cretaceous Cimmerian unconformity is recorded in the centre of the Brittany and North Celtic Sea Basins. The "lateral thermal processes" (heterogeneous stretching and conductive and convective lateral heat flow) invoked to account for the uplift by heating the lithosphere without accompanying crustal thinning may have been focused by the low density granitic batholiths of the Cornubian Massif. Alternatively, the rift/wrench movements and related subsidence which counteracted regional uplift in the South-West Channel and Brittany Basins may have been inhibited by the relatively strong massif.

Following uplift there was a period of Barremian-Aptian stability in the Western Approaches Basin (Figures 9.1. and 9.2) , during which a thin veneer of early Cretaceous clastics were deposited over the Cimmerian unconformity. Regional subsidence throughout the Western Approaches Trough commenced in the late Cretaceous and, combined with eustatic sea-level rise, resulted in the deposition of the Chalk. The mechanisms of late Cretaceous subsidence vary across the Western Approaches Trough and Cornubian Massif and are intimately linked to the geodynamic processes of the late Jurassic-early Cretaceous period. Subsidence in the Brittany Basin was driven by thermal relaxation following lithospheric extension. Subsidence in the Western Approaches Basin was driven by cooling following thermally-driven uplift and erosion with a subsidiary component of post-extensional relaxation. The Cornubian Massif subsided as a consequence of lithospheric cooling following uplift and erosion.

In the Western Approaches Trough early Alpine plate convergence and eustatic sea-level changes resulted in several relatively minor

Palaeocene and early Eocene hiatuses. However, deformation, and the consequent development of compressional structures on the north Biscay margin, did not occur until the late Eocene-late Oligocene (Masson and Parson, 1983). The Melville Basin was subjected to several hundred metres of uplift and consequent erosion at this time (Figures 9.1 and 9.2), witnessed by the abnormally low porosity of the Chalk. In the St. Mary's, Brittany and South-West Channel Basins, where pre-uplift sediments outcrop over much of the seabed, over a kilometre of erosion occurred and uplift probably continued into Miocene times (Figure 9.3). Uplift was driven by lithospheric compression transmitted from plate convergence associated with the northward movement of Africa relative to northern and central Europe (Figure 6.6). In the Brittany and South-West Channel Basins uplift resulted in inversion of the late Jurassic-early Cretaceous depocentres and the development of a major anticline. Compressional structures are not apparent in seismic reflection data over the Western Approaches Basin, or the Cornubian Massif, where the crust must have been sufficiently strong to transmit the stresses to the north without itself deforming. It is proposed that compression of the sub-crustal lithosphere without accompanying crustal compression largely accounts for the uplift of these areas. This may have been enhanced by lesser crustal compression, not apparent on the seismic data and, in the northern Melville Basin, halokinesis.

Unlike the former Variscan thrusts, the transfer faults in the Melville Basin were reactivated during the Tertiary. Sinistral reactivation of the Sticklepath-Lustleigh fault zone onshore south-west England was responsible for the development of the transtensional Eocene-Oligocene Bovey and Petrockstow Basins (Holloway and Chadwick, 1986) and is also invoked to account for extension across the Melville wrench zone within the broad Tertiary compressional setting.

REFERENCES

Alexander, S.A. & Fyfe, J.A. 1988. The Use of the B.G.S. Offshore Database with the Oracle Database Management System. British Geological Survey, Marine Geophysics and Offshore Services Research Programme Report 88/1.

Allmendinger, R.W., Farmer, H., Hauser, E., Sharp, J., Von Tish, D., Oliver, J. & Kaufman, S. 1986. Phanerozoic tectonics of the Basin and Range - Colorado Plateau Transition from COCORP data and geologic data: a review. In: Barazangi, M. & Brown, L. (eds.) Reflection Seismology. American Geophysical Union Geodynamcs Series, 14, 257-267.

Andreieff, P., Bouysse, P., Horn, R. & Monciardini, C. 1972. Contribution a l'étude géologique des approches occidentales de la Manche. Mémoires du Bureau de Recherches Géologiques et Minières, 79, 31-48.

Andreieff, P., Bouysse, P., Curry, D., Fletcher, B.N., Hamilton, D., Monciardini, C. & Smith, A.J. 1975. The stratigraphy of the post-Palaeozoic sequences in part of the western Channel. Philosophical Transactions of the Royal Society of London, A279, 79-97.

Artemjev, M.E, & Artyushkov, E.V. 1969. Origin of rift basins. International Geology Review, 11, 582-593.

Arthaud, F. & Matte, P. 1977. Late Palaeozoic strike-slip faulting in southern Europe and northern Africa: result of a right-lateral shear zone between the Appalachians and the Urals. Geological Society of America Bulletin, 88, 1305-1320.

Auffret, G.A., Pastouret, L., Cassat, G., De Charpal, O. & Guennoc, P. 1979. Dredged rocks from the Armorican and Celtic margins. In: Montadert, L., Roberts, D.G. et al (eds.) Initial Reports of the Deep Sea Drilling Project, 48, 995-1008.

Avedik, F., Camus, A.L., Ginsburg, A., Montadert, L., Roberts, D.G. & Whitmarsh, R.B. 1982. A seismic refraction and reflexion study of the continent-ocean transition beneath the north Biscay margin. Philosophical Transactions of the Royal Society of London, A305, 5-25.

Badham, J.P.N. 1982. Strike-slip orogens - an explanation for the Hercynides. Journal of the Geological Society of London, 139, 493-504.

Badley, M.E., Price, J.D., Rambech Dahl, C. & Agdestein, T. 1988. The structural evolution of the northern Viking Graben and its bearing upon extensional modes of basin formation. Journal of the Geological Society of London, 145, 455-472.

Bally, A.W. 1980. Basins and subsidence - a summary. In: Bally, A.W., Bender, P.L.,McGetchin, T.R. & Walcott, R.I. (eds.) Dynamics of Plate Interiors. American Geophysical Union Geodynamics Series, 1, 5-20.

Barnes, R.P. & Andrews, J.R. 1986. Upper Palaeozoic ophiolite generation and obduction in south Cornwall. Journal of the Geological Society of London, 143, 117-124.

Barr, D. 1987. Lithospheric stretching, detached normal faulting and footwall uplift. In: Coward, M.P., Dewey, J.F. and Hancock, P.L. (eds.) Continental Extensional Tectonics. Special Publication of the Geological Society of London, 28, 75-94.

Barton, P.J., Matthews, D.H., Hall, J. & Warner, M.R. 1984. Moho beneath the North Sea compared on normal incidence and wide-angle seismic records. Nature, 308, 55-56.

Barton, P.J. & Wood, R.J. 1984. Tectonic evolution of the North Sea Basin: crustal stretching and subsidence. Geophysical Journal of the Royal Astronomical Society, 79, 987-1022.

Bathurst, R.G.C. 1975. Carbonate Sediments and their Diagenesis. Developments in Sedimentology, 12. Elsevier, The Netherlands.

Beach, A. 1987. A regional model for linked tectonics in north-west Europe. In: Brooks, J. & Glennie, K. (eds.) Petroleum Geology of North West Europe, 43-48. Graham and Trotman, London.

Beaumont, C. 1981. Foreland basins. Geophysical Journal of the Royal Astronomical Society, 65, 291-329.

Beaumont, C., Keen, C.E. & Boutilier, R. 1982. A comparison of foreland and rift margin sedimentary basins. Philosophical Transactions of the Royal Society of London, A305, 295-317.

Beloussov, V.V. 1960. Development of the earth and tectogenesis. Journal of Geophysical Research, B65, 4127-4146.

Bennet, G., Copestake, P. & Hooker, M.P. 1985. Stratigraphy of Britoil 72/10-1A well, Western Approaches. Proceedings of the Geologists' Association, 96, 255-261.

Berggren, W.A., Kent, D.V., Flynn, J.J. & Van Couvering, J.A. 1985. Cenozoic geochronology. Geological Society of America Bulletin, 96, 1407-1418.

Bessis, F. 1986. Some remarks on the study of subsidence of sedimentary basins. Applications to the Gulf of Lions margin (Western Mediterranean). Marine and Petroleum Geology, 3, 37-63.

BIRPS & ECORS. 1986. Deep seismic reflection profiling between England, France and Ireland. Journal of Geological Society of London, 143, 45-52.

Blundell, D.J. 1975. The geology of the Celtic Sea and Western Approaches. Canadian Society of Petroleum Geologists Memoir, 4, 341-362.

Blundell, D.J. 1979. The geology and structure of the Celtic Sea. In: Banner, F.T., Collins, M.B. & Massie, K.S. (eds.) The Northwest European Shelf Seas, 1, Geology and Sedimentology, 43-60 (Chapter 4). Elsevier, The Netherlands.

Blundell, D.J. & Raynaud, B. 1986. Modelling lower crust reflections observed on BIRPS profiles. In: Barazangi, M. & Brown, L. (eds.) Reflection Seismology: A Global Perspective. American Geophysical Union Geodynamics Series, 13, 287-295.

Bois, C., Cazes, M., Damotte, B., Galdeano, A., Hirn, A., Mascle, A., Matte, P., Raoult, J.F. & Torreilles, G. 1986. Deep seismic reflection profiling of the crust in northern France: the ECORS project. In: Barazangi, M. & Brown, L. (eds.) Reflection Seismology: A Global Perspective. American Geophysical Union Geodynamics Series, 13, 21-29.

Bond, G. 1978. Speculations on real sea-level changes, and vertical motions of continents at selected times in the Cretaceous and Tertiary periods. Geology, 6, 247-250.

Bond, G.C. & Kominz, M.A. 1984. Construction of tectonic subsidence curves for the early Paleozoic miogeocline, southern Canadian Rocky Mountains: implications for subsidence mechanisms, age of breakup, and crustal thinning. Geological Society of America Bulletin, 95, 155-173.

Bott, M.H.P. 1971. Evolution of young continental margins and formation of shelf basins. Tectonophysics, 11, 319-327.

Bott, M.H.P. 1980. Mechanisms of subsidence at passive continental margins. In: Bally, A.W., Bender, P.L., McGetchin, T.R. & Walcott, R.I. (eds.) Dynamics of Plate Interiors. American Geophysical Union Geodynamics Series, 1, 27-35.

Bott, M.H.P., Holder, A.P., Long, R.E. & Lucas, A.L. 1970. Crustal structure beneath the granites of south-west England. In: Newall, G. & Rast, N. (eds.) Mechanism of Igneous Intrusion. Geological Journal Special Publication, 2, 93-102.

Brewer, J.A. & Smythe, D.K. 1984. MOIST and the continuity of reflector geometry along the Caledonian-Appalachian orogen. Journal of the Geological Society of London, 141, 105-120.

Brooks, M., Trayner, P.M. & Trimble, T.J. 1988. Mesozoic reactivation of Variscan thrusting in the Bristol Channel area, UK. Journal of the Geological Society of London, 145, 439-444.

Brown, L., Barazangi, M., Kaufman, S. & Oliver, J. 1986. The first decade of COCORP: 1974-1984. In: Barazangi, M. & Brown, L. (eds.) Reflection Seismology: A Global Perspective. American Geophysical Union Geodynamics Series, 13, 107-120.

Bullard, E.C. & Gaskell, T.F. 1941. Submarine seismic investigations. Proceedings of the Royal Society of London, A177, 476-499.

Busby, J.P. 1987. An interactive fortran 77 program using GKS graphics for 2.5D modelling of gravity and magnetic data. Computers & Geosciences, 13, 639-644.

Chadwick, R.A. 1985a. Permian, Mesozoic and Cenozoic structural evolution of England and Wales in relation to the principles of extension and inversion tectonics. In: Whittaker, A. (ed.) Atlas of Onshore Sedimentary Basins in England and Wales: Post-Carboniferous Tectonics and Stratigraphy, 9-25. Blackie, Glasgow and London.

Chadwick, R.A. 1985b. Cenozoic sedimentation, subsidence and tectonic inversion. In: Whittaker, A. (ed.) Atlas of Onshore Sedimentary Basins in England and Wales: Post-Carboniferous Tectonics and Stratigraphy, 61-63. Blackie, Glasgow and London.

Chadwick, R.A. 1985c. Seismic reflection investigations into the stratigraphy and structural evolution of the Worcester Basin. Journal of the Geological Society of London, 142, 187-202.

Chadwick, R.A. 1986. Extension tectonics in the Wessex Basin, southern England. Journal of the Geological Society of London, 143, 465-488.

Chapman, T.J. in press. The Permian-Cretaceous structural evolution of the Western Approaches Basin (Melville Sub-basin), U.K. In: Cooper, M.A. & Williams, G.D. (eds.) Inversion Tectonics. Geological Society of London Special Publication.

Chenet, P., Montadert, L., Gairaud, H. & Roberts D.G. 1982. Extension ratio measurements on the Galicia, Portugal, and northern Biscay continental margins: implications for evolutionary models of passive continental margins. In: Watkins, J.S. & Drake, C.L. (eds.) Studies in Continental Margin Geology. American Association of Petroleum Geologists Memoir, 34, 703-715.

Christie-Blick, N. & Biddle, K.T. 1985. Deformation and basin formation along strike-slip faults. In: Biddle, K.T. & Christie-Blick, N. (eds.) Strike-Slip Deformation, Basin Formation and Sedimentation. Society of Economic Paleontologists and Mineralogists Special Publication, 37, 1-34.

Cochran, J.R. 1983. Effects of finite rifting times on the development of sedimentary basins. Earth and Planetary Science Letters, 66, 289-302.

Cocks, L.R.M. & Fortey, R.A. 1982. Faunal evidence for oceanic separations in the Palaeozoic of Britain. Journal of the Geological Society of London, 139, 465-478.

Colter, V.S. & Havard, D.J. 1981. The Wytch Farm Oil Field, Dorset. In: Illing, L.V. & Hobson, G.D. (eds.) Petroleum Geology of the Continental Shelf of North-West Europe, 494-503. Heyden & Son Ltd., London.

Cook, D.R. 1987. The Goban Spur - exploration in a deep-water frontier basin. In: Brooks, J. & Glennie, K. (eds.) Petroleum Geology of North West Europe, 623-632. Graham and Trotman, London.

Cooles, G.P., Dungworth, G., Goodwin, N.S., Lister, S.W., Lowe, S.P. & Taylor, S. 1981. Organic geochemistry. In: Evans, C.D,R., Lott, G.K. & Warrington, G. (compilers) The Zephyr (1977) wells, South-Western Approaches and western English Channel. Institute of Geological Sciences Report 81/8, 37-44. HMSO, London.

Coward, M.P. 1986. Heterogeneous stretching, simple shear and basin development. Earth and Planetary Science Letters, 80, 325-336.

Coward, M.P. & McClay, K.R. 1983. Thrust tectonics of south Devon. Journal of the Geological Society of London, 140, 215-228.

Coward, M.P. & Smallwood, S. 1984. An interpretation of the Variscan tectonics of SW Britain. In: Hutton, D.H.W. & Sanderson, D.J. (eds.) Variscan Tectonics of North Atlantic Region. Special Publication of the Geological Society, 14, 89-102.

Crawshay, L.R. 1908. On rock remains in the bed of the English Channel. An account of the dredgings carried out by SS. "Oithona" in 1906. Journal of the Marine Biological Association of the United Kingdom, 8, 99-117.

Curry, D., Martini, E., Smith, A.J. & Whittard, W.F. 1962. The geology of the Western Approaches of the English Channel - I. Chalky rocks from the upper reaches of the continental slope. Philosophical Transactions of the Royal Society of London, B245, 267-290.

Curry, D., Hersey, J.B., Martini, E. & Whittard, W.F. 1965. The geology of the Western Approaches of the English Channel - II. Geological interpeation aided by boomer and sparker records. Philosophical Transactions of the Royal Society of London, B248, 315-351.

Curry, D., Hamilton, D. & Smith, A.J. 1971. Geological evolution of the Western English Channel and its relation to the nearby continental margin. In: Delaney, F.M. (ed.) Institute of Geological Sciences Report 70/14, 129-142.

Darbyshire, D.P.F. & Shepherd, T.J. 1985. Chronology of granite magmatism and associated mineralization, SW England. Journal of the Geological Society of London, 142, 1159-1177.

Davis, B.K. 1987. Velocity changes and burial diagenesis in the Chalk of the southern North Sea Basin. In: Brooks, J. & Glennie, K. (eds.) Petroleum Geology of North West Europe, 307-313. Graham and Trotman, London.

Day, A.A, Hill, M.N., Laughton, A.S. & Swallow, J.C. 1956. Seismic prospecting the Western Approaches of the English Channel. Quarterly Journal of the Geological Society of London, 112, 15-44.

Day, G.A. & Edwards, J.W.F. 1983. Variscan thrusting in the basement of the English Channel and SW Approaches. Proceedings of the Ussher Society, 5, 432-436.

Dewey, J.F. 1982. Plate tectonics and the evolution of the British Isles. Journal of the Geological Society of London, 139, 371-412.

D'Heur, M. 1984. Porosity and hydrocarbon distribution in the North sea chalk reservoirs. Marine and Petroleum Geology, 1, 211-238.

Dietz, R.S. 1963. Collapsing continental rises: an actualistic concept of geosynclines and mountain building. Journal of Geology, 71, 314-333.

Dobinson, A. 1984. Geophysical Track Atlas at 1:500000 Scale of Marine Geophysics Programme Surveys conducted on the UK Continental Shelf 1967-1983. British Geological Survey, Marine Geophysics Programme Report 112.

Donato, J.A. & Tully, M.C. 1981. A regional interpretation of North Sea gravity data. In: Illing, L.V. & Hobson, G.D. (eds.) Petroleum Geology of the Continental Shelf of North-West Europe, 65-75. Heyden & Son Ltd., London.

Dresser Atlas. 1974. Log Review 1. Dresser Industries Incorporated, U.S.A.

Durrance, E.M. & Laming, D.J.C. 1982. The Geology of Devon. University of Exeter, Exeter.

Edmonds, E.A., McKeown, M.C. & Williams, M. 1975. British Regional Geology: South-West England (Fourth Edition). HMSO, London.

Edwards, J.W.F. 1984a. Interpretations of seismic and gravity surveys over the eastern part of the Cornubian platform. In: Hutton, D.H.W. and Sanderson, D.J. (eds.) Variscan Tectonics of the North Atlantic Region. Special Publication of the Geological Society, 14, 119-124.

Edwards, J.W.F. 1984b. Discussion of an interpretation of the Variscan structures of SW England. Journal of the Geological Society of London, 141, 191-192.

Edwards, J.W.F., Armstrong, E.J. & Ham, D. 1983. Geophysical interpretations south-west of the Scilly Isles. British Geological Survey Report 84/1, 46-49. HMSO, London.

Evans, C.D.R. (compiler) 1986. Little Sole Bank, Solid Geology. British Geological Survey 1:250 000 Offshore Map Series.

Evans, C.D.R., Lott, G.K. & Warrington G. (compilers) 1981. The Zephyr wells, South-Western Approaches and western English Channel. Institute of Geological Sciences Report 81/8. HMSO, London.

Evans, C.D.R. & Hughes, M.J. 1984. The Neogene succession of the South Western Approaches, Great Britain. Journal of the Geological Society of London, 141, 315-326.

Evans, C.D.R., Day, G.A., Edwards, J.W.F., Gatliff, R.W. & Hillis, R.R. in press. Geology of the South-West Approaches. British Geological Survey Offshore Report Series.

Exley, C.S. 1966. The granitic rocks of Haig Fras. Nature, 210, 365-367.

Falvey, D.A. 1974. The development of continental margins in plate tectonic theory. Australian Petroleum Exploration Association Journal, 14, 95-106.

Falvey, D.A. & Middleton, M.F. 1981. Passive continental margins: evidence for a prebreakup deep crustal metamorphic subsidence mechanism. Oceanologica Acta 4, Colloque C3, Proceedings 26th International Geological Congress, Geology of continental margins symposium, Paris, 7-17 July, 1980, 103-114.

Falvey, D.A. & Deighton, I. 1982. Recent advances in burial and thermal geohistory analysis. Australian Petroleum Exploration Association Journal, 22, 65-81.

Fisher, M.J. & Jeans, C.V. 1982. Clay mineral stratigraphy in the Permo-Triassic red bed sequences of BNOC 72/10-1A, Western Approaches, and the south Devon coast. Clay Minerals, 17, 79-89.

Fletcher, B.N. & Evans, C.D.R. (compilers) 1987. Haig Fras, Solid Geology. British Geological Survey 1:250 000 Offshore Map Series.

Floyd, P.A. 1982. Chemical variation in Hercynian basalts relative to plate tectonics. Journal of the Geological Society of London, 139, 505-520.

Floyd, P.A. 1984. Geochemical characterisitcs and comparisons of the basic rocks of the Lizard complex and the basaltic lavas within the Hercynian troughs of SW England. Journal of the Geological Society of London, 141, 61-70.

Fuchs, K. 1969. On the properties of deep crustal reflectors. Zeitschrift für Geophysik, 35, 133-149.

Fyfe, J.A., Abbotts, I. & Crosby, A. 1981. The subcrop of the mid-Mesozoic unconformity in the UK area. In: Illing, L.V. & Hobson, G.D. (eds.) Petroleum Geology of the Continental Shelf of North-West Europe, 236-244. Heyden & Son Ltd., London.

Garrison, R.E. 1981. Diagenesis of oceanic carbonate sediments: a review of the DSDP perspective. In: Warme, J.E., Douglas, R.G. & Winterer, E.L. (eds.) The Deep Sea drilling Project: a Decade of Progress. Society of Economic Paleontologists and Mineralogists Special Publication, 32, 181-207.

Gartner, S. & Keany, J. 1978. The terminal Cretaceous event: a geologic problem with an oceanographic solution. Geology, 6, 708-712.

Genc, H.T. 1988. Gravity and other geophysical studies of the crust of southern Britain. Unpublished PhD Thesis, University of Edinburgh.

Ginzburg, A., Whitmarsh, R.B., Roberts, D.G., Montadert, L., Camus, A. & Avedik, F. 1985. The deep seismic structure of the northern continental margin of the Bay of Biscay. Annales Geophysicae, 3, 499-510.

Goode, A.J.J. & Merriman, R.J. 1987. Evidence of crystalline basement west of the Land's End Granite, Cornwall. Proceedings of the Geologists' Association, 98, 39-43.

Graciansky, P.C. de & Bourbon, M. 1985. The Goban Spur of the Northeast-Atlantic margin during late Cretaceous times. In: Graciansky, P.C. de, Poag, C.W. et al (eds.) Initial Reports of the Deep Sea Drilling Project, 80, 863-883.

Graciansky, P.C. de & Poag, C.W. 1985. Geologic history of Goban Spur, northwest Europe continental margin. In: Graciansky, P.C. de, Poag, C.W. et al (eds.) Initial Reports of the Deep Sea Drilling Project, 80, 1187-1216.

Hailwood, E.A., Bock, W., Costa, L., Dupeuple, P.A., Muller, C. & Schnitker, D. 1979. Chronology and biostratigraphy of northeast Atlantic sediments, DSDP Leg 48. In: Montadert, L., Roberts, D.G. et al (eds.) Initial Reports of the Deep Sea Drilling Project, 48, 1119-1141.

Hale, L.D. & Thompson, G.A. 1982. The seismic reflection character of the continental Mohorovicic discontinuity. Journal of Geophysical Research, B87, 4625-4635.

Hall, J. 1986. The physical properties of layered rocks in deep continental crust. In: Dawson, J.B., Carswell, D.A., Hall, J. & Wedepohl, K.H. (eds.) The Nature of the Lower Continental Crust. Geological Society of London Special Publication, 24, 51-62.

Hallam, A. 1971. Mesozoic geology and the opening of the North Atlantic. Journal of Geology, 79, 129-157.

Hallam, A. 1984. Pre-Quaternary sea-level changes. Annual Review of Earth and Planetary Science, 12, 205-243.

Hallam, A. & Sellwood, B.W. 1976. Middle Mesozoic sedimentation in relation to tectonics in the British area. Journal of Geology, 84, 301-321.

Hamilton, D. 1979. The geology of the English Channel, South Celtic Sea and continental margin, South Western Approaches. In: Banner, F.T., Collins, M.B. & Massie, K.S. (eds.) The Northwest European Shelf Seas, 1, Geology and Sedimentology, 61-87 (Chapter 5). Elsevier, The Netherlands.

Hancock, J.M. 1976. The petrology of the Chalk. Proceedings of the Geologists' Association, 86 (for 1975), 499-535.

Haq, B.U., Hardenbol, J. & Vail, P.R. 1987. Chronology of fluctuating sea levels since the Triassic. Science, 235, 1156-1167.

Harland, W.B., Cox, A.V., Llewellyn, P.G., Pickton, C.A.G., Smith, A.G. & Walters, R. 1982. A Geological Time Scale. Cambridge University Press, Cambridge.

Harrison, R.K., Snelling, N.J., Merriman, R.J., Morgan, G.E. & Goode, A.J.J. 1977. The Wolf Rock, Cornwall: new chemical, isotopic age and palaeomagnetic data. Geological Magazine, 114, 249-328.

Haxby, W.F., Turcotte, D.L. & Bird, J.M. 1976. Thermal and mechanical evolution of the Michigan basin. Tectonophysics, 36, 57-75.

Hegarty, K.A., Weissel, J.K. & Mutter, J.C. 1988. Subsidence history of Australia's southern margin: constraints on basin models. American Association of Petroleum Geologists Bulletin, 72, 615-533.

Hellinger, S.J. & Sclater, J.G. 1983. Some comments on two-layer extensional models for the evolution of sedimentary basins. Journal of Geophysical Research, B88, 8251-8269.

Hellinger, S.J., Sclater, J.G. & Giltner, J. in press. Mid-Jurassic through Mid-Cretaceous extension in the Central Graben of the North Sea: part 1, estimates from subsidence.

Hendriks, E.M.L. 1939. The Start-Dodman-Lizard boundary zone in relation to the Alpine structure of Cornwall. Geological Magazine, 76, 385-402.

Hillis, R.R. & Day, G.A. 1987. Deep events in U.K. South Western Approaches. Geophysical Journal of the Royal Astronomical Society, 89, 243-250.

Hobbs, R.W., Peddy, C. & the BIRPS group. 1987. Is lower crustal layering related to extension? Geophysical Journal of the Royal Astronomical Society, 89, 239-242.

Holder, M.T. & Leveridge, B.E. 1986. A model for the tectonic evolution of south Cornwall. Journal of the Geological Society of London, 143, 125-134.

Holliger, K. & Klemperer, S.L. in press. A comparison of the Moho interpreted from gravity data and from deep seismic data in the northern North Sea. Geophysical Journal.

Holloway, S. & Chadwick, R.A. 1986. The Sticklepath-Lustleigh fault zone: Tertiary sinistral reactivation of a Variscan dextral strike-slip fault. Journal of the Geological Society of London, 143, 447-452.

Hsü, K.J. 1965. Isostasy, crustal thinning, mantle changes, and the disappearance of land masses. American Journal of Science, 263, 97-109.

Hurich, C.A. & Smithson, S.B. 1987. Compositional variation and the origin of deep crustal reflections. Earth and Planetary Science Letters, 85, 416-426.

Jackson, J.A. & McKenzie, D.P. 1983. The geometrical evolution of normal fault systems. Journal of Structural Geology, 5, 471-482.

Jansa, L.F. & Wade, J.A. 1975. Paleogeography and sedimentation in the Mesozoic and Cenozoic, southeastern Canada. In: Yorath, C.J. & Parker, E.R. (eds.) Canada's Continental Margins and Offshore Petroleum Exploration. Canadian Society of Petroleum Geologists Memoir, 4, 79-102.

Jansa, L.F., Bujak, J.P. & Williams, G.L. 1980. Upper Triassic salt deposits of the western North Atlantic: Canadian Journal of Earth Sciences, 17, 547-559.

Jarvis, G.T. & McKenzie, D.P. 1980. Sedimentary basin formation with finite extension rates. Earth and Planetary Science Letters, 48, 42-52.

Jenkins, D.G. & Shackleton, N. 1979. Parallel changes to species diversity and palaeotemperatures in the Lower Miocene. Nature, 278, 50-51.

Jones, T.D. & Nur, A. 1984. The nature of seismic reflections from deep crustal fault zones. Journal of Geophysical Research, B89, 3153-3171.

Kamerling, P. 1979. The geology and hydrocarbon habitat of the Bristol Channel Basin. Journal of Petroleum Geology, 2, 75-93.

Karner, G.D. & Watts, A.B. 1982. On isostasy at Atlantic-type continental margins. Journal of Geophysical Research, B87, 2923-2948.

Karner, G.D., Lake, S.D. & Dewey, J.F. 1987. The thermal and mechanical development of the Wessex Basin, southern England. In: Coward, M.P., Dewey, J.F. & Hancock, P.L. (eds.) Continental Extensional Tectonics. Special Publication of the Geological Society of London, 28, 517-536.

Kazmin, V. 1987. Two types of rifting: dependence on the condition of extension. Tectononphysics, 143, 85-92.

Keen, C.E., Boutilier, R., de Voogd, B., Mudford, B. & Enachescu, M.E. 1987. Crustal geometry and extensional models for the Grand Banks, eastern Canada: constraints from deep seismic reflection data. In: Beaumont, C. & Tankard, A.J. (eds.) Sedimentary Basins and Basin-Forming Mechanisms. Canadian Society of Petroleum Geologists Memoir, 12, 101-115.

Kennedy, W.J. 1987. Late Cretaceous and early Palaeocene Chalk Group sedimentation in the greater Ekofisk area, North Sea Central Graben. Bulletin Centres Recherches Exploration-Production Elf Aquitaine, 11, 91-126.

Kent, D.V. & Gradstein, F.M. 1985. A Cretaceous and Jurassic geochronology. Geological Society of America Bulletin, 96, 1419-1427.

Kirby, G.A. 1979. The Lizard Complex as a thrust ophiolite mass. Nature, 282, 58-60.

Kirton, S.R. & Hitchen, K. 1987. Timing and style of crustal extension N of the Scottish mainland. In: Coward, M.P., Dewey, J.F. & Hancock, P.L. (eds.) Continental Extensional Tectonics. Special Publication of the Geological Society of London, 28, 501-510.

Klemperer, S.L. 1988. Crustal thinning and nature of extension in the northern North Sea from deep seismic reflection profiling. Tectonics, 7, 803-821.

Klemperer, S.L. & the BIRPS group. 1987. Reflectivity of the crystalline crust: hypotheses and tests. Geophysical Journal of the Royal Astronomical Society, 89, 217-222.

Kusznir, N.J. & Karner, G.D. 1985. Dependence of the flexural rigidity of the continental lithosphere on rheology and temperature. Nature, 316, 138-142.

Kusznir, N.J., Karner, G.D. & Egan, S. 1987. Geometric, thermal and isostatic consequences of detachments in continental lithosphere extension and basin formation. In: Beaumont, C. & Tankard, A.J. (eds.) Sedimentary Basins and Basin-Forming Mechanisms. Canadian Society of Petroleum Geologists Memoir, 12, 185-203.

Kusznir, N.J. & Park, R.G. 1987. The extensional strength of the continental lithosphere: its dependence on geothermal gradient, and crustal composition and thickness. In: Coward, M.P., Dewey, J.F. & Hancock, P.L. (eds.) Continental Extensional Tectonics. Geological Society of London Special Publication, 28, 35-53.

Lake, S.D. & Karner, G.D. 1987. The structure and evolution of the Wessex Basin, southern England: an example of inversion tectonics. Tectonophysics, 137, 347-378.

Lalaut, P., Sibuet, J-C. & Williams, C.A. 1981. Carte Gravimetrique de l'Atlantique Nord-Est, CNEXO.

Laming, D.J.C. 1969. Facies interpretations in the New Red Sandstone, S.W. England (abstract only). Proceedings of the Ussher Society, 2, 111-112.

Leeder, M.R. 1982. Upper Palaeozoic basins of the British Isles - Caledonide inheritance versus Hercynian plate margin processes. Journal of the Geological Society of London, 139, 479-491.

Lefort, J.P. 1977. Possible "Caledonian" subduction under the Domnonean domain North Armorican area. Geology, 5, 523-526.

Lefort, J.P., Peucat, J.J., Deunff, J. & Le Herisse, A. 1985. The Goban Spur Palaeozoic basement. In: Graciansky, P.C. de, Poag, C.W. et al (eds.) Initial Reports of the Deep Sea Drilling Project, 80, 677-679.

LePichon, X. & Sibuet, J-C. 1981. Passive margins: a model of formation. Journal of Geophysical Research, B86, 3708-3720.

Leveridge, B.E., Holder, M.T. & Day, G.A. 1984. Thrust nappe tectonics in the Devonian of south Cornwall and the western English Channel. In: Hutton, D.H.W. & Sanderson, D.J. (eds.) Variscan Tectonics of North Atlantic Region. Special Publication of the Geological Society, 14, 89-102.

Lloyd, A.J., Savage, R.J.G., Stride, A.H. & Donovan, D.T. 1973. The geology of the Bristol Channel floor. Philosophical Transactions of the Royal Society of London, A274, 595-626.

Lott, G.K., Knox, R.W.O'B., Bigg, P.J., Davey, R.J. & Morton, A.C. 1980. Aptian-Cenomanian stratigraphy in boreholes from offshore south-west England. Institute of Geological Sciences Report, 80/8. HMSO, London.

Lubimova, E.A. & Nikitina, V.N. 1975. On heat flow singularities over mid-ocean ridges. Journal of Geophysical Research, B80, 232-243.

Ludwig, W.J., Nafe, J.E. & Drake, C.L. 1970. Seismic Refraction. In: Maxwell, A.E. (ed.) The Sea, 4, 53-84 (Chapter 2). Wiley, New York.

McGeary, S. & Warner, M.R. 1985. Seismic profiling in the continental lithosphere. Nature, 317, 795-797.

McGetchin, T.R., Burke, K.C., Thompson, G.A. & Young, R.A. 1980. Mode and mechanisms of plateau uplifts. In: Bally, A.W., Bender, P.L., McGetchin, T.R. & Walcott, R.I. (eds.) Dynamics of Plate Interiors. American Geophysical Union Geodynamics Series, 1, 99-111.

McKenzie, D.P. 1978. Some remarks on the development of sedimentary basins. Earth and Planetary Science Letters, 40, 25-32.

McKenzie, D.P. 1984. A possible mechanism for epeirogenic uplift. Nature, 307, 616-618.

McKerrow, W.S. & Ziegler, A.M. 1972. Palaeozoic oceans. Nature, 240, 92-94.

Magara, K. 1976. Thickness of removed sedimentary rocks, paleopore pressure, and paleotemperature, southwestern part of Western Canada Basin. American Association of Petroleum Geologists Bulletin, 60, 554-565.

Mapstone, N.B. 1975. Diagenetic history of a North Sea chalk. Sedimentology, 22, 601-614.

Masson, D.G. & Roberts, D.G. 1981. Late Jurassic-early Cretaceous reef trends on the continental margin SW of the British Isles. Journal of the Geological Society of London, 138, 437-443.

Masson, D.G. & Parson, L.M. 1983. Eocene deformation on the continental margin SW of the British Isles. Journal of the Geological Society of London, 140, 913-920.

Masson, D.G., Montadert, L. & Scrutton, R.A. 1985. Regional geology of the Goban Spur continental margin. In: Graciansky, P.C. de, Poag, C.W. et al (eds.) Initial Reports of the Deep Sea Drilling Project, 80, 1115-1139.

Masson, D.G. & Miles, P.R. 1986. Development and hydrocarbon potential of Mesozoic sedimentary basins around margins of North Atlantic. American Association of Petroleum Geologists Bulletin, 70, 721-729.

Matthews, S.C., Chauvel, J.J. & Robardet, M. 1980. Variscan geology of northwestern Europe. In: Geology of Europe, Colloque C6, 26th International Geological Congress, Paris, 69-76.

Meissner, R. 1973. The Moho as a transition zone. Geophysical Surveys Dordrecht, 1, 195-216.

Meissner, R. 1986. Twenty years of deep seismic reflection profiling in Germany - a contribution to our knowledge of the nature of the lower Variscan crust. In: Dawson, J.B., Carswell, D.A., Hall, J. & Wedepohl, K.H. (eds.) The Nature of the Lower Continental Crust. Geological Society of London Special Publication, 24, 1-10.

Meissner, R., Matthews, D.H. & Vever, T. 1986. The "Moho" in and around Great Britain. Annales Geophysicae, 4B, 659-664.

Merkel, R.H. 1981. Well Log Formation Evaluation. American Association of Petroleum Geologists Continuing Education Course Note Series #14.

Miller, J.A. & Mohr, P.A. 1964. Potassium-argon measurements on the granites and some associated rocks from southwest England. Geological Journal, 4, 105-126.

Mimran, Y. 1977. Chalk deformation and large-scale migration of calcium carbonate. Sedimentology, 24, 333-360.

Mimran, Y. 1985. Tectonically controlled freshwater carbonate cementation in Chalk. In: Schneidermann, N. & Harris, P.M. (eds.) Carbonate Cements. Society of Economic Paleontologists and Mineralogists Special Publication, 36, 371-379.

Montadert, L., Roberts, D.G., De Charpal, O. & Guennoc, P. 1979. Rifting and subsidence of the northern continental margin of the Bay of Biscay. In: Montadert, L., Roberts, D.G. et al (eds.) Initial Reports of the Deep Sea Drilling Project, 48, 1025-1060.

Morgan, P. & Ramberg, I.R. 1987. Physical changes in the lithosphere associated with thermal relaxation afetr rifting. Tectonophysics, 143, 1-11.

Morton, A.C. 1987. Petrography and geochemistry of Permian extrusive rocks from well 73/12-1, SW Approaches. British Geological Survey, Stratigraphy and Sedimentology Research Group Report, SRG/87/16.

Mudford, B.S. 1987. A quantitative analysis of lithospheric subsidence due to thinning by simple shear. Canadian Journal of Earth Sciences, 25, 20-29.

Munns, J.W. 1984. The Valhall field: a geological overview. Marine and Petroleum Geology, 2, 23-43.

Murrell, S.A.F. 1986. Mechanics of tectogenesis in plate collision zones. In: Coward, M.P. & Ries A.C. (eds.) Collision Tectonics. Special Publication of the Geological Society of London, 19, 95-111.

Naylor, D. & Mounteney, S.N. 1975. Geology of the North-West European Continental Shelf, 1. Graham, Trotman & Dudley Ltd., London.

Naylor, D. & Shannon, P. 1982 The Geology of Offshore Ireland and West Britain. Graham and Trotman Ltd., London.

Neugebauer, J. 1974. Some aspects of cementation in chalk. In: Hsu, K.J. & Jenkyns, H.C. (eds.) Pelagic Sediments: on Land and under the Sea. International Association of Sedimentologists Special Publication, 1, 149-176.

Odin, G.S. & Matter, A. 1981. De glauconiarum origine. Sedimentology, 28, 611-641.

Odin, G.S., Curry, D., Gale, N.H. & Kennedy, W.J. 1982. The Phanerozoic time scale in 1981. In: Odin, G.S. (ed.) Numerical Dating in Stratigraphy, 957-960. John Wiley & Sons, Ltd., New York.

Owen, T.R. 1974. The geology of the Western Approaches. In: Nairn, A.E.M. & Stehli, F.G. (eds.) The Ocean Basins and Margins, 2, The North Atlantic, 233-272 (Chapter 8). Plenum Press, New York.

Pantin, H.M. & Evans, C.D.R. 1984. The Quaternary history of the central and southern Celtic Sea. Marine Geology, 57, 259-293.

Parsons, B. & Sclater, J.G. 1977. An analysis of the variation of ocean floor bathymetry and heat flow with age. Journal of Geophysical Research B82, 803-827.

Phinney, R.A. & Jurdy D.M. 1979. Seismic imaging of the deep crust. Geophysics, 44, 1637-1660.

Pinet, B., Montadert, L., Mascle, A., Cazes, M. & Bois, C. 1987. New insights on the structure and the formation of sedimentary basins from deep seismic profiling in western Europe. In: Brooks, J. & Glennie, K. (eds.) Petroleum Geology of North West Europe, 43-48. Graham and Trotman, London.

Pitman, W.C. 1978. Relationship between eustacy and stratigraphic sequences of passive margins. Geological Society of America Bulletin, 89, 1389-1403.

Pitman, W.C. & Andrews, J.A. 1985. Subsidence and thermal histories of small pull-apart basins. In: Biddle, K.T. & Christie-Blick, N. (eds.) Strike-Slip Deformation, Basin Formation and Sedimentation. Society of Economic Paleontologists and Mineralogists Special Publication, 37, 45-49.

Poag, C.W., Reynolds, L.A., Mazzullo, J.M. & Kiegwin, L.D. 1985. Foraminiferal, lithic, and isotopic changes across four major unconformities at Deep Sea Drilling Project site 548, Goban Spur. In: Graciansky, P.C. de, Poag, C.W. et al (eds.) Initial Reports of the Deep Sea Drilling Project, 80, 539-555.

Pomerol, C. 1972. Introduction. Mémoires du Bureau de Recherches Géologiques et Minières, 79, 11-12.

Powers, M.C. 1967. Fluid-release mechanisms in compacting marine mudrocks and their importance in oil exploration. American Association of Petroleum Geologists Bulletin, 51, 1240-1254.

Pryor, W.A. 1973. Permeability-porosity patterns and variations in some Holocene sand bodies. American Association of Petroleum Geologists Bulletin, 57, 162-189.

Rat, P., Gillot, E., Magniez, F. & Pascal, A. 1985. Paleoenvironmental study of Barremian-Albian sediments at Deep Sea Drilling Project site 549 in the eastern North Atlantic. In: Graciansky, P.C. de, Poag, C.W. et al (eds.) Initial Reports of the Deep Sea Drilling Project, 80, 905-925.

Rawson, P.F. & Riley, L.A. 1982. Latest Jurassic - early Cretaceous events and the "late Cimmerian unconformity" in North Sea area. American Association of Petroleum Geologists Bulletin, 66, 2628-2648.

Reston, T.J. & Blundell, D.J. 1987. Seismic modelling of the lower crust (abstract only). Geophysical Journal of the Royal Astronomical Society, 89, 483.

Robinson, K.W., Shannon, P.M. & Young, D.G.G. 1981. The Fastnet Basin: an integrated analysis. In: Illing, L.V. & Hobson, G.D. (eds.) Petroleum Geology of the Continental Shelf of North-West Europe, 444-454. Heyden & Son Ltd., London.

Rollin, K.E. 1988. A detailed gravity survey between Dartmoor and Bodmin Moor: the shape of the Cornubian Granite Ridge and a new Tertiary basin. Proceedings of the Geologists' Association, 99, 15-25.

Rowley, D.B. & Sahagian, D. 1986. Depth-dependent stretching: a different approach. Geology, 14, 32-35.

Royden, L. & Keen, C.E. 1980. Rifting processes and thermal evolution of the continental margin of eastern Canada determined from subsidence curves. Earth and Planetary Science Letters, 51, 343-361.

Royden, L., Sclater, J.G. & Von Herzen, R.P. 1980. Continental Margin Subsidence and Heat Flow: Important parameters in formation of petroleum hydrocarbons. American Association of Petroleum Geologists Bulletin, 64, 173-187.

Rubey, W.W. & Hubbert, M.K. 1959. Role of fluid pressure in mechanics of overthrust faulting II - overthrust belt in geosynclinal area of western Wyoming in light of fluid pressure hypothesis. Geological Society of America Bulletin, 70, 167-206.

Rutten, M.G. 1969. The Geology of Western Europe. Elsevier, The Netherlands.

Sanderson, D.J. 1984. Structural variation across the northern margin of the Variscides in NW Europe. In: Hutton, D.H.W. & Sanderson, D.J. (eds.) Variscan Tectonics of the North Atlantic Region. Special Publication of the Geological Society of London, 14, 149-165.

Savostin, L.A., Sibuet, J-C., Zonenshain, L.P., LePichon, X. & Roulet, M-J. 1986. Kinematic evolution of the Tethys belt from the Atlantic Ocean to the Pamirs since the Triassic. Tectonophysics, 123, 1-35.

Schlanger, S.O. & Douglas, R.G. 1974. The pelagic ooze-chalk-limestone transition and its implications for marine stratigraphy. In: Hsu, K.J. & Jenkyns, H.C. (eds.) Pelagic Sediments: on Land and under the Sea. International Association of Sedimentologists Special Publication, 1, 117-148.

Schlumberger. 1974. Well Evaluation Conference North Sea. Services Techniques Schlumberger, France.

Schlumberger. 1987. Log Interpretation Principles/Applications. Schlumberger Educational Services, U.S.A..

Scholle, P.A. 1977. Chalk diagenesis and its relation to petroleum exploration: oil from chalks, a modern miracle? American Association of Petroleum Geologists Bulletin, 61, 982-1009.

Sclater, J.G. & Christie, P.A.F. 1980. Continental stretching: an explanation of the post-mid-Cretaceous subsidence of the Central North Sea Basin. Journal of Geophysical Research, B85, 3711-3739.

Sclater, J.G., Royden, L., Horvath, F., Burchfiel, B.C., Semken, S. & Stegena, L. 1980. The formation of the intra-Carpathian basins as determined from subsidence data. Earth and Planetary Science Letters, 51, 139-162.

Scotese, C., Bambach, R.K., Barton, C., Van der Voo, R. & Ziegler, A.M. 1979. Palaeozoic base maps. Journal of Geology, 87, 217-278.

Shackleton, R.M., Ries, A.C. & Coward, M.P. 1982. An interpretation of the Variscan structures in SW England. Journal of the Geological Society of London, 139, 533-541.

Shorey, M.D. & Sclater, J.G. in press. Mid-Jurassic through mid-Cretaceous extension in the Central Graben of the North Sea part 2: estimates from faulting observed on a seismic reflection line.

Sibuet, J.C., Mathis, B., Pastouret, L., Auzende, J.M., Foucher, J.P., Hunter, P.M., Guennoc, P., Graciansky, P.C. de, Montadert, L. & Masson, D.G. 1985. Morphology and basement structures of the Goban Spur continental margin (Northeast Atlantic) and the role of the Pyrenean orogeny. In: Graciansky, P.C. de, Poag, C.W. et al (eds.) Initial Reports of the Deep Sea Drilling Project, 80, 1153-1165.

Sleep, N.H. 1971. Thermal effects of the formation of Atlantic continental margins by continental break up. Geophysical Journal of the Royal Astronomical Society, 24, 325-350.

Sloss, L.L. & Speed, R.C. 1974. Relationships of cratonic and continental margin tectonic episodes. In: Dickinson, W.C. (ed.) Tectonics and Sedimentation. Society of Economic Paleontologists and Mineralogists Special Publication, 22, 98-119.

Smith, A.J., Stride, H. & Whittard, W.F. 1965. The geology of the Western Approaches of the English Channel - IV. A recently discovered Variscan granite west-north-west of the Scilly Isles. Proceedings of the Colston Research Society, 17, 287-301.

Smith, D.B., Brunstrom, R.G.W., Manning, P.I., Simpson, S. & Shotton, F.W. 1974. A correlation of Permian rocks in the British Isles. Geological Society of London Special Report, 5.

Smith, N.J.P. (compiler) 1985. Map 2: Contours on the top of the pre-Permian Surface of the United Kingdom (South). Scale 1:1 000 000. British Geological Survey.

Snyder, S.W., Muller, C., Sigal, J., Townsend, H. & Poag, C.W. 1985. Biostratigraphic, paleoenvironmental, and paleomagnetic synthesis of the Goban Spur region, Deep Sea Drilling Project leg 80. In: Graciansky, P.C. de, Poag, C.W. et al (eds.) Initial Reports of the Deep Sea Drilling Project, 80, 1169-1186.

Steckler, M.S. 1985. Uplift and extension at the Gulf of Suez: indications of induced mantle convection. Nature, 317, 135-139.

Steckler, M.S. & Watts, A.B. 1978. Subsidence of the Atlantic-type continental margin off New York. Earth and Planetary Science Letters, 41, 1-13.

Strong, D.F., Stevens, R.K., Malpas, J. & Badham, J.P.N. 1975. A new tale for the Lizard (abstract only). Proceedings of the Ussher Society, 3, 252.

Styles, M.T. & Rundle, C.C. 1984. The Rb-Sr isochron age of the Kennack gneiss and its bearing on the age of the Lizard complex, Cornwall. Journal of the Geological Society of London, 141, 15-19.

Talwani, M. & Ewing, M. 1960. Rapid computation of gravitational attraction of three-dimensional bodies of arbitary shape. Geophysics, 25, 203-225.

Tankard, A.J. & Welsink, H.J. 1987. Extensional tectonics and stratigraphy of Hibernia Oil Field, Grand Banks, Newfoundland. American Association of Petroleum Geologists Bulletin, 71, 1210-1232.

Taylor, S.R & Lapre, J.F. 1987. North Sea chalk diagenesis: its effect on reservoir location and properties. In: Brooks, J. & Glennie, K. (eds.) Petroleum Geology of North West Europe, 483-495. Graham and Trotman, London.

Thorpe, R.S., Cosgrove, M.E. & Van Calsteren, P.W.C. 1986. Rare earth element, Sr- and Nd-isotope evidence for petrogenesis of Permian basaltic and K-rich volcanic rocks from south-west England. Mineralogical Magazine, 50, 481-490.

Trappe, H., Wever, T. & Meissner, R. 1988. Crustal reflectivity pattern and its relation to geological provinces. Geophysical Prospecting, 36, 265-281.

Tucker, R.M. & Arter, G. 1987. The tectonic evolution of the North Celtic Sea and Cardigan Bay basins with special reference to basin inversion. Tectonophysics, 137, 291-307.

Vail, P.R., Mitchum, R.M. & Thompson, S. 1977. Seismic stratigraphy and global changes of sea level, part 4: global cycles of relative changes of sea level. In: Payton, C.E. (ed.) Seismic Stratigraphy - Applications to Hydrocarbon Exploration. American Association of Petroleum Geologists Memoir, 26, 83-97.

Van Hinte, J.E. 1976a. A Cretaceous time scale. American Association of Petroleum Geologists Bulletin, 60, 498-516.

Van Hinte, J.E. 1976b. A Jurassic time scale. American Association of Petroleum Geologists Bulletin, 60, 489-497.

Van Hinte, J.E. 1978. Geohistory analysis - application of micropaleontology in exploration geology. American Association of Petroleum Geologists Bulletin, 62, 201-222.

Van Hinte, J.E. & Deighton, I.C. 1987. Burial and thermal geohistory modelling ofsedimentary basins. Joint Association for Petroleum Exploration Course Notes, 57. Imperial College, London 24-26 March 1987.

Van Hoorn, B. 1987. The South Celtic Sea/Bristol Channel Basin: origin, deformation and inversion history. Tectonophysics, 137, 309-334.

Walker, A.B. 1987. Background & induced seismicity monitoring for the HDR geothermal programme in Cornwall. British Geological Survey, Global Seismology Report, 323.

Walter, L.M. 1985. Relative reactivity of skeletal carbonates during dissolution: implications for diagenesis. In: Schneidermann, N. & Harris, P.M. (eds.) Carbonate Cements. Society of Economic Paleontologists and Mineralogists Special Publication, 36, 3-16.

Warner, M.R. 1987. Seismic reflections from the Moho - the effect of isostasy. Geophysical Journal of the Royal Astronomical Society, 88, 425-435.

Warrington, G. 1983. Late Triassic and earliest Jurassic palynomorph assemblages from the western English Channel. Proceedings of the Ussher Society, 5, 473-476.

Warrington, G. & Owens, B. 1977. Micropalaeontological biostratigraphy of offshore samples from south-west Britain. Institute of Geological Sciences Report 77/7. HMSO, London.

Warrington, G., Audley-Charles, M.G., Elliott, R.E., Wyndham, B.E., Ivimey-Cook, H.C., Kent, P., Robinson, P.L., Shotton, F.W. & Taylor, F.M. 1980. A correlation of Triassic rocks in the British Isles. Geological Society of London Special Report, 13.

Watts, A.B. & Steckler, M.S. 1979. Subsidence and eustacy at the continental margins of eastern North America. In: Talwani, M., Hay, W. & Ryan, W.B.F. (eds.) Deep Drilling Results in the Atlantic Ocean: Continental Margins and Paleoenvironment. American Geophysical Union Maurice Ewing Symposium Series, 3, 218-234.

Watts, A.B., Karner, G.D. & Steckler, M.S. 1982. Lithospheric flexure and the evolution of sedimentary basins. Philosophical Transactions of the Royal Society of London, A305, 249-281.

Watts, N.L. 1983. Microfractures in chalks of Albuskjell field, Norwegian sector, North Sea: possible origin and distribution. American Association of Petroleum Geologists Bulletin, 67, 201-234.

Wernicke, B. 1981. Low-angle normal faults in the Basin and Range province: nappe tectonics in an extending orogen. Nature, 291, 645-648.

Wernicke, B. 1985. Uniform sense normal simple shear of the continental lithosphere. Canadian Journal of Earth Science, 22, 108-125.

Wernicke, B. & Burchfiel, B.C. 1982. Modes of extensional tectonics. Journal of Structural Geology, 4, 105-115.

White, N.J. 1988. Extension and subsidence of the continental lithosphere. Unpublished PhD Thesis, University of Cambridge.

White, N.J., Jackson, J.A. & McKenzie, D.P. 1986. The relationship of normal faults and that of the sedimentary layers in their hanging walls. Journal of Structural Geology, 8, 897-909.

White, N.J. & McKenzie, D.P. 1988. Formation of the "steer's head" geometry of sedimentary basins by differential stretching of the crust and mantle. Geology, 16, 250-253.

White, R.S., Spence, G.D., Fowler, S.R., McKenzie, D.P., Westbrook, G.K. & Bowen, A.N. 1987. Magmatism at rifted continental margins. Nature, 330, 439-444.

Wilkinson, I.P. & Halliwell, G.P. 1980. Offshore micropalaeontological biostratigraphy of southern and western Britain. Institute of Geological Sciences Report 79/9. HMSO, London.

Wilson, A.C. & Taylor, R.T. 1976. Stratigraphy and sedimentation in west Cornwall. Transactions of the Royal Geological Society of Cornwall, 20, 246-259.

Wise, D.U. 1974. Continental margins, freeboard and the volumes of continents and oceans through time. In: Burke, K. & Drake, C.L. (eds.) The Geology of Continental Margins, 45-58. Springer, Berlin/New York.

Wise, S.W., Jr. 1973. Calcareous nannofossils from cores recovered during leg 18, Deep Sea Drilling Project: biostratigraphy and observations on diagenesis. In: Musich, L.F. & Weser, O.E. (eds.) Initial Reports of the Deep Sea Drilling Project, 18, 569-615.

Worth, R.H. 1908. The dredgings of the Marine Biological Association (1895-1906), as a contribution to the knowledge of the geology of the English Channel. Journal of the Marine Biological Association, United Kingdom, 8, 118-188.

Wyllie, M.R.J., Gregory, A.R. & Gardner, L.W. 1956. Elastic wave velocities in heterogeneous and porous media. Geophysics, 21, 41-70.

Zervos, F.A. 1987. A compilation and regional interpretation of the northern North Sea gravity map. In: Coward, M.P., Dewey, J.F. & Hancock, P.L. (eds.) Continental Extensional Tectonics. Special Publication of the Geological Society of London, 28, 477-494.

Ziegler, P.A. 1981. Evolution of the sedimentary basins in North-West Europe. In: Illing, L.V. & Hobson, G.D. (eds.) Petroleum Geology of the Continental Shelf of North-West Europe, 3-39. Heyden and Son Ltd., London.

Ziegler, P.A. 1982. Geological Atlas of Western and Central Europe. Shell International Petroleum, Maatschappij B.V..

Ziegler, P.A. 1987a. Evolution of the Western Approaches Trough. Tectonophysics, 137, 341-346.

Ziegler, P.A. 1987b. Late Cretaceous and Cenozoic intra-plate compressional deformations in the Alpine foreland - a geodynamic model. Tectonophysics, 137, 389-420.

Ziegler, P.A. 1987c. Celtic Sea - Western Approaches area: an overview. Tectonophysics, 137, 285-289.

Ziegler, P.A. & Van Hoorn, B. in press. Evolution of the North Sea rift system. American Association of Petroleum Geologists Memoir.

APPENDIX A

DATABASE

A.1 DATA COVERAGE MAPS

Maps A.1-A.6 show the principal data sources used in the project.

Map A.1 shows the locations of all the commercial and BGS wells referred to in the text, and the Deep Sea Drilling Project (DSDP) well and dredge sites. Where "X" refers to a number and "A" a letter commercial wells in the British sector of the Western Approaches Trough are of the form XX/XX-1 (e.g. 72/10-1), whereas those in the French sector have names (e.g. Brezell-1). DSDP well locations are of the form DSDPXXX (e.g. DSDP400), dredges are of the form AAXX-XX (e.g SU01-01). British Geological Survey (BGS) wells are of the form SLSXX (e.g. SLS34) or XX/XX (e.g. 74/41).

Map A.2 is a track chart for the British Institutions Reflection Profiling Syndicate (BIRPS)/Etude de la Croûte Continentale et Océanique par Réflexion et Réfraction Sismiques (ECORS) South West Approaches Trough (SWAT) lines in the area.

Maps A.3 and A.4 are track charts for the GECO 1978/1979 and Petty-Ray 1973 speculative reflection seismic surveys respectively.

Map A.5 is a track chart for the gravity lines from which Hunting Geology and Geophysics interpolated gridded Bouguer gravity data. The gridded data were, in turn, used to produce the Bouguer gravity maps of Figures 2.7 and 8.2 and were used as the input for the gravity backstripping procedure (Section 8.2.1).

Map A.6 is a track chart for the aeromagnetic map of Figure 2.8.

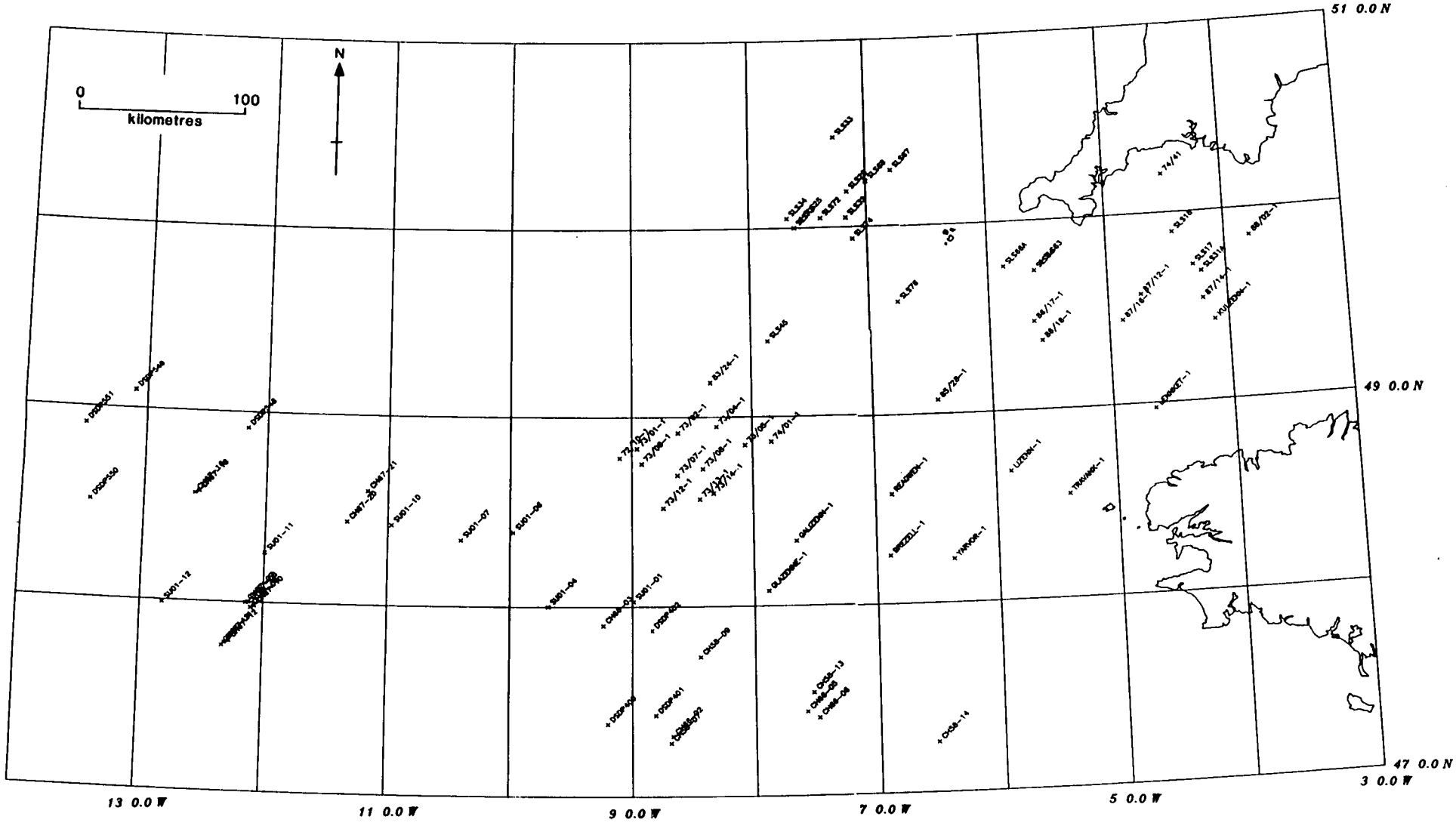

Map A.1 Location of commercial, BGS and DSDP wells and DSDP dredges.

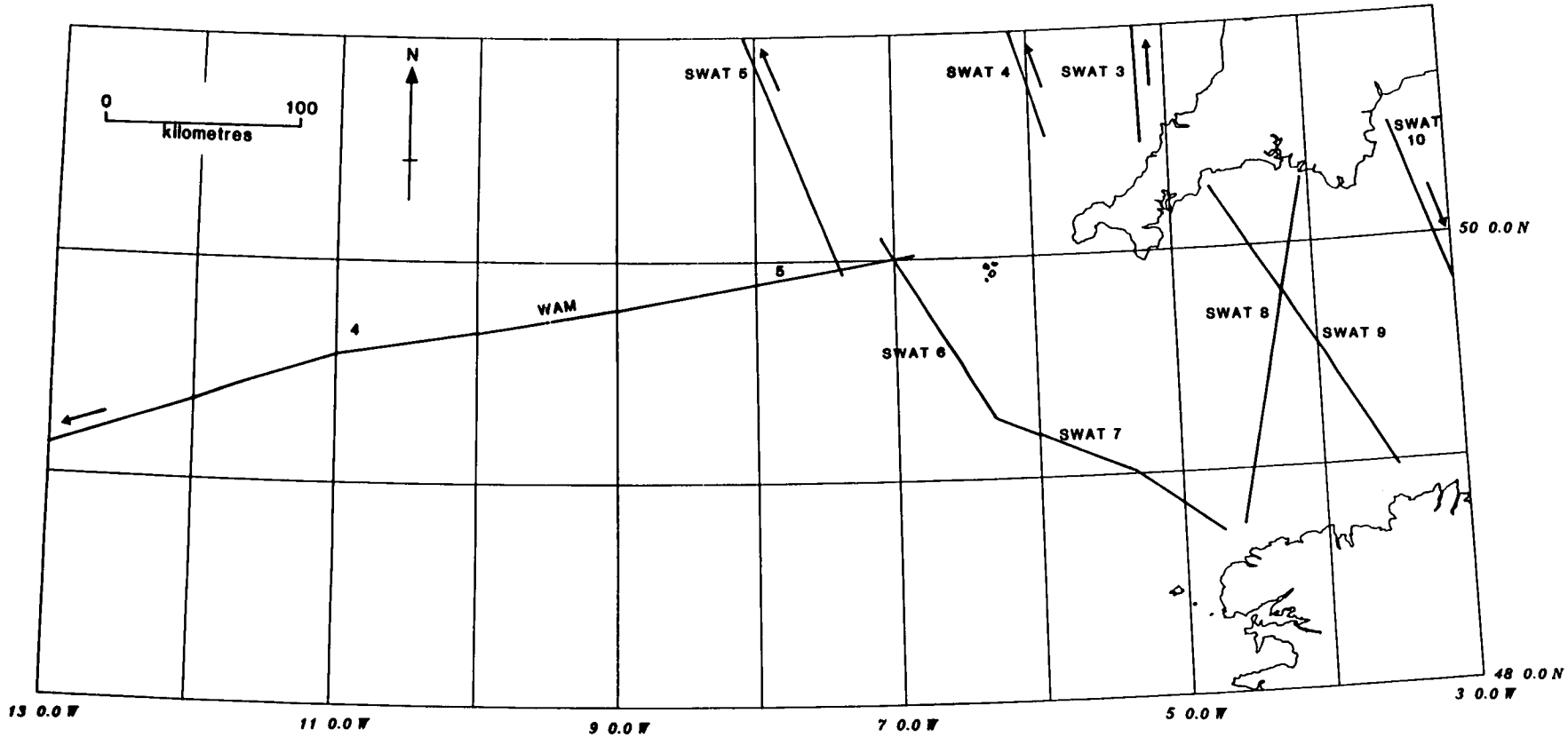

Map A.2 BIRPS/ECORS deep seismic reflection lines.

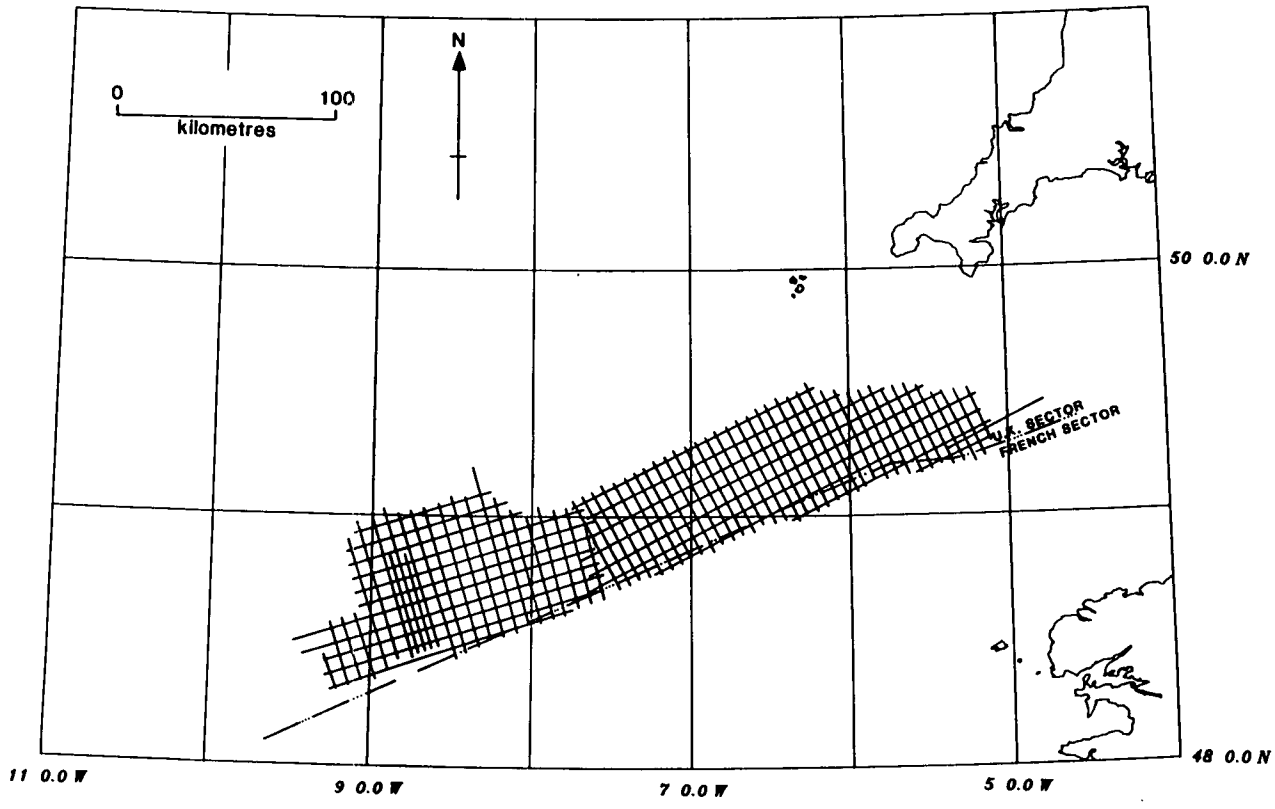

Map A.3 GECO 1978/1979 speculative seismic reflection data.

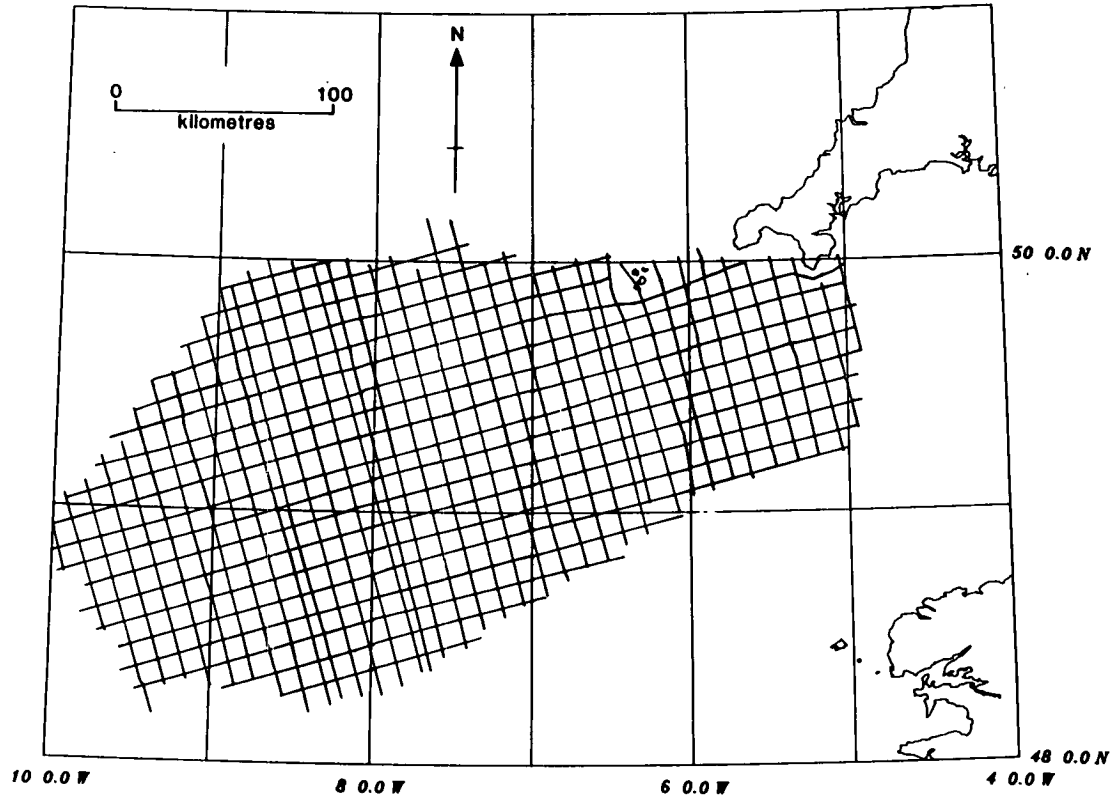

Map A.4 Petty-Ray 1973 speculative seismic reflection data.

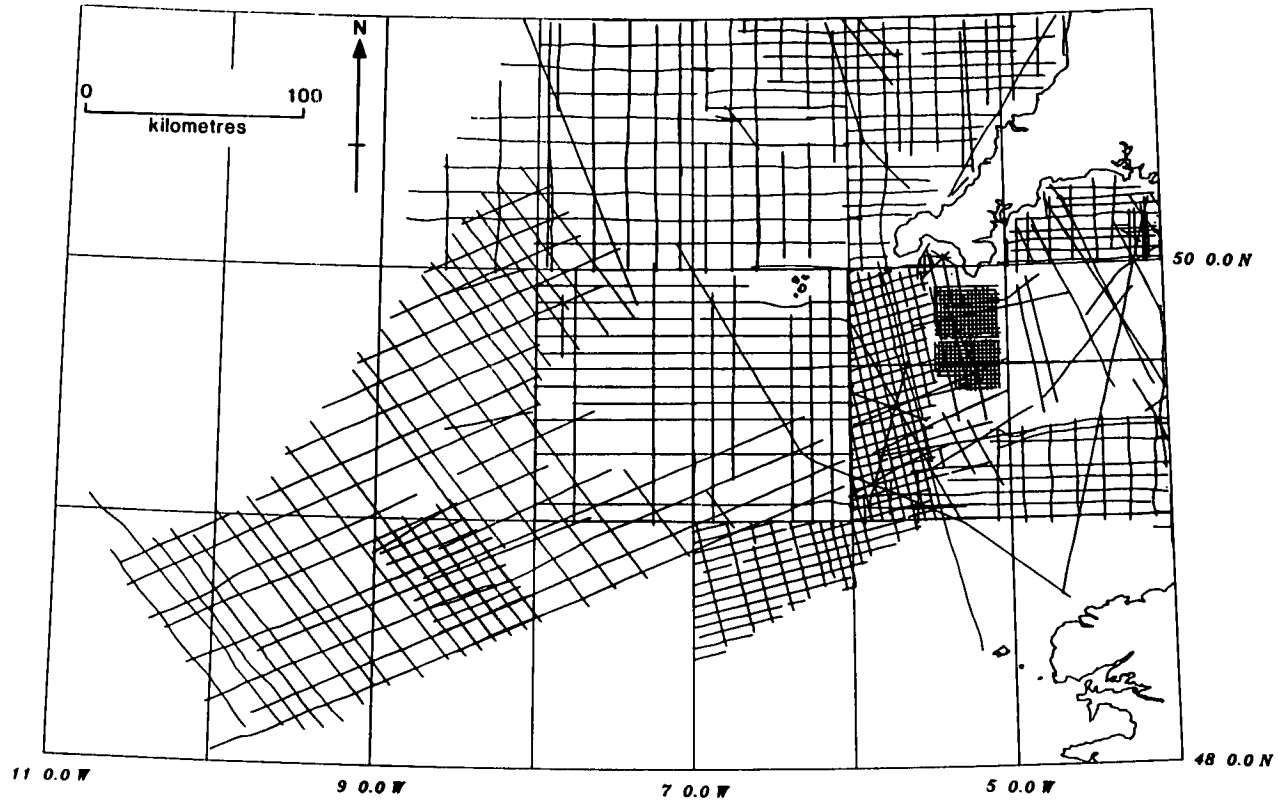

Map A.5 Gravity track chart.

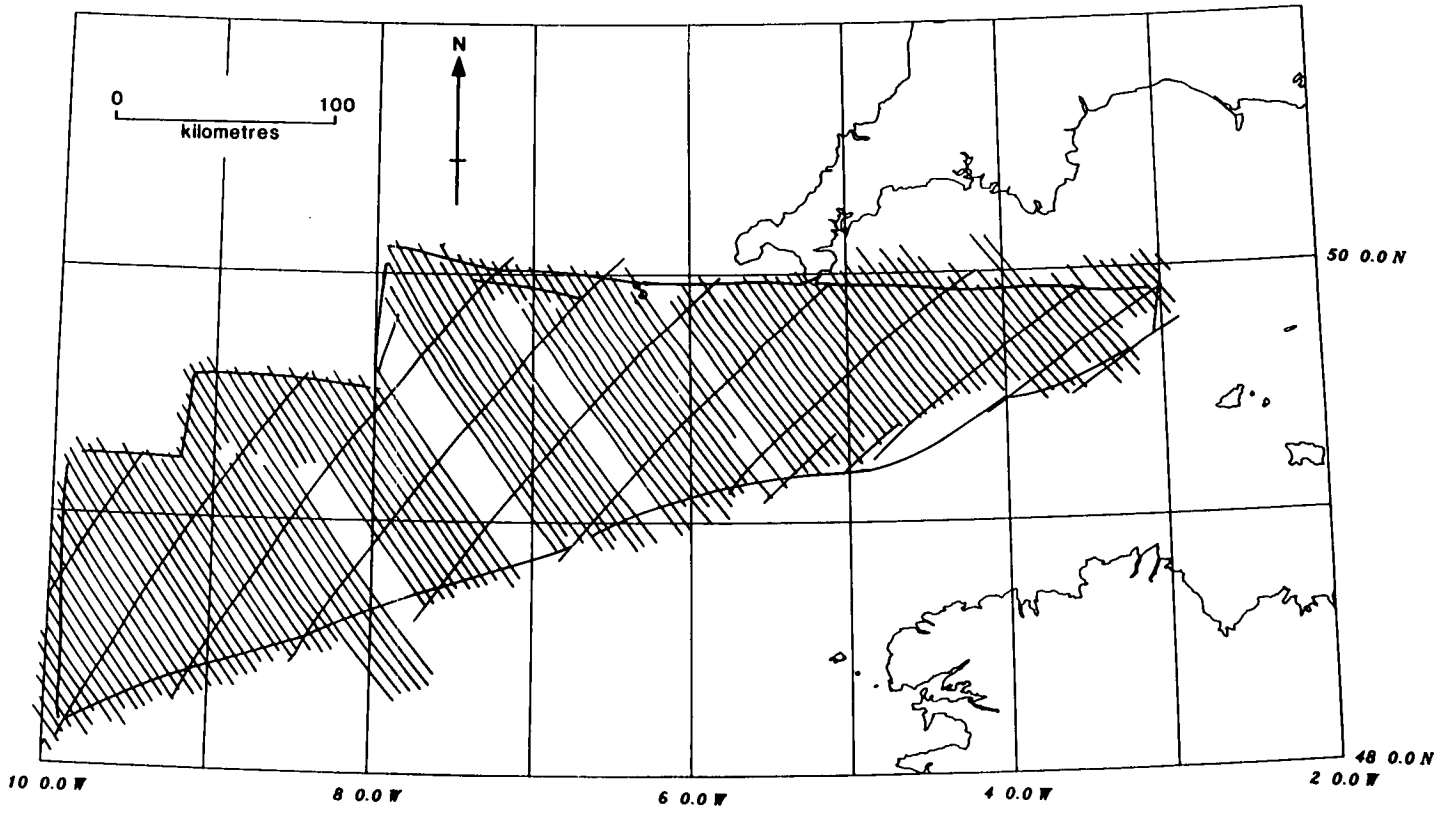

Map A.6 Aeromagnetic track chart.

APPENDIX B

PROSPECTIVITY OF THE WESTERN APPROACHES TROUGH

B.1 INTRODUCTION

The majority of well and seismic data utilized in this project were acquired in the search for commercial hydrocarbons. In addition to numerous speculative seismic surveys thirty-two commercial wells have been drilled in the Western Approaches Trough (twenty in the British sector and twelve in the French sector). This appendix briefly outlines the possible hydrocarbon plays in the area.

B.2 SOURCE ROCKS

The rich Liassic shales in the Western Approaches Trough provide a good potential source rock. Total organic carbon values for the Liassic of well 88/2-1 range from 2.3-7.7% by weight in the Hettangian, 0.50-3.3% by weight in the Sinemurian and up to 11.3% in the Pliensbachian (Cooles et al, 1981). Rock Eval analyses indicated a moderately good potential for both oil and gas (Cooles et al, 1981). In well 73/13-1 the early Sinemurian shale, particularly the top 100m, contains greater than 2% total organic carbon .

Taking the oil generation threshold at 75°C, an average sea-bed temperature of 10°C, an average geothermal gradient of 25°Ckm^{-1}, and ignoring erosion, then oil generation should commence in a source rock at approximately 2.6km below sea-bed. Deeper, undrilled parts of the southern Liassic outlier in the Melville Basin only just lie within this depth and little oil generation would be anticipated. However, in well 88/2-1 Cooles et al (1981) predicted shallow oil generation depths (threshold 1160±960m, peak 2210±2400m) on the basis of vitrinite reflectance data. Cimmerian and Eocene-Miocene uplift and erosion (Sections 2.7 and 2.9.3 respectively) combined with increased heatflow during Atlantic rifting (Kamerling, 1979) have generated shallower kitchen areas than predicted by simple modelling. Drilling results suggest, however, that Liassic source rocks in the southern

Melville outlier are only early mature and that significant quantities of oil have not been generated.

In the Brittany Basin the Liassic is more deeply buried than in the Western Approaches Basin due to the absence of Cimmerian uplift (Section 2.7). It, and younger Jurassic source rocks removed from the Western Approaches Basin by Cimmerian erosion, have been buried to sufficient depth for oil and gas generation and migration.

Any post-Variscan organic-rich Carboniferous sediments deposited in the Western Approaches Basin are also tentatively proposed as potential (?)gas-prone source rocks. Although the Devono-Carboniferous Variscan basement is overmature in well 83/24-1 (Cooles et al, 1981), post-orogenic sedimentation may locally have started in the Carboniferous and host a potentially mature source rock (Section 2.5.3).

B.3 RESERVOIR ROCKS

Early wells in the Western Approaches Basin concentrated on plays involving migration from the Liassic shales into overlying Jurassic sandstones equivalent to the Pennard (mid Liassic) and Bridport (Toarcian) Sandstones of onshore southern England. In well 72/10-1 not only was the maturity of the Liassic unfavourable at 1.2-1.3km below sea-bed, but the target sandstones had been removed by Cimmerian erosion (Bennet et al, 1985). Jurassic sandstones have only been recovered from well 73/1-1 where 15m of Hettangian sandstone with a porosity of 15% were proven (Section 2.6.1).

Subsequently the Triassic Sherwood Sandstone, structurally uplifted above Liassic source rock, became a reservoir target. Porosities up to 20% are preserved in the Sherwood Sandstone (Figure 3.3). This play is analogous to one of the successful plays in the Wytch Farm Oil Field (Colter and Havard, 1981).

Lower Cretaceous sandstones, directly overlying the Liassic due to Cimmerian erosion in the Melville Basin, are another potential reservoir. Porosities in the Lower Cretaceous sandstones reach almost 40% (Figure 3.3). In the Brittany Basin although porosities are slightly lower (not exceeding 30%) the sandstones are still a good potential reservoir

(Sections 2.8.1-2.8.3). Higher in the sequence the Chalk and the Eocene limestones and sandstones present potential reservoir horizons.

In the Brittany and South-West Channel Basins middle and late Jurassic reservoir horizons, removed from the Western Approaches Basin by Cimmerian erosion, are present but not correlatable between the three available wells. In well Lennket-1 the top 100m of the mid Jurassic dolomite is an excellent potential reservoir while undifferentiated late Jurassic "Purbeckian" sandstones have porosities up to 10% (Figure 3.3) but rather low permeabilities. In well Lizenn-1 Oxfordian sandstones also have porosities up to 10% (Figure 3.3). In well Brezell-1 the Tithonian sandstones, which are continuous with the early Cretaceous "Wealden" sediments, have porosities up to 20% (Figure 3.3).

The lack of commercially viable hydrocarbon deposits in these reservoirs, particularly in the Brittany Basin, where the source rocks have almost certainly reached maturity, must reflect unfavourable migration paths and/or trapping configurations.

B.4 CAP ROCKS

The Sherwood Sandstone Group is overlain by the Mercia Mudstone Group which comprises thick mudstones and evaporites with only minor silty sandstones and is a good stratigraphic trap. Similarly, potential Jurassic sandstone and carbonate reservoirs are interbedded with mudstones which should provide reasonable traps although they are locally rather silty. In well Lennket-1 the undifferentiated "Purbeckian" sandstones are interbedded with anhydrite. In the northern Melville Basin any Jurassic sandstones such as those in well 73/1-1 may be locally capped in the vicinity of the salt swells, however, as discussed above, significant oil generation has probably not occurred in the northern Liassic outlier of the Melville Basin. Traps for potential Lower Cretaceous and later reservoirs are less well developed with the early Eocene London Clay equivalent having the best potential. Other interbedded early Cretaceous and Tertiary mudstones are generally silty, and older chalks, although often of low porosity, probably contain significant fracture permeability.

B.5 CONCLUSIONS

Although oil shows have been reported in the Western Approaches Trough no significant finds have been recorded to date and the area is unlikely to receive further commercial attention without an upturn in the financial climate of oil exploration. The commercial failure of the area has been a boon to academic research providing an excellent database of unreleased wells and speculative seismic data which would not have otherwise been made available.

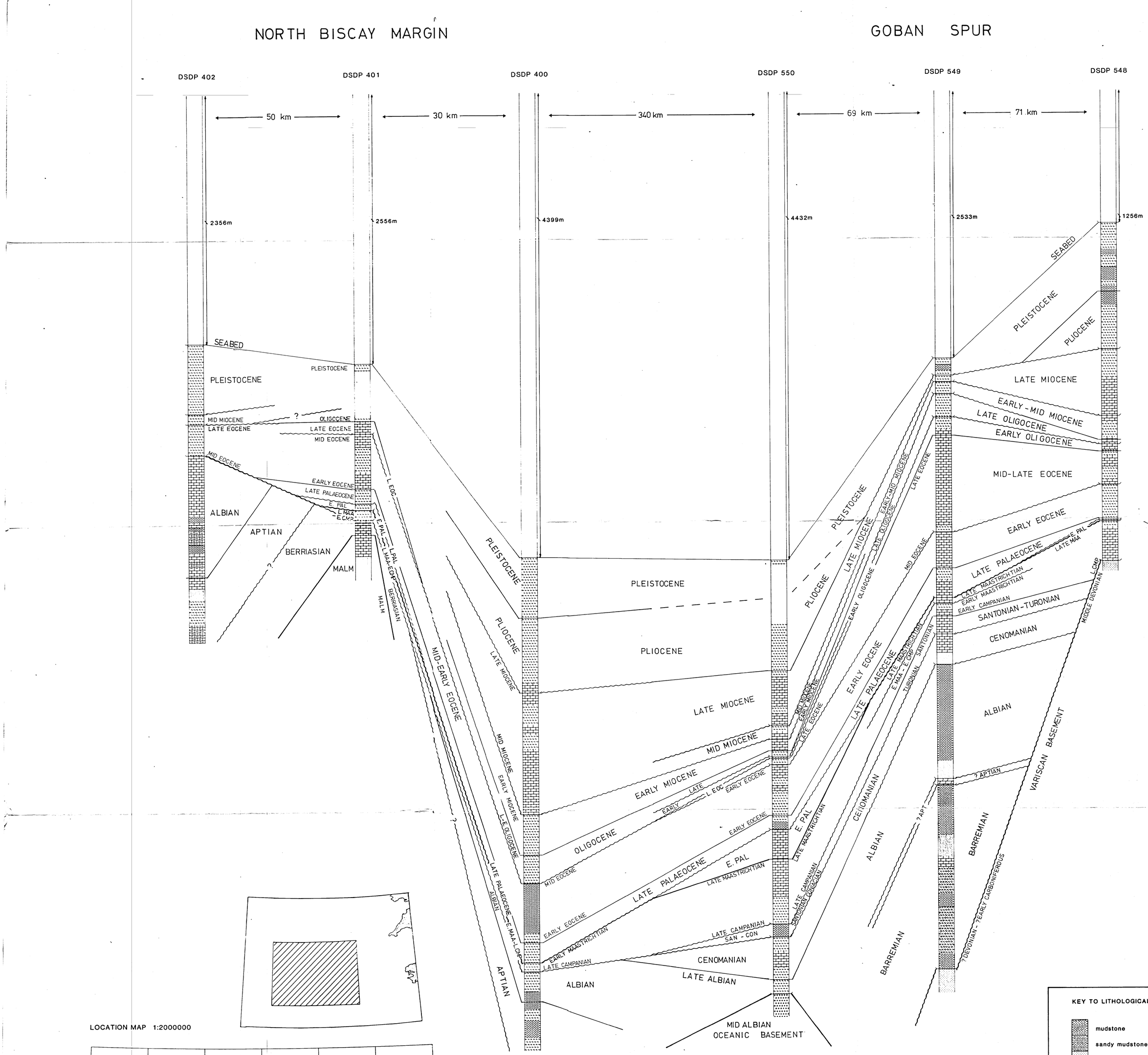

FIGURE 2.2 DEEP SEA DRILLING PROJECT
LEGS 48 AND 80 - BOREHOLE CORRELATION
Vertical Scale - water column 1 : 15 000
sub-seabed 1 : 2 500

CORNUBIAN MASSIF

MELVILLE BASIN

BRITTANY BASIN

SOUTH-WEST CHANNEL BASIN

ST. MARY'S BASIN

PLYMOUTH BAY BASIN

BGS 83/24-1 | BRITOIL 72/10-1 | BRITOIL 73/1-1 | CHEVRON 73/6-1 | AMERADA HESS 73/2-1 | PHILLIPS 73/7-1 | CHEVRON 73/8-1 | PLACID 73/12-1 | MURPHY 73/13-1 | MURPHY 73/14-1 | ARCO 73/5-1 | BRITISH GAS 74/1-1 | SNEA Brezell-1 | SNEA Lizen-1 | SNEA Lennket-1 | Britoil 85/28-1 | Murphy 86/17-1 | Britoil 86/18-1 | BP 87/12-1 | BGS 87/16-1 | BGS 87/14-1 | BGS 88/2-1

SEALEVEL

70 km | 12 km | 9 km | 28 km | 24 km | 16 km | 33 km | 23 km | 9km | 34km | 16 km | 97 km | 89 km | 95 km | 32 km | 74 km | 12 km | 66 km | 19 km | 50 km | 47 km

SEABED

FIRST RETURNS

MIOCENE

OLIGOCENE

MID-LATE EOCENE

EARLY EOCENE

MAASTRICHTIAN - CAMPANIAN

SANTONIAN - CENOMANIAN

ALBIAN-APTIAN

LIAS

PERMO-TRIAS

DEVONO-CARB

MERCIA MUDSTONE GROUP

SHERWOOD SANDSTONE GROUP

AYLESBEARE GROUP

ARMORICAN BASEMENT

MAJOR LATE JURASSIC/EARLY CRETACEOUS DOWNTHROW

PALAEOCENE

OLIGOCENE

EOCENE

MAASTRICHTIAN-CAMPANIAN

SANTONIAN-CENOMANIAN

ALBIAN-APTIAN

LIAS

PENARTH GROUP

MERCIA MUDSTONE GROUP

SHERWOOD SANDSTONE GROUP

AYLESBEARE GROUP

? PERMO-CARBONIFEROUS

BRITTANY AND SOUTH-WEST CHANNEL BASINS INVERTED IN TERTIARY

MAA-CMP

SANTONIAN-CENOMANIAN

ALBIAN-APTIAN

BARREMIAN-HAUTERVIAN

VALANGINIAN-BERRIASIAN

MALM

DOGGER

LIAS

? AYLESBEARE GROUP

MAJOR LATE JURASSIC/EARLY CRETACEOUS DOWNTHROW

ARMORICAN BASEMENT

EOCENE

CAMPANIAN

SANTONIAN-CENOMANIAN

ALBIAN-APTIAN

MERCIA MUDSTONE GROUP

SHERWOOD SANDSTONE GROUP

AYLESBEARE GROUP

DEVONO - CARBONIFEROUS

fault

PALAEOCENE

MAASTRICHTIAN - CAMPANIAN

SANTONIAN - CENOMANIAN

LIAS

MIDDLE DEVONIAN

KEY TO LITHOLOGICAL SYMBOLS

- mudstone
- sandy mudstone
- sandstone
- marl
- limestone
- argillaceous limestone
- chalk
- calcareous sandstone
- dolomite
- conglomerate/breccia
- slate
- halite
- anhydrite
- quartzite
- water/unknown
- igneous extrusive
- gneiss

LOCATION MAP 1:2000000

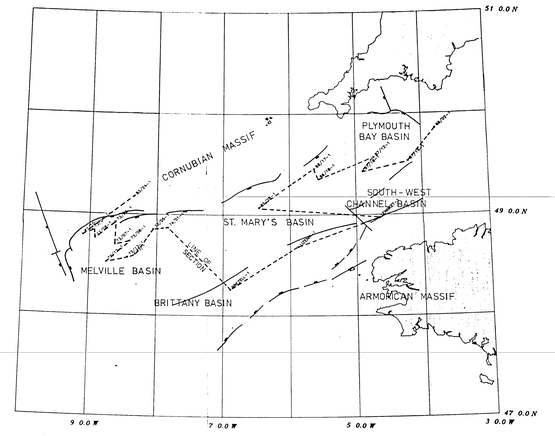

FIGURE 2.1 COMMERCIAL BOREHOLE CORRELATION - WESTERN APPROACHES TROUGH. Vertical Scale 1:6500